The role of perineuronal nets in the anterior bed nucleus of the stria terminalis in regulating emotional behaviour and neuronal transmission

Submitted by Kathryn Murrall to the University of Exeter as a thesis for the degree of

Doctor of Philosophy, September, 2022

Abstract

Anxiety disorders are the most common mental health disorders suffered globally, affecting upwards of 300 million people. Despite the prevalence of anxiety disorders, the currently available therapies lack efficacy, with only 50-85% of patients experiencing at least a 50% improvement in symptoms, and can cause adverse reactions. As such, greater insight into the molecular underpinnings of anxiety disorders is essential to provide a rationale for novel effective treatments.

Exposure to severe or prolonged stress promotes the development of anxiety, through aberrant changes to neuronal plasticity in the cortex, hippocampus and amygdala, three well-characterised brain regions involved in the stress response. However, the role of the bed nucleus of the stria terminalis (BNST), uniquely placed to modulate the stress response, in anxiety disorders is not fully understood.

Here, I investigated the role of specialised organisations of extracellular matrix, perineuronal nets (PNNs), within the BNST in regulating emotional behaviour and neuronal transmission in relation to stress.

The experimental work presented in this thesis characterises the spatiotemporal development of PNNs in the anterior BNST and identifies the anteromedial BNST as the region with densest PNN expression. Morphological studies determine that the structure of PNNs in the anteromedial BNST is the most vulnerable seven days following exposure to repeated restraint stress, a period which coincides with increased anxiety-like behaviour in the elevated plus maze and changes to plasticity of BNST neurons. However, such behavioural changes cannot be recapitulated by PNN degradation, suggesting that PNN alterations are highly specific following stress.

Altogether these experiments provide evidence of a relationship between stress and PNNs in the BNST and open an avenue for future research, which may one day inform discovery of novel therapeutics for anxiety disorders.

Acknowledgements

Firstly, I would like to thank my funding body, Leverhulme, and my supervisors: Prof. Pawlak, for giving me the opportunity and freedom to pursue this PhD project, Dr. Mucha, for your advice and support throughout, and Dr. Mosienko for your continued guidance and mentorship, I truly would not have made it to the end without you and will be forever grateful for your late addition to my supervisory team.

I would also like to express my gratitude to Dr. Sherlock, Dr. Brown, Callum, and Brinda for the various scripts I was able to use to facilitate my data analysis. I appreciate all your patience and assistance along the way. Special thanks to Brinda for your help with the MEA, and for taking the time to teach me something completely new in an incredibly short space of time.

A massive thank you to my parents, Bec, and my wider family, for all the love and encouragement you show me daily. Your reassurance has undoubtedly helped me to persevere. Special thanks to my friends in Liverpool, Exeter, and further afield, for all the laughs and adventures over the years, your friendship has been the best tonic throughout this journey. Finally, my biggest thanks go to Iain, without whom the last few years would not have been possible.

Table of contents

List of figures

List of tables

List of abbreviations

AMPA - α-amino-3-hydroxy-5-methyl-4-isoxazolepropionic acid

ANOVA – analysis of variance

aCSF – artificial cerebral spinal fluid

ACTH - adrenocorticotropic hormone

BNST – bed nucleus of the stria terminalis

ChABC – chondroitinase ABC

CNS – central nervous system

CRF – corticotropin releasing factor

CRH – corticotropin releasing hormone

Crtl1 – cartilage linking protein 1

CSPG – chondroitin sulfate proteoglycan

ECM – extracellular matrix

EPM – elevated plus maze

fMRI – functional magnetic resonance imaging

GAG – glycosaminoglycan

GFAP – glial fibrillary acidic protein

HAPLN – hyaluronan and proteoglycan link protein

HAS – hyaluronan synthase

HCN – hyperpolarisation-activated cyclic nucleotide

HEK – human embryonic kidney

HPA – hypothalamic-pituitary-adrenal

LTD – long term depression

LTP – long term potentiation

mPFC – medial prefrontal cortex

NMDA – *N*-Methyl-D-Aspartate

NMDAR – *N*-Methyl-D-Aspartate receptor

nNOS – neuronal nitric oxide synthase

OCD – obsessive compulsive disorder

OFT – open field test

PBS – phosphate buffered saline

PFA – paraformaldehyde

pMEA – perforated multielectrode array

PNN – perineuronal net

PTSD – post-traumatic stress disorder

PV – parvalbumin

PVN – paraventricular nucleus of the thalamus

qRT-PCR – quantitative real time polymerase chain reaction

SSRI – selective serotonin reuptake inhibitor

SNRI – selective serotonin and noradrenaline reuptake inhibitor

STFU – bed nucleus of the stria terminalis, fusiform part

STLD – bed nucleus of the stria terminalis, lateral division 2

STLI – bed nucleus of the stria terminalis, lateral division 1

STLJ – bed nucleus of the stria terminalis, juxtacapsular part

STLP – bed nucleus of the stria terminalis, lateral division, posterior part

STLV – bed nucleus of the stria terminalis, lateral division, ventral part

STMA – bed nucleus of the stria terminalis, medial division, anterior part

STMAL - bed nucleus of the stria terminalis, medial division anterolateral part

STMAM - bed nucleus of the stria terminalis, medial division, anteromedial part

STMP - bed nucleus of the stria terminalis, medial division, posterior part

STMPI - bed nucleus of the stria terminalis, medial division, posterior intermediate part

STMPL - bed nucleus of the stria terminalis, medial division, posterolateral part

STMPM – bed nucleus of the stria terminalis, medial division, posteromedial part

STMV - bed nucleus of the stria terminalis, medial division, ventral part

TTX - tetrodotoxin

UCMS – unpredictable chronic mild stress

WFA – wisteria floribunda agglutinin

YLD – years lived with disability

Chapter 1 – General introduction

1.1 Anxiety

Anxiety is characterised by a state of negative valence and high arousal resulting in increased vigilance in the absence of imminent threat (Davis, et al., 2010). Anxiety is either considered to be ‘state’ or ‘trait’ in nature; enhanced arousal and vigilance in uncertain situations is representative of state or ‘phasic’ anxiety, also referred to as fear, which can be evolutionarily beneficial. Conversely, persistent and non-adaptive vigilance and high arousal in ambiguous situations is reflective of trait or ‘sustained’ anxiety (Sylvers, et al., 2011). Anxiety is deemed to be pathological when disruptive or disproportionate to the level of threat; perception of threat may be internally generated or innocuous stimuli may be misinterpreted as threatening (Calhoon & Tye, 2015).

The term ‘anxiety disorders’ covers a range of related disorders including generalised anxiety, social phobia, specific phobia and panic disorder (American Psychiatric Association, 2013). Post-traumatic stress disorder (PTSD) and obsessive-compulsive disorder (OCD) were also classified as anxiety disorders until 2013, when they became separately classified under DSM-5 criteria (American Psychiatric Association, 2013; Kupfer, 2015). PTSD and OCD may still be conflated with anxiety disorders for experimental research purposes, however, as many of the presenting symptoms are similar: uncontrollable and intrusive thoughts of worry, hyperarousal and hypervigilance, and increased heart and respiration rate (Davis, et al., 2010; Calhoon & Tye, 2015; Bandelow, et al., 2016).

Anxiety disorders have the highest incidence of any psychiatric disorder, with an estimated prevalence of 301.4 million cases globally in 2019 (GBD 2019 Mental Disorders Collaborators, 2022). Notably, since 1990 the global prevalence and burden of anxiety have not reduced, despite interventions evidenced to lessen their impact (GBD 2019 Disease and Injuries Collaborators, 2020). Case numbers have also risen sharply as a result of the global Covid-19 pandemic; prevalence of anxiety disorders was estimated to be around 374 million globally in 2020, with upwards of 70 million cases attributed to the effects of the pandemic (COVID-19 Mental Disorders Collaborators, 2021).

Anxiety disorders are pervasive, often chronic and are reported to be the eighth leading cause of disability globally, as measured by years lived with disability

(YLD) (James, et al., 2018; GBD 2019 Mental Disorders Collaborators, 2022). In 2017, YLD counts for anxiety disorders were 27,121.4 (thousands) compared to YLD counts for Alzheimer's and other dementias, for example, at 6,570.4 (thousands) (James, et al., 2018). As with the majority of mental disorders, these estimates are likely to be on the conservative side due to differing attitudes towards mental health disorders in different countries and the inadequacy of self-report questionnaires, which fail to take into account the variation with which psychiatric conditions may be experienced (Stein, et al., 2017; Baxter, et al., 2013; Baxter, et al., 2014).

Anxiety disorders are some of the most difficult disorders to treat. Response to treatment for anxiety disorders is highly variable, reflective of the individuality of the experienced symptoms. Research suggests that only 50-85% of patients respond to currently available pharmacological and psychological treatments, determined by at least a 50% reduction in experienced symptoms, and even fewer achieve recovery, defined by minimal anxiety symptoms (Bystritsky, 2006; Garakani, et al., 2020).

Patients may also experience different anxiety disorders simultaneously, which are often associated, and there is high comorbidity between anxiety disorders and other conditions (Thibaut, 2017; van Steensel, et al., 2011; Kessler, et al., 2015). 41.6% of those with a 12-month major depressive disorder also had one or more concomitant anxiety disorder as reported in a world-wide survey and 40% of those with an autism spectrum disorder will simultaneously experience an anxiety disorder (Kessler, et al., 2015; van Steensel, et al., 2011). Consequently, anxiety disorders frequently remain undiagnosed or misdiagnosed (Thibaut, 2017; Wittchen, et al., 2002). Therefore, studies which seek to further elucidate the molecular underpinnings of anxiety disorders are critical to provide rationale for the development of future therapeutics.

1.1.1 Differentiating between fear and anxiety

Threat detection, evaluation and interpretation are key processes which contribute to the selection of fear or anxiety-like responses to stimuli. Though the brain regions which contribute to the underlying circuitry of fear and anxiety are broadly similar, and the terms are often used interchangeably, it is important to

distinguish between the two states. Fear is a phasic response to an imminent, identifiable threat which dissipates upon stimulus removal; though threatening stimuli which are imagined or perceived as present may also trigger a fear response (Davis, et al., 1989; Blanchard, et al., 1993; Davis, et al., 2010; Knight & Depue, 2019). Conversely, anxiety is an apprehensive state elicited by unpredictable prospective threat which is physically or psychologically more remote (Blanchard, et al., 1993; de Jongh, et al., 2003; Davis, et al., 2010; Avery, et al., 2016).

One of the primary differences in the underlying circuitry of fear and anxiety-like responses, in both rodents and humans, lies in the relative contribution of the amygdala and the BNST (Davis, et al., 2010; Avery, et al., 2014). Early lesional studies of the rodent central amygdala and BNST demonstrated unique roles for the two regions. Central amygdala lesions reduce conditioned fear responses but have no effect on anxiety-like responses, whereas BNST lesions attenuate anxiety-like behaviour, disrupt cortisol release, and do not affect conditioned fear responses (Walker & Davis, 1997; Walker, et al., 2003; Duvarci, et al., 2009; Sullivan, et al., 2004; Hammack, et al., 2004).

Humans also show distinction between amygdala and BNST involvement in fear and anxiety states. A functional magnetic resonance imaging (fMRI) study comparing phobic to control participants found increased BNST activity when presented with phobia-related images, and in the anticipatory period prior to presentation, with no increase in amygdala activity (Straube, et al., 2007). Conversely, enhanced amygdala activity during brief presentation of phobogenic stimuli has been reported (Dilger, et al., 2003; Larson, et al., 2006). Furthermore, a potential role for the BNST in so-called ‘threat monitoring’ has been uncovered in humans. In an fMRI study where participants were shown videos of a line fluctuating in height, and were told whenever the line exceeded a certain threshold they would accumulate an electric shock to be delivered at the end of the task, though they were never actually shocked, robust activity of the BNST was identified during the task, but only minimal activity in the amygdala (Somerville, et al., 2010).

The proximity of a threat also affects human BNST activity. An fMRI study where a tarantula approached, and retreated from, a participant’s foot identified an increase in BNST activity as the tarantula moved closer (Mobbs, et al., 2010).

Amygdala activity was higher when the tarantula was approaching compared to retreating, consistent with significantly higher experienced fear ratings – a subjective measure determined by a self-report questionnaire. Taken together, these data support unique roles for the amygdala and BNST – the BNST manages potential and non-imminent threats, in complement with the amygdala which is responsible for pairing unconditional stimuli with immediate threats.

1.1.2 Translational rodent models of fear and anxiety

Paradigms used to model fear in rodents are generally based on the measurement of immediate responses to unconditioned or conditioned stimuli. One such assay is the acoustic startle response, which is characterised by the contraction of facial and skeletal muscles in response to an unexpected high decibel noise (Prosser & Hunter, 1936). Another is Pavlovian fear conditioning where cues such as a light or an audible tone - the conditioned stimulus - predict the onset of footshocks - the unconditioned stimulus (Pavlov, 1927). Over time, the pairing of stimuli is learned, such that the conditioned stimulus alone is sufficient to induce the response which would be elicited by delivery of the unconditioned stimulus, in this case freezing behaviour (Maren, et al., 1997; Kim & Jung, 2006; Corcoran & Quirk, 2007). A confound of cued fear conditioning is that animals will also form associations with the environment where the association between conditioned and unconditioned stimuli is learned (Bouton, 1993). As such, contextual fear conditioning, a form of Pavlovian conditioning, can also be used to study fear learning and behaviour. In contextual fear conditioning, the entire environment the animal is placed in serves as the conditioned stimulus, which is still paired with an aversive unconditioned stimulus. Freezing behaviour is measured when the animal is re-exposed to the context in which the unconditioned stimulus was previously delivered (Fanselow, 2000).

Ethological assays designed to model anxiety-like behaviour capitalise on the innate approach/avoidance conflict in rodents in nature; the desire to explore novel areas, generally to find resources, coupled with the desire to avoid open, bright areas, where potential exposure to threat from predators is greater (La-Vu, et al., 2020). Rodents with an anxious phenotype will typically spend a greater

amount of time in enclosed areas or zones deemed to be ‘safe’ within behavioural apparatus, in comparison to controls. The most used behavioural assays to measure anxiety in rodents are the elevated plus maze (EPM), open field test (OFT), light-dark box and the hole board.

The EPM apparatus consists of two enclosed arms and two open, brightly lit arms arranged in the shape of a plus around a central square, elevated a distance off the ground (Pellow, et al., 1985). Rodents are given an allotted amount of time to freely explore the maze and time spent in, and number of entries to the open arms of the maze provide a measure of anxiety-like behaviour. Rodents with an anxious phenotype will generally spend less time in, and make fewer entries to, the open arms of the maze (Pellow, et al., 1985; Rodgers & Dalvi, 1997; Korte & De Boer, 2003). A variation of the EPM is the elevated zero maze, which is ring shaped and consists of four alternative walled and open quadrants. Whilst the zero maze eliminates the somewhat ambiguous central square of the EPM, in other aspects it remains identical.

The OFT is an open arena with a central portion demarcated (Hall & Ballachey, 1932). Animals are given a set amount of time to freely explore the arena and similar to the EPM the time spent in, and number of entries to, the central portion indicate the extent of anxiety-like behaviour (Seibenhener & Wooten, 2015). Rodents with an anxious phenotype will spend more time in the outer section of the open field and will make fewer entries to the central zone of the field. Like the OFT, the hole board assay consists of an open arena with evenly spaced holes in the floor, which a rodent can poke their head into. Measurement of this ‘head-dipping’ behaviour is the basis for quantification of anxiety-like behaviour; rodents with an anxious phenotype will head-dip less than controls (Brown & Nemes, 2008). This assay is also used to measure repetitive behaviours as well as exploratory behaviours.

The light dark box consists of an arena with two chambers, one dark and one brightly lit (Bourin & Hascoet, 2003). Animals have free access to both chambers and are allowed to explore for a set time. Rodents with an anxious phenotype will spend less time in, and make fewer entries to, the light half of the arena; increased avoidance of the brightly lit compartment is indicative of anxiety-like behaviour (Kulesskaya & Voikar, 2014). Additional measures in the light-dark box

may include length of time spent freezing, latency to enter the light chamber and general locomotor activity (Ambrogi Lorenzini, et al., 1984).

It is important to consider that the tests described above each have their own strengths and limitations and that no one test provides superior measurements over the others. Notably, these tests are only capable of measuring innate anxiety-like behaviours, as rodents cannot qualitatively communicate their feelings or comment on their emotional state. As such, ethological tests can inform research into the underlying neurocircuitry of the behaviours they measure, and even the development of novel compounds to address these behaviours. However, they are limited in drawing parallels with the subjective human experience of anxiety, which must be taken into consideration in any experimental research employing rodent models to study such behaviours.

1.1.3 Neural circuitry of anxiety

The pathways and interlinking microcircuitry which govern threat perception and evaluation and downstream behavioural responses in the context of anxiety are complex. However, the macrocircuit of information flow consists of four key nodes: the amygdala, BNST, the ventral hippocampus and medial prefrontal cortex (mPFC) (Namburi, et al., 2015; Kim, et al., 2013; Adhikari, et al., 2010; Calhoon & Tye, 2015). Specifically, the basolateral amygdala receives information regarding sensory stimuli from sensory cortices and the thalamus (McDonald, 1998; Mishkin & Aggleton, 1981). The information is then relayed, via the ventral hippocampus, to the mPFC, which directly projects to the motor cortex to mediate risk avoidance and defensive behaviours (Felix-Ortiz, et al., 2013; Schoenfeld, et al., 2014). The basolateral amygdala also relays sensory information to the BNST, which sends direct projections to the lateral hypothalamus, which also mediates risk avoidance, and the brainstem, particularly the parabrachial nucleus, periaqueductal gray and dorsal vagal complex, which drive an increase in physiological measures of anxiety: heart rate, respiration rate and freezing behaviour (Kim, et al., 2013). Crucially, the information flow between the four key nodes of the anxiety circuit is bidirectional, allowing simultaneous evaluation and interpretation of the emotional value of environmental stimuli (Calhoon & Tye, 2015).

1.2 The bed nucleus of the stria terminalis

1.2.1 Anatomy of the bed nucleus of the stria terminalis

The bed nucleus of the stria terminalis (BNST) is a bilateral, multinucleate, limbic brain region situated in the basal forebrain. Sometimes, although perhaps misleadingly, referred to as part of the 'extended amygdala', as the two regions have uniquely defined roles. The BNST first appears at the base of the lateral ventricle and extends to where the hypothalamus begins (Alheid & Heimer, 1988; Glangetas & Georges, 2016). Though the BNST is physiologically heterogeneous and anatomically complex, in rodents the region can largely be split into anterior and posterior divisions (Figure 1.1). The anterior division is organised around the white matter of the anterior commissure and the posterior division around the fibrous structure of the stria terminalis (Dumont, 2009).

In humans, the BNST is larger than in rodents, though its structure is less complex (Lesur, et al., 1989). The human BNST consists of medial, central and lateral divisions, subdivided along a medial-lateral, rather than an anterior-posterior, axis, which join a ventral division more posteriorly (Walter, et al., 1991; Lebow & Chen, 2016). These subdivisions are largely similar to those described in rodents, however (Walter, et al., 1991; Ju & Swanson, 1989).

The rodent BNST is one of the most structurally complex regions in the central nervous system (CNS). It is made up of approximately 12-18 subnuclei, depending on the classification used to divide the region. Notably, the BNST has been more robustly characterised in the rat brain than in the mouse brain. The original classification was described in the rat and is largely based on cytoarchitectural features (Ju & Swanson, 1989; Dong, et al., 2001a; Swanson, 2004). The second classification is more detailed in its parcellation of the individual subnuclei and is based on ventral, lateral, medial and intermediate divisions within the BNST (Franklin & Paxinos, 2007). Both classifications broadly divide the BNST into anterior and posterior regions. The posterior BNST is mainly involved in reproductive and social behaviours and is the main source of sexual dimorphism in the BNST (Hines, et al., 1985; Simerly, 2002; Greenberg, et al., 2013). However, the current work will focus on the anterior BNST, since the subnuclei in this region have been implicated in anxiogenesis and associated anxiety-like behaviours (Davis, et al., 2010; Kim, et al., 2013).

In the Ju & Swanson (1989) classification, the anterior BNST consists of the following subnuclei: anterodorsal, anterolateral, anteromedial, dorsal, dorsomedial, fusiform, juxtacapsular, magnocellular, oval, rhomboid and ventral (Figure 1.1A). The posterior BNST consists of the principal, transverse and interfascicular subnuclei (Ju & Swanson, 1989). Adding to complexity, in the literature there is additional and sometimes conflicting nomenclature used to describe various groups of individual subnuclei. The anteromedial, anterolateral and juxtacapsular subnuclei have collectively been referred to as the dorsolateral BNST (Kash, et al., 2008; Salimando, et al., 2020). Conversely, the anterolateral, oval and juxtacapsular subnuclei have also been collectively referred to as the dorsolateral BNST (Kasten, et al., 2020). The rhomboid, anterolateral, juxtacapsular and oval subnuclei are sometimes referred to as the 'anterolateral group' (Dabrowska, et al., 2013; Smithers, et al., 2019), which in some cases also includes the fusiform nucleus (Dong & Swanson, 2004).

In the Franklin & Paxinos (2007) classification, the anterior BNST is divided into the following subnuclei: fusiform (STFU), lateral division 1 (STLI), lateral division 2 (STLD), juxtacapsular (STLJ), lateral division posterior part (STLP), lateral division ventral part (STLV), medial division anterior part (STMA), medial division anterolateral part (STMAL), medial division anteromedial part (STMAM), medial division posterior part (STMP) and medial division ventral part (STMV; Figure 1.1A). The posterior BNST is divided into the medial division, posterior intermediate part (STMPI), medial division, posterolateral part (STMPL) and medial division posteromedial part (STMPM).

Throughout the data chapters in this thesis, I will use the second anatomical classification of the BNST, as detailed by Franklin and Paxinos (2007) in the mouse. However, throughout the introductory chapter, nomenclature of the various anatomical parts of the BNST will be used as given in the original papers.

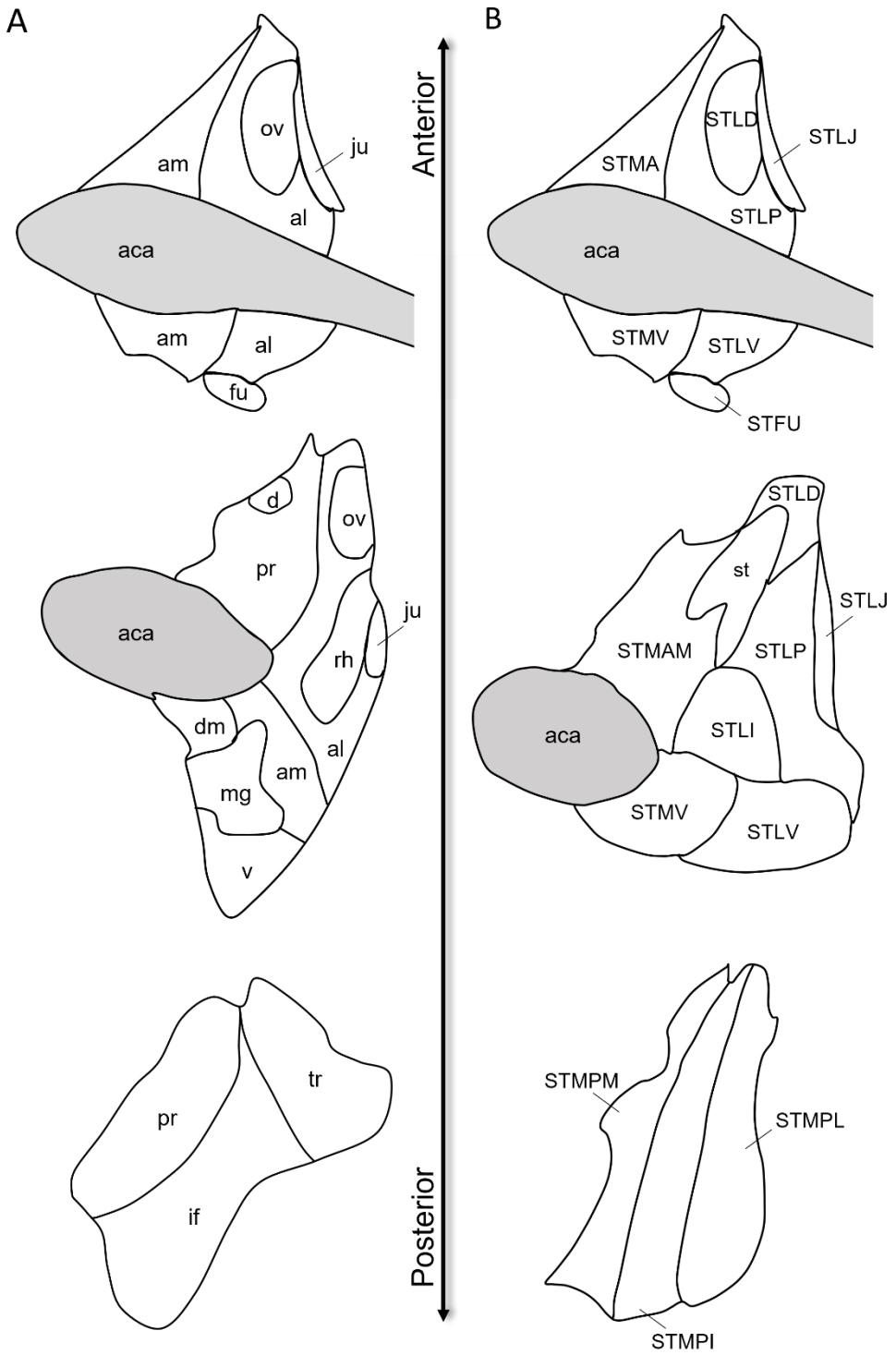

Figure 1.1 Nomenclature of subnuclei in the bed nucleus of the stria terminalis. In the rodent, the BNST is organised around the white matter of the anterior commissure (aca) along an anterior-posterior axis. Two classifications for naming the BNST subnuclei predominate. The first is based on cytoarchitecture (A; Ju & Swanson, 1989) and the second is based on relative location – lateral, medial, ventral, and intermediate - of the subnuclei (B; Franklin & Paxinos, 2007). Abbreviations: al, anterolateral; am, anteromedial; d, dorsal; dm, dorsomedial; fu, fusiform; if, interfascicular; ju, juxtacapsular; ov, oval; mg, magnocellular; pr, principal; rh, rhomboid; tr, transverse; v, ventral. st, stria terminalis; STFU, fusiform part; STLD, lateral division 2; STLI, lateral division; STLJ, lateral division juxtacapsular part; STLP, lateral division posterior part; STMA, anteromedial part; STMAM, medial division anteromedial part; STMV, medioventral part; STMPI, medial division posterior intermediate part; STMPL, medial division posterolateral part; STMPM, medial division posteromedial part.

1.2.2 Connectivity of the bed nucleus of the stria terminalis

In humans, three ipsilateral fibre pathways of the BNST have been described, using diffusion-weighted magnetic resonance imaging: the anterior bundle, the ventral bundle, and the posterior bundle (Kruger, et al., 2015). The ventral bundle connects the BNST to the hypothalamus and medial amygdala and the posterior bundle connects the BNST to the lateral amygdala. Both pathways match previously reported pathways found in rodents (Weller & Smith, 1982). However, the anterior bundle connects the BNST with the mPFC and orbitofrontal cortex through the nucleus accumbens and the head of the caudate body and has not been previously reported in rodents (Kruger, et al., 2015). Further structural and functional connections between the BNST and basal ganglia, including the caudate putamen and pallidum, and hippocampus have been identified, alongside a novel connection with the paracingulate gyrus, not previously reported in humans or rodents (Avery, et al., 2014).

In experiments involving rodents, the anterior BNST is broadly divided into three nodes, as constituent individual nuclei are small and therefore difficult to specifically target *in vivo.* These subdivisions are termed anterolateral, anteromedial and anteroventral (Figure 1.2A). Neurons within the three distinct regions can project to other neurons in the same region, neurons in a different BNST region, or more distant brain regions. Glutamate uncaging studies revealed that intraregional connections in the BNST are predominantly GABAergic, with more inhibitory post-synaptic potentials (IPSPs) elicited than excitatory post-synaptic potentials (EPSPs) (Turesson, et al., 2013). However, in the ventral part of the anteromedial BNST, and in the anteroventral region, a more even distribution of glutamatergic and GABAergic connections was identified.

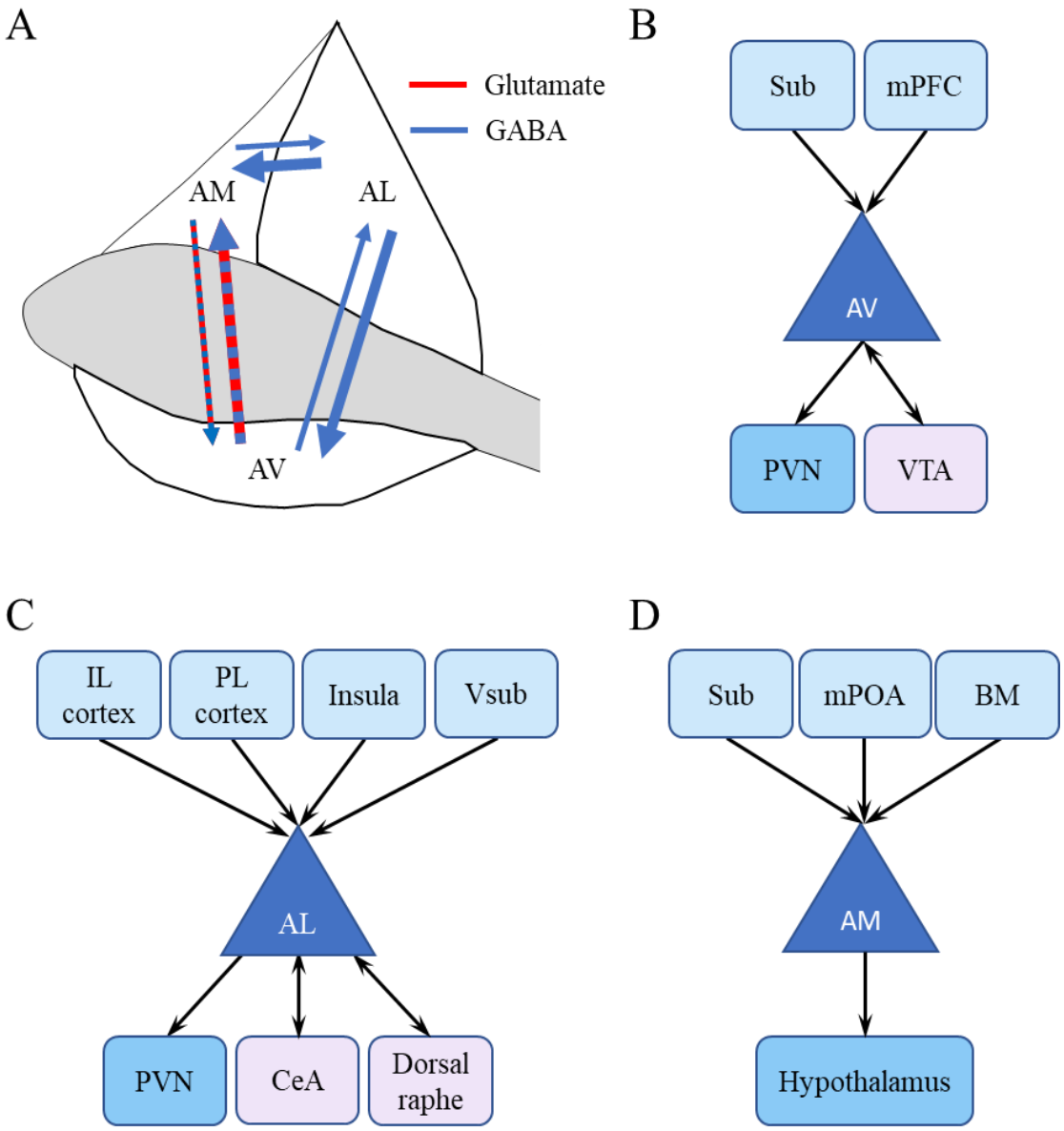

Figure 1.2 Connectivity of the rodent anterior bed nucleus of the stria terminalis. (A) The internal connections of the anterior BNST, split grossly into anterolateral (AL), anteromedial (AM) and anteroventral (AV) divisions. GABAergic projections predominate in the BNST, except between the AM and AV subdivisions, where a mixture of glutamatergic and GABAergic connections have been defined (Turesson, et al., 2013). The AL division reciprocally projects to both AM and AV regions, however the outward projections are far stronger than the incoming projections. (B) The AV subdivision of the BNST receives input from the subiculum and medial prefrontal cortex (mPFC), reciprocally connects with the ventral tegmental area (VTA) and projects to the PVN. (C) The AL division of the BNST receives input from the infralimbic (IL) prelimbic (PL) and insula cortices along with the ventral subiculum of the hippocampus (Vsub), reciprocally projects to the central amygdala (CeA) and dorsal raphe, and projects to the paraventricular nucleus of the hypothalamus (PVN). (D) The AM region of the BNST receives projections from the subiculum (Sub), medial preoptic area (mPOA) and the basomedial amygdala (BM) and projects to the hypothalamus.

Interregional connections within the BNST are highly diverse (Figure 1.2A). Whilst the anterolateral part is reciprocally connected to both the anteromedial part and anteroventral part, the outward projections are far stronger than the return projections, and all reciprocal projections are GABAergic (Turesson, et al., 2013). Conversely, the anteromedial part and anteroventral part are also reciprocally connected, but these connections may be glutamatergic or GABAergic and the anteromedial part projects more strongly to the anteroventral part than vice versa (Turesson, et al., 2013).

Considering the connections formed between the BNST and more distant brain regions, the three subdivisions send and receive projections from distinct brain regions. The anterolateral division receives projections from the infralimbic, prelimbic and insular cortices and the ventral subiculum of the hippocampus (Figure 1.2B) (McDonald, et al., 1999; Reynolds & Zahm, 2005; Li & Kirouac, 2008; Forray & Gysling, 2004). In turn, the anterolateral division reciprocally projects to the lateral part of the central amygdala and the dorsal raphe, and projects to the paraventricular nucleus of the hypothalamus (PVN) (Dong & Swanson, 2004; Sun, et al., 1991). The anteromedial division receives inputs from the subiculum, hypothalamic nuclei including the medial preoptic area and the basomedial amygdala (Figure 1.2C) (Dong & Swanson, 2006; Gomez & Newman, 1992; Cullinan, et al., 1993). In turn, the anteromedial BNST projects strongly to the hypothalamus, particularly the shell of the ventromedial hypothalamic nucleus (Dong & Swanson, 2006). The afferent projections of the anteroventral division of the BNST are largely from the subiculum and mPFC (Figure 1.2D) (Radley, et al., 2009; Radley & Sawchenko, 2011). Most of the BNST innervation of the PVN comes from the anteroventral division, and strong projections to the ventral tegmental area have also been documented (Sawchenko & Swanson, 1983; Moga & Saper, 1994; Georges & Aston-Jones, 2002; Sartor & Aston-Jones, 2013).

In addition to the three broad subdivisions of the anterior BNST, rodent studies have also singled out the oval nucleus, part of the anterolateral division, due to its distinct physiology and innervation compared to the rest of the region (Dong, et al., 2001a; Dabrowska, et al., 2016; Gungor & Pare, 2016). The oval nucleus receives no innervation from the basolateral amygdala, medial amygdala or subiculum but does receive projections from brainstem nuclei, the periaqueductal

gray and the insula (Dong, et al., 2001a; Cullinan, et al., 1993; McDonald, et al., 1999; Reynolds & Zahm, 2005; Saper & Loewy, 1980; Li, et al., 2016). GABAergic efferent projections from the oval nucleus project to the ventral tegmental area, central amygdala and lateral hypothalamus (Dong, et al., 2001a). Notably, the oval nucleus receives corticotropin releasing factor (CRF) inputs from the central amygdala, parabrachial nucleus, mPFC, and hippocampus (Crestani, et al., 2013). Furthermore, the oval nucleus contains a population of CRF containing cells which send CRF projections to the PVN, dorsal raphe and the ventral tegmental area, to a lesser extent, in both rats and mice (Dabrowska, et al., 2016). CRF is a critical regulator of the stress response, binding to CRFR1 receptors in the anterior pituitary gland following stressor exposure to initiate activation of the hypothalamic-pituitary-adrenal (HPA) axis (Chrousos & Gold, 1992). Though the oval nucleus produces its own CRF, it is currently unclear how these cells alter the activity of neurons within the BNST, and further afield, regarding the stress response and generation of anxiolytic/anxiogenic behaviours.

1.2.3 Regulation of the hypothalamic-pituitary-adrenal axis by the bed nucleus of the stria terminalis

The HPA axis is the homeostatic mechanism which drives the mammalian stress response, and that of other vertebrates. The HPA axis is a neuroendocrine pathway whereby corticotropin releasing hormone (CRH) and vasopressin, are released from the PVN (Figure 1.3). This subsequently stimulates release of adrenocorticotropic hormone (ACTH) in the pituitary gland which acts on the adrenal gland to produce cortisol. Cortisol then stimulates mobilisation of energy stores, maintenance of blood pressure and negatively feeds back to the PVN and pituitary gland to internally regulate the HPA axis (McEwen & Stellar, 1993; Herman, et al., 2003; Pecoraro, et al., 2005).

Limbic brain regions including the mPFC, amygdala and hippocampus are well documented to exert influence over the HPA axis (Figure 1.3). The mPFC and hippocampus predominantly repress HPA axis secretion, whereas activation of the amygdala stimulates glucocorticoid secretion (Feldman, et al., 1995; Jacobson & Sapolsky, 1991; Herman & Cullinan, 1997; Herman, et al., 2005).

Stressor exposure can cause alterations in the mPFC, hippocampus and amygdala which consequently affect HPA axis activity and are associated with the aetiology of stressor-related conditions including depression and anxiety-related disorders such as PTSD (McEwan, 1998; Choi, et al., 2007).

The afferent projections of the amygdala, hippocampus and mPFC largely terminate prior to the PVN, therefore these regions do not communicate directly with the PVN (Sawchenko & Swanson, 1983; Cullinan, et al., 1993). The BNST is well positioned to regulate the HPA axis as it receives direct projections from limbic brain regions, including the amygdala and hippocampus, and projects strongly to the PVN (Figure X; Sun, et al., 1991; Radley, et al., 2009; Radley & Sawchenko, 2011; Dong & Swanson, 2004; Moga & Saper, 1994).

Lesional studies have provided evidence to support different, and sometimes directly opposing, actions of the individual BNST subnuclei on the HPA axis (Dunn, 1987; Feldman, et al., 1990; Gray, et al., 1993). Lesioning of the lateral BNST inhibits amygdala and hippocampus driven neuroendocrine responses, particularly dampening the rise in plasma cortisol induced by amygdala stimulation and blunting the elevation of ACTH in the plasma following stimulation of the hippocampus (Feldman, et al., 1990; Zhu, et al., 2001). Basal levels of corticosterone and ACTH are unaffected by lesioning the anterior BNST, suggesting that HPA axis response to stress, and not basal tone of the HPA axis, is regulated by this group of subnuclei (Choi, et al., 2007). Reduced expression of corticotropin releasing hormone (CRH) mRNA was reported in the PVN following lesioning of the anterior BNST (Herman, et al., 1994) with a later study failing to replicate such difference (Choi, et al., 2007). Anterior BNST lesions reduced c-Fos mRNA in the PVN, suggesting reduced cellular activity of the PVN, but not PVN CRH mRNA (Choi, et al., 2007). Both studies reinforce the importance of the connection between the BNST and PVN in mediating the stress response (Herman, et al., 1994; Choi, et al., 2007). Lesions in the medial BNST, conversely, have no observed functional effect on stress responsiveness (Gray, et al., 1993). Electrical stimulation of the lateral BNST in rats results in reduced levels of corticosterone in the plasma. However, stimulation of the medial BNST increases plasma corticosterone (Dunn, 1987).

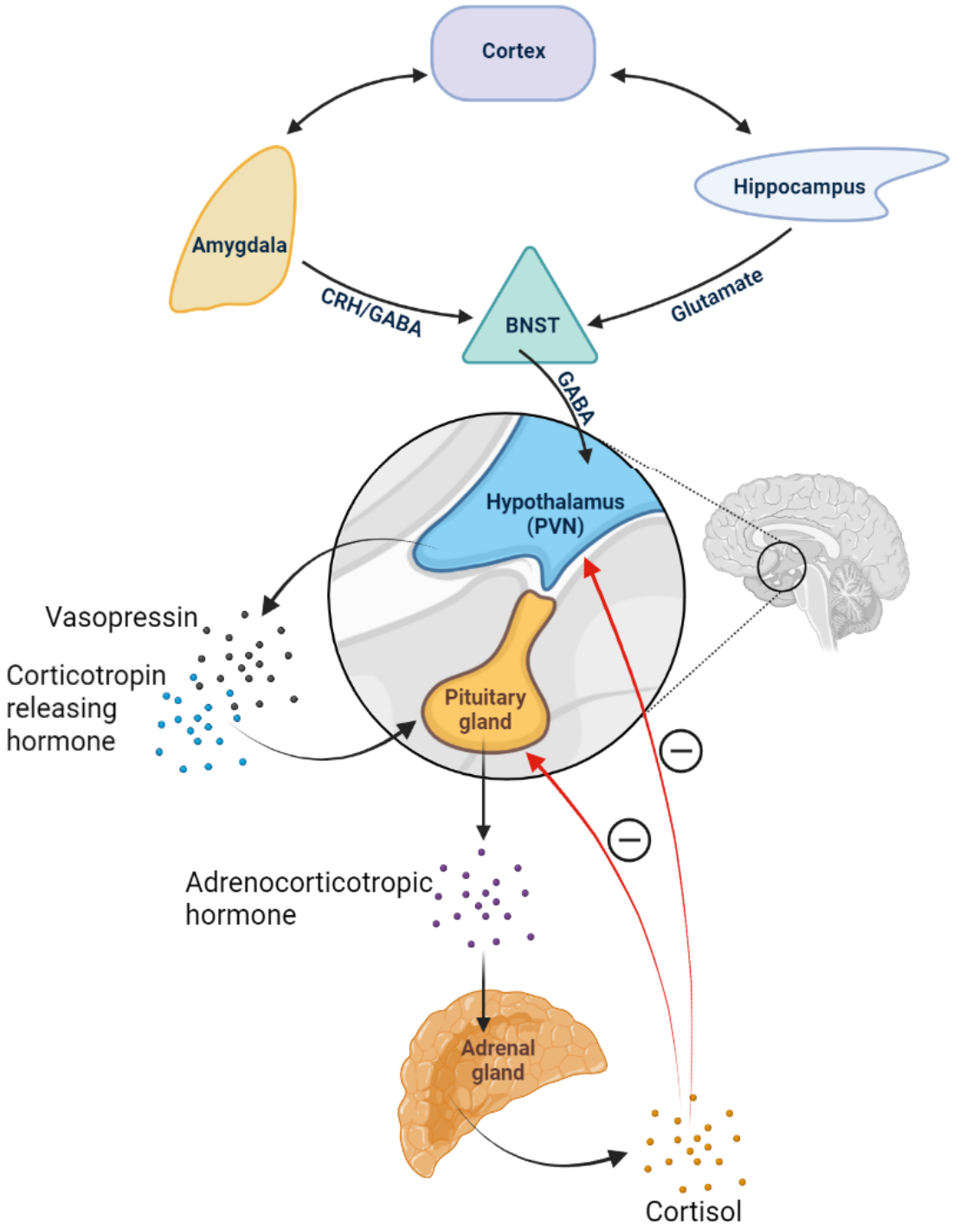

Figure 1.3. Schematic illustration of the regulation of the hypothalamic pituitary adrenal axis by the bed nucleus of the stria terminalis. Stress-inducing stimuli activate cortical neurons that send projections to the amygdala and hippocampus. Activated amygdala CRH and GABAergic neurons and hippocampal glutamatergic neurons signal to the BNST. BNST GABAergic neurons projecting to the paraventricular nucleus of the hypothalamus are then activated (there are projections existing in the brain, independently of stress stimuli – however, stress activates those neurons/projections). The hypothalamus produces vasopressin and corticotropin releasing factor, which stimulate release of adrenocorticotropin hormone from the pituitary gland. Adrenocorticotropin releasing hormone acts on the adrenal gland to release cortisol, which negatively feeds back to the pituitary gland and the hypothalamus. Adapted from Arnett et al. (2016), created with Biorender.

1.2.4 Role of the bed nucleus of the stria terminalis in the generation of anxiolytic and anxiogenic behaviours

Recruitment of the BNST is critical for the initiation of sustained anxiety responses. Specifically, excitatory signalling in the BNST has been shown to drive emotional behaviours, with interruption of intra- and inter-BNST signalling provoking increases or decreases in anxiety-like behaviours (Kim, et al., 2013; Jennings, et al., 2013; Glangetas, et al., 2017). Notably, as with its modulation of the HPA axis, activity of individual BNST subnuclei differentially influence features of the anxiety phenotype (Kim, et al., 2013; Jennings, et al., 2013; Giardino, et al., 2018; Yamauchi, et al., 2018; Xiao, et al., 2021). Optogenetic inhibition of the oval nucleus of the BNST produces anxiolytic behaviour in the elevated plus maze (EPM) and open field behavioural paradigms (Kim, et al., 2013). Conversely, stimulating the oval BNST results in enhanced behavioural and physiological measures of anxiety including increased respiratory rate. Furthermore, optogenetic inhibition of basolateral amygdala projections to the anterodorsal BNST increases anxiety-like behaviours in the behavioural paradigms and respiration rate, whereas stimulating these fibres reduces anxiety-like behaviours (Kim, et al., 2013). Altogether these data support an anxiogenic role for the oval BNST and an anxiolytic role for the anterodorsal BNST under basal conditions.

Activation of distinct BNST afferents results in diverse behavioural outcomes (Jennings, et al., 2013). Optogenetic activation of the glutamatergic BNST afferents projecting to the VTA produces an aversive, anxiogenic behavioural phenotype in mice. In contrast, activation of the GABAergic projections from the BNST to the VTA produces an anxiolytic phenotype. Notably, direct inhibition of GABAergic neurons in the VTA is sufficient to recapitulate the anxiolytic phenotype (Jennings, et al., 2013). Furthermore, direct optogenetic activation of the projections from the anterodorsal BNST to the lateral hypothalamus is also sufficient to diminish anxiety-like behaviour (Kim, et al., 2013). Conversely, in a more recent study, optogenetic activation of dorsolateral BNST afferents which project to the central amygdala was found to elicit anxiogenic behaviour in the EPM (Yamauchi, et al., 2018). Optogenetic and chemogenetic activation of two distinct groups of cells within the BNST, CRF-containing neurons in the anterolateral BNST and cholecystokinin-containing neurons in the anteromedial

BNST, both of which project to the lateral hypothalamus, elicit anxiogenic behaviour in both open field and EPM tests (Giardino, et al., 2018). In summary, the structure of the BNST is extremely diverse and complex, and various intra- and inter-BNST connections contribute to the expression of diverging behavioural states.

1.2.5 Bed nucleus of the stria terminalis plasticity: implications for anxiety

In the CNS, synaptic plasticity is characterised by activity-dependent modulation of both the strength of transmission and the structure of synapses (Citri & Malenka, 2008). Plasticity of neurons is necessary for them to meet the ever-changing requirements of the neuronal environment, in response to external stimuli and experience. Short-term plasticity refers to changes generally lasting from milliseconds to several minutes which are important in modulation of transient behavioural states, adaptation to short-term sensory inputs and in short-lasting memory. Conversely, long-term plasticity refers to more permanent changes which can persist for several hours, and frequently longer (Manilow & Malenka, 2002). Long-term potentiation and long-term depression are the two most studied forms of long-term plasticity, resulting in a permanent increase or decrease in the strength of transmission of a particular synapse. Activation of signalling cascades and changes in gene expression are required to facilitate such alterations (Bosiacki, et al., 2019).

Persistent alteration in neural network plasticity is one of the likely mechanisms underpinning pathophysiological anxiety (Vyas, et al., 2002; Mitra & Sapolsky, 2008; Maggio & Segal, 2011; Cook & Wellman, 2004; Radley, et al., 2004; Radley, et al., 2006; Pego, et al., 2008). Chronic results in shortening and debranching of apical dendrites, neuronal atrophy, and a reduction in hippocampal volume – processes, mediated by cellular and molecular events downstream from increased glucocorticoid secretion (Watanabe, et al., 1992; Magarinos & McEwen, 1995). BNST neurons have also been observed to undergo morphological and synaptic changes in response to stress-inducing stimuli, which may consequently facilitate generation of stress-induced anxiety-like behaviour (Conrad, et al., 2011; Vyas, et al., 2003; Glangetas, et al., 2013; Glangetas, et al., 2017; Pego, et al., 2008). Chronic restraint stress sufficient to

induce anxiety-like behaviour results in increased dendritic arborisation in the BNST (Vyas, et al., 2003). Chronic unpredictable stress-induced hyper-anxiety was correlated with increased BNST volume, as a result of dendritic remodelling (Pego, et al., 2008).

Stressors other than chronic restraint also affect neuronal plasticity in the BNST. The gestational stress of protein restriction *in utero*, which increases anxiety-like behaviour in offspring, relative to non-restricted controls, also influences structural plasticity in the BNST (Torres, et al., 2018). Protein-restricted rats showed diminished dendritic arborisation and reduced dendritic length in the BNST. Conversely, neurons in the oval nucleus of the BNST increase in length following chronic restraint in wild-type rats (Roman, et al., 2012). Decreased expression of the CRH1 receptor was also reported in rats which had undergone protein restriction *in utero* (Torres, et al., 2018). Moreover, expression of CRH mRNA in the BNST was reported to be increased following repeated corticosterone injection, prolonged social stress and repeated mild stressor exposure (Makino, et al., 1994; Choi, et al., 2006; Kim, et al., 2006).

Physiological correlates of BNST neuroplasticity may also be altered in response to prolonged or repeated stressor exposure. Following repeated exposure to morphine, excitatory post-synaptic currents are enhanced in BNST neurons projecting to the ventral tegmental area (Dumont, et al., 2008). In electrophysiological slice studies of mice chronically administered corticosterone, blunting of long-term potentiation (LTP), a form of long-term synaptic plasticity, was reported in the BNST (Conrad, et al., 2011). Furthermore, such LTP blunting is correlated with increased anxiety-like behaviour. Dampening of LTP in BNST slices from mice which had undergone acute social isolation was also reported. However, acute isolation had no significant influence on anxiety-like behaviour (Conrad, et al., 2011). The study by Conrad et al. (2011) suggests that physiological changes in BNST plasticity precede development of anxiety-like behaviour, irrespective of stressor type, and that a certain threshold of activity may be required to tip the balance of behaviour in favour of anxiogenesis.

More recently, a role for *N*-Methyl-D-Aspartate receptors (NMDAR) in the BNST has been uncovered with respect to BNST plasticity and generation of anxiety-like behaviours (Glangetas, et al., 2017; Salimando, et al., 2020; Ressler, et al., 2020). High frequency stimulation of the ventral subiculum/CA1 region of the

hippocampus triggers NMDAR dependent plasticity in the anteromedial BNST, a region known to receive projections from the ventral subiculum/CA1 (Glangetas, et al., 2017). Local infusion of D,L,2-amino-5-phosphonovalerate (AP5), an antagonist which inhibits the glutamate binding site of NMDARs, in the anteromedial BNST reverses the direction of the evoked plasticity to long-term depression (LTD), though the mechanism of reversal remains unclear. Furthermore, evoked LTP in the anteromedial BNST as a result of high frequency stimulation of the ventral subiculum/CA1 coincides with anxiolytic behavioural effects in both basal and anxiogenic situations, whereas inhibition of evoked LTP promotes anxiogenic behaviour (Glangetas, et al., 2017).

A further study using mice genetically deficient in the GluN2D NMDAR subunit revealed an increase in negative emotional behaviour in the OFT, elevated zero maze and forced swim test, though no behavioural differences were captured in the light/dark box (Salimando, et al., 2020). Enhanced activity of CRF-containing BNST neurons in the knockout mice accompanies observed anxiety- and depressive-like behavioural changes. Conversely, synaptic potentiation is blunted in the BNST of GluN2D-deficient mice following tetanic stimulation, in the early stages, suggesting a role for this NMDAR subtype in the induction of short-term plasticity in the BNST (Salimando, et al., 2020). NMDAR in the BNST have also been implicated in backwards/temporally randomised fear conditioning, where conditioned stimuli poorly predict the onset of an unconditioned stimulus e.g. a footshock (Ressler, et al., 2020). Specifically, freezing behaviour is reduced following intra-BNST infusion of AP5, suggesting that NMDAR plasticity in the BNST is critical for encoding these conditioned stimuli. Furthermore, spontaneous activity of BNST neurons is enhanced in the immediate period following early footshocks in conditioning trials, when they are still unexpected (Bjorni, et al., 2020).

Altogether, the data summarised here further support a role for the BNST in threat perception and the development of anxiety-like behaviours, with a likely reliance on plastic changes within the BNST to facilitate such development. While the exact mechanisms responsible for driving changes in anxiety-like behaviour are yet to be fully elucidated, various studies highlight the importance of LTP blunting in the BNST in the development of anxiogenic behaviours, and the emerging

importance of NMDAR-dependent plasticity (Glangetas, et al., 2017; Conrad, et al., 2011; Salimando, et al., 2020).

1.3 The extracellular matrix

The neuronal extracellular matrix (ECM) is the non-cellular component of the CNS which provides a three-dimensional network of biochemical and structural support for the neurons and glia which it surrounds (Dityatev & Schachner, 2003) . Increasingly, the ECM is referred to as the fourth element of a tetrapartite synapse, additionally consisting of pre- and post-synaptic terminals and glial cells (Dityatev, et al., 2007). Communication between neurons and their ECM is critical both in development and in adulthood, providing guidance cues for neuronal proliferation, differentiation, axonal pathfinding and synaptogenesis (Rozario & DeSimone, 2010). The ECM can largely be divided into three distinct types: the 'loose' ECM found throughout the body; membrane bound molecules on cells; and the more unique organisation of perineuronal nets (PNNs), generally associated with the parvalbumin positive subclass of inhibitory neurons (Sorg, et al., 2016). The focus of this section will be on perineuronal nets which are lattice like structures that wrap around individual neurons in the CNS.

1.3.1 Structure and composition of perineuronal nets

PNNs are specialised forms of extracellular matrix expressed within the CNS. They were first discovered by Camillo Golgi in 1893 (1893) and then described in detail by Spreafico *et al* (1999). PNNs are reticular structures which ensheath both cell bodies and proximal dendrites of subpopulations of neurons (Celio, et al., 1998). The characteristic net-like shape of PNNs is owed to the perisynaptic arrangement of astrocytic processes and multiple constituent components linked together (Figure 1.4). PNNs consist of a hyaluronan backbone synthesised by membrane bound hyaluronan synthase (HAS) enzymes (Figure 1.4). Hyaluronan is attached to chondroitin sulfate proteoglycans (CSPGs) via hyaluronan and proteoglycan link proteins (HAPLNs; Figure 1.4). Tenascin binds to multiple CSPGs and acts as a cross-linking molecule (Brauer, et al., 1982; Lafarga, et al., 1984; Carulli, et al., 2007; Galtrey & Fawcett, 2007; Kwok, et al., 2010; Figure 1.4). The constituent components of PNNs may be synthesised by neurons, glial cells or both. PNNs have therefore been referred to as a type of glial associated matrix (Bruckner, et al., 1993; Giamanco & Matthews, 2012).

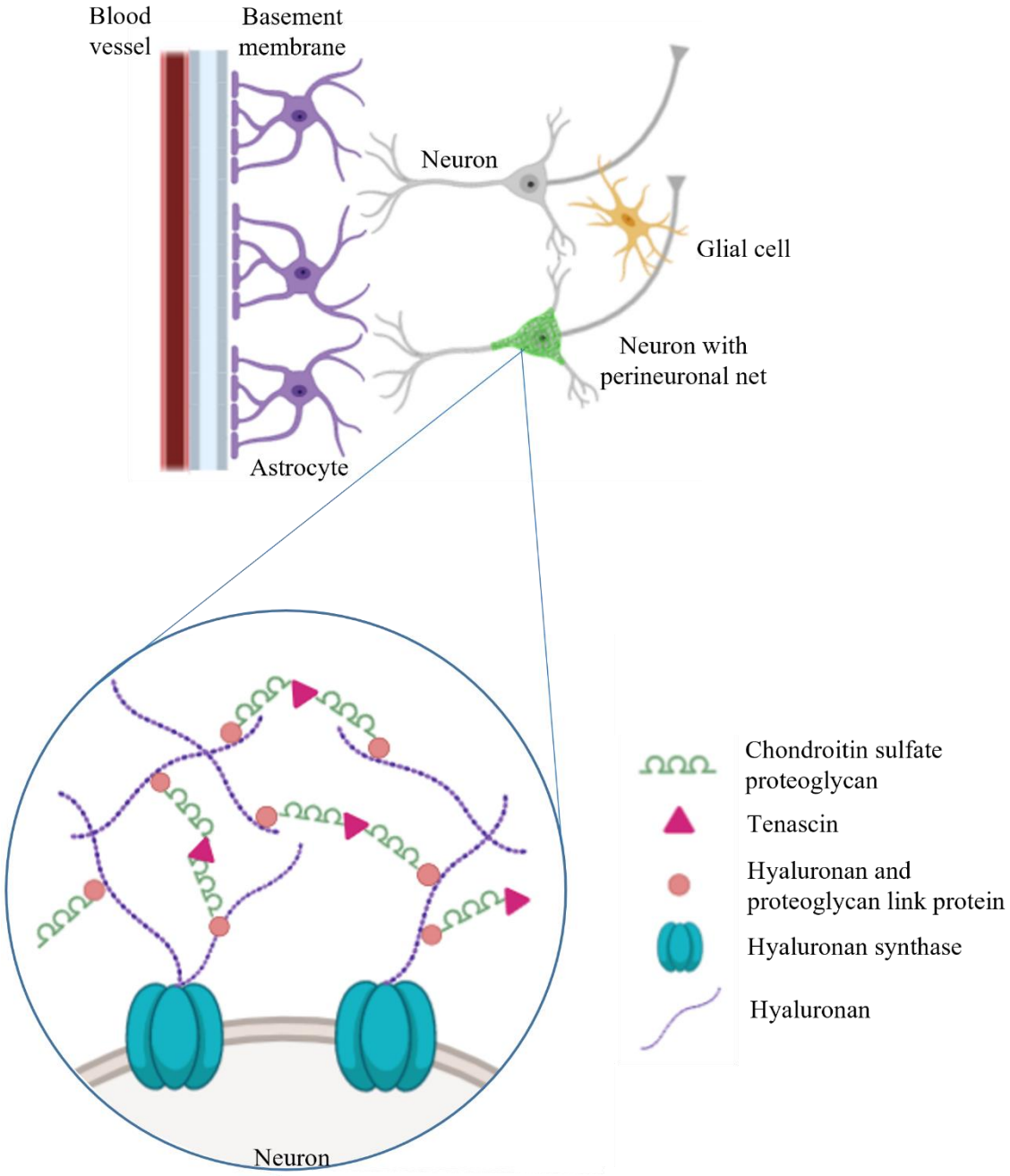

Figure 1.4 Schematic representation of the organisation of perineuronal net components. Perineuronal nets surround cell bodies and proximal dendrites of neurons. Both neurons and glial cells synthesise the constituents of perineuronal nets. The characteristic net-like shape is owed to the organisation of astrocytic processes and the way the individual components of perineuronal nets link together. The net is composed of a hyaluronan backbone, secreted by hyaluronan synthase enzymes bound to the plasma membrane. Hyaluronan is linked to chondroitin sulfate proteoglycans by link proteins, which stabilise this interaction. Tenascin then acts a cross-linking protein across multiple chondroitin sulfate proteoglycans. Adapted from Tsien (2013). Created with BioRender.com.

As PNNs consist of multiple constituent components, several methods have been employed to visualise them. The most common method is a lectin-based staining with *Wisteria floribunda* agglutinin (WFA) (Hartig, et al., 1992). WFA is a plant derived lectin which selectively labels the *N*-acetyl-galactosamine residues on CSPG molecules (Figure 1.5). Similarly, *Vicia villosa* agglutinin, another plant-based lectin, may be used to visualise PNNs (Nakagawa, et al., 1986). Both lectins may be conjugated to fluorescent molecules, such as fluorescein, for quick detection (Slaker, et al., 2016; Souter & Kwok, 2020). Antibodies against specific PNN components including hyaluronan, tenascin and CSPGs such as aggrecan may also be employed, to immunolabel PNNs (Matthews, et al., 2002; Dityatev, et al., 2007; Giamanco, et al., 2010). The use of these different methods has shown considerable heterogeneity among PNNs. Of note are the different glycosylation patterns of aggrecan which exist within distinct, but overlapping, populations of PNNs (Matthews, et al., 2002). Novel detection methods which further address PNN heterogeneity, would provide greater insight into the specificity of PNNs (Matthews, et al., 2002; Irvine & Kwok, 2018).

Hyaluronan and hyaluronan synthesizing enzymes

Hyaluronan is an unsulfated glycosaminoglycan (GAG) which forms the backbone of PNN structure. Hyaluronan is synthesised by a family of membrane-bound enzymes, hyaluronan synthases (HAS), of which there are three members (HAS1-3; Table 1.1). These enzymes have not been widely studied, however it has been determined that knockout of HAS2 is embryonic lethal and double knockout of HAS1 and HAS3 results in accelerated wound closure, suggesting an additional role in the inflammatory response (Camenisch, et al., 2000; Mack, et al., 2012).

Hyaluronan can bind other ECM molecules such as HAPLNs and CSPGs via its *N*-terminal hyaluronan binding domains (Fraser, et al., 1997). Hyaluronan is produced, both *in vivo* and *in vitro,* by astrocytes and neurons independently (Cargill, et al., 2012; Asher & Bignami, 1991; Bruckner, et al., 1993; Fowke, et al., 2017; Table 1.1). In cultured cortical neurons, in the absence of co-cultured astrocytes, 93% of neurons express hyaluronan, however only ~50% express a PNN (Fowke, et al., 2017). Hyaluronan is therefore also expressed outside the

specialised PNN organisation, and its expression is not a determinant of whether a neuron will form a PNN.

Hyaluronan is necessary for formation of PNNs in human embryonic kidney (HEK) cell culture (Kwok, et al., 2010). HEK cells do not form a pericellular matrix under regular culture conditions but do express most PNN components themselves. Upon expression of HAS3 in HEK cells, a layer of pericellular matrix forms around cells. The pericellular matrix is more diffuse than PNN matrix, but stains positively with WFA. Hyaluronan expression alone is not sufficient to trigger PNN-like matrix formation. However, co-expression of HAS3, a CSPG and a HAPLN, specifically aggrecan and HAPLN1 respectively, results in formation of a condensed, PNN-like matrix (Kwok, et al., 2010).

Hyaluronan can be degraded by the enzyme hyaluronidase, which leads to overall disruption of PNNs both *in vitro* and *in vivo.* The specificity of hyaluronidase as an enzyme to disrupt PNNs was demonstrated *ex vivo* by Deepa et al. (2006) in fresh, flash frozen slices. Similarly, *in vivo* infusions of hyaluronidase into the hippocampus and medial prefrontal cortex resulted in decomposition of PNNs, as determined by a significant reduction of WFA staining (Hylin, et al., 2013). PNN formation in cell culture, especially using non-neuronal cell lines, may not reflect morphology of PNNs *in vivo*. As PNN development is experience driven, neuronal activity is typically required for PNNs to develop *in vivo* (Dityatev, et al., 2007; Reimers, et al., 2007).

Table 1.1 Perineuronal net components

PNN component family	Members expressed in the CNS	Importance in perineuronal net structure	Reference
Hyaluronan	• Hyaluronan	• Backbone of PNN	Fraser et al, 1997
Hyaluronan synthesising enzymes	• HAS1 • HAS2 • HAS3	• Membrane bound • Secrete hyaluronan	Camenisch et al, 2000 Mack et al, 2012
Hyaluronan and proteoglycan link proteins	• HAPLN1 (Crtl1) • HAPLN2 (Bral1) • HAPLN4 (Bral2)	• Bind chondroitin sulphate proteoglycans • Stabilise interaction	Binette at al, 1994
Chondroitin sulphate proteoglycans	• Aggrecan • Brevican • Neurocan • Phosphacan • Versican	• Core protein attached to glycosaminoglycan chains • Principal perineuronal net constituent • Aggrecan is most critical	Galtrey & Fawcett, 2007 Sherman & Back, 2008
Tenascins	• Tenascin-C • Tenascin-R	• Cross-link across multiple chondroitin sulphate proteoglycans • Form ternary structure with hyaluronan	Anlar & Gunel-Ozcan, 2012 Weber at al, 1999

Hyaluronan and proteoglycan link proteins

HAPLNs are a small family of glycoproteins which can bind to CSPGs and hyaluronan to form ternary structures (Binette, et al., 1994). There are four known hyaluronan and proteoglycan link proteins, HAPLN1, 2, 3, and 4 (Table 1.1). Of these, HAPLN2 and 4 are specific to neural tissue. HAPLN2 and 4 upregulation in the adult rodent nervous system temporally coincides with the expression pattern of brevican, the most abundant CSPG (Hirakawa, et al., 2000; Bekku, et al., 2003).

HAPLN1 (also known as cartilage linking protein 1, Crtl1) stabilises hyaluronan-lectican aggregates and increases the affinity of lecticans for hyaluronan (Sim, et al., 2009). HAPLN1 upregulation also coincides with PNN formation, and, when co-expressed with HAS3 in HEK cells, is sufficient for PNN formation *in vitro* (Carulli, et al., 2010; Kwok, et al., 2010).

PNN expression is highly attenuated in a mouse conditional CNS HAPLN1 knockout (Carulli, et al., 2010; Table 1.2). WFA staining for PNNs in HAPLN1 knockout mice is sparse around cell somas and absent around dendrites. With the exception of neurocan, expression levels of CSPGs in the HAPLN1 knockout are equivalent to control mice. HAPLNs therefore have a critical role in bringing PNN components together by stabilising interactions between them, evidenced by more diffuse CSPG expression in the HAPLN1 knockout (Carulli, et al., 2010).

Table 1.2 Perineuronal net component knockout models

Component	Gene modified	WFA staining?	Effect on expression of other components	Reference
Brevican	Deletion of coding region by LacZ insertion into exon 2 of Bcan gene	+	↑ Neurocan	Brakebusch et al, 2002
Neurocan	LacZ and cre-lox directed inactivation of Ncan gene	+++	No change	Zhou et al, 2001
Versican	Knockout of Cspg2 gene	-	Die at birth, no PNN development	Mjaatvedt et al, 1998
Aggrecan	Cartilage matrix deficiency (Cmd) mice	-	Die at birth, no PNN development	Rittenhouse et al, 1978 Giamanco et al, 2010
	Heterozygous Cmd mice	+++	No change	Suttkus et al, 2014
	Conditional Cre-lox deletion of exon 4 of Acan gene	-	↓↓↓ Crtl1 ↓↓↓ Tenascin-R ↓↓↓ Versican ↓↓↓ Neurocan	Rowlands et al, 2018
Link protein	Disruption of exon 4 in the Crtl1 gene by pGK-neo^r-poly(A) cassette	+*	↓ Neurocan	Carulli et al, 2010
Tenascin	p5′PGKneo3′TK targeting of Tn-r gene	+*	↓↓ Hyaluronan ↓↓ Neurocan ↓↓ Phosphacan ↓ Brevican	Bruckner et al, 2000

* Indicates abnormal perineuronal nets which are granular and diffuse in appearance

Chondroitin sulfate proteoglycans

CSPGs are composed of a core protein with one or more covalently attached GAG chains. GAG chains contain repeating disaccharide units that consist of one glucuronic acid and one *N*-acetyl-galactosamine residue forming long, linear polysaccharides (Sherman & Back, 2008; Figure 1.5). *N*-acetyl-galactosamine residues can be sulfated by one of two sulfotransferase enzymes which generate either 4- or 6- sulfation patterns (Mikami & Kitagawa, 2013; Figure 1.5). The most widely studied family of CSPGs are the lecticans: aggrecan, brevican, neurocan and versican (Galtrey & Fawcett, 2007; Table 1.1). Lecticans are crucial components of PNN structure and contribute significantly to PNN function (Table 1.1).

The lecticans are each encoded by a single gene (aggrecan, *ACAN*; brevican *BCAN*; neurocan, *NCAN* and versican, *VCAN*) and share similar homology. All lecticans have a G1 domain at the N-terminus and a G3 domain at the C-terminus (Siebert, et al., 2014). Distinctively, aggrecan has an additional G2 domain near its G1 domain (Figure 1.5). The most notable difference between lecticans is the number of GAG chains attached to the core protein, with five or fewer found in brevican and neurocan and over 100 found in aggrecan. The sulfation pattern of these GAG chains mediates the functions of the CSPG. The *N*- terminal of CSPGs is highly similar in structure to HAPLNs, and the hyaluronan binding domains in both molecules are termed ‘link-protein modules’ (Sim, et al., 2009; Figure 1.5).

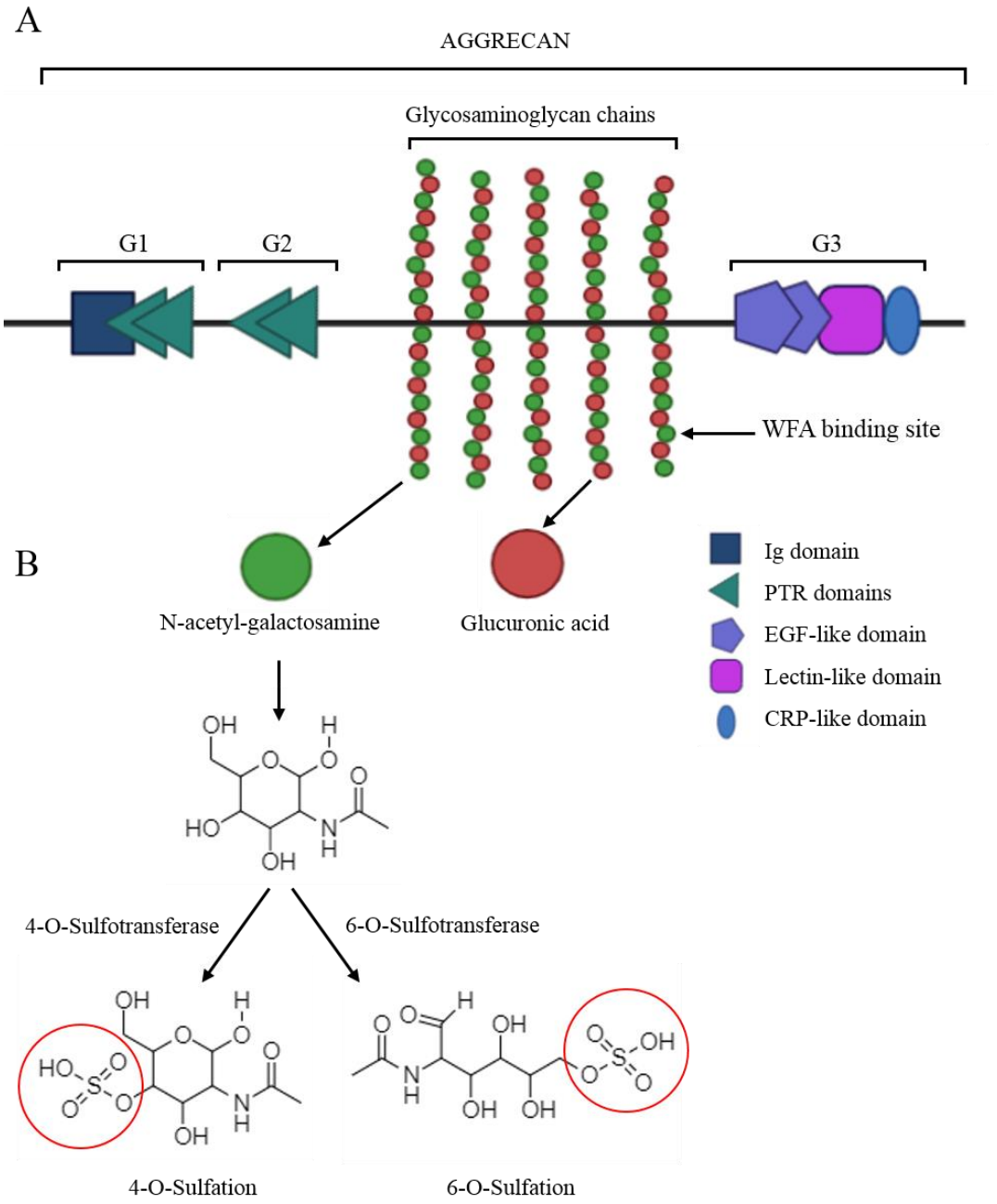

Figure 1.5 Chondroitin sulfate proteoglycan structure. A schematic representation of the structure of a chondroitin sulfate proteoglycan; aggrecan. (A) The N-terminal G1 domain is the binding site for hyaluronan and consists of immunoglobulin (Ig) and proteoglycan tandem repeats (PTR) domains. The G2 domain is the globular aggrecan domain. The glycosaminoglycan chains consist of repeating units of *N*-acetyl-galactosamine and glucuronic acid. WFA, a lectin-based stain used to visualise perineuronal nets binds to the *N*-acetyl-galactosamine residues within the glycosaminoglycan chains. The G3 domain consists of epidermal growth factor (EGF) like domains, a lectin-like domain and a complement regulatory protein (CRP) like domain. The G3 domain is where the chondroitin sulfate proteoglycan binds to tenascins. (B) *N*-acetyl-galactosamine may be sulfated by two sulfotransferase enzymes; 4-O-sulfotransferase or 6-O-sulfotransferase. Therefore, there can be different sulfation patterns of chondroitin sulfate proteoglycans. This, combined with variety of available core proteins and amount of covalently attached glycosaminoglycan chains, contributes to diversity among chondroitin sulfate proteoglycans. Adapted from Berretta et al. (2015) and Avram et al. (2014), created with BioRender.com. Structures drawn with ChemDraw software (CambridgeSoft, UK).

The contribution of individual CSPGs to PNN formation has been assessed using knockout and knockdown mouse models (Table 1.2). Mice deficient in brevican are still able to form PNNs, however they are less densely expressed than in wild-type controls (Brakebusch, et al., 2002). Neurocan is upregulated in brevican-deficient mice, possibly as a compensatory mechanism. Conversely, mice deficient in neurocan have unchanged levels of brevican, and tenascin-C, thus the compensation is not reciprocal (Zhou, et al., 2001). Neurocan knockout mice are able to form visually normal PNNs, therefore neurocan is less crucial to PNN structure. The contribution of versican to PNN formation and structure has not been investigated yet as knockout of *Cspg2*, the gene encoding versican, is embryonic lethal in mice due to heart defects and no knockdown model has been created to date (Mjaatvedt, et al., 1998; Table 1.2).

Aggrecan has been argued to be the most important CSPG in PNN structure and composition (Carulli, et al., 2007; Suttkus, et al., 2014; Rowlands, et al., 2018). Until recently, however, the contribution of aggrecan to PNN structure and formation was impossible to study using knockout models, as aggrecan knockout is embryonic lethal (Rittenhouse, et al., 1978; Table 1.2). The cartilage matrix deficiency (*cmd*) model produces a highly truncated form of aggrecan which is not processed in the endoplasmic reticulum or secreted (Watanabe, et al., 1994). Organotypic slices derived from the *cmd* model do not stain positively with WFA, demonstrating a crucial role for aggrecan in PNN formation (Giamanco, et al., 2010). Furthermore, conditional knockout of aggrecan, achieved by knocking out the Acan gene in a cre-lox dependent manner, is sufficient to prevent the expression of PNNs stained by WFA (Rowlands, et al., 2018). Tissue from the conditional knockout model also stains negatively for Crtl1, tenascin-R, versican and neurocan (Table 1.2). Thus, aggrecan expression is critical for promoting PNN assembly and for PNN maintenance. In the rat spinal cord aggrecan is present in all PNNs. Moreover, aggrecan mRNA is upregulated at the same time as PNN formation in the spinal cord begins. Aggrecan expression therefore may be a temporal trigger for PNN synthesis (Galtrey, et al., 2008; Table 1.2).

Whilst knockout models of various PNN components can be useful to study formation and maintenance, PNNs may be degraded entirely to investigate other aspects of their function. CSPGs, as the principal constituents of PNNs, are most commonly targeted to induce PNN degradation (Moon, et al., 2001; Massey, et

al., 2006; Sullivan, et al., 2018). The enzyme chondroitinase ABC (ChABC), derived from the bacteria *Proteus vulgaris*, cleaves the GAG chains of CSPG molecules (Moon, et al., 2001). *In vivo*, infusions of ChABC in the visual cortex, amygdala, or spinal cord result in significantly reduced WFA staining (Lensjo, et al., 2017b; Gogolla, et al., 2009; Massey, et al., 2006). Furthermore, ChABC treatment of organotypic slice cultures with ChABC results in a loss of WFA staining (Sullivan, et al., 2018).

Tenascins

Tenascins are a family of large fibrous glycoproteins of which there are four variants in vertebrates, -W, -C –X and –R (Table 1.1). Tenascin-R is exclusively found in the developing and adult nervous system and is a crucial PNN component (Anlar & Gunel-Ozcan, 2012). Tenascin-C expression is more ubiquitous, and is also expressed in the nervous system, however it is not incorporated into PNNs (Anlar & Gunel-Ozcan, 2012). Tenascin-R binds to lecticans, with highest affinity for brevican, and is expressed in perineuronal nets (Weber, et al., 1999).

In a tenascin-R deficient mouse model, PNNs show the same regional distribution and maturational time course as PNNs in wild-type control animals (Bruckner, et al., 2000; Table 1.2). However, PNNs in the tenascin-R deficient mouse, show far less intense labelling with WFA in various cortical regions and are more granular in appearance (Bruckner, et al., 2000). Hyaluronan, neurocan and phosphacan expression is greatly reduced in the tenascin-R knockout, in addition to brevican, to a lesser extent, which may explain the granular PNNs (Bruckner, et al., 2000). Furthermore, PNNs in organotypic slice cultures derived from tenascin-R knockout mice show similar deficits in structural appearance to those observed in the model *ex vivo* (Morawski, et al., 2014). When tenascin-R knockout slice cultures were co-cultured with organotypic slices from wild-type mice, which produce soluble factors including a tenascin-R isoform, the deficient PNNs could not be rescued (Morawski, et al., 2014). Therefore, endogenous tenascin-R is crucial for PNN formation and maintenance and cannot be supplemented. The critical contribution of tenascin-R to PNN formation and maintenance may lie in its function as a cross-linking molecule. Tenascin-R

stabilises the interaction between hyaluronan and CSPGs, including aggrecan (Galtrey, et al., 2008; v'ant Spijker & Kwok, 2017). In the absence of tenascin-R, the interaction between hyaluronan and CSPGs is weaker, therefore other PNN components are less likely to be recruited and organised into a mature PNN structure.

1.3.2 Perineuronal net functionality

PNNs have two major generalised functions throughout the CNS; they protect neurons from damage and restrict neuronal plasticity in adulthood. In restricting neuronal plasticity, PNNs may also exhibit functions specific to the brain region where they are expressed. Here I will discuss what is known about the protective effects of PNNs; the three ways in which they reduce neuronal plasticity; and how PNN expression manifests functionally in different brain regions.

1.3.2.1 Protective function of perineuronal nets

PNNs act as a protective barrier for the neurons they surround against oxidative stress caused by free radical production systems (Suttkus, et al., 2014). In the absence of PNNs, after ChABC treatment, parvalbumin (PV) neurons are more vulnerable to oxidative stress (Zhao & Fawcett, 2013; Cabungcal, et al., 2013). Furthermore, vulnerability to oxidative stress is dependent on PNN maturity, with more mature PNNs offering greater protection to the neurons they surround (Cabungcal, et al., 2013).

However, PNNs themselves are vulnerable to oxidative stress, therefore the extent of the protection they can offer neurons is a balance between the capacity of the net maintenance system and the damage to the system through oxidative stress (Zhao & Fawcett, 2013). In mice deficient in aggrecan, tenascin-R or HAPLN1, neurons are especially vulnerable to oxidative stress, compared to wild-type controls, as the PNN structure is mildly impaired (Cabungcal, et al., 2013). Tenascin-R deficient mice exhibit the greatest levels of damage from oxidative stress (Cabungcal, et al., 2013). PNNs in Tenascin-R mice show the most variance from wild-type PNN structure, in that they are more granular, less ‘net-like’, hence offering the least protection to the neurons they surround.

PNNs can also protect against other damaging species within the body, such as amyloid-β (Aβ), the main component of plaque aggregates seen in Alzheimer's disease pathology. Treatment of cortical neuronal cultures with Aβ1-42 induces significant neurotoxicity in neurons not ensheathed by PNNs. However, PNN-associated neurons are protected from such damage (Miyata, et al., 2007). After net degradation with ChABC, Aβ1-42 neurotoxic damage is comparable to that observed in PNN-free neurons (Miyata, et al., 2007).

PNNs do not protect against damage induced by increasing concentrations of glutamate, with wild-type cultures exhibiting similar levels of neurotoxicity to ChABC treated cultures (Miyata, et al., 2007). Thus, PNNs may regulate the excitability of the cells they surround in order to additionally protect themselves from glutamate induced excitotoxicity.

1.3.2.2 Role of perineuronal nets in the control of synaptic plasticity

Experience driven alterations of synaptic strength are critical for both sensory development and learning and memory (Hebb, 1949; Bliss & Collingridge, 1993; Griffiths, et al., 2008). PNNs are highly dynamic and turn over through the lifespan of the neuron, allowing them to have some degree of control over synaptic plasticity. There are at least three known mechanisms through which PNNs have been shown to limit synaptic plasticity in neurons; (1) acting as a physical barrier to limit formation of new synaptic connections (2) inhibiting lateral mobility of α-amino-3-hydroxy-5-methyl-4-isoxazolepropionic acid (AMPA) type glutamate receptors at the synapse and (3) acting as a scaffold for inhibitory molecules of synapse formation (Figure 1.6; Wang & Fawcett, 2012).

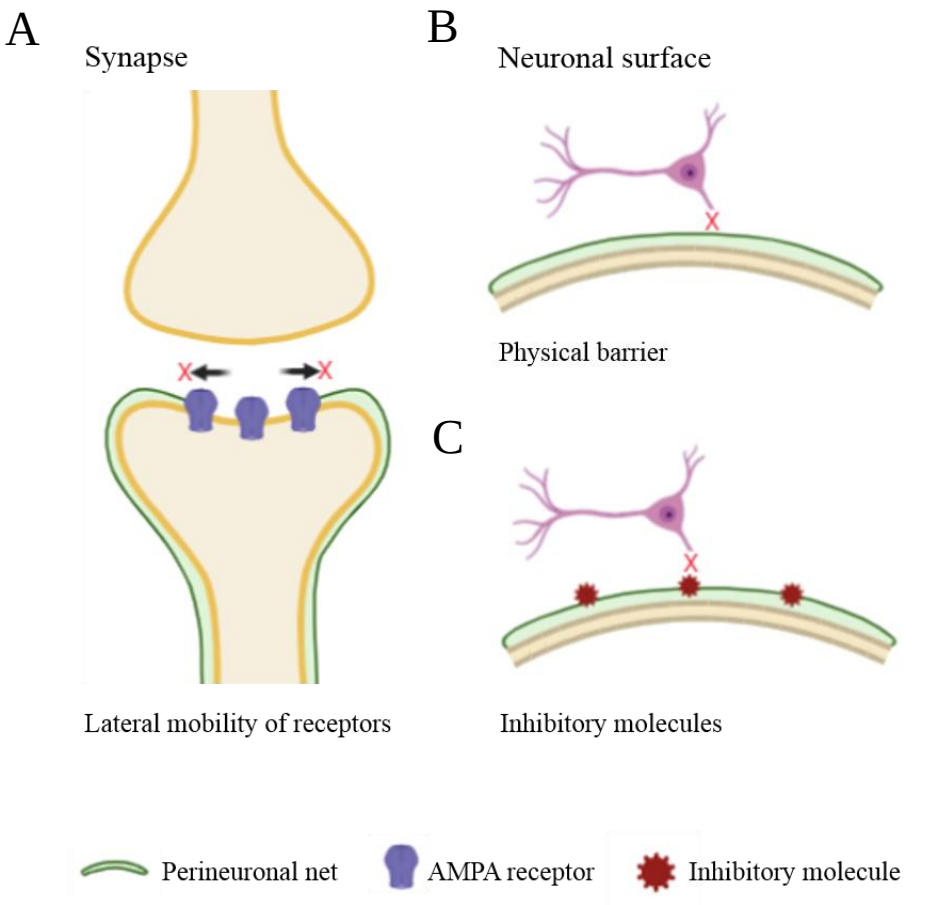

Figure 1.6 Schematic representation of perineuronal net function in the central nervous system. Perineuronal nets are critical modulators of synaptic plasticity, that is, changes in synapse structure and strength of synaptic transmission. Their functions relevant to plasticity can be broadly divided into three: (A) inhibiting lateral diffusion of α-amino-3-hydroxy-5-methyl-4-isoxazolepropionic acid (AMPA) type glutamate receptors at the synapse; (B) forming a physical barrier around neurons to limit formation of new synaptic connections and (C) acting as a scaffold for inhibitory molecules of synapse formation. Adapted from v'ant Spijker and Kwok (2017), created with BioRender.com.

Perineuronal nets as a physical neuronal barrier

PNNs ensheath neurons and proximal dendrites, creating a physical barrier between the neuron and the extracellular space (Figure 1.6). Acting as a physical barrier, PNNs reduce anatomical plasticity, that is the ability of a particular neuron to form new physical connections with other surrounding neurons. CSPGs within PNN structures are strong inhibitory molecules which inhibit axon growth *in vitro* (McKeon, et al., 1991; Smith-Thomas, et al., 1994). Furthermore, *in vivo*, axonal regeneration is terminated upon reaching CSPG rich regions (Davies, et al., 1999). CSPGs collapse growth cones and inhibit neural regeneration, thus inhibiting neuronal plasticity (Cheah, et al., 2016).

The physical presence of PNNs restricts neuronal outgrowth, in turn, reducing formation of new synapses. ChABC mediated degradation of PNNs in the rat cuneate nucleus partially denervates forepaw dorsal column axons and promotes sprouting of primary afferents from the spared forepaw (Massey, et al., 2006). PNN degradation by ChABC injection directly into the spinal canal promotes axonal regeneration after chronic spinal cord injury (Shinozaki, et al., 2016). Furthermore, degradation of PNNs in the cerebellum results in increased sprouting of Purkinje neurites (Corvetti & Rossi, 2005).

The physical barrier created by PNNs also supports neuronal function by acting as a buffering reservoir for cations close to the synapse (Hartig, et al., 1999). Ion buffering is facilitated by the large negative charge on both hyaluronan and CSPG molecules. As PNNs predominantly surround fast-spiking interneurons, which exhibit high synaptic activity, such a buffer is necessary for neurotransmission (v'ant Spijker & Kwok, 2017). PNNs have a fixed structure with a high local charge density which allows them to both sort ions and act as an ion exchanger, in addition to hindering free diffusion of ions through the extracellular space (Morawski, et al., 2015).

Perineuronal nets as inhibitors of lateral receptor movement

PNNs can restrict synaptic plasticity by limiting the lateral mobility of α-amino-3-hydroxy-5-methyl-4-isoxazolepropionic acid (AMPA) receptors at the synapse (Frischknecht, et al., 2009; Figure 1.6). Most fast excitatory synaptic transmission in the CNS is dependent on AMPA receptors and as such, modulation of AMPA receptors underlies transmission plasticity (Lee, et al., 2000). Disruption of PNNs with hyaluronidase *in vitro* allows AMPA receptors to diffuse over longer distances compared to when the ECM is intact (Frischknecht, et al., 2009). PNNs form a passive diffusion barrier to control the exchange of AMPA receptors from the extrasynaptic space to the synapse. However, they do not influence intrasynaptic mobility (Frischknecht, et al., 2009). During high frequency firing, therefore, PNNs permit synaptic desensitisation by hindering exchange of desensitised receptors (Frischknecht, et al., 2009; Frischknecht & Gundelfinger, 2012; Heine, et al., 2008). Degradation of PNNs with ChABC enhances neuronal excitability *ex vivo* (Dityatev, et al., 2007). *In vivo* brevican and GluR1, the most

extensively studied AMPA receptor subunit, form a complex which is implicated in spatial memory retrieval (Saroja, et al., 2014). Further investigation of the interaction between GluR1 and brevican may provide additional mechanistic insight into how PNNs specifically impede, or perhaps modulate, lateral diffusion of receptors.

Perineuronal nets as a scaffold for molecular interaction

PNNs provide an interface between neurons and the extracellular space (Figure 1.6). PNNs, specifically the chondroitin sulfate molecules within the structure, can bind molecules which influence neuronal development and synaptic plasticity (Djerbal, et al., 2017). A key class of molecules that can bind to PNNs are semaphorins, which are important in development of the nervous system, though semaphorin expression also extends into adulthood (Giger, et al., 1998). Semaphorins are important for maintenance of pre-existing synaptic connections and regulation of newly developing ones. Initially thought to be chemorepulsive guidance molecules, semaphorins can also be chemoattractants (Polleux, et al., 2000; Dick, et al., 2013). Semaphorins therefore guide development of nerve projections and contribute to new synapse formation. Semaphorin-3A is the most widely studied semaphorin and binds to the GAG chondroitin-4,6-sulfate, highly enriched in PNNs. Local injection of ChABC into the rat cerebral cortex results in a lack of semaphorin-3A on the neuronal surface (Vo, et al., 2013). Semaphorin-3A expression is significantly reduced on attenuated PNNs in mice lacking HAPLN1 (Vo, et al., 2013). Notably, HAPLN1-deficient mice also exhibit persistent plasticity into adulthood (Carulli, et al., 2010). PNNs present semaphorin-3A to axons approaching the neuron they surround, to repulse them, thus influencing structural synaptic plasticity (de Winter, et al., 2016).

PNNs also control synaptogenesis by modulating integrin signalling. Neurons and astrocytes mediate excitatory synaptogenesis through activation of integrin receptors leading to protein kinase C activation and facilitation of synapse formation (Hama, et al., 2004; Kyung Park & Goda, 2016). CSPGs in PNNs block integrin activation and signalling to other molecules, inhibiting excitatory synaptogenesis. ChABC degradation of PNNs in organotypic hippocampal

cultures restores integrin activity and leads to a persistent and significant increase in spine motility (Orlando, et al., 2012).

1.3.2.3 Region-specific perineuronal net functionality

PNNs are critical for maintaining low levels of synaptic plasticity into adulthood. Enzymatic degradation of PNNs, however, can reopen the window of high, experience driven plasticity known as the critical period. Specifically targeting degradation of PNNs to singular brain regions facilitates the study of functional changes that occur in the absence of PNNs (Pizzorusso, et al., 2002; Gogolla, et al., 2009; Lensjo, et al., 2017b).

Synaptic plasticity has long been associated with the encoding, storage, and retrieval of memories (Hebb, 1949; Kandel & Schwartz, 1982; Martin, et al., 2000). As PNNs have a crucial role in the control of synaptic plasticity, they have subsequently been implicated in various types of memory (Gogolla, et al., 2009; Hylin, et al., 2013; Banerjee, et al., 2017). Fear conditioning and other associated paradigms have long been used to study emotional memory in rodents, and more recently have been employed to elucidate the role of PNNs in memory formation and maintenance (Davis, 1992; Myers & Davis, 2007; Gogolla, et al., 2009).

Fear memories can be extinguished by repeated exposure to the conditioned stimulus alone (Myers & Davis, 2007). However, in adulthood, fear response can recover after a context shift, referred to as renewal, or spontaneously after re-exposure to the unconditioned stimulus, referred to as reinstatement (Bouton, et al., 2006). Conversely, in development, fear conditioned memories can seemingly be unlearned by the process of extinction; rats younger than three weeks do not exhibit context-dependent renewal or reinstatement after previous fear conditioning (Kim & Richardson, 2007a; Kim & Richardson, 2007b). The development of PNNs in the rat basolateral amygdala coincides with the reported switch in fear memory resilience (Gogolla, et al., 2009). Degradation of PNNs in the basolateral amygdala of adult rats reverts synaptic plasticity to a juvenile-like state, preventing both spontaneous reinstatement and context-dependent renewal of the fear response (Gogolla, et al., 2009). The effects of PNN degradation in the basolateral amygdala are specifically anterograde in nature, meaning that fear memories acquired prior to removal of basolateral amygdala

PNNs are unaltered. Therefore, memories formed in the absence or presence of PNNs are likely to be formed through physiologically different mechanisms and rely on distinct neural correlates, though these are yet to be elucidated. By extension, memories formed in developing juveniles are likely to be physiologically different to those formed in adults, following critical period closure.

PNNs in other limbic brain regions, including the hippocampus, a brain region heavily implicated in determining memory context, and the mPFC, a brain region critical for the formation of extinction memories, are also involved in the expression of fear memory (Hylin, et al., 2013). Degradation of PNNs with hyaluronidase or ChABC in the adult rat hippocampus, prior to fear conditioning, results in an impairment of contextual, but not cue-induced fear memory expression (Hylin, et al., 2013). Furthermore, in a trace fear conditioning paradigm where a trace period with no stimulus presentation follows paired conditioned and unconditioned stimulus presentation, rats with disrupted hippocampal PNNs show disrupted long-term fear memory (Hylin, et al., 2013). Rats with degraded PNNs exhibited significantly less freezing behaviour following presentation of the conditioned stimulus and in the trace period. Infusion of PNN degrading enzymes into the mPFC of adult rats caused them to acquire conditioned stimulus elicited fear more slowly than vehicle treated controls (Hylin, et al., 2013). Moreover, rats with disrupted PNNs in the mPFC showed impaired cue-induced fear expression, but not contextual fear expression, when presented with conditioned stimulus. Freezing behaviour was additionally reduced in the trace period (Hylin, et al., 2013).

PNNs expressed in sensory brain regions are also implicated in the expression of fear conditioned behaviour (Banerjee, et al., 2017; Thompson, et al., 2017). PNNs in the auditory cortex of adult mice are necessary for acoustically elicited conditioned fear learning (Banerjee, et al., 2017). Disruption of PNNs with ChABC in the auditory cortex prior to fear conditioning results in lower levels of freezing behaviour following presentation of the conditioned stimulus, compared to vehicle injected control animals, both 24 and 48 hours after initial training (Banerjee, et al., 2017). However, three months after PNN degradation, when PNNs are expected to be re-aggregated, no difference is observed between ChABC and vehicle injected mice when fear conditioned to a novel tone. Disruption of PNNs immediately after initial training, in the memory acquisition phase, does not affect

short-term memory; no differences were observed between ChABC and vehicle injected mice when tested 30 minutes after PNN disruption (Banerjee, et al., 2017). However, fear memory expression was reduced in ChABC-treated mice compared to controls both 24 and 48 hours after initial training, suggesting that PNNs in the auditory cortex are selectively important for long-term memory, specifically for the consolidation of acoustic memories.

PNNs in the secondary visual cortex have also been implicated in the recall of remote fear memories. ChABC mediated PNN digestion in the secondary visual cortex after training, but one week before testing, results in disruption of remote visual fear memory, but not contextual memory, recall (Thompson, et al., 2017). Moreover, degradation of PNNs one day after training does not affect remote fear memory, further implicating PNNs in longer term changes in sensory cortices.

PNNs are also involved in non-fear related memories. (Romberg, et al., 2013; Yang, et al., 2015; Saroja, et al., 2014). In a Cartilage Linking Protein 1 gene (*CRTL1*) knockout mouse model, where PNNs are highly attenuated globally due to lack of cartilage link protein, mice show enhanced novel object memory compared to wild-type controls (Romberg, et al., 2013). Furthermore, local degradation of PNNs specifically in the perirhinal cortex of wild-type mice similarly produces enhanced novel object recognition (Romberg, et al., 2013). Enhanced recognition in both the Crtl1 knockout model and locally injected animals is robust and long-term. All experimental groups recognise the novel object as familiar up to 48 hours after initial testing, compared to the control groups which show no memory of the familiar object by 24 hours. The enhanced recognition in ChABC-treated mice declines in the weeks following PNN degradation and follows the time course of PNN regeneration. Recognition comparable to control mice is observed ~6-8 weeks after ChABC treatment (Romberg, et al., 2013). As novel object recognition requires long-term depression in the perirhinal cortex (Brown, et al., 1987; Griffiths, et al., 2008), it is likely that the mechanism of enhanced recognition in ChABC treated mice is as a result of facilitated long-term depression in the region (Romberg, et al., 2013).

The implications of PNN digestion have also been studied in neurodegenerative disease models. Both transgenic mice expressing mutated human tau protein and mice with adenovirally mediated local expression of mutated, P301S, human tau in the perirhinal cortex, show progressive deficits in synaptic transmission and

object recognition memory (Allen, et al., 2002; Delobel, et al., 2008; Yang, et al., 2015). PNN degradation in the perirhinal cortex in both animal models restores object recognition memory to a level indistinguishable from wild-type controls (Yang, et al., 2015). However, enhanced object recognition memory is not maintained 5 weeks after ChABC treatment.

PNNs contribute to diverse forms of learning and memory and exert their effects in a largely region-specific manner. Local disruption of PNNs, therefore, can provide a wealth of information about the specific roles of brain regions where they are expressed. Altogether, PNNs may exert their effects on memory by stabilising the neural network of the memory network, or engram. It has been proposed that long term memories may, in some way, be encoded in the pattern of the holes in PNNs (Tsien, 2013). While an interesting conceptual theory, no empirical evidence has emerged thus far to support or oppose the hypothesis.

I hypothesise that PNNs are differently expressed throughout various anatomical parts of the BNST throughout development and are essential for maintaining normal synaptic transmission and emotional response following stress.

The overall aims of the thesis are to:
(1) determine the spatiotemporal development of PNNs in the BNST

(2) examine the composition of BNST PNNs and identify PNN expressing neuronal populations in the BNST

(3) identify the effects of restraint stress on PNN expression and morphology and neuronal activity in the BNST

(4) investigate the impact of PNN digestion in the BNST on anxiety-like behaviour and underlying neuronal activity.

Altogether, the results presented in this thesis lay the groundwork for future research on PNNs in the BNST and how they might contribute to stressor-related disorders. Enhanced knowledge of the underlying physiological and behavioural changes which accompany development of stressor-related disorders will help to inform the development of more successful treatments in the future.

Chapter 2 – Spatiotemporal distribution and composition of perineuronal nets in the bed nucleus of the stria terminalis

2.1 Introduction

Perineuronal net development

PNNs in different brain regions form at different rates during development. Overall, development of PNNs in most rodent brain regions begins between postnatal day (P) 14 and P21 (Table 2.1). PNN maturity, where PNNs reach their highest levels of expression and exhibit mature morphology, is largely reached by early adulthood, throughout the brain, in both rodents and humans (Bruckner, et al., 2000; Bruckner & Grosche, 2001; Pizzorusso, et al., 2002; Rogers, et al., 2019); Table 2.1).

Formation of PNNs coincides with 'critical period' closure in various brain regions. The critical period occurs in early neuronal development and signifies a time where synaptic plasticity is especially sensitive to experience and environmental influence (Sengpiel, 2007; Nabel & Morishita, 2013). When PNNs are expressed at the end of the critical period, synaptic plasticity is vastly reduced and switches from a juvenile phenotype to an adult phenotype (Happel & Frischknecht, 2016). Functional changes can occur as a result of this switch. For example, in the medial entorhinal cortex, maturation of PNNs coincides with the formation of the grid cell pattern, whereas in the amygdala PNN maturity coincides with a switch in fear memory resilience (Lensjo, et al., 2017a; Gogolla, et al., 2009).

Many studies have addressed some aspects of PNN development in distinct brain regions. However, not all studies have characterised the full developmental profile of PNNs. From the studies that have been conducted thus far in rodents, PNNs first develop in the brainstem at P4 and spinal cord at P7 (Bruckner, et al., 2000; Galtrey, et al., 2008; Table 2.1). PNNs are detected in the medial entorhinal cortex at P12 and hippocampus, globus pallidus and somatosensory cortex at P14 (Lensjo, et al., 2017a; Yamada & Jinno, 2013; Bruckner, et al., 1993). At P16, PNNs begin to develop in the amygdala (Gogolla, et al., 2009). PNN formation starts around P21 in the visual and auditory cortices and hypothalamic arcuate nucleus and in the piriform cortex around P28 (Bruckner, et al., 2000; Wen, et al., 2018; Mirzadeh, et al., 2019; Ueno, et al., 2019; Table 2.1). PNNs are mature in all examined regions of the rodent brain by P80 (Table 2.1).

In humans, less is known about PNN development. Post-mortem labelling of human brain tissue has provided a small amount of developmental data (Rogers, et al., 2019). In the human medial prefrontal cortex and hippocampus PNNs begin to develop at 54 days and 2 years, respectively (Rogers, et al., 2019; Table 2.1). PNNs in these two regions reach maturity by approximately 14 years of age. It is important to consider, however, that generally only one healthy control subject for each developmental stage was available for the study, and three different tissue preparation methods were employed between subjects: fresh frozen, PFA fixed and frozen-fixed.

Development of PNNs is promoted by neural activity *in vitro* (Bruckner & Grosche, 2001; Dityatev, et al., 2007). Furthermore, development of PNNs is delayed by lack of stimulation/neural activity *in vivo* across multiple species (Pizzorusso, et al., 2002; Balmer, et al., 2009). Depriving developing zebra finches, a species of songbird, of a song tutor delays development of PNNs in the song nucleus HVC (abbreviation is actual name) and, in turn, delays developmental song learning (Balmer, et al., 2009). PNN expression is also reduced in the visual cortex of dark reared animals, prolonging the critical period (Pizzorusso, et al., 2002). During dark rearing, neurocan does not condense into PNN structures. However, after a week of normal visual experience under a natural light/dark cycle following dark rearing, neurocan levels in PNNs are equivalent to those in non-dark reared animals. Environmental enrichment can prevent the effects of dark rearing on PNNs in the visual cortex and even leads to early critical period closure (Bartoletti, et al., 2004; Baroncelli, et al., 2016). Furthermore, animals raised in an enriched environment under a natural light/dark cycle express greater numbers of PNNs in the hippocampus CA2 region, but fewer PNNs in the cerebellum (Carstens, et al., 2016; Foscarin, et al., 2011).

Reduction or a delay in PNN formation is not a consequence of all adverse environmental experiences, however. For example, mice that are maternally separated and weaned earlier following birth, as a model of early life stress, express more intense PNNs around PV-positive interneurons in the ventral dentate gyrus, but not the CA1 region of the hippocampus (Murthy, et al., 2019). Male rats exposed to a scarcity/adversity model of early life stress exhibit greater numbers of PNNs specifically in the right amygdala, however the same increase was not observed in females (Guadango, et al., 2020). In summary, these data

suggest that environmental experiences may affect PNNs in different ways, in different brain regions, through development, depending on a variety of factors including type of stimulus, or lack thereof, and even sex of the studied animal.

Table 2.1 Perineuronal net development through the central nervous system

Brain Region	Species	Perineuronal nets first detected	Perineuronal net maturity	Reference
Hypothalamic arcuate nucleus	Mice (C57BL/6)	P21	P30	Mirzadeh et al. 2019
Somatosensory cortex	Mice (C57BL/6N)	P14	P77	Bruckner et al. 2000
Piriform cortex	Mice (C57BL/6N)	P28	P77	Ueno et al. 2019
Visual cortex	Mice (C57BL/6)	P22	P70	Bruckner et al. 2000
	Rats (Long Evans)	P21	P63	Liu et al. 2013
Primary auditory cortex	Mice (C57BL/6)	P21	P60*	Wen et al. 2018
Globus pallidus	Mice (C57BL/6)	P14	NA	Bruckner et al. 2000
Brainstem	Mice (C57BL/6)	P4	NA	Bruckner et al. 2000
Amygdala	Mice (C57BL/6J)	P16	P45*	Gogolla et al. 2009
Medial entorhinal cortex	Rats (Long Evans)	P12	P30	Lensjø et al. 2017a
Hippocampus	Mice (C57BL/6N)	P14	P60*	Yamada and Jinno. 2013
Hippocampus	Human	2 years•	14 years•	Rogers et al. 2019
Medial prefrontal cortex	Human	54 days•	14 years•	Rogers et.al 2019
Spinal cord	Rat (Sprague-Dawley)	P7	P21	Geltrey et al. 2008

* Indicates the last time-point of investigation in the study. • indicates availability of only a single data point for each age

Differences in regional and neuronal specificity of perineuronal nets

PNNs are typically highly expressed in sensory and motor brain regions including both sensory and motor cortices and basal ganglia structures (Bruckner, et al., 1999; Bruckner, et al., 2000; Adams, et al., 2001). In these brain regions PNNs are predominantly expressed around fast-spiking PV-positive interneurons. More recently, interest has been drawn to PNNs expressed in regions associated with learning and memory including the hippocampus and mPFC (Yamada, et al., 2015; Carstens, et al., 2016; Lensjo, et al., 2017a; Slaker, et al., 2015). There is a vast array of literature on the function of PNNs, however few publications specifically focus on their characterisation in distinct brain regions, particularly their spatiotemporal expression and development. In the current section, I will briefly summarise what is known about the differential expression of PNNs across the brain.

PNNs can be found predominantly in layers 2-5 of the cortex (Bruckner, et al., 1999). They are highly expressed in sensory and motor cortices in addition to prefrontal and temporal cortices (Bruckner, et al., 2000; Slaker, et al., 2015). PNNs begin to form around P21, which follows the later stages of interneuronal migration in the developing post-natal brain (Wonders & Anderson, 2006). In all investigated cortical regions, the largest populations of PNNs are expressed around GABAergic interneurons (Hartig, et al., 1999; Baig, et al., 2005). Predominantly these interneurons are fast-spiking PV-positive interneurons. In the somatosensory cortex specifically, where two PV-positive interneuronal populations have been identified; one co-expressing somatostatin and the other co-expressing metallopeptidases, PNNs are formed exclusively around the metallopeptidase co-expressing interneurons (Rossier, et al., 2015). Cortical PV and PNN co-expressing cells regulate pyramidal neurons which form excitatory projections outside of the cerebral cortex (Lensjo, et al., 2017b). In the neocortex, PNNs can surround excitatory pyramidal neurons themselves, though this is rare, and generally PNNs associate with PV-positive interneurons as is the case in most cortical regions (Alpar, et al., 2006).

In the hippocampus, PNNs are most densely expressed in the CA2 region, with smaller populations in CA1, CA3 and the dentate gyrus (Lensjo, et al., 2017a; Kochlamazashvili, et al., 2010; Jansen, et al., 2017). Predominantly, PNNs form around PV-positive neurons in the hippocampus, as in the cortex, specifically

around basket cells and bistratified neurons (Schuppel, et al., 2002; Yamada, et al., 2015). Both basket cells and bistratified neurons regulate pyramidal cells locally in the hippocampus. A small population of PNNs in the CA2 region of the hippocampus also form around pyramidal neurons and their excitatory synapses (Carstens, et al., 2016).

In the amygdala, specifically the lateral and basal nuclei, PNNs are expressed at a lower density in comparison to the cortex and hippocampus (Hartig, et al., 1995; Gogolla, et al., 2009; Morikawa, et al., 2017). PNNs in the amygdala form around GABAergic interneurons positive for PV or calbindin, which in turn regulate amygdala pyramidal neurons (Hartig, et al., 1995). In the lateral amygdala, a large population of PNN expressing cells are positive for calcium calmodulin-dependent kinase II, a marker of excitatory neurons (Morikawa, et al., 2017).

PNNs are expressed in the lateral and basolateral nuclei of the cerebellum, in addition to the cerebellar cortex (Lafarga, et al., 1984; Blosa, et al., 2016; Mabuchi, et al., 2001). In the cerebellum, PNNs ensheath PV-positive Golgi neurons, which are large, excitatory neurons that form synapses onto granule cells (Carulli, et al., 2006). A population of Purkinje cells also express PNNs. However, they are organised in a much thinner layer around cells than PNNs in other brain regions (Mabuchi, et al., 2001). Purkinje cells are also PV-positive and project to the deep cerebellar nuclei.

In the hypothalamus, PNNs are expressed in the perifornical area of the anterior hypothalamus, a region containing distinct populations of calretinin and enkephalin positive, and PV-negative, cells (Horii-Hayashi, et al., 2015). Co-localisation experiments were not performed as part of this study, therefore it is yet to be determined which of these populations, if any, are the ones which co-express PNNs.

While PNNs have a largely similar structure and composition in different regions of the brain, heterogeneity within and between PNN populations also lies in the neurons they surround. PNNs identified around fast-spiking PV-positive inhibitory interneurons make up the largest populations of PNNs in both cortical and hippocampal regions (Hartig, et al., 1999; Baig, et al., 2005; Yamada & Jinno, 2013). However, more recently, populations of PNNs have also been identified around excitatory neurons in the hippocampus and amygdala (Carstens, et al.,

2016; Morikawa, et al., 2017). The different properties of the neurons which express PNNs may reflect diverse roles for PNNs in different brain regions.

The existence of PNNs in the BNST was first documented by Horii-Hayashi *et al.* (2015) who performed a global study to investigate PNNs in the CNS. The presence of PNNs in the BNST was indicated in a table, however no labelling images were provided to corroborate the findings. More recently, PNNs were examined in the posterior medial part of the BNST in the mouse and marmoset (Ciccarelli, et al., 2021). No study to date has identified the expression and characterised the spatiotemporal development of PNNs in the anterior BNST or determined the chemical nature of the neurons they surround. Here, successive ages of mice were examined to establish a comprehensive picture of PNN expression in the BNST through development, and into adulthood. I chose C57BL/6 mice in the current study since it is the most commonly used strain of mice in the research community – hence, results obtained in my thesis could be compared to published studies investigating PNN development in other brain regions in mice (Table 2.1). No known differences in expression or distribution of PNNs have been reported between various wild-type mouse strains to date. The current study is the first to examine PNNs, specifically in the anterior BNST, in detail.

2.2 Aims

In the current chapter I will address the following four main aims:

(1) determine the time course of PNN development in the BNST

(2) investigate the spatial expression of PNNs in the BNST

(3) examine the composition of PNNs in the BNST

(4) identify a population(s) of neurons surrounded by PNNs within the BNST

2.3 Methods

2.3.1 Animals

Male, wild-type C57BL/6J mice at successive life stages: P10, P20, P30, P60, P210 and P365, were used in these experiments. Mice were group housed, in groups of 3-4 for adults, in individually ventilated cages, in temperature-controlled rooms, on a 12-hour light/dark cycle, with lights on at 6:30am, with *ad libitum* access to food (Teklad Global 14, 14% protein diet, Envigo) and water. All procedures were carried out in accordance with the UK Animal (Scientific Procedures) Act 1986. Experiments were approved by the UK Home Office and University of Exeter Local Ethics Committee.

2.3.2 Development of perineuronal nets

Tissue preparation

Mice were anaesthetised with sodium pentobarbital (50 mg kg^{-1}) and transcardially perfused with ice cold phosphate buffered saline (PBS; Sigma) and room temperature paraformaldehyde (PFA, 4% in PBS; Sigma) and thereby killed. Following dissection and overnight fixation with 4% PFA at 4°C, brains were washed in PBS, transferred to a cryoprotective solution (30% sucrose in PBS) for dehydration, and stored at 4°C until they were submerged. After brains were fully submerged in sucrose, on average this took 24 hours, 30 µm coronal anterior BNST sections, approximately bregma 0.62 mm to 0.02 mm (Figure 2.1), were cut on a cryostat (Bright Instruments, UK). Sections were collected in 24-well plates, in PBS, and were stored at 4 °C for a maximum of two weeks.

Labelling

Every third section of BNST, approximately 90 µm between sections, was taken for PNN labelling. First, sections were incubated for 1 hour at room temperature in blocking solution (10% foetal bovine serum (Sigma, UK) in 0.1% PBST: Triton X-100 in PBS (Sigma, UK). Sections were then incubated for an hour at room temperature in FITC conjugated WFA (1:500; VectorLabs, UK) in blocking solution (1:500), protected from light. Sections were washed in PBS before

mounting on Poly-D-Lysine coated slides (VWR, UK) with fluorsave mounting medium (Merck, UK). Slides were left to dry overnight before sections were imaged using a Zeiss LSM 5 Exciter confocal microscope (Zeiss, Germany). A single field of view was imaged per slice, with a 10x or 40x (oil) objective. A laser with a wavelength of 488 nm was used for excitation of the green fluorophore.

Image preparation

The Franklin and Paxinos mouse brain atlas (Franklin & Paxinos, 2007) was used as a guide to create masks of bregma points throughout the BNST, from approximately bregma 0.62 mm to 0.02 mm (Figure 2.1). Masks were made transparent and were overlaid onto microscopy images of the BNST in accordance with bregma point, using the anterior commissure as an anatomical reference guide, to separate the distinct subnuclei. For clarity, subnuclei of interest are highlighted in white (Figure 2.1).

Image analysis

For manual counting of PNNs, images with mask overlays were opened in ImageJ (v1.53e; NIH, USA) and the count tool was used to identify PNN positive cells. PNN identification was based on the criteria that they must be independently visible and distinctly reticular. Meshes of PNN units were not counted, as individual units could not be separated.

Intensity of PNNs was measured using a MATLAB (Mathworks, USA) script, designed in collaboration with Dr Ben Sherlock (Appendix 2). Images with mask overlays were analysed by the script, which parcellated each distinct BNST subnucleus. Output values of average pixel intensity per BNST region were subsequently collated. To account for background fluorescence, the average pixel intensity of a separate region, adjacent to the BNST, where no PNNs were expressed, was measured. Background fluorescence was normalised across slices by subtracting the average pixel intensity of the BNST adjacent region, which did not express PNNs, from the measured BNST regions within the same slice.

Statistical analysis

Graphpad Prism (Graphpad Software Inc, USA) was used to perform all statistical analyses. A Shapiro-Wilk test was used to test for normality of sample distributions. One-way analysis of variance (ANOVA), which assumes equal variance and normal distribution of samples, was then used to compare group means and Tukey's multiple comparisons test was used to determine significant differences. Equal variance was not specifically assessed prior to ANOVA. Multiple comparisons were corrected for using a Dunnett post-hoc test. For the analysis of PNN number and intensity over time number of animals for each group were as follows: P30 = 5, P60 = 5, P210 = 6 and P365 = 6. Data are presented as mean ± SEM unless otherwise stated.

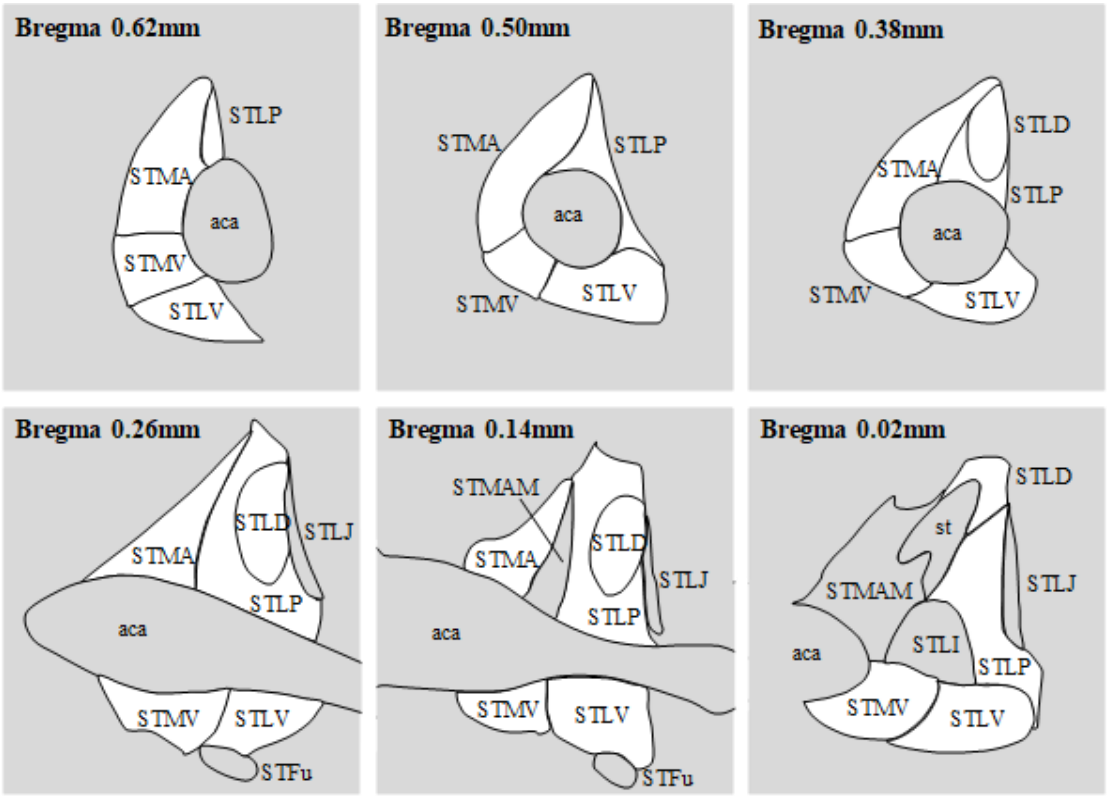

Figure 2.1 Schematic illustration of bed nucleus of the stria terminalis subnuclei mask overlays. Masks were created from bregma point 0.62 mm to 0.02 mm using the Franklin and Paxinos mouse brain atlas (2007). Subnuclei of interest are highlighted in white. Abbreviations: aca, anterior commissure; STFu, bed nucleus of the stria terminalis, lateral division, fusiform part; STLD, bed nucleus of the stria terminalis, lateral division 2; STLI, bed nucleus of the stria terminalis, lateral division 1; STLJ, bed nucleus of the stria terminalis, lateral division, juxtacapsular part; STLP, bed nucleus of the stria terminalis, lateral division, posterior part; STLV, bed nucleus of the stria terminalis, lateral division, ventral part; STMA, bed nucleus of the stria terminalis, medial division, anterior part; STMAL; bed nucleus of the stria terminalis, medial division, anterolateral part; STMAM, bed nucleus of the stria terminalis, medial division, anteromedial part; STMP, bed nucleus of the stria terminalis, medial division, posterior part; STMV, bed nucleus of the stria terminalis, medial division, ventral part.

2.3.3 Immunolabelling for perineuronal net components and cellular markers

Tissue preparation

Brains were dissected and fixed overnight in 4% PFA in PBS at 4°C. Following washing with PBS, 50 µm coronal BNST sections between bregma 0.62 mm and 0.02 mm, were cut using a Leica VT1200 Semiautomatic Vibrating Blade Microtome (Leica, UK). Sections were collected in 24-well plates, in PBS, and were stored at 4 °C for a maximum of two weeks. For longer storage, of up to six months, sections were transferred to a cryoprotective solution (25% glycerol, 25% ethylene glycol and 0.1 M phosphate buffer consisting of 23 mM NaH_2PO_4 x $1H_2O$ and 77 mM Na_2HPO_4 x 2 H_2O; all reagents from Sigma, UK).

Immunolabelling

All immunolabelling was performed using free-floating sections. Following incubation in blocking solution for one hour at room temperature on an orbital shaker (IKA, UK), vibratome prepared BNST sections were incubated with primary antibody (Table 2.2) in blocking solution, overnight at 4°C on a Nutator shaker (Clay Adams®, US). Sections were then washed 3 times, for 15 minutes each in PBS, before incubation with fluorophore-conjugated secondary antibody (Table 2.2) in PBST, protected from light. Sections were finally incubated in FITC conjugated WFA (1:500 in blocking solution) for an hour at room temperature, protected from light. Sections were washed in PBS before mounting on Poly-D-Lysine coated slides (VWR, UK) with fluorsave mounting medium (Merck, UK). Slides were left to dry overnight before sections were imaged using a Zeiss LSM 5 Exciter confocal microscope (Zeiss, Germany). A single field of view was imaged per slice, with a 10x or 40x (oil) objective. Lasers with wavelengths of 488 nm, 594 nm and 647 nm were used for excitation of green, red and far-red fluorophores, respectively. For all immunolabelling experiments, steps were taken to limit photobleaching of FIT-C, therefore all images were taken first of the FIT-C labelling prior to imaging of the red fluorophore, and then the far-red fluorophore, where three fluorophores were used.

Selection of interneuronal markers for immunolabelling

Markers of interneurons of interest for immunolabelling experiments were chosen based on consultation with the genomic Allen Mouse Brain Atlas (https://mouse.brain-map.org/). A thorough search of *in situ* hybridisation experiments for each interneuronal marker was performed, and only markers with observable RNA expression in the BNST were taken forward for immunolabelling.

Table 2.2 Antibodies for immunolabelling

Target	Primary Antibody	Conc.	Secondary Antibody	Conc.
Aggrecan	Aggrecan (mouse), Novus Biologicals (NB120-11570)	1:200	Donkey anti-mouse 594	1:1000
Brevican	Brevican (mouse), Novus Biologicals (NBP2-22401)	1:500	Donkey anti-mouse 594	1:1000
Calbindin	Calbindin D28k (chicken), Synaptic Systems (214006)	1:500	Donkey anti-chicken Cy3	1:1000
Calretinin	Calretinin (rabbit), Synaptic Systems (214111)	1:500	Donkey anti-rabbit 555	1:1000
C-fos	C-fos (rabbit), Cell Signaling (2250)	1:500	Donkey anti-rabbit 647	1:1000
Glial fibrillary acidic protein	GFAP (chicken), Abcam (ab4674)	1:1000	Goat anti-chicken 647	1:1000
Neurocan	Neurocan (mouse), Abcam (ab26003)	1:500	Donkey anti-mouse 594	1:1000
Neuronal cell bodies	NeuN (rabbit), Cell Signaling (12943)	1:1000	Donkey anti-rabbit 555	1:1000
	Or			
	NeuN (mouse), Chemicon	1:1000	Donkey anti-mouse 594	1:1000
Neuronal nitric oxide synthase	nNOS (rabbit), Cell Signaling (4231)	1:500	Donkey anti-rabbit 555	1:1000
Neuropeptide Y	NPY (rabbit), Cell Signaling (11976)	1:500	Donkey anti-rabbit 555	1:1000
Parvalbumin	Parvalbumin (rabbit), Swant (PV27)	1:500	Donkey anti-rabbit 555	1:1000
Somatostatin	Somatostatin (rat), Invitrogen (MA5-16987)	1:500	Goat anti-rat Texas Red	1:1000
Versican	Versican (mouse), Novus biologicals (NBP2-22408)	1:500	Donkey anti-mouse 594	1:1000
Chondroitin sulphate proteoglycans	WFA, conjugated to FITC, VectorLaboratories (FL-1351-2)	1:500	NA	NA

2.4 Results

2.4.1 Morphological comparison of perineuronal nets in the bed nucleus of the stria terminalis to those in other brain regions

WFA, which selectively labels N-acetylgalactosamine residues on glycoproteins within the extracellular matrix, labelled a population of PNN expressing cells in the BNST of male, adult mice, aged 8 weeks (Figure 2.2). The labelling protocol was optimised, using successive dilutions of WFA (1:100, 1:200, 1:500 and 1:1000; images not shown). A dilution of 1:500 resulted in clearly labelled PNNs while reducing intensity of the labelling of the background ECM. Labelling was repeated in 10 mice, where they all qualitatively showed the same result. PNNs ensheath cell bodies and proximal dendrites in the BNST, however their appearance is less reticular, lacking the distinct lattice-like structure observed in PNNs in the cortex and hippocampus, and more granular, similar to PNNs in the basolateral amygdala (Figure 2.2). PNNs in the BNST do not show the same organisation pattern as in the cortex, hippocampus, or amygdala. They are more densely clustered together in a small region, compared to the few, evenly spaced PNNs in the amygdala, the random, widespread expression of PNNs in the cortex and the highly organised PNNs in the hippocampus (Figure 2.2).

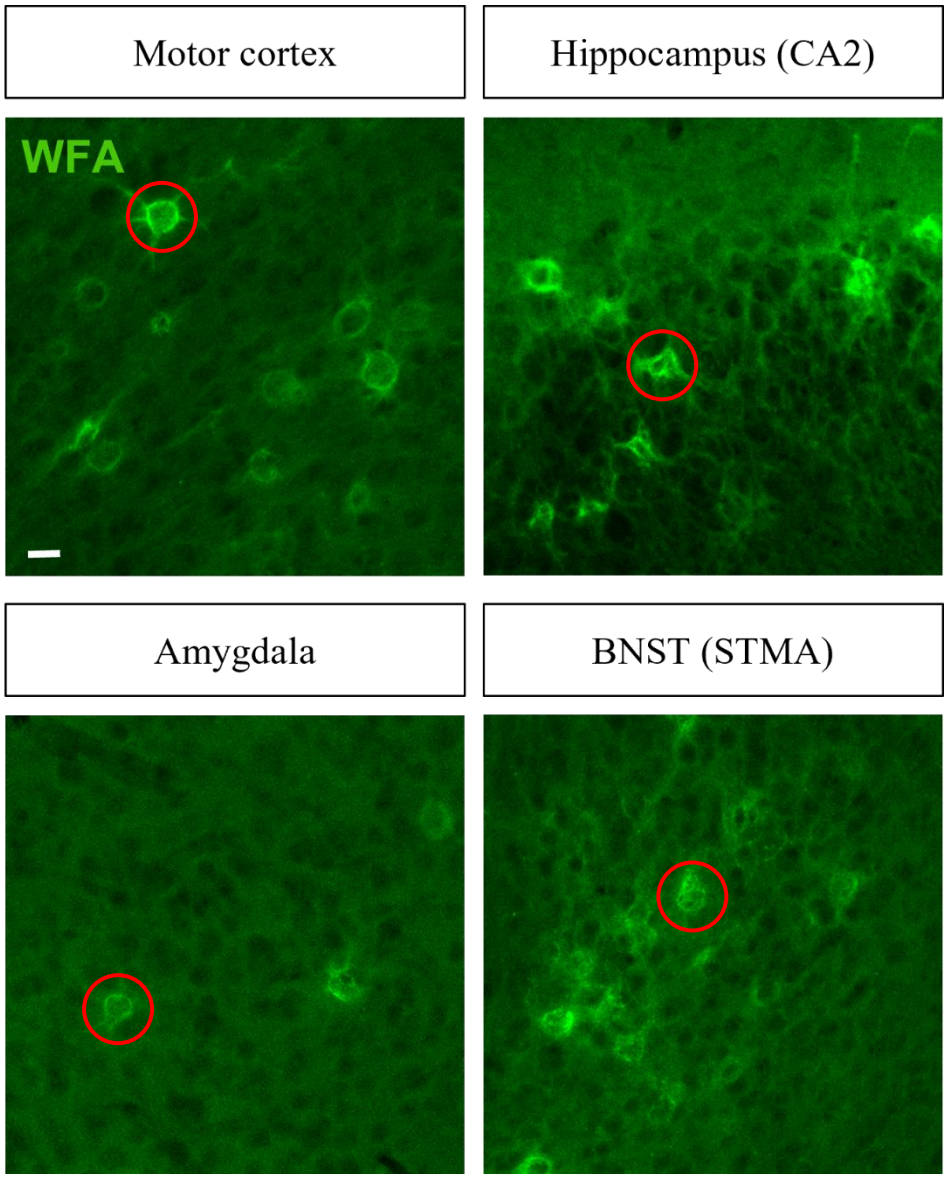

Figure 2.2 Comparison of perineuronal net appearance across different brain regions in adult mice. WFA labelling in the motor cortex, CA2 region of the hippocampus, lateral amygdala and anteromedial BNST (STMA) revealed PNNs in all analysed regions (green). Examples of single PNNs in each brain region are identified within the red circles. Perineuronal nets in the BNST form in small, clustered regions compared to the cortex, hippocampus and amygdala, where PNN-positive cells are more diffusely spread over a greater area. Perineuronal nets are more densely expressed than in the amygdala, with a more similar density to hippocampal perineuronal nets. The morphology of perineuronal nets in the BNST is closest to those expressed in the amygdala, with less deposition around proximal dendrites than in the cortex or hippocampus. Representative images, experiments were performed independently with similar results on 8-10 animals. Scale bar = 20µm.

2.4.2 Temporal development of perineuronal nets in the bed nucleus of the stria terminalis

To investigate the development of PNNs in the BNST over time, BNST sections from mice aged P10, P20, P30, P60, P210 and P365 were labelled with WFA. Time points were chosen to represent successive life stages of the mouse, which also correspond to human life stages. The two early time points, P10 and P20, represent early life, P20 in particular was chosen as PNNs have been identified in other brain regions by this time; P30 represents early adolescence; P60, late adolescence; P210, mature adult and finally P365, middle age.

There were no PNNs detected by WFA labelling in the BNST at P10 (Figure 2.3). By P20, WFA labelling was positive and revealed matrix beginning to condense, shown by higher intensity WFA labelling, but no evident PNNs were detected. The characteristic shape of PNNs was apparent in the BNST at P30, with more intense WFA labelling around neuronal cell bodies and proximal dendrites, denoted by the white arrows and orange triangles, respectively (Figure 2.3). At P60, PNNs were visually similar to those documented in other brain regions, including the hippocampus and amygdala (Figure 2.2). However, in comparison, PNN structure in the BNST is less reticular and more granular in appearance.

PNNs were also visualised at two much later time points: P210 and P365 (Figure 2.3). PNNs have previously been determined to be developmental features important in the closure of the critical period of synaptic plasticity (Pizzorusso, et al., 2002; Gogolla, et al., 2009; Balmer, et al., 2009; Sengpiel, 2007; Nabel & Morishita, 2013). However, PNNs are also proposed to remodel through adulthood, based on activity in local microcircuits (Devienne, et al., 2021). I was, therefore, interested to investigate PNNs within the BNST beyond their initial maturation in early adulthood. WFA labelling revealed that at P210 and P365 PNNs in the BNST are more densely expressed than at earlier time points, and in some instances form clusters around adjacent neurons (Figure 2.3).

WFA labelling of BNST slices was repeated in 5-6 mice for each time point, where all qualitatively showed the same result. Further quantification of PNNs in various subregions of BNST at different developmental stages was performed using two independent methods (Chapter 2.4.3).

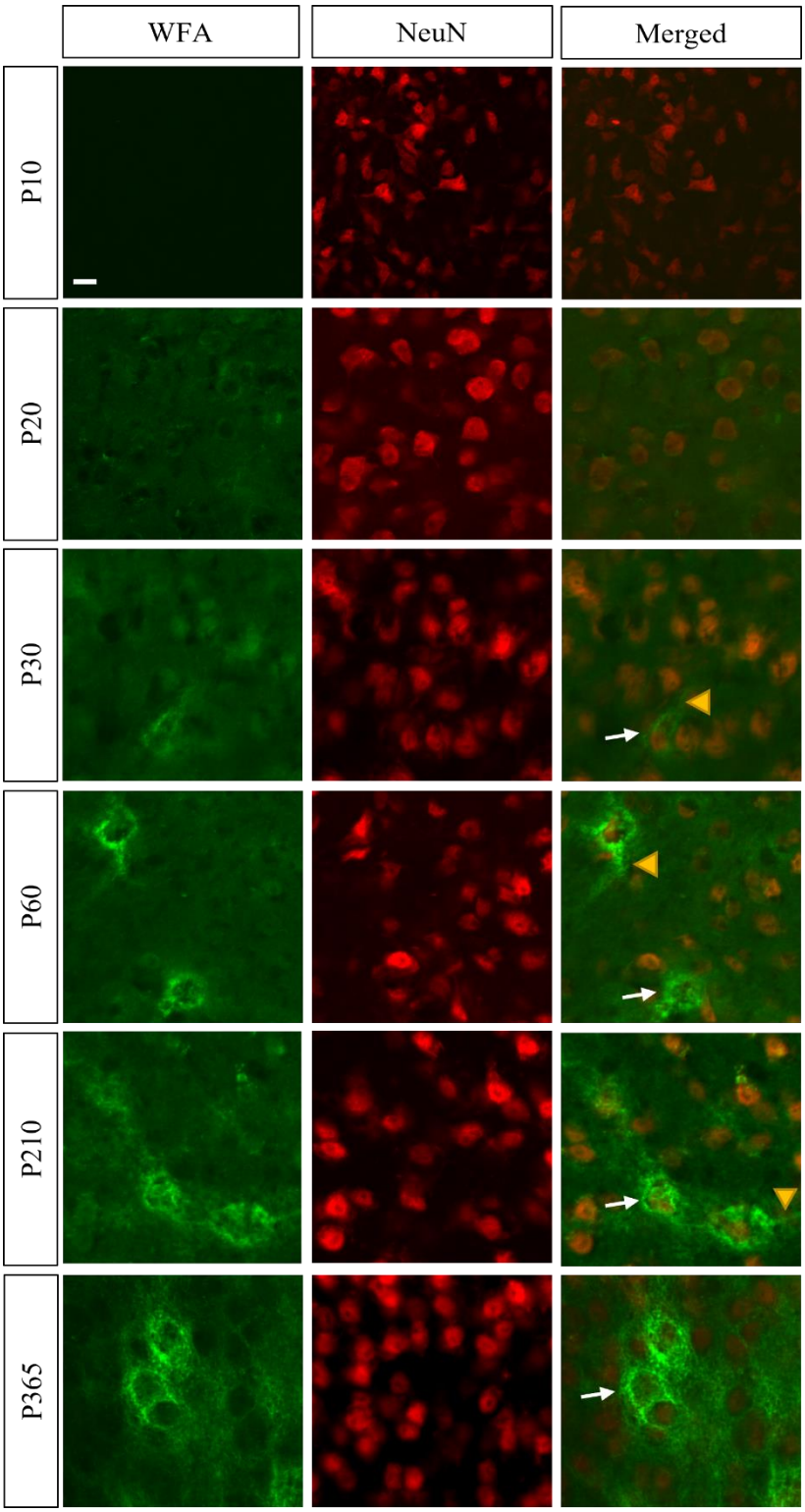

Figure 2.3 Temporal development of perineuronal nets in the bed nucleus of the stria terminalis. WFA labelling in the BNST is negative at post-natal day 10 (P10) (green fluorescence). By P20, WFA labelling is positive, and by P30, the characteristic 'net' shape can be clearly identified around neuronal cell bodies (red fluorescence). Beyond initial maturation, WFA labelling of perineuronal nets becomes more intense in the BNST from P60 onwards, with labelling seen around both neuronal cell bodies (labelled by NeuN) and their proximal dendrites. Nets are also more likely to be clustered together than independent from one another. Arrows indicate perineuronal nets around neuronal cell bodies, triangles indicate extension of perineuronal nets to proximal dendrites. Representative images, experiments were performed independently with similar results on 6 animals per age group. Scale bar = 20µm.

2.4.3 Spatiotemporal development of perineuronal nets in the bed nucleus of the stria terminalis

To quantify the development of PNNs in the BNST, manual and automatic methods were employed. Number of PNNs was counted first manually in Image J. PNN intensity was also measured computationally using a MATLAB script that I developed in collaboration with Dr Ben Sherlock (Living Systems Institute, University of Exeter; Appendix 2). This method provided the advantage of unbiased and automated quantification of PNNs within various BNST subnuclei with the possibility of analysing numerous images at once.

Each N in these studies represents one animal, with total PNN number/intensity calculated across six slices per animal, averaged across the left and right BNST.

P10 and P20 time points were excluded from quantitative analysis of PNN spatiotemporal expression since no PNNs were detected in mouse brain at these time points (Figure 2.3). PNN expression within the BNST was thus investigated, in detail, at P30, P60, P210 and P365. PNN identification was based on the criteria that they must be independently visible and distinctly reticular. Meshes of PNN units were not counted, as individual units could not be separated. Examples of individual PNN units can be found in Figure 2.1, indicated by the red circles. PNNs were expressed in the STMA at P30, and across the BNST from P60 (Figure 2.4). Upon quantification of BNST PNNs, it was generally observed that they were more numerous and intense through development (Figure 2.5; Figure 2.6).

PNN expression increased significantly with age in the STMA (Figure 2.5B; $F(3, 18) = 16.48$, $P = <0.0001$). The number of PNNs doubled between P30 and P60, and between P60 and P210 (Figure 2.5B; P30: 6.10 ± 1.55, $p = <0.0001$; P60: 16.59 ± 3.69, $p = 0.0079$; vs. P210: 31.42 ± 3.51). There was no difference in PNN expression between P210 and P365 (Figure 2.5B; P365: 28.00 ± 1.75).

PNN number increased significantly over time in the STMV (Figure 2.5C; $F(3, 18) = 3.787$, $P = 0.0288$). Specifically, a greater number of PNNs were expressed at P365 compared with P30 (Figure 2.5C; P30: 4.50 ± 2.01, $p = 0.0198$; vs. P365: 12.05 ± 1.51). No difference in PNN number was observed in the STMV at P60 or P210 in comparison to P30 (P60: 8.55 ± 1.87; P210: 10.02 ± 1.16). PNN

number did not change over time in the STLV (Figure 2.5D; P30: 5.70 ± 1.67; P60: 7.95 ± 2.23; P210: 8.13 ± 1.64; P365: 6.67 ± 1.51).

In both lateral subnuclei of the BNST, STLP and STLD, number of PNNs increased throughout development. In the STLP, PNN expression increased with age (Figure 2.5E; $F(3, 18) = 11.96$, $P = 0.0002$). Specifically, more PNNs were expressed at P210 than at P30 or P60 time points (Figure 2.5E; P30: 3.9 ± 0.60; $p = 0.0002$; P60: 6.5 ± 1.02, $p = 0.0360$; vs. P210: 9.67 ± 0.33). Twice as many PNNs were expressed in the STLP at P365 compared with P30 (Figure 2.5E; P30: 3.9 ± 0.60, $p = 0.0009$; vs. P365: 8.88 ± 0.33). In the STLD, number of PNNs significantly increased with age (Figure 2.5F; $F(3, 18) = 7.102$, $P = 0.0024$). There were seven times more PNNs in the STLD at P60 compared to P30 (Figure 2.5F; P30: 0.60 ± 0.60, $p = 0.0244$; vs. P60: 7.10 ± 1.60). There was no difference in the number of PNNs detected in the STLD at P210 or P365 compared with any other time point (Figure 2.5F; P210: 9.41 ± 2.02; P365: 5.50 ± 0.50).

PNNs increased in number with age in various BNST subnuclei (Figure 2.5). However, there was also a difference in PNN expression throughout development across BNST subnuclei, with the anteromedial part of the BNST (STMA) expressing greater numbers of PNNs than the STLP at adulthood (P60) (Appendix 1 Table 6.2; $F(4, 20) = 3.312$, $P = 0.0309$; STLP: 6.51 ± 1.03, $p = 0.0366$; vs. STMA: 16.59 ± 3.69). At P210, the STMA expressed at least three times more PNNs than any other subnucleus (Appendix 1 Table 6.3; $F(4, 25) = 23.15$, $P = <0.0001$; STLV: 8.13 ± 1.64, $p = <0.0001$; STMV: 10.02 ± 1.16, $p = <0.0001$; STLP: 9.67 ± 0.88, $p = <0.0001$; STLD: 9.42 ± 2.02, $p = <0.0001$; vs. STMA: 31.42 ± 3.51). See Appendix 1 Table 6.1 for comparisons of PNN number across BNST subnuclei at P30 and Appendix 1 Table 6.4 for P365 comparisons, respectively.

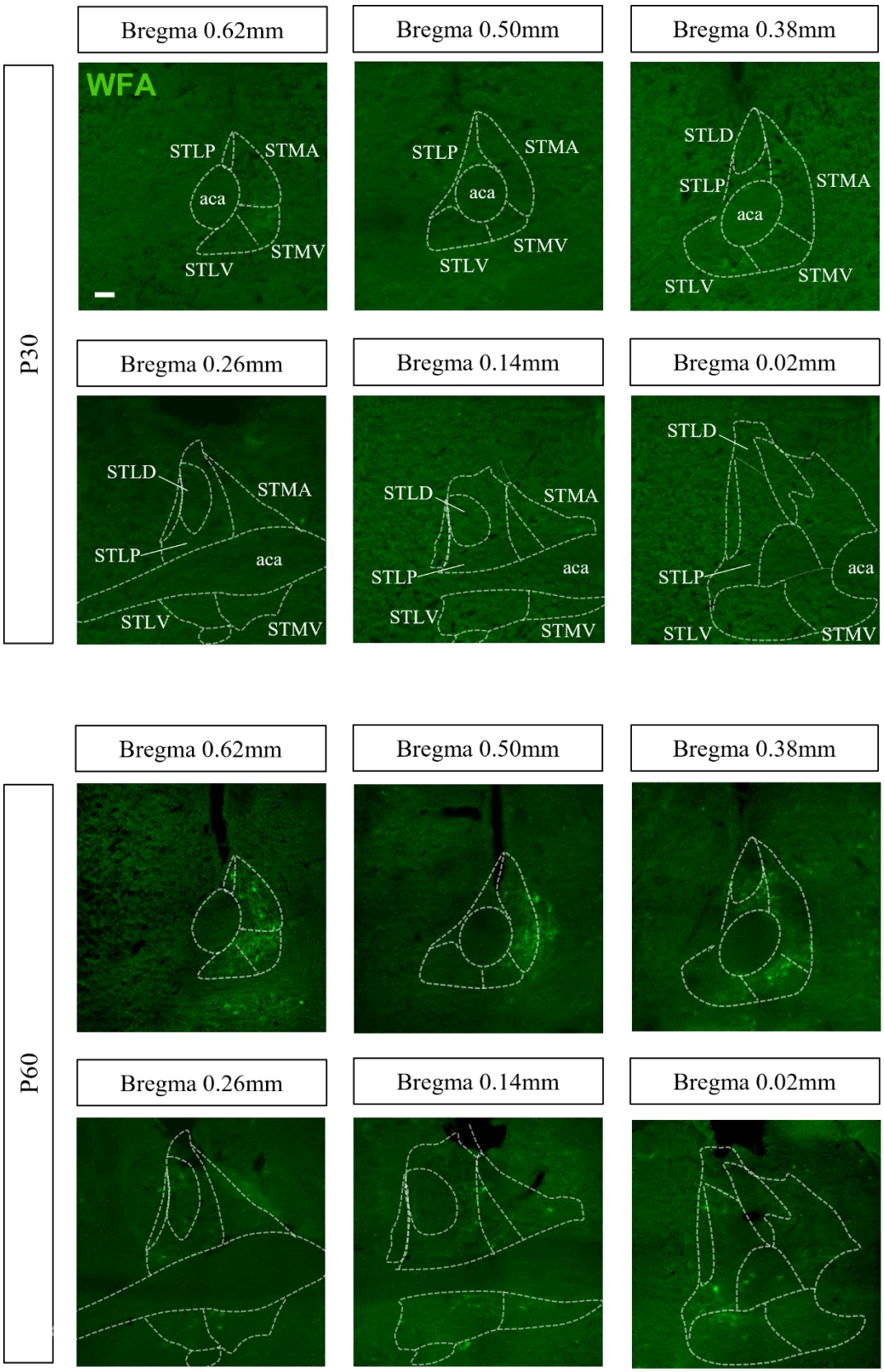
P30
Bregma 0.62mm
Bregma 0.50mm
Bregma 0.38mm
WFA
STLP
STMA
aca
STMV
STLV
STLD
Bregma 0.26mm
Bregma 0.14mm
Bregma 0.02mm
P60
Bregma 0.62mm
Bregma 0.50mm
Bregma 0.38mm
Bregma 0.26mm
Bregma 0.14mm
Bregma 0.02mm

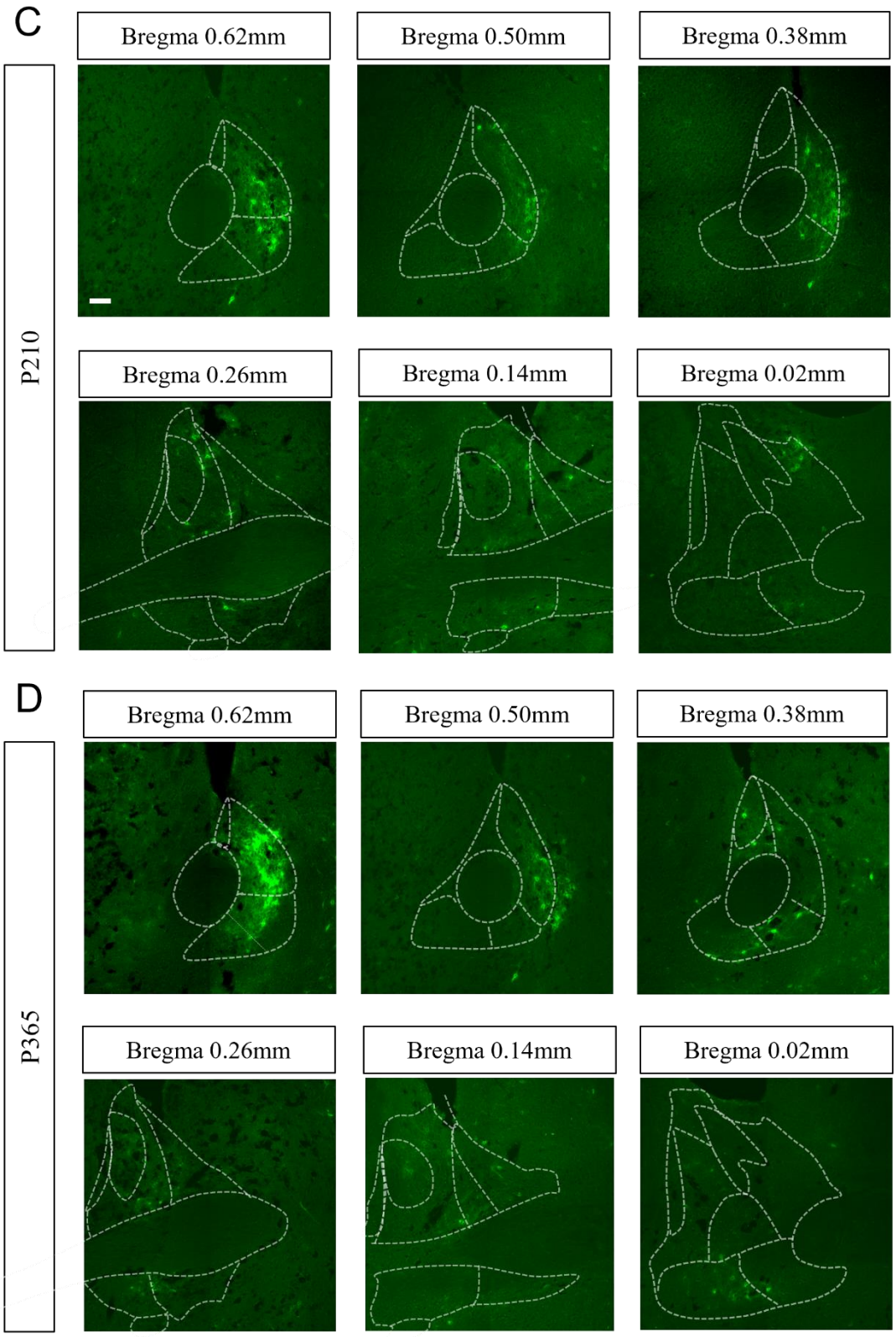

Figure 2.4 Spatiotemporal distribution of perineuronal nets in the bed nucleus of the stria terminalis. WFA labelled PNNs in the BNST show a similar distribution throughout development, (A) P30, to adulthood, (B) P60, and beyond, (C) P210 and (D) P365 (green fluorescence). PNNs are more highly expressed in the medial subnuclei when the BNST is organised around the anterior commissure, and the dorsomedial and ventromedial nuclei when the anterior commissure bisects the region. Abbreviations: PNNs, perineuronal nets; STMV, BNST, medial division, ventral part; STLV, BNST, lateral division, ventral part; STMA, BNST, medial division, anterior part; STLP, BNST, lateral division, posterior part; STLD, BNST, lateral division, dorsal part; aca, anterior commissure. Representative images, experiments were performed independently with similar results in 6 animals per age group. Scale bar = 100µm.

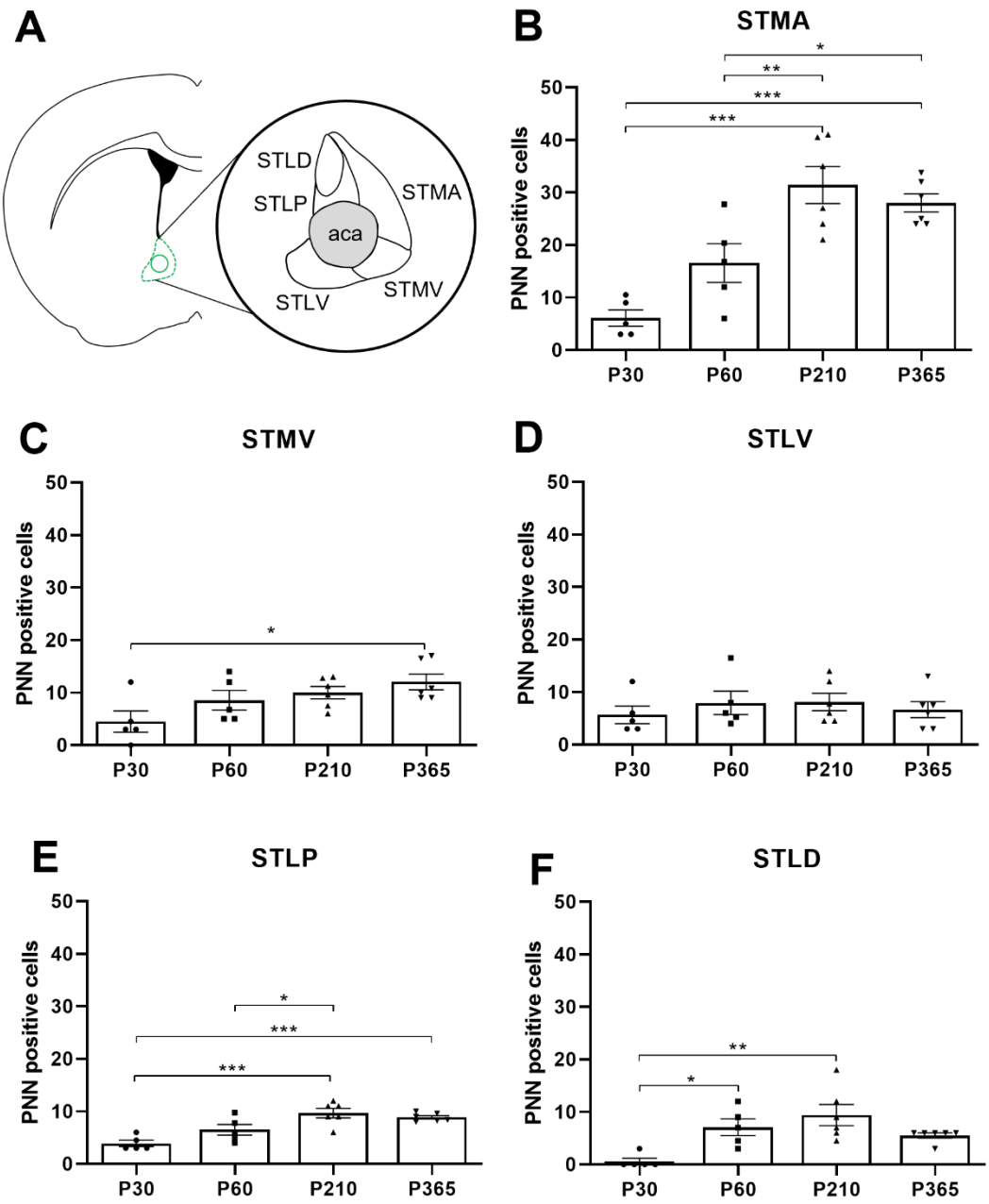

Figure 2.5 Perineuronal net number within anterior subnuclei of the bed nucleus of the stria terminalis throughout development. Serial images throughout the BNST, with mask overlays to define subnuclei, were used to determine PNN number manually. Images were analysed with the count tool on ImageJ. PNNs were only counted if they met certain criteria; a distinct reticular shape, independently discernible from the rest of the matrix. (A) Location of the BNST on a coronal image of the brain (bregma 0.38mm) with annotated view of the subnuclei investigated (aca denotes the anterior commissure). (B) Number of PNNs in the medial division, anterior part (STMA) of the BNST through development. (C) Number of PNNs in the medial division, ventral part (STMV) of the BNST through development. (D) Number of PNNs in the lateral division, ventral part (STLV) of the BNST through development. (E) Number of PNNs in the lateral division, posterior part (STLP) of the BNST through development. (F) Number of PNNs in the lateral division 2, (STLD) of the BNST through development. N (P30/P60) = 5 mice, N (P210/P365) = 6 mice, 6 brain sections per animal. Data are presented as bar plots with mean±SEM; *p < 0.05, **p < 0.01, ***p < 0.001 vs an indicated group, one-way ANOVA with Tukey's *post hoc* testing.

The same sections were used for automated analysis of PNN intensity as were used for manual counting of PNNs. Using the newly created MATLAB script to determine WFA labelling intensity of PNNs, it was determined that PNN intensity increased over time, but not in all BNST subnuclei. In the anterior part of medial BNST (STMA) WFA labelling of PNNs had greater intensity through development (Figure 2.6A; $F(3, 18) = 5.245$, $P = 0.0089$). WFA labelling was twice as intense at P60, P210 and P365 compared to P30 (Figure 2.6A; P60: 6413 ± 899.2, $p = 0.0166$; P210: 6127 ± 486.2, $p = 0.0244$; P365: 6234 ± 644.6, $p = 0.0188$; vs. P30: 3411 ± 79.61).

In the ventromedial division of BNST (STMV), and both lateral subnuclei of BNST (STLP and STLD) there was no change in intensity of WFA labelling (STMV – Figure 2.6B; P30: 2508 ± 637.0; P60: 2814 ± 383.6; P210: 2596 ± 141.0; P365: 2365 ± 270.2; STLP – Figure 2.5D; P30: 2126 ± 484.2; P60: 2283 ± 343.4; P210: 1534 ± 158.6; P365: 2589 ± 165.7; STLD – Figure 2.6E; P30: 1977 ± 23.6; P60: 3082 ± 788.7; P210: 1905 ± 307.3; P365: 2931 ± 410.4).

Labelling of PNNs in the lateral subnucleus of the BNST (STLV) increased in intensity with age (Figure 2.6C; $F(3, 18) = 4.263$, $P = 0.0193$). More intense WFA labelling within the STLV was observed at P60 and P365, compared to P30 (Figure 2.6C; P60: 3523 ± 177.8, $p = 0.0342$; P365: 3500 ± 298.5, $p = 0.0298$; vs. P30: 2443 ± 259.6). No difference in WFA intensity was observed at P210 compared with the other time points under investigation (Figure 2.6C; P210: 3381 ± 192.5).

Automated analysis using the newly created MATLAB script also revealed greatest PNN expression, by intensity, in the STMA at adulthood (P60) (Appendix 1 Table 6.6; STLV: 3523 ± 177.8, $p = 0.0179$; STMV: 2814 ± 383.6, $p = 0.0027$; STLP: 2283 ± 343.4, $p= 0.0006$; STLD: 3082 ± 788.7, $p = 0.0055$; vs. STMA: 6413 ± 899.2). See Appendix 1 Table 6.5, 1.7 and 1.8 for comparisons of WFA labelling intensity across BNST subnuclei at P30, P210 and P365, respectively.

As both quantification methods identified the STMA as the subnucleus with the most numerous/intensely labelled PNNs, further analysis will focus on the STMA as the subnucleus of interest.

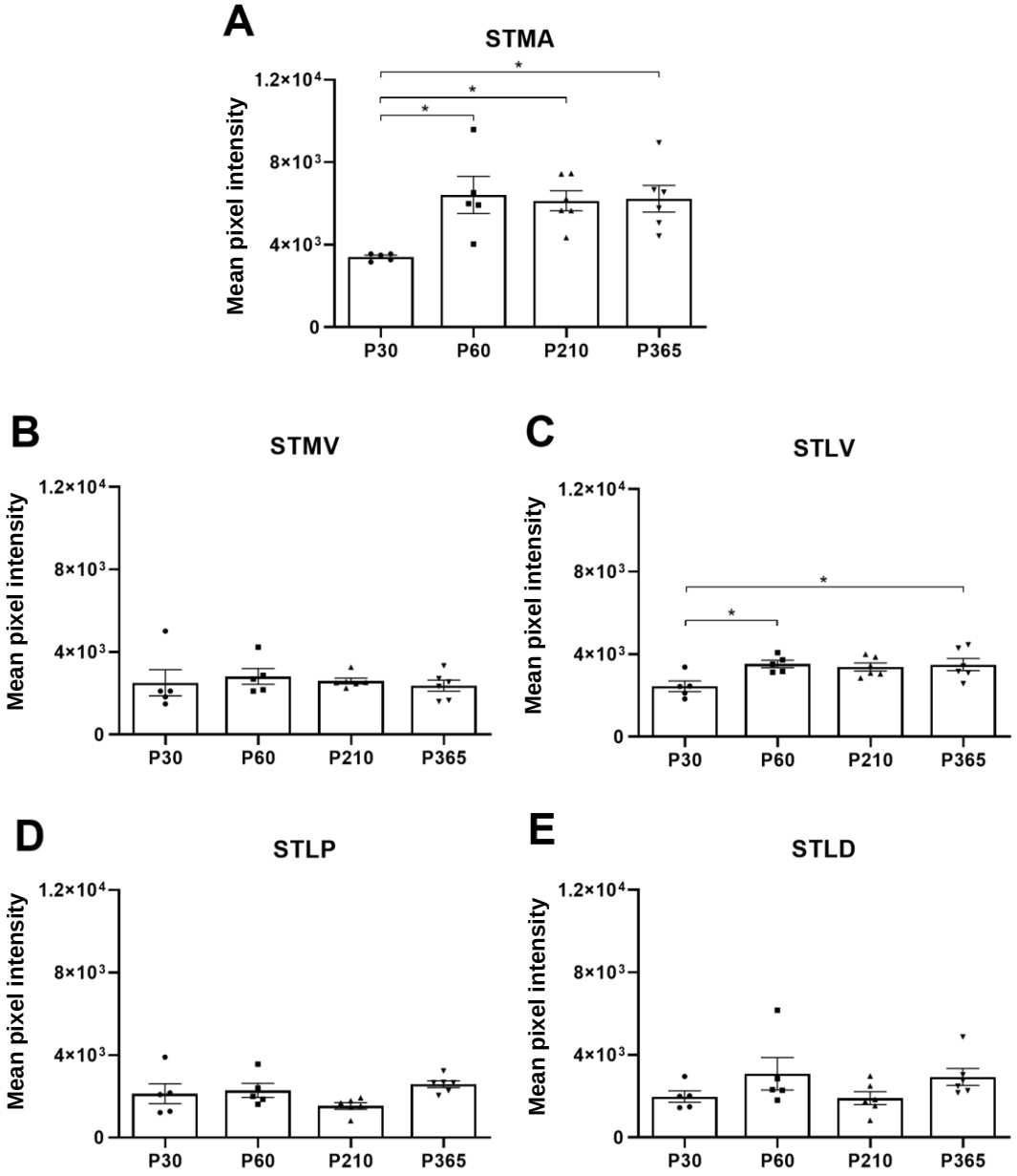

Figure 2.6 Intensity of perineuronal nets within anterior subnuclei of the bed nucleus of the stria terminalis throughout development. Serial images throughout the BNST, with mask overlays to define subnuclei, were run through a MATLAB script. Intensity values calculated by the script were normalised to a control region of the BNST with no PNN expression to eliminate the intensity of background fluorescence. (A) PNN intensity development in the medial division, anterior part (STMA) of the BNST. (B) Development of PNN intensity in the medial division, ventral part (STMV) of the BNST. (C) Development of PNN intensity in the lateral division, ventral part (STLV) of the BNST. (D) PNN intensity development in the lateral division, posterior part (STLP) of the BNST. (E) Development of PNN intensity in the lateral division 2, (STLD) of the BNST. N (P30/P60) = 5 mice, N (P210/P365) = 6 mice, 6 brain sections per animal. Data are presented as bar plots with mean±SEM; *$p < 0.05$, **$p < 0.01$, ***$p < 0.001$ vs an indicated group, one-way ANOVA with Tukey's *post hoc* testing.

2.4.4 Cell type specificity of perineuronal nets in the bed nucleus of the stria terminalis

To elucidate the neuronal subtype(s) surrounded by PNNs in the STMA, immunolabelling was performed for an array of interneuronal markers. The markers were chosen based on their expression across the BNST according to the genomic Allen Mouse Brain Atlas (https://mouse.brain-map.org/). The interneuronal markers targeted were: parvalbumin, somatostatin, neuropeptide Y, neuronal nitric oxide synthase (nNOS), calbindin and calretinin (Figure 2.7). Positive labelling in the BNST was observed in cell bodies for somatostatin, neuropeptide Y, calbindin and calretinin. Diffuse positive labelling was observed for nNOS, however labelling for parvalbumin was negative in the BNST (Figure 2.7). No co-localisation of WFA labelled PNNs and cell bodies positive for any of the interneuronal markers tested was observed in the BNST. Labelling for each interneuronal marker was performed in at least four separate animals, where they all showed qualitatively the same result.

Image analysis revealed that PNNs in the BNST are expressed exclusively around neurons (NeuN-positive cells; Figure 2.8). PNN positive neurons are also often found in close proximity to astrocytes, which label positively for glial fibrillary acidic protein (GFAP). Co-labelling for NeuN and GFAP was performed using sections across the BNST (at least four) in five mice where they all qualitatively showed the same result.

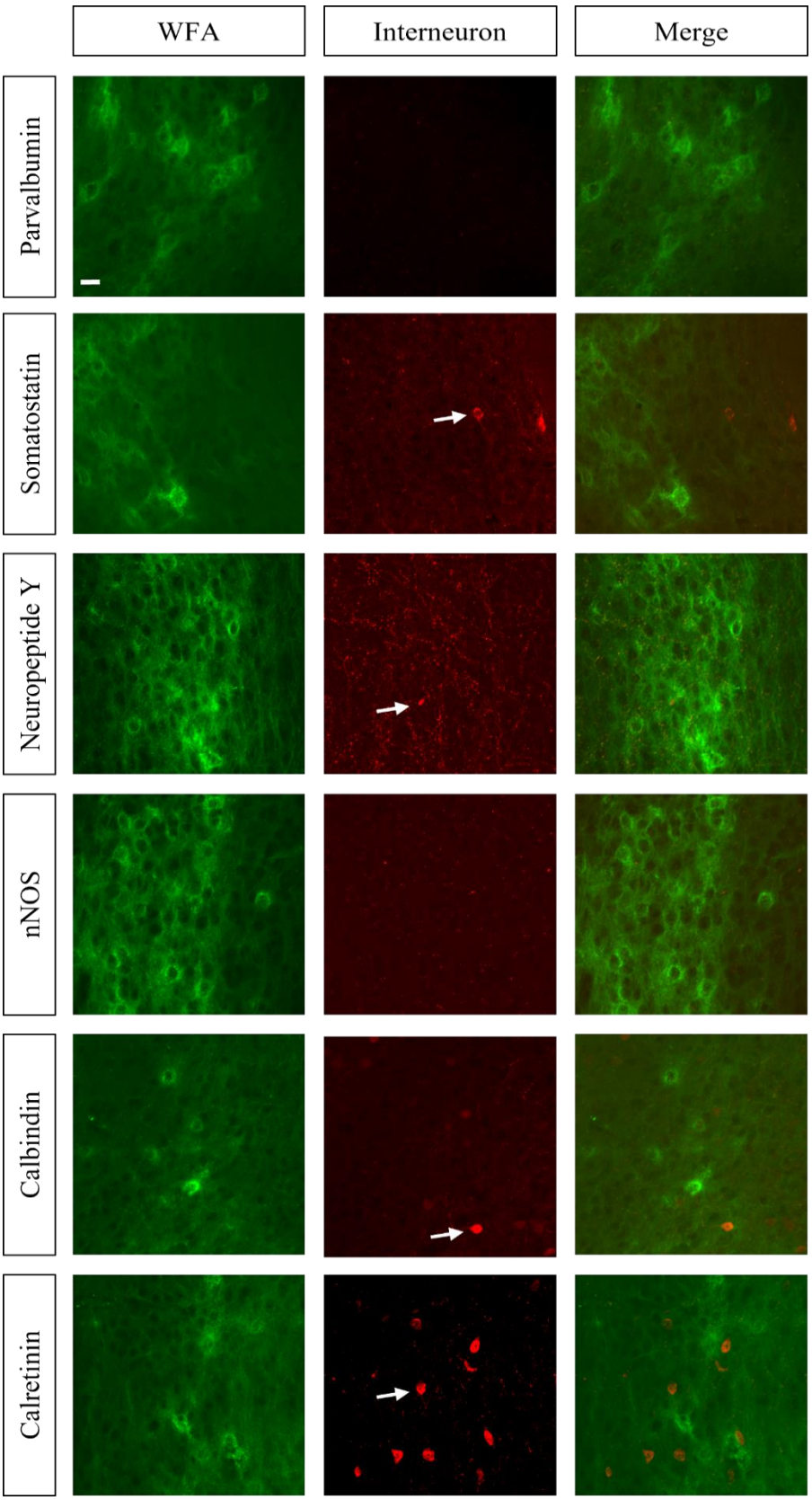

Figure 2.7. Perineuronal net and interneuronal marker labelling in the anteromedial bed nucleus of the stria terminalis. The anteromedial BNST of P60 male mice contains cells expressing the common interneuronal markers somatostatin, neuropeptide-Y, calbindin and calretinin (red fluorescence). The anteromedial BNST is completely devoid of parvalbumin expression, but some dendritic processes are positive for expression of neuronal nitric oxide synthase (nNOS). None of the cells expressing these interneuronal markers colocalised with WFA positive PNNs (green fluorescence). Representative images, experiments were performed independently with similar results on 4 animals. Scale bar = 20µm.

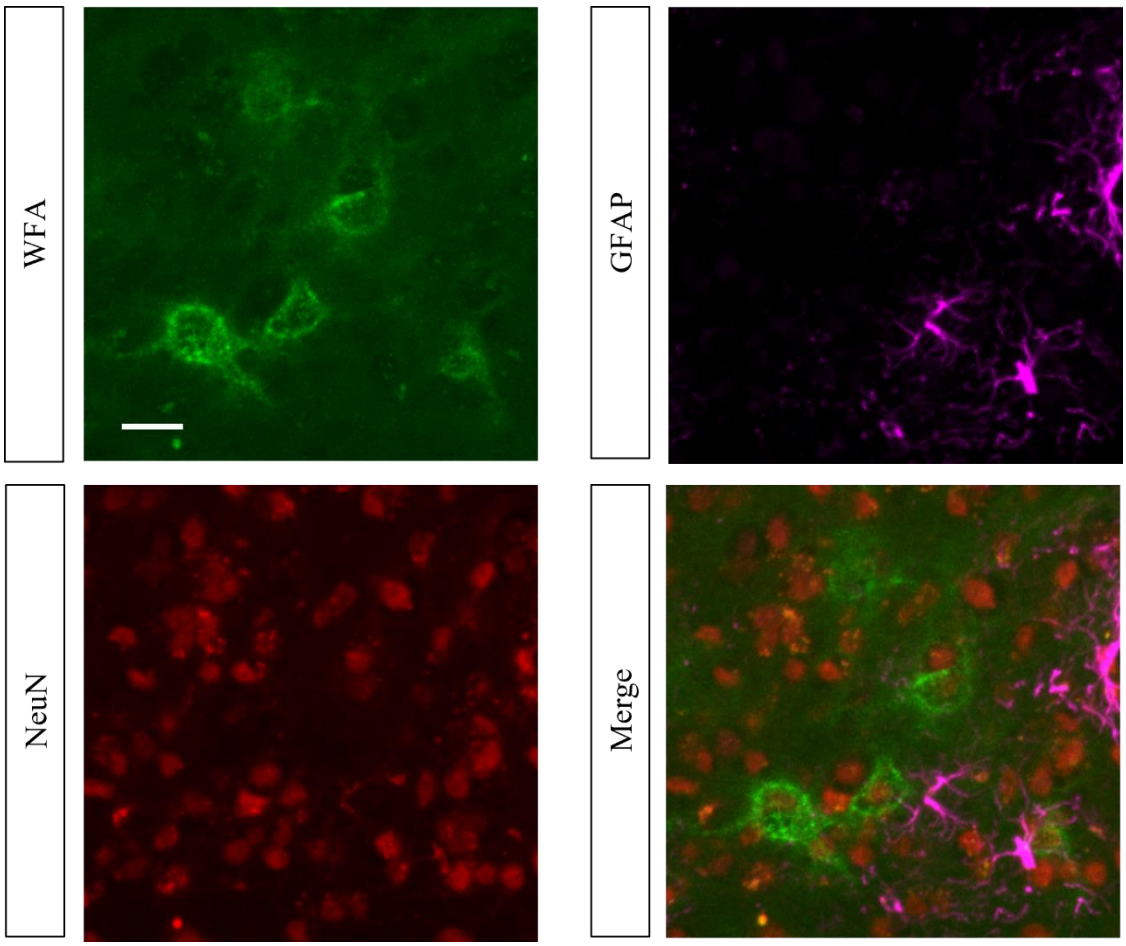

Figure 2.8 Cell type distribution of perineuronal nets in the anteromedial bed nucleus of the stria terminalis. WFA labelling (green) revealed PNN expression in the anteromedial BNST of P60 male mice. Immunolabelling for neuronal (red) and astrocytic (magenta) markers, NeuN and GFAP respectively, revealed that PNNs are exclusively expressed around neurons in the BNST. PNN expressing neurons are, however, typically adjacent to astrocytes in the BNST. Representative images, experiments were performed independently with similar results on 5 animals. Scale bar = 20µm.

2.4.5 Chemical composition of perineuronal nets in the bed nucleus of the stria terminalis

To investigate the presence of individual components within PNNs in the anterior BNST, immunolabelling for aggrecan, brevican and neurocan was performed, specifically using STMA sections. Markers for immunolabelling perineuronal net components were selected based on the availability of antibodies to label the tissue of interest: mouse BNST. Three CSPGs were chosen as potential future experiments may have included targeting of these genes and their gene products *in vivo.* As expression could not be accurately determined, however, representative images are presented for general interest.

No positive labelling was detected for aggrecan in the BNST. Positive labelling for both brevican and neurocan was observed in the BNST; labelling for both markers was diffusely spread across the tissue (Figure 2.9). The labelling protocol was performed in between 6-8 animals, on 3-4 BNST sections, for each CSPG marker, and all showed qualitatively similar results. Labelling for CSPGs was stronger in the cortex when tested during antibody optimisation, but CSPG labelling still did not directly co-localise with WFA labelling as documented in the literature by other groups (Morawski et al., 2010; Rowlands et al., 2018; see Appendix 1, Figure 6.2 for cortical labelling).

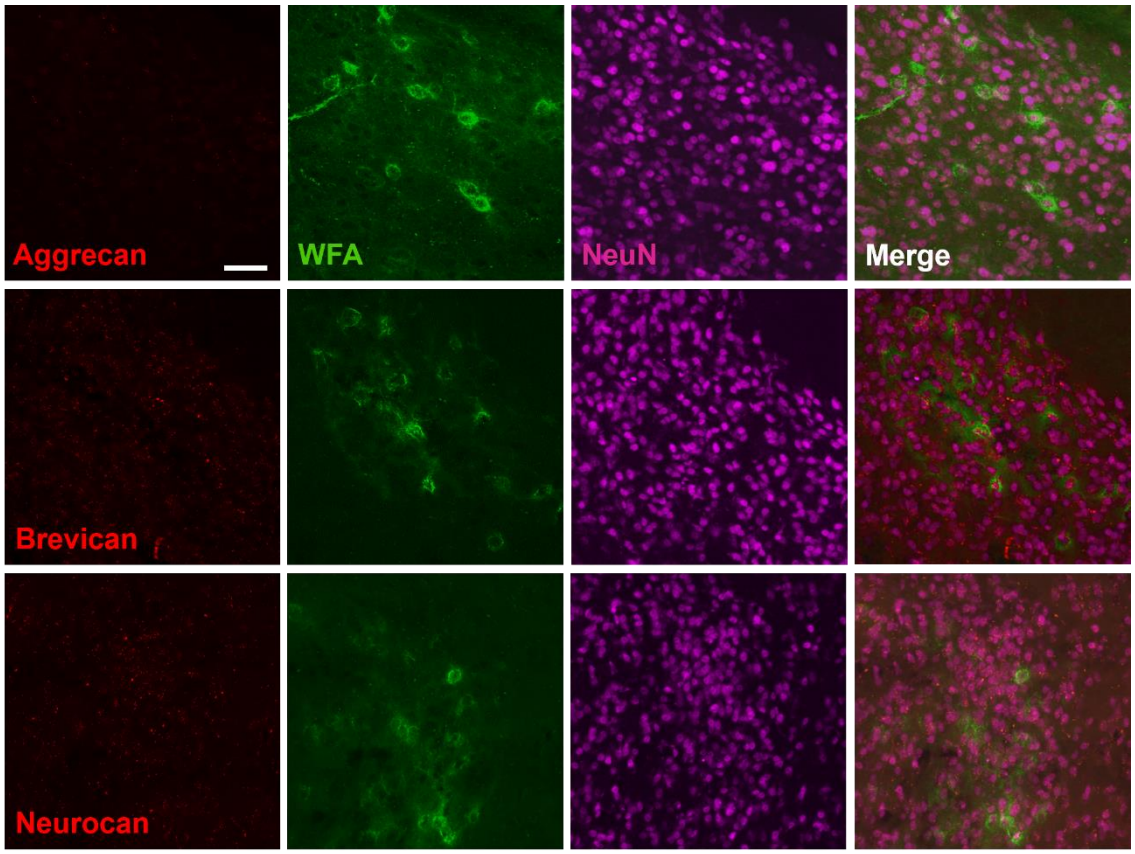

Figure 2.9. Perineuronal net component labelling in the anteromedial bed nucleus of the stria terminalis. Representative images of immunolabelling for (A) aggrecan, (B) brevican and (C) neurocan (red) with WFA labelled perineuronal nets (green) and NeuN labelling to show neuronal cell bodies (magenta). Brevican and neurocan labelling was diffusely spread across the tissue, but no labelling was detected when targeting aggrecan in the BNST. Representative images, experiments were performed independently with similar results on 4 animals. Scale bar = 50µm.

2.5 Discussion

In the current chapter, the formation and expression of PNNs in the anterior BNST has been investigated in detail for the first time. Labelling with WFA revealed a developmental time course of PNNs in the BNST, with earliest expression detected at P30 and greatest expression, both numerically and based on WFA labelling intensity, at P210 (Figure 2.5 and Figure 2.6). Overall, PNN number exclusively increased in the BNST subnuclei with age (Figure 2.5). The subnucleus with the greatest PNN expression in adulthood was identified to be the STMA (Appendix 1 Table 1.3; Appendix 1 Table 1.6). Immunolabelling to determine the nature of PNNs in the BNST found PNNs to be expressed exclusively around neurons (Figure 2.8) and revealed diffuse expression of PNN components brevican and neurocan (Figure 2.9). Additional labelling for interneuronal markers showed a lack of co-localisation between PNNs and tested interneuronal markers (Figure 2.7).

Two primary methods are currently used for detecting PNNs in the CNS: fluorescently coupled lectins and antibodies against specific PNN components. Lectins including WFA and *vicia villosa agglutinin*, which bind N-acetylgalactosamine residues on the GAG chains of chondroitin sulfate proteoglycans (CSPGs), are the most widely used method for PNN detection (Nakagawa, et al., 1986; Kosaka & Heizmann, 1989; Hartig, et al., 1992). Antibodies against PNN components, including aggrecan and hyaluronan, are more targeted and are therefore more useful for the detection of specific molecules of interest within PNNs (Matthews, et al., 2002; Dityatev, et al., 2007; Giamanco, et al., 2010; Yamada & Jinno, 2016). However, significant molecular heterogeneity has been identified in studies comparing the two methods (Matthews, et al., 2002; Irvine & Kwok, 2018). Multilevel approaches may, therefore, be the best currently available way of addressing this heterogeneity.

In the current study, WFA labelling was predominantly used to detect PNNs in the BNST due to the convenience of the method, particularly the short duration of the labelling protocol. Antibody methods were additionally employed to identify PNN components in the BNST. However, labelling was diffuse for brevican and neurocan and completely absent for aggrecan, the component hypothesised to be necessary for PNN formation and structural maintenance (Carulli, et al., 2007; Suttkus, et al., 2014; Rowlands, et al., 2018). Previously, the existence of different

glycosylation patterns of aggrecan which are present within distinct, but overlapping, populations of PNNs were identified (Matthews, et al., 2002). The antibody used in this study may, therefore, not have been specific to the particular isoform of aggrecan expressed in the BNST. Conversely, aggrecan may not be expressed in the BNST in any form and another CSPG or component might be more important for structural integrity of PNNs within the BNST. The poor labelling observed for other PNN components, brevican and neurocan, was likely due to poor antibody quality, as labelling was also diffuse in other brain regions with known PNN expression.

A confound of this immunolabelling may have been that the primary antibodies were raised in mouse, the same species as the tissue for labelling; the labelling in BNST looks to be non-specific. As there were no problems with other antibodies used for labelling in BNST slices treated exactly the same way, it is unlikely there were problems with antibody access in the fixed tissue sections. The versican and brevican antibodies did not have associated publications, however the neurocan antibody had been used by other groups, but not for the purposes of detecting PNNs, and was used to label rat tissue (Li, et al., 2016). As labelling of CSPGs was not successful in BNST sections, quantification of CSPG co-localisation with WFA labelled PNNs could not be performed.

PNNs have previously been identified in a wide variety of brain regions including sensory and motor cortices, the hippocampus, amygdala, thalamic regions and the cerebellum (Bruckner, et al., 2000; Yamada & Jinno, 2013; Gogolla, et al., 2009; Mirzadeh, et al., 2019; Lafarga, et al., 1984; Mabuchi, et al., 2001). PNNs were first identified in the mouse BNST by Horii-Hayashi et al. (2015), in a study screening multiple brain regions for PNNs. Only PNN presence within the BNST was indicated in the original paper – however, no representative images or detailed immunolabelling analysis of PNNs within the BNST was performed. More recently, PNNs were identified specifically in the posterior medial division of the BNST, part of the reproductive circuit, in both the mouse and marmoset (Ciccarelli, et al., 2021).

In the current study of the anterior BNST, PNNs were exclusively identified around neuronal cell bodies and proximal dendrites of neurons (Figure 2.8). While PNNs were not found to be organised around glial cells, they were often found in close proximity to one another. Such observations are unsurprising, as the

synthesis of various PNN components, including neurocan, brevican, tenascin-R, phosphacan and cartilage linking protein (Crtl1) is glial-dependent (Giamanco & Matthews, 2012).

PNN organisation changes during development, from a more granular and diffuse structure in the earlier post-natal period to a more reticular structure towards adulthood (Ueno, et al., 2017b). Notably, some prefrontal regions including the PFC maintain PNNs with a granular morphology in adulthood, hypothesised to be due to the highly plastic nature of the PFC (Ueno, et al., 2017). Granular PNNs have more structural vulnerability and could therefore theoretically undergo morphological changes more readily (Ueno, et al., 2017; Kolb & Gibb, 2015; Carulli & Verhaagen, 2021). WFA labelling in the BNST revealed similarly granular PNNs (Figure 2.2), which lacked the distinct lattice-like structure observed in PNNs in the visual cortex or hippocampus (Lensjo, et al., 2017a). However, unlike in the PFC, some proximal dendrites of BNST PNNs were labelled with WFA, which was visually denser (Figure 2.3). The BNST, like the PFC, is a plastic brain region, particularly in response to stress and chronic exposure to drugs (Daniel & Rainnie, 2016; Le, et al., 2018; McElligott & Winder, 2009). Altogether, the morphological structure of PNNs within the BNST combined with previous evidence of neuronal plasticity in the BNST, suggests that BNST PNNs could be prone to remodelling and/or structural damage, more so than PNNs in other brain regions.

As key regulators of synaptic plasticity, PNNs form at the end of so-called critical periods of high synaptic plasticity, which are particularly sensitive to experience and environmental influence (Pizzorusso, et al., 2002; Gogolla, et al., 2009; Balmer, et al., 2009; Sengpiel, 2007; Nabel & Morishita, 2013). Critical periods are essential for development of both sensory systems, such as song learning or the establishment of ocular dominance, and memory systems, particularly those pertaining to emotional memories such as those created during fear conditioning. Critical periods in different brain regions occur at different times during post-natal development. Consequently, the time at which PNNs begin to be expressed across brain regions is also variable. In mice, PNNs are first detected in the brainstem at P4, somatosensory cortex and hippocampus at P14, amygdala at P16 and piriform cortex at P28 (Bruckner, et al., 2000; Yamada & Jinno, 2013; Gogolla, et al., 2009; Ueno, et al., 2019). Comparatively, here WFA labelling in

the BNST was first detected at P20, in broad agreement with the P21 time point identified by Horii-Hayashi et al. (2015). The distinct morphological structure of PNNs was not detected by labelling here until P30, however (Figure 2.3). P30 is comparatively late for PNNs to develop, though the BNST is a brain region which is under development for an extended period and is hypothesised to continue developing into adulthood (Chung, et al., 2002; Clauss, 2019). Notably, the period prior to P21 is the critical period for the development of anxiety via serotonin receptor activation in mice (Gross, et al., 2002; Gordon & Hen, 2004). Given the established role of the BNST in anxiety and the misinterpretation of non-threatening stimuli, the BNST is likely to play a role in the critical period associated with anxiety. This may explain the presence of PNNs in the BNST. Further, PNNs in the BNST may stabilise connections between the BNST and the central amygdala, as between post-natal weeks three to seven is the time in which resting functional connectivity between the BNST and central amygdala is increased in preadolescent primates (Oler, et al., 2017).

As PNNs begin to be expressed in different regions at different times they also mature, or reach their peak expression, at different rates. In mouse, PNNs in the amygdala mature around P45, while in the hippocampus PNNs reach maturity at P60, and in the somatosensory and piriform cortices PNNs mature at an even later time point, P77 (Gogolla, et al., 2009; Yamada & Jinno, 2013; Bruckner, et al., 2000; Ueno, et al., 2019). However, PNN development in amygdala and hippocampus has not yet been investigated beyond these time points. Hence, the conclusions drawn from the available data may not truly reflect the complete time course of PNN development in these regions.

In a human study investigating the expression of PNNs in *post-mortem* brains, PNNs were shown to mature in the hippocampus and medial prefrontal cortex around 14 years of age (Rogers, et al., 2019). As with the experiments performed in mice, however, the study did not investigate PNNs beyond this age. Moreover, tissues were only available for a limited number of subjects, therefore accurate conclusions about the complete time course of PNN development cannot be drawn from the available data.

Preliminary evidence from rodent and human studies suggests that PNNs mature in adolescence, which is consistent with their developmental role in various brain regions (Pizzorusso, et al., 2002; Gogolla, et al., 2009; Balmer, et al., 2009).

However, it has been hypothesised that the BNST is a brain region which continues to develop into adulthood (Chung, et al., 2002; Clauss, 2019). Therefore, two comparatively later time points of PNN expression (P210 and P365) were investigated in the current study. In mice, P210 and P365 roughly correspond to ‘mature adult’ and ‘middle age’, respectively (Flurkey, et al., 2007).. The comparatively late development of PNNs in the BNST, up to P60 in some subnuclei and beyond this time point in others, suggests that any potential critical period which the BNST might facilitate is likely to be lengthier than those studied in other brain regions (Pizzorusso, et al., 2002; Gogolla, et al., 2009; Balmer, et al., 2009). Conversely, PNNs in the BNST may not be responsible for regulation of a critical period. As PNNs are experience driven, those in the BNST may develop as a result of gained experiences, most likely those of an emotional nature, given the established connections of the BNST in both rodents and humans (Davis, et al., 2010; Pego, et al., 2008; Avery, et al., 2016).

PNNs were quantified in this chapter using two distinct methods: WFA labelling intensity and PNN number. Both methods are used widely in PNN research, though most studies only consider one or the other (Gogolla, et al., 2009; Ueno, et al., 2017b; Guadango, et al., 2020). Here, each method produced slightly different results, at a granular level, however there was agreement between both methods in that PNN expression increases throughout development in the BNST. There are advantages and disadvantages to each method of PNN quantification. Quantification of PNN number provides tangible values which are easily understood; however, the method may be open to researcher biases when determining what is, or is not, considered a PNN. Conversely, quantification of PNN intensity is especially useful for measuring the structural integrity of a PNN, and automated programmes to measure intensity can reduce researcher biases, but changes in absolute PNN number cannot be identified. As such, using both methods is preferable, to capture differences in both PNN number and structure.

WFA labelling of the BNST at different developmental time points, to examine the spatiotemporal expression of PNNs, revealed specific subnuclei locations of high density PNN expression; particularly the STMA (Figure 2.4; Appendix 1 Table 1.3; Appendix 1 Table 1.6). The STMA is one of the lesser studied BNST subnuclei, but the presently established connections between the STMA and other brain regions suggest the STMA could mediate anxiogenic effects of the

BNST (Gungor & Pare, 2016). The STMA receives olfactory projections from the medial amygdala, contextual projections from the subiculum and dense glutamatergic projections from the basomedial amygdala (Cullinan, et al., 1993; McDonald, et al., 1999). Given that threatening odours and contexts can generate an anxiogenic response, evidence suggests the STMA could, in part, be responsible for mediation of the anxiogenic response to such stimuli.

In the early stages of PNN characterisation in other brain regions, PNNs were predominantly found around fast-spiking PV-positive GABAergic interneurons (Hartig, et al., 1992; Schuppel, et al., 2002; Dityatev, et al., 2007). While PNNs are still largely expressed around PV-positive neurons, increasing research has identified heterogeneity among PNN expressing neurons in other regions and in other species (Hausen, et al., 1996; Carstens, et al., 2016; Morikawa, et al., 2017; Horii-Hayashi, et al., 2015). Contrary to the PV-positive PNN ensheathed neurons in the rodent cortex, in human cortices, particularly somatosensory and motor, PNNs are more commonly expressed around mostly excitatory, pyramidal cells (Hartig, et al., 1994; Hausen, et al., 1996). In the rat basolateral amygdala, PNNs surround both PV-positive and -negative neurons, whereas in the mouse, PNNs are exclusively expressed around excitatory neurons (Baker, et al., 2017; Morikawa, et al., 2017).

Co-labelling for interneuronal markers in the BNST did not allow the determination of the chemical nature of the neurons surrounded by PNNs (Figure 2.7). PV labelling in the BNST was negative and no cell bodies expressing the marker were identified in any part of the anterior BNST (Figure 2.7). WFA labelled PNNs within the BNST did not co-localise with any tested interneuronal markers including somatostatin, neuropeptide Y, calbindin and calretinin (Figure 2.7). Immunolabelling for these markers did identify populations of positively labelled neurons, however, in agreement with previous studies which have identified neuronal populations expressing somatostatin, neuropeptide Y, calbindin and calretinin in the rodent BNST (Bota, et al., 2012; Allen, et al., 1983; Pleil, et al., 2012; Gos, et al., 2014; Nguyen, et al., 2016). Notably, in mouse the BNST has a density of calbindin expressing neurons twice as great as the basolateral amygdala, ten times as great as the subiculum and twenty times as great as the CA3 region of the hippocampus, with comparable calbindin density to the paraventricular nucleus of the thalamus and infralimbic region of the prefrontal

cortex (Bjerke, et al., 2021). Somatostatin and calretinin are also abundant in the BNST; ~17% of anterodorsal BNST neurons express somatostatin and ~10% express calretinin, though comparable data for other brain regions are not available (Nguyen, et al., 2016). Excitatory neurons expressing CAMKII or excitatory amino acid carrier (EAAC) have been reported in the BNST; therefore PNNs in the BNST may surround excitatory neurons, which is comparatively rare but has been reported in the amygdala (Morikawa, et al., 2017).

Whilst the chemical nature of PNN expressing neurons in the BNST remains elusive, given previous evidence from other brain regions, the common feature which relates the majority of PNN expressing cells studied thus far is that they are fast spiking and likely to project to pyramidal neurons (Blosa, et al., 2013; Cabungcal, et al., 2013; Rossier, et al., 2015; Slaker, et al., 2018). The complex organisation and unique composition of the BNST may contribute to a novel role for PNNs in the central nervous system.

2.6 Conclusions

In this chapter, PNNs have been characterised in the anterior BNST for the first time. PNNs appear in the BNST at approximately P30, and continue to develop into adulthood, with greatest expression of PNNs at P210 in several of the studied subnuclei. Comparing PNN expression across BNST subnuclei, the anteromedial BNST expressed the greatest number of PNNs across developmental stages and will therefore be the region of focus in the proceeding studies. Populations of calretinin, calbindin, somatostatin and neuropeptide Y positive cells were identified in the BNST, however none of these were found to co-express PNNs. This suggests that PNNs in the BNST may not be expressed around interneurons and may instead be expressed around other neuronal subtypes, possibly even neurons which signal through glutamatergic, rather than GABAergic, transmission. Notably, no populations of PV-positive cells were detected in the BNST, indicating that BNST PNNs differ from those observed in other brain regions, where PNNs are usually located around PV-positive interneurons. This suggests that the PNNs in the BNST have unique features, and further investigation into what differentiates BNST PNNs from those in other brain regions may reveal more about their physiological role. The granular morphology of BNST PNNs also suggests that they may be more susceptible to remodelling. As plastic changes have been observed in the BNST following exposure to stressful stimuli, and PNNs are known regulators of neuronal plasticity, PNNs may be affected by exposure to stressful stimuli and may consequently influence the stress response.

Chapter 3 – Involvement of neurons and perineuronal nets within the bed nucleus of the stria terminalis in the stress response

3.1 Introduction

The effect of stress on perineuronal net expression

A shared feature in the underlying aetiology of many psychiatric disorders, including anxiety disorders, is an impairment in neurodevelopmental and adult neural plasticity systems including synaptogenesis, long term potentiation and synaptic pruning (Vyas, et al., 2002; Mitra & Sapolsky, 2008; Maggio & Segal, 2011; Cook & Wellman, 2004; Radley, et al., 2004; Radley, et al., 2006; Pego, et al., 2008; Lubbers, et al., 2014). The ECM and its various organisations, particularly PNNs, are well documented to be involved in the regulation of neuronal plasticity (McKeon, et al., 1991; Smith-Thomas, et al., 1994; Davies, et al., 1999; Cheah, et al., 2016; Frischknecht, et al., 2009; Dityatev, et al., 2007). PNNs may therefore affect the development and progression of psychiatric disorders. Moreover, PNNs may themselves be affected by stimuli known to facilitate the development of psychiatric disorders, including stress.

Studies using early life stress models have so far predominantly been focused on investigating the effect of stress on PNN expression (Ueno, et al., 2018; Murthy, et al., 2019; Santiago, et al., 2018). Juvenile mice (P21) subjected daily for 8 days to multiple stressors, including tail pinch, restraint stress and food and water deprivation show less intense WFA labelling in the dorsal anterior cingulate, infralimbic, and layer 2/3 motor cortices, compared to unstressed control mice when measured 2 days after the last stressor (Ueno, et al., 2018). Conversely, exposure to the multimodal stress protocol did not affect the number of PNNs in the hippocampus, mPFC or primary motor cortex (Ueno, et al., 2018). The early life stress model employed in the study by Ueno et al. (2018) did not affect anxiety-like behaviour measured in the EPM. The effect of the 8-day stress paradigm in the study on depression-like behaviour was inconclusive, since no difference in behaviour was observed in a tail suspension test and increased immobility time was observed only during the first few minutes of a forced swim test (Ueno, et al., 2018). Hence, increased expression of PNNs in key brain regions may be protective against development of aversive behaviours.

Maternal separation and early weaning increases PNN deposition around ventral hippocampal PV-positive interneurons and promotes anxiety-like behaviour in stressed mice compared to unstressed controls when measured in adulthood (P60-70; Murthy, et al., 2019). Inhibitory neurons in the hippocampus play an important role in the development of anxiety-like behaviour induced by early life stress (Adhikari, et al., 2010). A subpopulation of hippocampal neurons develop greater expression of PNNs following maternal separation and early weaning (Murthy, et al., 2019). Thus, change in PNN expression in the hippocampus could play a role in the development of anxiety-like behaviours.

An alternative model of early life trauma, where rat pups are reared in an environment with insufficient nest building materials, results in increased threat responses to predator odour (Walker, et al., 2017). In a similar model, rats subjected to early life stress exhibit reduced WFA labelling intensity of PNNs in the anterior, but not posterior, basolateral amygdala upon weaning, and also show enhanced response to predator odour compared to controls (Santiago, et al., 2018). The behavioural effect of increased threat to predator odour is recapitulated when rats raised in conventional bedding are subjected to PNN degradation in the basolateral amygdala (Santiago, et al., 2018). Therefore, PNNs in the basolateral amygdala, or lack thereof, may have a role in supporting the enduring behavioural effects of early life stress.

More limited work has been undertaken to investigate the effects of stress on PNN expression in adolescents and adults (Yu, et al., 2020; Chen, et al., 2016). Unpredictable chronic mild stress (UCMS) is a paradigm most commonly employed in adult rodents to induce behavioural changes related to enhanced stress response; for example, increased anxiety- and depression-like behaviours. During the UCMS paradigm, rodents are exposed daily for 2-4 weeks to alternating mild, non-painful stressors including absence of bedding, cage tilting, and short periods of restraint stress (Willner, et al., 1992; Surget & Belzung, 2008). UCMS results in decreased PNN density and aggrecan expression in the prelimbic cortex of adult rats (Yu, et al., 2020). PNN density and neurocan expression are consistently reduced in the prelimbic cortex of rats which show vulnerability to UCMS, compared to resilient and control groups. Therefore, increased PNN density in the prelimbic cortex may protect against the development of depressive-like behaviours induced by stress.

PNN expression may also be altered by pharmacological agents used to treat psychiatric disorders, suggesting a potential novel mechanism through which these treatments might act (Ohira, et al., 2013; Guirado, et al., 2014; Umemori, et al., 2015; Chen, et al., 2016; Alaiyed, et al., 2019). Administration of fluoxetine, a selective serotonin reuptake inhibitor (SSRI) used to treat anxiety and depression, results in a reduction of WFA-labelled PNNs in the hippocampus and mPFC of mice (Ohira, et al., 2013; Guirado, et al., 2014). Furthermore, exposure to fluoxetine *in utero* delays the formation of PNNs in both the hippocampus and amygdala (Umemori, et al., 2015). Conversely, following UCMS, fluoxetine elevates PNN expression in the mPFC, and in turn reduces susceptibility to developing UCMS-induced anxiety- and depressive-like behaviours (Chen, et al., 2016).

Venlafaxine, a serotonin and noradrenaline reuptake inhibitor (SNRI) clinically used to treat depression and anxiety, actively promotes proteolysis of PNNs (Alaiyed, et al., 2019). The therapeutic mechanisms of action of SNRIs are yet to be fully elucidated; changes to PNN expression induced by SNRI treatment may be directly related to the efficacy of SNRIs, though this hypothesis is yet to be fully explored. Conversely, there are other antidepressant drugs whose actions are directly affected by PNNs (Donegan & Lodge, 2017). For example, following PNN degradation in mouse ventral hippocampus, the antidepressant effect of rapidly acting antidepressant ketamine is lost (Donegan & Lodge, 2017).

Altogether, PNNs may have a key role in response to stress and, in turn, the development of depressive- and anxiety-like behaviours. PNN expression may be altered as a result of stress and may also affect and indeed mediate the action of established pharmacological treatments for psychiatric disorders. The functional contribution of PNNs to the stress response are evidently complex. However, further elucidation of the role of PNNs in the stress response may provide insight into the mechanisms underlying the development of stress-associated disorders and bring us one step closer towards effective new treatments.

Here, a restraint stress model was employed to investigate the effect of stress on the expression of PNNs. Restraint is a commonly used emotional stress model of anxiety-like behaviour in rodents, which, in comparison to human anxiety disorders, most closely recapitulates post-traumatic stress disorder symptoms

(Mendonca & Guimaraes, 1996; Padovan & Guimaraes, 2000; Chiba, et al., 2012). Both acute and chronic restraint stress were previously shown to engage the rodent BNST (Adami, et al., 2017; Oliveira, et al., 2015; Schmidt, et al., 2019; Vyas, et al., 2003). However, for procedural simplicity, and to prevent development of co-morbidities often seen with chronic stress paradigms (depressive-like behaviours) which make measurement of singular behaviours more challenging, a repeated acute restraint stress model of 2-hour restraint for three consecutive days was chosen as the stressor here. Three days of consecutive restraint has previously been shown to increase ACTH and corticosterone levels and anxiety-like behaviour, with this exact protocol (2h stress daily for three days) documented to induce the stress response by increasing plasma corticosterone, indicative of HPA activation (Gameiro, et al., 2006; Sadler & Bailey, 2016). Notably, this stress protocol previously reported quantitatively similar results in C57BL/6 mice and the more anxious BALB/c mouse line (Sadler & Bailey, 2016). As the possibility of using transgenic mice in later studies here was considered, and most transgenic lines are bred on a C57BL/6 background, c57BL/6 mice were used in this study to make results comparable across future studies.

To examine anxiety-like behaviour in mice, the EPM was chosen as it is one of the ethological paradigms to have face, construct, and predictive validity. The face validity of the EPM is demonstrated by the ability to measure the perceived fear/anxiety rodents show for open brightly lit spaces; greater anxiety-like behaviour is shown by mice that spend more time in the closed arms of the maze. The EPM also has construct validity, whereby anxiogenic drugs reduce time spent in the open arms of the maze and anxiolytic drugs increase this time (Pellow, et al., 1985). Finally, the EPM has predictive validity; animals that make more entries and spend more time in the open arms of the maze also make increased entries to the central zone of the OFT, furthermore, exposure to the open arms of the maze increases plasma corticosterone levels and risk-assessment behaviour in both rats and mice (Rodgers, et al., 1999). The EPM also shows translational relevance; in the human EPM, participants spent more time in the ‘safe’ closed arms of the maze and avoided spending time in the open arms (Biedermann, et al., 2017). These behaviours were further supported by subjective anxiety ratings by participants, an aspect which cannot be tested in the

rodent EPM. Furthermore, participants showed increased physiological measures of anxiety including heart and respiration rate and skin conductance, demonstrating cross-species validity of the EPM.

The BNST is a key region in the development and expression of anxiety-like behaviours, which are likely to be facilitated by plastic changes in the region (Conrad, et al., 2011; Vyas, et al., 2003; Glangetas, et al., 2013; Glangetas, et al., 2017; Pego, et al., 2008). Results reported in Chapter 2 demonstrate differential expression of PNNs across BNST subnuclei, with greatest expression of PNNs in the anteromedial division (STMA). PNNs within the BNST are likely to play a key role in regulating emotional behaviour given the involvement of PNNs in restricting synaptic plasticity. However, the direct contribution of PNNs in the BNST to the development of anxiety-like behaviours following stress has not yet been discovered.

3.2 Aims

In the current chapter I will address the following three main aims:

(1) determine BNST engagement and subsequent changes to anxiety-like behaviour in a mouse model of repeated restraint stress
(2) examine alterations to composition and structure of perineuronal nets in mouse BNST following repeated restraint stress
(3) identify changes in neuronal firing, detected extracellularly, in mouse BNST as a consequence of repeated restraint stress

3.3 Methods

3.3.1 Animals

Male, wild-type C57BL/6J mice aged between 8-13 weeks, were used in these experiments. Mice were housed in groups of 3-4, in individually ventilated cages, in temperature-controlled rooms, on a 12-hour light/dark cycle, with lights on at 6:30am, with *ad libitum* access to food (Teklad Global 14, 14% protein diet, Envigo) and water. All procedures were carried out in accordance with the UK Animal (Scientific Procedures) Act 1986. Experiments were approved by the UK Home Office and University of Exeter Local Ethics Committee.

3.3.2 Mouse model of anxiety-like behaviour

Repeated acute restraint stress model

Mice were subjected to a two-hour restraint stress session for three consecutive days to induce anxiety-like behaviour. Mice were restrained in ventilated 50 mL polypropylene, conical, centrifuge tubes, which allowed a close fit to mice (Starlab, UK; Figure 3.1). Restraint was performed in a procedural room, in the home cage. Restraint took place between 10.00am and 12.00pm each day, after which mice were released back into the home cage. Mice were allowed to acclimate for a further hour, before being returned to the housing room at 1.00pm. Mice were continually observed during the restraint stress procedure. Centrifuge tubes were cleaned after use and reused for further cohorts of mice. Control animals were left undisturbed in their cages until the next phase of the experiment.

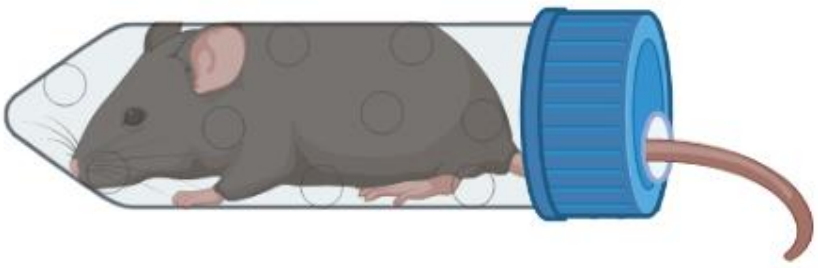

Figure 3.1. Schematic illustration of restraint stress apparatus. Mice were restrained in modified 50 mL polypropylene centrifuge tube restrainers, with air holes drilled for ventilation and a hole in the cap for the tail. Figure created using BioRender.

Evaluation of anxiety-like behaviour – elevated plus maze

The EPM is a commonly used behavioural paradigm for the assessment of anxiety-like behaviour in rodents (Pellow, et al., 1985; Rodgers & Dalvi, 1997; Korte & De Boer, 2003). The method centres around the approach-avoidance conflict; the balance between a rodent's desire for novelty and exploration and their aversion to open, elevated, and brightly illuminated spaces.

The EPM used here was constructed by the Technical Services team at the University of Exeter Mechanical Workshop. The maze was fabricated from melamine coated medium-density fibreboard and consisted of two open arms (30 cm in length) and two closed arms (30 cm in length, with 12 cm high walls), with a 10 cm x 10 cm central square, elevated 60 cm off the floor on metal legs (Figure 3.2). The open arms of the maze were brightly lit for the duration of the experiment, with illumination levels of 254 lx; anxiety-like behaviour is triggered in the EPM at illumination levels of ~3 lx and is not light-intensity dependent above this threshold (Becerra Garcia, et al., 2005).

EPM testing was performed accordingly with Attwood et al. (2011). Mice were individually placed in the centre square of the maze, facing an open arm, and were allowed to freely explore for five minutes. 70% ethanol was used to clean the EPM between sessions in order to prevent any odorant cues. EPM sessions were video recorded using a ceiling mounted webcam and Logitech software (Logitech, Switzerland). Video recordings were analysed after completion of behavioural experiments using Viewer^2 software (Biobserve GmbH, Germany). Using the software, the arms of the maze were manually identified as 'zones'. Mice were identified by three focus points: the tip of the nose, the middle of the body and the base of the tail using the contrast between the dark fur of the mouse and the white floor of the EPM. Focus points were adjusted manually for each mouse to ensure optimum tracking. The focus point located at the middle of the body was used to determine the location of the mouse in the maze. When the point at the middle of the body crossed the threshold of one of the maze arms, an entry to the arm, or 'zone', was recorded. Number of zone entries, along with time spent in each zone, were automatically counted by the Viewer^2 software.

The outcome measures assessed to determine anxiety-like behaviour in the EPM were as follows: the total number of open arm entries, the length of time spent in the open arms of the EPM, the anxiety index, calculated by the number of open arm entries divided by the total number of entries to all arms of the EPM. Additionally, total number of entries and distance travelled have been assessed as measures of activity in the maze.

Four groups of mice were used for this experiment, with individual mice constituting the 'experimental unit'. A control group which received no treatment and was subjected to the EPM at the same time as mice 24 hours post-stress, and three experimental groups which were all subjected to two hours of restraint stress for three consecutive days and tested in the EPM at discrete time points following the final day of restraint: 24 hours, 7 days and 14 days. N numbers for each group were as follows: control, 10; 24 hours post-stress, 9; 7 days post-stress, 7; 14 days post-stress, 4. The groups of the greatest experimental interest for comparison, control and 24 hours post-stress, were prioritised in terms of number of mice to determine the primary outcome of whether the restraint protocol was sufficient to induce anxiety-like behaviour in the EPM. The sample sizes to assess the secondary outcome of persistence of anxiety-like behaviour in the EPM following stress are smaller and therefore likely underpowered.

Animals were assigned to groups randomly and the experimenter was blinded to the treatment when conducting analysis. A Shapiro-Wilk test was used to test for normality of sample distributions. A one-way ANOVA which assumes equal variance and normal distribution of samples, was then used to compare group means was performed to determine differences between the control group and experimental groups, and a Tukey test was used to correct for multiple comparisons. Equal variance was not specifically assessed prior to ANOVA. Multiple comparisons were corrected for using a Dunnett post-hoc test. As groups have unequal sample sizes, caution should be taken when interpreting results. All data are presented as dot plots with mean ± SEM; $*p < 0.05$, $**p < 0.01$, $***p < 0.001$.

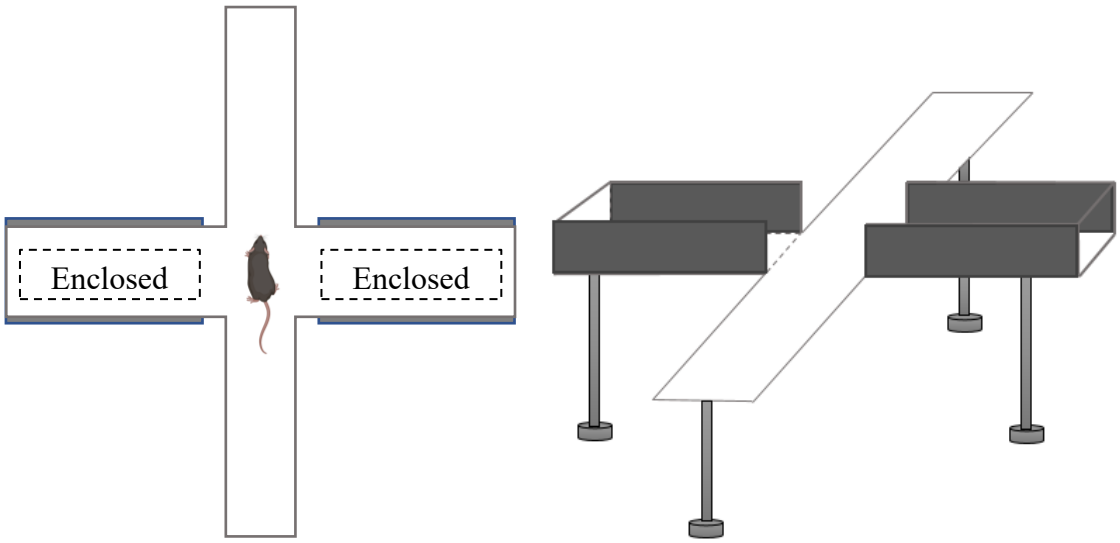

Figure 3.2. Schematic illustration of elevated plus maze apparatus, aerial and 3D side view. The elevated plus maze consists of two sets of bisecting pairs of arms. Two, facing each other, are open and brightly lit. The other two, also facing each other, are enclosed by walls. Figure created using BioRender.

3.3.3 Labelling of recently active neurons

Two groups of mice were used in these experiments. The experimental group consisted of ten mice that were subjected to two hours of restraint for three consecutive days. Control mice were age matched and did not undergo the restraint stress protocol. Following the final session of restraint stress, a two hour session on the third consecutive day, mice were returned to their home cages for one hour, prior to being culled by sodium pentobarbital anaesthesia (50 mg kg^{-1}) and transcardial perfusion with PBS and PFA (4%).

Brains were fixed overnight in 4% PFA and slices were prepared as in section 2.3.3. Every third section through the anterior BNST, bregma 0.62 mm to 0.02 mm, was used for c-Fos immunolabelling; six BNST sections were used for immunolabelling for each mouse (Franklin & Paxinos, 2007). Slices were incubated in blocking solution for one hour at room temperature on a horizontal rotator, set at a slow speed to gently agitate the slices. Slices were subsequently incubated in blocking solution with anti-c-Fos antibody (1:500; Cat No 2250; Cell Signaling Technology, USA) overnight at 4 °C. Slices were washed 3 times for 15 minutes with PBST and finally incubated in blocking solution with secondary antibody (anti-rabbit AlexaFluor® 647; 1:1000; ThermoFisher Scientific) for one hour at room temperature, protected from light. Slices were then washed with PBS prior to mounting on Poly-D-Lysine coated slides (VWR, UK) with fluorsave

reagent (Merck, UK). Slides were dried overnight before imaging with a Zeiss LSM 5 Exciter confocal microscope (Zeiss, Germany).

A single field of view image was taken for each slice, with six slices used for quantification in total for each animal. Images were overlaid with the anterior BNST masks previously described in section 2.3.2. Counting of c-Fos positive cells was performed using the count tool within ImageJ, with each c-Fos positive cell manually selected by the experimenter and automatically counted by the programme (v1.53e; NIH, USA). As only one in three slices through the BNST were used for quantification, final counts of c-Fos positive cells were extrapolated by multiplying original counts by three. An unpaired, two-tailed t-test was performed between the two groups to determine whether numbers of c-Fos positive cells were significantly different following restraint stress. All data are presented as dot plots with mean ± SEM; $*p < 0.05$, $**p < 0.01$, $***p < 0.001$.

3.3.4 Perineuronal net characterisation following repeated acute restraint stress

Quantification of perineuronal net component expression

Mice were subjected to the restraint stress protocol and were sacrificed 7 or 14 days post-stress. Control group mice were age matched and did not undergo restraint. Mice were anaesthetised with sodium pentobarbital (50 mg kg^{-1}) and transcardially perfused with ice cold PBS supplemented with protease inhibitors and diethyl pyrocarbonate. Left and right BNST were dissected manually from coronal slices, bregma 0.62 mm to 0.26 mm, under a dissection microscope (Leica SD6 Stereo Zoom, Leica, UK). BNST tissue was homogenised (QIAzol reagent, Qiagen, Germany) and total RNA was isolated (RNeasy™ Lipid Tissue Mini Kit, Qiagen, Germany). Amount of isolated RNA was quantified using a spectrophotometer (NanoDrop 2000, Thermo Scientific,USA). Between 11-42 ng/µl of RNA was isolated per mouse sample, in 30 µl elution. For each sample 150 ng template RNA was used for conversion to cDNA (EvoScript Universal cDNA Master Kit, Roche, Switzerland). qRT-PCR for PNN components was performed using the following programme (Mastercycler, Eppendorf, Germany): 95°C for 15 minutes, 95°C for 15 seconds, 55°C for 30 seconds, 72°C for 30 seconds; steps two, three and four were repeated 40 times with the primers

detailed in Table 3.1 for each target gene, and for β-actin, a housekeeping gene to which target gene expression was normalised.

Forward and reverse primer sequences were generated against target genes and compatibility checked using the NCBI primer-BLAST tool (Ye, et al., 2012). Primer3 (Untergasser, et al., 2012) was used to select primers with optimum properties; 18-24 bases in length, 40-60% GC content, melting temperature between 50°C and 60°C and melting temperature of forward and reverse primers being within 5°C of each other, and absence of complementary regions. See Appendix 3 for visualisation of full gene sequences and primer positions. For brevican expression quantification, four mice were analysed per group. For neurocan and tenascin-R expression quantification, three mice were analysed per group. Three technical repeats were performed for each qRT-PCR reaction, and values were averaged per animal. Ct values were obtained from the qPCR analyser when the first reliable product signal was detected. Gene expression values were calculated using the Livak $2^{-\Delta\Delta CT}$ method (Livak & Schmittgen, 2001). Relative differences between the control gene (β-actin) and experimental genes of interest were calculated, per animal, and averaged (ΔCt). The difference of gene expression from the average for each animal was then determined (ΔΔCt), and $2^{-\Delta\Delta Ct}$ was calculated for each animal and averaged. The difference of $2^{-\Delta\Delta Ct}$ from the average was calculated per animal as the fold change; the average for the control group was 1. The relative gene expression for the post-stress experimental groups of animals was calculated by comparing relative fold changes in expression to the $2^{-\Delta\Delta Ct}$ average for the control animals.

Table 3.1. qRT-PCR primers used to determine expression of perineuronal net components

Gene	Gene ID	Forward /reverse	Sequence	Position (nt bases)	Product length (nt)	Melting temperature (°C)
Brevican	12032	F	GATGGAGAGCGAGTCTCGTG	1323-1342	153	59.97
		R	TCTGAGGACTCGGTAGGTGG	1475-1456		60.03
Neurocan	13004	F	GGGCTCTAGGGCTGAAGAAA	59-78	153	60.84
		R	CTAGGAGAAGCAGCCACAGC	211-192		60.3
Tenascin-R	21960	F	CAACAGCCTTGGGGATACTC	48-67	199	59.55
		R	GAGATTCCGTATGGCAGCAT	246-227		60.07
β-Actin	11461	F	TCCTTAGCTTGGTGAGGGTG	2701-2720	210	59.02
		R	CCTGCTTGCTGATCCACATC	2910-2891		58.98

Perineuronal net expression and morphology

Mice underwent the restraint stress protocol and were culled at 7 or 14 days post-stress, as described in section 2.3.2. The control group of mice were age matched and did not undergo restraint. BNST sections were sliced and labelled with WFA as described in section 2.3.3. For each animal, three 50 µm sections, containing the STMA nucleus, sampled 150 µm apart, were taken for counting and morphological analysis.

BNST masks were overlaid on the captured images and PNNs were counted in the STMA only, using the count tool within ImageJ (NIH, USA). For morphological analysis, magnified images of PNNs were acquired as three-layer z-stacks, with 0.1 µm between stacks and image size of 1024 x 1024 pixels, with the second layer of the stack being of optimum focus on the PNN surface. Each individual PNN was considered an experimental unit, with 5-6 PNNs imaged per animal, with 7 mice in each group. PNNs show variability, even in the same brain region, in the same animal, therefore each PNN was considered statistically independent. Total N numbers for each group were as follows: control, 41; 7 days post-stress, 40; 14 days post-stress, 40.

PNN morphology was analysed using the script 'Analysis of Perineuronal Net Units', APNU v1.1, previously developed and described by Kaushik et al. (2020). Briefly, after manual selection of the central point within each hole of an individual PNN unit, the programme calculated an outline of the PNN from the three confocal layer images. The output text file from the script provided values for a number of distinct parameters including: hole area (Area3Dhole), hole perimeter (Per3DECM) and intensity of matrix surrounding the hole (IntMean3DECM). In addition, PNN flatness was measured by the standard deviation of ECM intensity across the three Z planes (zSDECM), and PNN leakiness was measured by the minimum intensity of ECM in 3D space (IntMin3DECM).

One-way ANOVA was performed to investigate differences in morphological parameters between groups, with Tukey's *post hoc* test to account for multiple comparisons. All data are presented as bar plots with mean ± SEM; $*p < 0.05$, $**p < 0.01$, $***p < 0.001$.

3.3.5 Electrophysiological recording of putative single units in the bed nucleus of the stria terminalis following stress

Solutions

A sucrose-based solution and an artificial cerebral spinal fluid solution (aCSF) continuously bubbled with carbogen (95% O_2/5% CO_2) were prepared for electrophysiological recordings (Table 3.2). Sucrose solution was used for cutting brain slices, while aCSF solution was used to maintain slices both in the holding chamber and during recordings.

Table 3.2. Composition of sucrose-based and artificial cerebral spinal fluid solutions

Component	Sucrose (mM) pH 7.3, 290-300 Osm	aCSF (mM) pH 7.3, 290-300 Osm
Sucrose	189	-
D-glucose	10	10
$NaHCO_3$	26	24
KCl	3	3
$MgSO_4$	5	1
$CaCl_2$	0.1	2
NaH_2PO_4	1.25	1.25
NaCl	-	124

Slice preparation

Two groups of mice were used for these experiments: one group was exposed to the restraint stress protocol; these mice were killed 7 days following the final day of restraint. The second group, control mice, were age matched and were not subjected to restraint. Mice were killed by cervical dislocation, followed by decapitation, and the brain was quickly removed. The brain was sliced in ice cold sucrose solution, ~4°C, and a 400 µm coronal slice containing the STMA nucleus of the BNST was collected (bregma 0.62 mm to 0.02 mm). It was only possible to obtain one section of the STMA, at the thickness required for electrophysiological recording, per animal. Therefore, slices were hemisected to

maximise the tissue available to make recordings from. Slices were transferred to a holding chamber containing aCSF bubbled with carbogen and were incubated in a water bath for 30 minutes at 37°C, and then at room temperature for a further 30 minutes.

Multielectrode array recording

Slices were placed, recording side down, into a 60pMEA100/30iR-Ti-gr perforated multielectrode array (pMEA; Multi Channel Systems, Germany). The array comprised 59 recording electrodes and one reference electrode, with each electrode 100 µm apart, in a 6 x 10 layout. Each electrode had a diameter of 30 µm and the whole array covered an approximate total area of 707 μm^2, to record from the entire STMA nucleus (Figure 3.3).

Slices were acclimatised in pre-warmed, ~34°C, oxygenated aCSF in the pMEA recording chamber for 30 minutes prior to recording. Slices were held in place by vacuum generated negative pressure, through the perforations of the pMEA, and by a weighted slice harp (Warner Instruments, USA) to ensure recording stability. The recording chamber was continuously perfused with pre-warmed oxygenated aCSF from above and below at a combined rate of 0.9 mL min^{-1} (top flow 0.8mL min^{-1} and bottom flow 0.1mL min^{-1}; Figure 3.3).

Recordings were sampled at 50 kHz, and data were acquired using MC_RACK software, using a MEA1060 system and MEA1060UP amplifier (all Multi Channel Systems, Germany). Multi-unit activity was extracted via a second-order high-pass Butterworth filter with a cut-off frequency of 200 Hz and multiunit spikes crossing a threshold of -16.5 µV were extracted for further analysis.

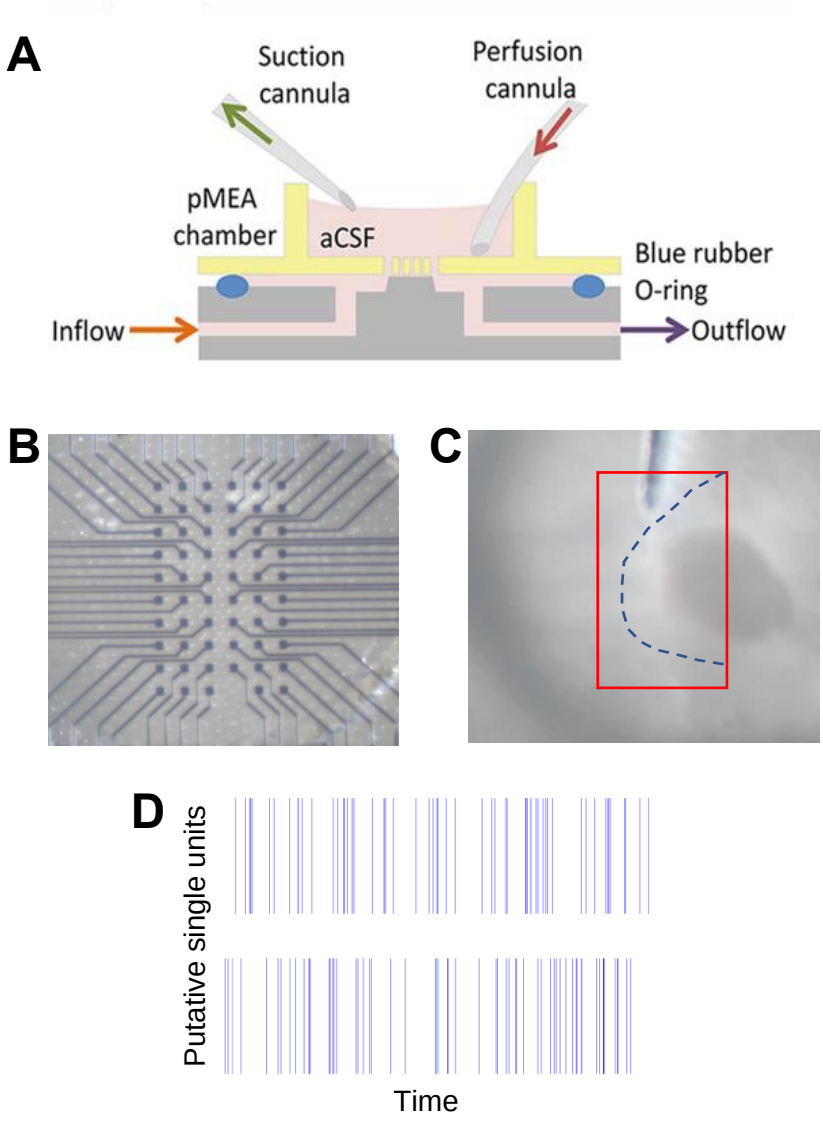

Figure 3.3 Perforated multielectrode array set up. (A) Schematic illustration of multielectrode array set up for electrophysiological recording. The brain slice was placed in the perforated multielectrode array (pMEA) chamber, held by negative pressure and a weighted slice harp. The chamber was continually perfused with aCSF via the perfusion cannula and a constant volume of liquid was maintained by the suction cannula. The blue rubber O-ring prevents escape of liquid from the chamber. Adapted from Belle et al. (2021). (B) The array consisted of 59 recording electrodes and one reference electrode, which were all spaced 100 µm apart, in a 6x10 layout. The diameter of each electrode was 30µm and the whole array covered an approximate total area of 707 μm^2. (C) The pMEA was able to capture the entire anteromedial BNST (STMA) during recording as shown by the representative image with the pMEA area indicated in red, and the STMA nucleus indicated by the dashed line. (D) The STMA was not spontaneously active; only 2 of 21 channels recorded spontaneously active putative single units in a baseline control recording of the STMA. The blue lines on the raster plot represent action potentials.

Experimental design

Neuronal excitability within BNST slices was measured as a response to *N*-Methyl-D-Aspartate (NMDA) mainly because, following the first few recordings, the STMA nucleus exhibited low levels of spontaneous activity on the pMEA (Figure 3.3D). Following 30 minutes of baseline recording, slices were perfused with 20 µM NDMA (Tocris, UK) for 10 minutes before a wash-off with aCSF until cell activity returned to baseline levels. To determine true signal, 500 nM tetrodotoxin (TTX; Tocris, UK) was applied to the slices until all activity ceased. Concentration of both NMDA and TTX were chosen based on previously published data to consistently increase neuronal activity and eradicate all electrical activity in brain slices, respectively (Hoehn et al., 1990; Partridge et al., 2016). 7 days after exposure to repeated restraint stress, performed as described in section 3.3.2, adult 8-13 weeks old mice were culled by cervical dislocation, followed by decapitation, for pMEA recordings. Age-matched mice which did not undergo restraint served as controls for pMEA experiments.

Analysis of putative single unit activity

Recordings for each individual electrode were extracted from the original files and multiunit spikes crossing an updated threshold of -18 µV were extracted for further analysis. The .mat file containing recordings from the individual electrodes in a single experiment was converted to single channel files for clustering analysis using in-lab written MATLAB code (Dr John Brown; MATLAB, R2020b, Mathworks, USA). Spike sorting software (MClust version 4.4, AD Redish, University of Minnesota) was used to cluster putative single units based on parameters of their waveforms: the energy, maximum depth (valley) and peak of the action potential waveform, the position of the waveform peak (peak index) and the contribution of the waveform to the first and second principal components, which account for variation within the data. A putative single unit/cell was selected as the experimental unit as the population of neurons recorded from was determined to be functionally heterogeneous by the differential responses of putative single units to experimental manipulation, including NMDA application and restraint stress. A cluster was validated as well separated if it satisfied two criteria: an isolation distance of ≥ 10, and an L-ratio of < 0.35 (Schmitzer-Torbert,

et al., 2005). A third metric, sensitivity to TTX, was used to separate signal from noise and therefore identify true single unit activity. A further in-lab written script (Dr John Brown; MATLAB, R2020b, Mathworks, USA) was used to select single channels within the STMA region of the BNST and compile these into a .mat file for further analysis.

A final newly written in-lab script (written collaboratively with Callum Walsh and Brinda Gurung) was used to extract values for specific parameters from the data. Units were categorised based on their response to NMDA: increasers (firing rate increase of ≥ 2 standard deviations), decreasers (firing rate decrease of ≥ 2 standard deviations) and non-responders (units whose firing rate did not lie outside of these boundaries). Though non-responding units were categorised in this way, the firing rate of non-responders did increase in response to 20 µm NMDA, however not to a sufficient magnitude to be classed as increasers.
For each responder subclass the following metrics were determined: the number of units categorised for each response group, mean firing rate at baseline, mean firing rate following NMDA application (z-scored to baseline), action potential halfwidth and action potential asymmetry. Firing rate data were transformed by z-scoring values to each individual slice's baseline firing rate, instead of reporting raw firing rate values in Hz, to account for differences in the basal firing rate between slices. Z-scoring the firing rate relative to each individual slice's baseline firing rate standardises the data and means that firing rates can be directly compared across all slices.

3.4 Results

3.4.1 Anxiety-like behaviour following repeated acute restraint stress

First, I investigated whether a repeated acute restraint stress paradigm, to be used throughout the study, indeed increased anxiety-like behaviour in mice. The restraint protocol consisted of three consecutive days of 2 hour restraint, and behaviour was measured the day after the final session of restraint, 7 days after restraint, or 14 days after restraint (Figure 3.4A).

Repeated acute restraint stress increased anxiety-like behaviour in mice as measured by decreased open arm entries and time spent in the open arms of the maze and increased anxiety index scores 1, 7 and 14 days following the last session of restraint (Figure 3.4). Stress significantly altered the number of entries mice made into the open arms of the EPM (Figure 3.4B; $F(3, 26) = 8.045$, $P = 0.006$). Specifically, stressed mice entered the open arms approximately 40% less often than control mice when tested 1, 7 or 14 days following stress (Figure 3.4B; 1 day post-stress: 4.4 ± 0.50 entries, $p = 0.027$; 7 days post-stress: 2.3 ± 0.57 entries, $p = 0.0002$; 14 days post-stress: 4.0 ± 0.41 entries, $p = 0.047$; vs. control: 7.0 ± 0.88 entries). No differences in open arm entries were identified between mice 1, 7 or 14 days post-stress.

The repeated acute restraint stress protocol significantly altered the length of time mice spent in the open arms of the EPM (Figure 3.4C; $F(3, 26) = 12.14$, $P < 0.0001$). Mice exposed to restraint stress spent significantly less time in the open arms of the maze 1, 7 and 14-days after stress (Figure 3.4C; 1 day post-stress: 28.6 s ± 3.8 s, $p = 0.0006$; 7 days post-stress: 17.4 s ± 4.8 s, $p < 0.0001$; 14 days post-stress: 28.0 s ± 2.8 s, $p = 0.0055$ vs. control: 59.7 s ± 6.8 s). No difference in time spent in the open arms of the maze was identified between mice at 1, 7 and 14 days post-stress.

Restraint stress significantly influenced the anxiety index scores of mice in the EPM, as measured by the number of open arm entries divided by the number of total arm entries (Figure 3.4D; $F(3, 26) = 6.531$, $P = 0.0019$). The anxiety index measures the relative approach behaviour of mice to the aversive element of the maze, the open arms, with lower scores indicating reduced approach behaviour and therefore greater aversion. Mice tested in the EPM 1 and 7 days post-stress exhibited reduced anxiety index scores (Figure 3.4D; 1 day post-stress: 0.28 ±

0.022, p = 0.024; 7 days post-stress: 0.22 ± 0.039, p = 0.0008; vs. control: 0.39 ± 0.027). There was no difference in the anxiety index of mice 14 days post-stress compared with control mice, nor were there any differences between post-stress mice at different time points (Figure 3.4D; 14 days post stress: 0.27 ± 0.031).

Stress also had a significant effect on the locomotor activity of mice in the EPM, as measured by the distance travelled in the maze (Figure 3.4E; $F(3,27) = 6.853$, $P = 0.0014$). Mice tested 7 days post-stress travelled significantly shorter distances in the maze compared to controls (Figure 3.4E; 7 days post-stress: 691 cm ± 94.8 cm, p = 0.0176; vs. control: 943 cm ± 52.6 cm). No differences were detected at 1 or 14 days post stress compared with stress naïve control mice, nor were any differences detected between mice at different experimental time points post-stress (Figure 3.4E; 1 day post-stress: 1039 cm ± 39.5 cm; 14 days post-stress: 745 cm ± 53.4 cm).

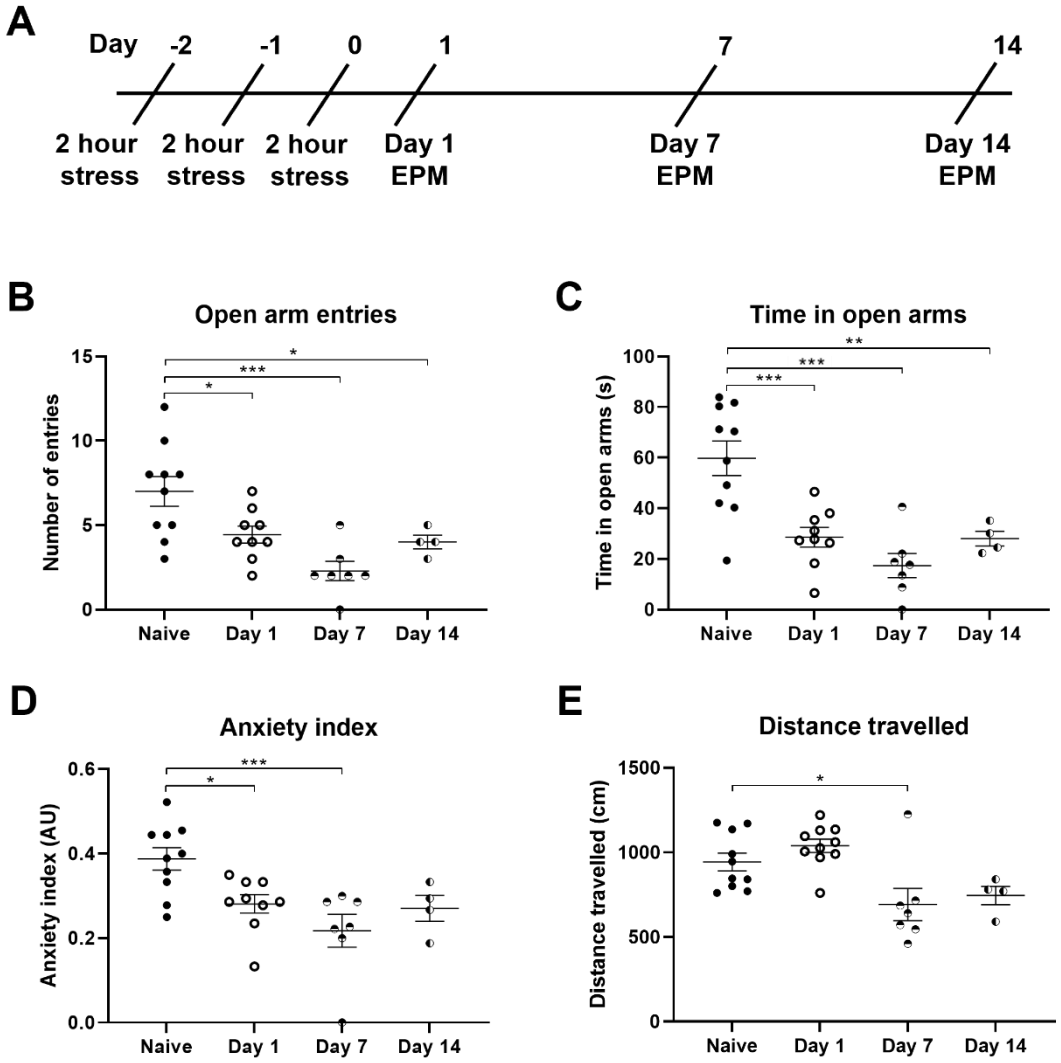

Figure 3.4 Quantification of anxiety-like behaviour in the elevated plus maze of mice exposed to repeated restraint stress. (A) Schematic timeline of the restraint stress protocol and subsequent behavioural testing. (B) Stress naïve mice entered the open arms of the maze more often in comparison to stressed mice on Day 1 ($p = 0.0273$), Day 7 ($p = 0.0002$), and Day 14 ($p=0.0474$) following stress. (C) The time spent in the open arms of the maze was longer for stress naïve naive mice compared to stressed mice at Day 1 ($p = 0.0006$), Day 7 ($p < 0.0001$), and Day 14 ($p = 0.0055$). (D) The anxiety index of stress naïve mice was higher than in mice at Day 1 ($p = 0.0244$) and Day 7 ($p=0.0008$) following the last restraint session. (E) The locomotor activity, measured by distance travelled in the maze, of stressed mice on Day 7 following the last restraint session was lower in comparison to the stress naïve control group ($p = 0.0176$). Control group N = 10; Day 1 group N = 10; Day 7 group N = 7; Day 14 group N = 4. Data are presented as bar plots with mean±SEM (B-E); $*p < 0.05$, $**p < 0.01$, $***p < 0.001$ vs an indicated group, one-way ANOVA with Tukey's *post hoc* testing.

3.4.2 Neuronal activation in the bed nucleus of the stria terminalis following repeated acute restraint stress

Repeated restraint stress had a significant effect on the activity of neurons in the anterior BNST, as determined by immunolabelling (Figure 3.5). Very few c-Fos positive cells were observed in BNST slices from stress naïve mice (Figure 3.5A). However, following restraint stress a greater number of c-Fos positive cells was detected in the BNST (Figure 3.5B). Quantification of c-Fos positive cells in the anterior BNST revealed that mice exposed to repeated restraint stress had approximately 20-fold more c-Fos positive cells compared to stress naïve mice (Figure 3.5D; stress: 191 ± 11.7, $p < 0.0001$; vs. control: 10 ± 1.1). Presented here are the total counts of c-Fos positive cells, with a single data point representing the total number of c-Fos positive cells in the right and left BNST of a single mouse.

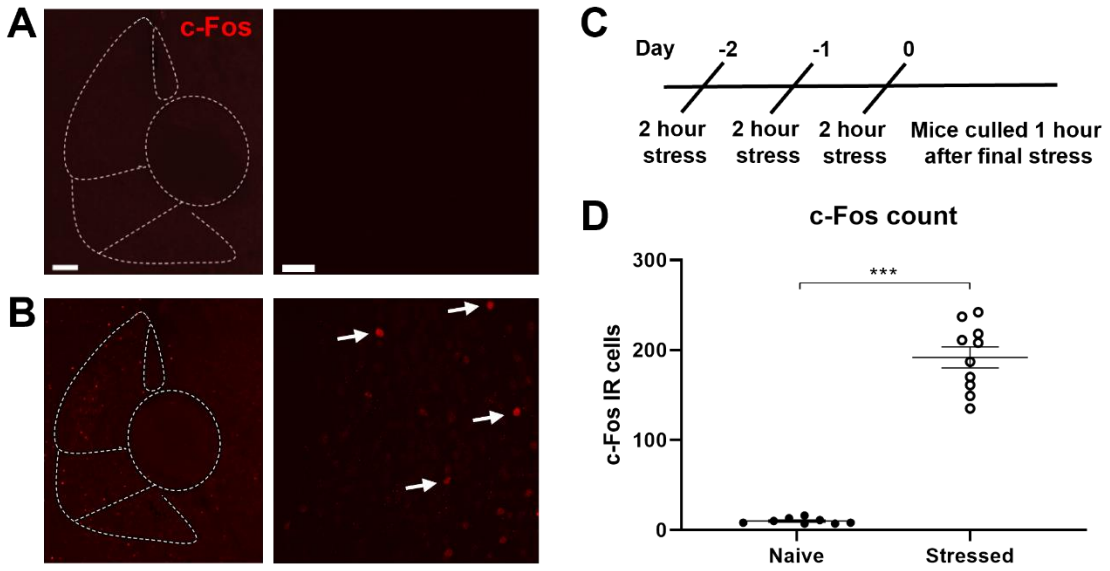

Figure 3.5 C-Fos labelling in the bed nucleus of the stria terminalis following repeated restraint stress. 10x (left; scale bar = 100 µm) and 20x (right; scale bar = 50 µm) representative images of BNST sections labelled for c-Fos (red) from stress-naïve mice (A) and stressed mice (B) that were sacrificed 1 hour following the last session of an acute repeated restraint stress protocol (C). Arrows indicate c-Fos positive cells in the BNST. Mice exposed to the restraint stress protocol expressed greater numbers of c-Fos positive cells than stress naïve mice (D; p=0.0001). Scale bar = 100 µm. Control group N = 8 animals, 6 slices per animal; Stressed group N = 10, 6 slices per animal. Data are presented as dot plot with mean±SEM (D); ***$p < 0.001$ vs an indicated group, t-test.

To establish whether neurons active during stress were surrounded by PNNs, I performed immunolabelling for c-Fos with WFA labelling for PNNs. The neuronal population activated by restraint stress and the population surrounded by PNNs were largely mutually exclusive (Figure 3.6). No more than one neuron expressing both c-Fos and a PNN was observed in each of the experimental animals; labelling was performed on all mice used to quantify c-Fos positive cells in the BNST following restraint. Labelling was therefore performed for eight control and ten experimental animals, assessing three fields of view per slice and six slices per animal, focusing on the STMA, and all showed qualitatively the same result (Figure 3.6). Hence, further quantification of co-localisation of c-Fos and WFA labelling was not performed as it is unlikely to occur more often than would be expected by chance.

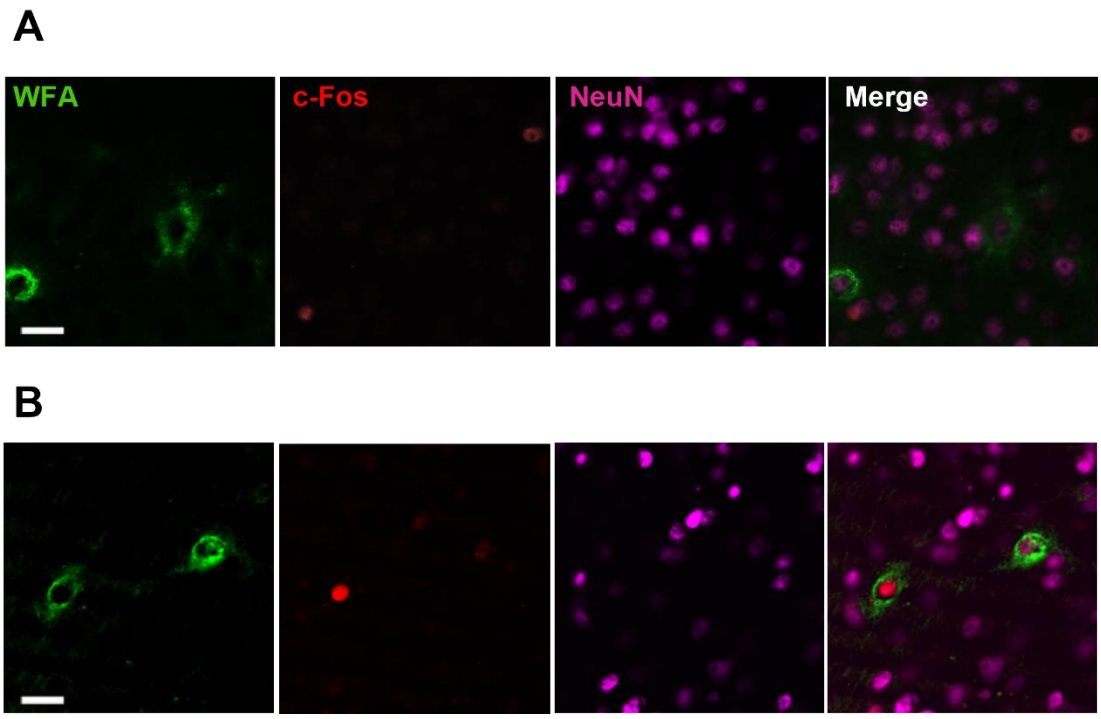

Figure 3.6 Perineuronal net and c-Fos co-localisation post-stress. Representative images of perineuronal nets (green) and activated neurons (red & magenta dual label) in the anterior bed nucleus of the stria terminalis of control mice (A) and following repeated acute restraint stress (B). Representative images, experiments were performed independently with similar results on 8 control and 10 stressed animals, 6 brain slices per animal, 3 field of views per brain slice. Scale bar = 20 µm.

3.4.3 Expression and morphology of PNNs within the BNST following repeated acute restraint stress

Acute restraint stress significantly affected the expression of major components of PNNs in the BNST, including the STMA subnucleus, both 7 and 14 days post-stress, as determined by qRT-PCR (Figure 3.7). The expression of brevican was not significantly altered by restraint (Figure 3.7A; control: 1.00 ± 0.17; 7 days post stress: 3.41 ± 1.18; 14 days post-stress: 1.05 ± 0.13). Restraint stress significantly affected the expression of neurocan (Figure 3.7B; $F(2,6) = 13.94$, $P = 0.0056$). Specifically, neurocan expression increased 30-40 fold 7 days post stress and ~40-80 fold 14 days post stress compared to control (Figure 3.7B; 7 days post stress: 36.97 ± 2.87, $p = 0.0265$; 14 days post-stress: 52.44 ± 11.91, $p = 0.0051$; vs. control: 1.00 ± 0.04). The expression of tenascin-R was also affected by restraint stress (Figure 3.7C; $F(2,6) = 5.471$, $P = 0.0444$). 14 days post-stress, the expression of tenascin-R increased 3 fold compared to expression in stress naïve control mice (Figure 3.7C; 14 days post-stress: 2.54 ± 0.59, $p = 0.0474$; vs. control: 1.00 ± 0.11). Expression of tenascin-R was equivalent in control mice and mice 7 days post-stress (Figure 3.7C; 7 days post-stress: 2.25 ± 0.07). Each data point represents a single mouse.

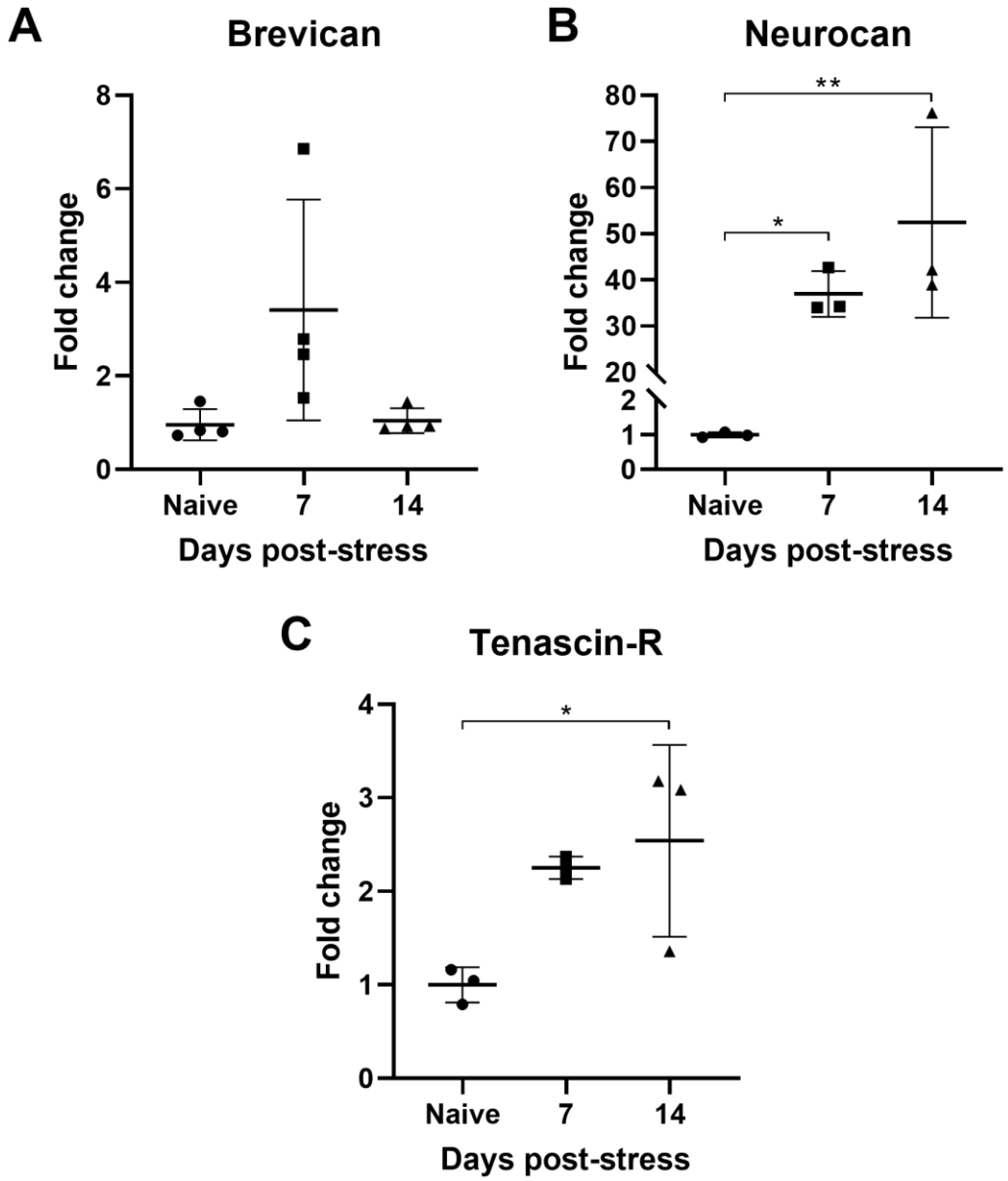

Figure 3.7 Gene expression of perineuronal net components in the bed nucleus of the stria terminalis following repeated acute restraint stress. (A) Expression of the brevican gene was not altered following stress. (B) Expression of the neurocan gene increased both 7 days ($p = 0.0265$) and 14 days ($p = 0.0051$) post-stress. (C) Tenascin-R gene expression increased 14 days ($p = 0.0474$) post-stress. Data are presented as dot plots with mean±SEM; N (brevican) = 4 animals; N (neurocan/tenascin-R) = 3 animals; *$p < 0.05$, **$p < 0.01$ vs an indicated group, one-way ANOVA with Tukey's post hoc test.

Despite increases in two of the major components of PNNs following restraint, the overall number of PNNs in the STMA was unaffected by restraint, as determined by counting the number of WFA-labelled PNNs (Figure 3.8B-D). Quantification of PNNs in the BNST of stress naïve mice and mice 7 and 14 days post stress revealed no differences in the number of PNNs expressed between groups (Figure 3.8C; control: 20.5 ± 2.3; 7 days post-stress: 15.0 ± 1.6; 14 days post-stress: 15.7 ± 1.6).

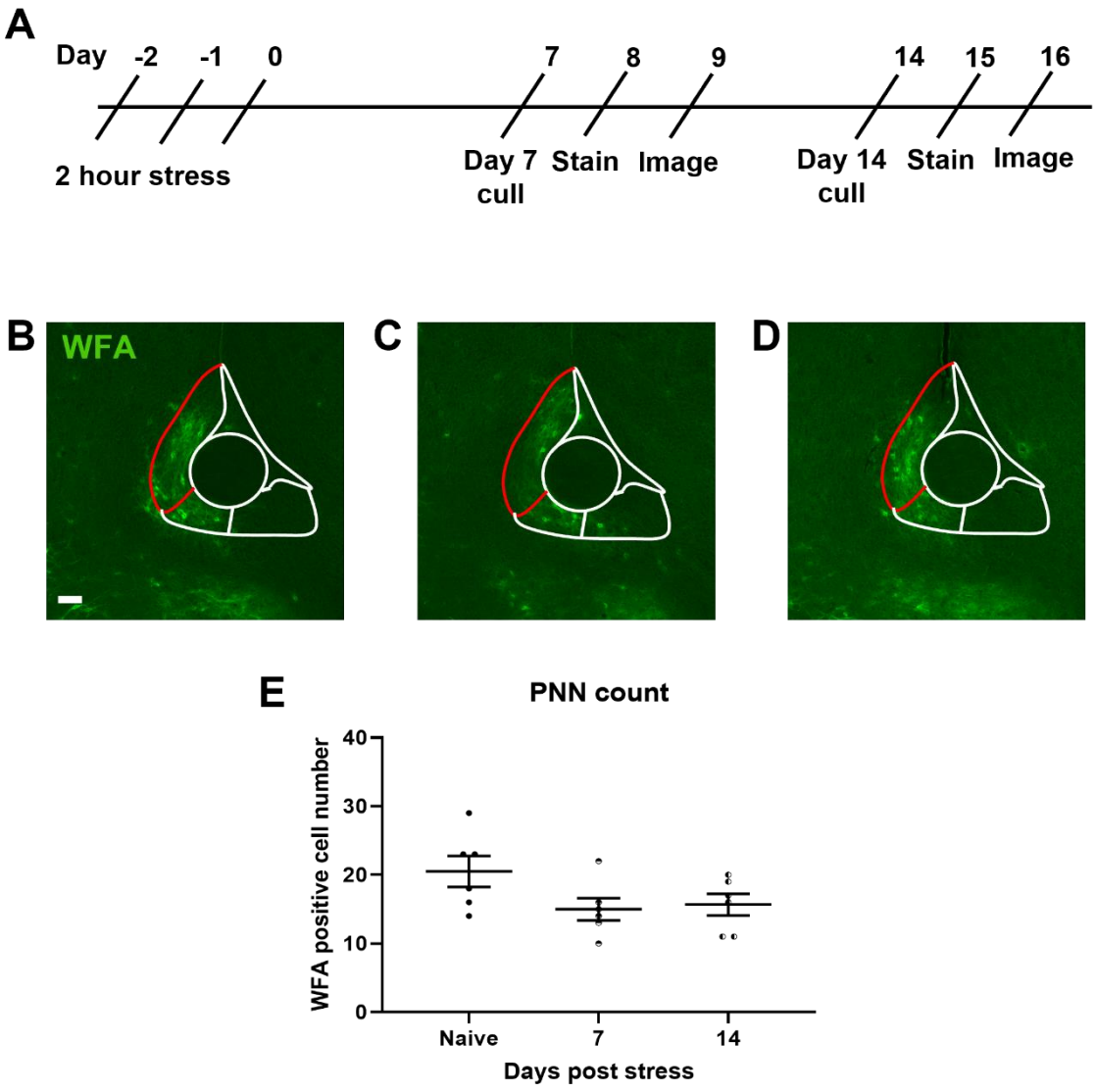

Figure 3.8 Perineuronal net expression in the anteromedial bed nucleus of the stria terminalis following repeated acute restraint stress. (A) A schematic timeline of the repeated acute restraint stress protocol and subsequent imaging. Representative images of WFA labelled perineuronal nets in the BNST of (B) stress naïve mice and mice (C) 7 days and (D) 14 days post-stress. The red outline indicates the anteromedial bed nucleus of the stria terminalis. Scale bars = 100 µm. (E) There was no significant difference in perineuronal net number in mice 7 or 14 days following an acute restraint stress protocol compared to stress naïve control mice. Data are presented as dot plots with mean±SEM (E); N (each group) = 6 animals, 6 slices per animal; one-way ANOVA.

Next, a detailed morphological study of PNNs in the STMA was undertaken, considering the lack of change in PNN number, but the significant alterations to PNN component expression. Each individual PNN was considered an experimental unit; PNNs show variability, even in the same brain region, in the same animal, therefore each PNN was considered statistically independent. Repeated acute restraint stress significantly affected the morphological properties of PNNs in the STMA, as determined by WFA labelling, microscopy and image analysis (Figure 3.9). As absolute scale was not factored into the analysis, values are relative and therefore presented in arbitrary units. Stress significantly influenced the area of the individual holes within the PNN unit (Figure 3.9C; $F(2,117) = 8.332$, $P < 0.0001$). Specifically, the area of the holes in the PNN matrix within the STMA was twice as great in mice 7 days post-stress compared with stress naïve controls and mice at 14 days post-stress (Figure 3.9C; stress naïve control: 0.009 ± 0.0006, $p < 0.0001$; 14 days post-stress: 0.01 ± 0.0007, $p < 0.0001$; vs. 7 days post-stress: 0.018 ± 0.002). The perimeter of PNN holes within the STMA was also affected by restraint stress (Figure 3.9D; $F(2,117) = 5.231$, $P < 0.0001$). The perimeter of holes within the PNN matrix in the BNST was at least 35% greater in mice 7 days post-stress compared to stress naïve controls and mice 14 days post-stress (Figure 3.9D; stress naïve controls: 0.46 ± 0.017, $p < 0.0001$; 14 days post-stress: 0.48 ± 0.016, $p < 0.0001$; vs. 7 days post-stress: 0.65 ± 0.031).

The intensity of the ECM surrounding each hole was altered following stressor exposure (Figure 3.9E; $F(2,117) = 5.782$, $P = 0.0007$). Specifically, the mean intensity of ECM was significantly reduced in PNNs within the BNST in mice 7 days post-stress compared to controls and mice 14 days after stress (Figure 3.9E; stress naïve controls: 669.9 ± 30.0, $p = 0.0005$; 14 days post-stress: 618.0 ± 25.2, $p = 0.027$; vs. 7 days post-stress: 509.1 ± 32.6).

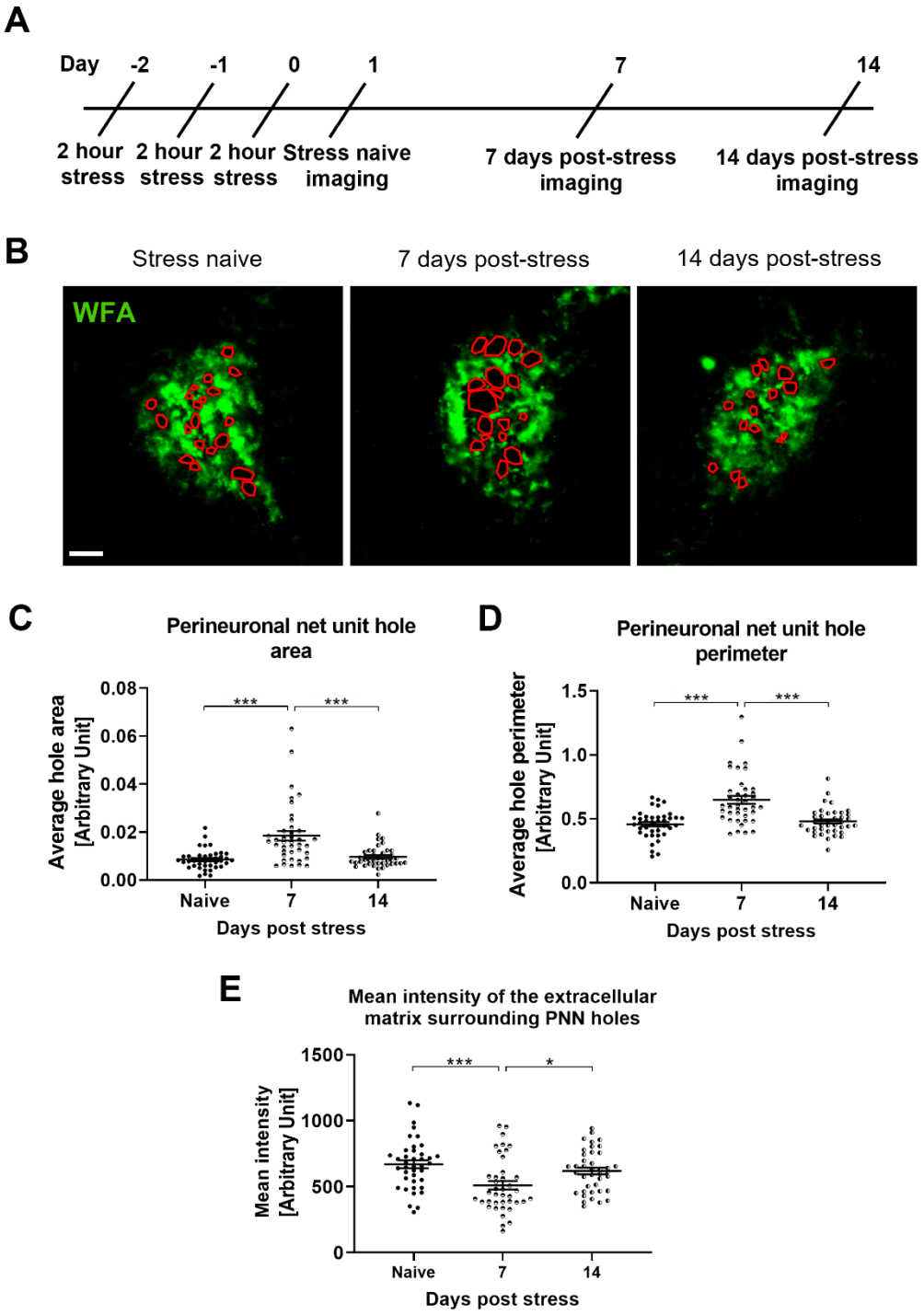

Figure 3.9 Perineuronal net morphology in the anteromedial bed nucleus of the stria terminalis following repeated acute restraint stress. (A) A schematic timeline of the restraint stress and imaging protocol. (B) Representative images of individual perineuronal net units from stress naïve and 7 and 14 days post-stress mice. Holes measured within the units are highlighted in red (scale bar = 5µm). (C) The average hole area within a perineuronal net unit in the BNST was greater 7 days post-stress ($p < 0.0001$) but decreased from 7 to 14 days post-stress ($p < 0.0001$). (D) The average hole perimeter within a perineuronal net unit in the BNST increased 7 days post-stress ($p < 0.0001$) but returned to baseline by 14 days post-stress ($p < 0.0001$). (E) The fluorescence intensity of the extracellular matrix surrounding the holes within the perineuronal net unit was reduced 7 days post-stress ($p = 0.0005$) but recovered 14 days post-stress ($p = 0.0269$). Data are presented as dot plots with mean±SEM (C-E); N (all groups) = 7 animals, 3 slices per animal, 5-6 perineuronal nets per slice; *p < 0.05, ***p < 0.001 vs an indicated group; one-way ANOVA with Tukey's post-hoc test.

PNN flatness and PNN leakiness were also used to investigate the morphology of PNNs following stress. The flatness of PNNs was determined by the standard deviation of the ECM intensity across z-planes to determine the arrangement of the PNN in 3D space (Figure 3.10A). No significant differences in the flatness of BNST PNNs post-stress were observed (Figure 3.10B; control: 0.18 ± 0.007; 7 days post-stress: 0.16 ± 0.007; 14 days post-stress: 0.19 ± 0.006). The leakiness of PNNs, a measure of structural complexity of the ECM, was determined by finding the values for the minimum intensity of the ECM around the perimeter of the PNN holes (Figure 3.10C). Significant differences in PNN leakiness were observed following stress (Figure 3.10D; $F(2,117) = 0.2474$, $P = 0.0036$). The minimum ECM intensity of PNNs 7 days post-stress was 27% lower, indicative of increased leakiness, compared to PNNs in stress naïve mice and mice 14 days post-stress (Figure 3.10D; control: 442.4 ± 29.4, $p = 0.0072$; 14 days post-stress: 433.5 ± 29.2, $p = 0.0135$; vs. 7 days post-stress: 315.5 ± 28.8).

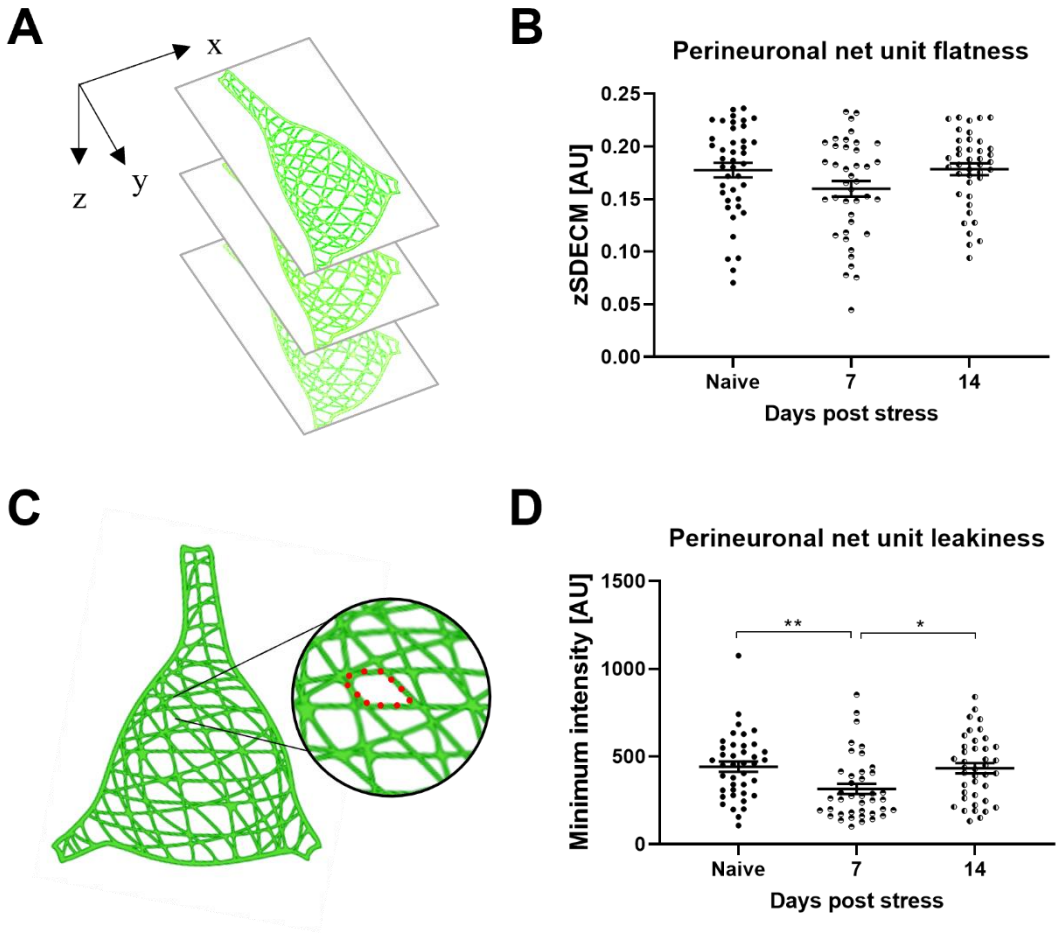

Figure 3.10 Perineuronal net flatness and leakiness in the anteromedial bed nucleus of the stria terminalis following repeated acute restraint stress. (A) A schematic representation of perineuronal net flatness, determined by the standard deviation of the fluorescence intensity of the extracellular matrix across z-planes. (B) Perineuronal net flatness in the anteromedial bed nucleus of the stria terminalis was not altered following stress. (C) A schematic representation of the way in which perineuronal net leakiness was determined; finding the minimum values of extracellular matrix fluorescence intensity around the perimeter of the individual holes within the perineuronal net unit, in 3D space. (D) The leakiness of perineuronal nets in the anteromedial bed nucleus of the stria terminalis increased 7 days following the last session of restraint compared to stress naïve controls ($p = 0.0072$), as evidenced by the reduction in minimum intensity of the extracellular matrix. Perineuronal nets leakiness subsequently decreased between 7 and 14 days post-stress ($p = 0.0135$). Data are presented as dot plots with mean±SEM (B, D); N (all groups) = 7 animals, 3 slices per animal, 5-6 perineuronal nets per slice; *$p < 0.05$, **$p < 0.01$ vs an indicated group; one-way ANOVA with Tukey's post-hoc test. Schematic diagrams created using BioRender.

3.4.4 Effect of acute stress on electrophysiological properties of putative single units within the anteromedial bed nucleus of the stria terminalis

Electrophysiological recordings were made in the STMA, due to the dense expression of PNNs, shown to be morphologically altered following restraint stress. The STMA showed very low levels of spontaneous activity, with only 2 of

21 channels recording spontaneous activity in a baseline recording of STMA (Figure 3.3D). Therefore, putative single unit response to NMDA was examined as an alternative, to investigate stress induced changes in neuronal excitability within the STMA.

Differential responses to NMDA application were identified through real-time observation of the MEA recording output. A portion of putative units were observed to increase firing in response to NMDA and a portion of units were observed to cease or reduce firing in response to NMDA (Figure 3.11). To address these differential responses, putative single units were classified into three groups: increasers, decreasers and non-responders, and analysed separately. To account for differences in baseline firing rates between individual slices, firing rates were z-scored to the baseline prior to analysis. Z-scored firing rates are presented as violin plots, to show the relative distribution of the data points, with mean and interquartile range indicated. The width of the violin indicates the relative number of data points with and equivalent firing rate.

Exposure to stress significantly modified the firing rate of putative single units in the STMA, in response to NMDA (Figure 3.11). The increaser responder subtype was sensitive to stress and units within slices from stressed mice fired significantly faster in response to NMDA than increaser units in control slices (Figure 3.11B; control: 1.21 ± 0.04, $p = 0.0005$; vs. stress: 1.37 ± 0.03). The difference in firing rate can also be observed in the plot of firing rate over the duration of the experiment (Figure 3.11A; control: dark green; stress: light green). Though non-responder units did not surpass either applied threshold to be responsive to NMDA, the average firing rate of non-responders marginally increased in the presence of NMDA following stress (Figure 3.11D; control: 0.25 ± 0.04, $p = 0.0093$; vs. stress: 0.08 ± 0.04). The difference can also be visualised in the firing rate plot for the duration of the experiment (Figure 3.11C; control: dark purple; stress: light purple). The decreaser unit subtype was unaffected by restraint stress (Figure 3.11F; control: -0.84 ± 0.04; vs. stress: -1.0 ± 0.06). The firing rate plots corroborate the lack of difference in response to NMDA in decreasers (Figure 3.11E; control: dark red; stress: light red).

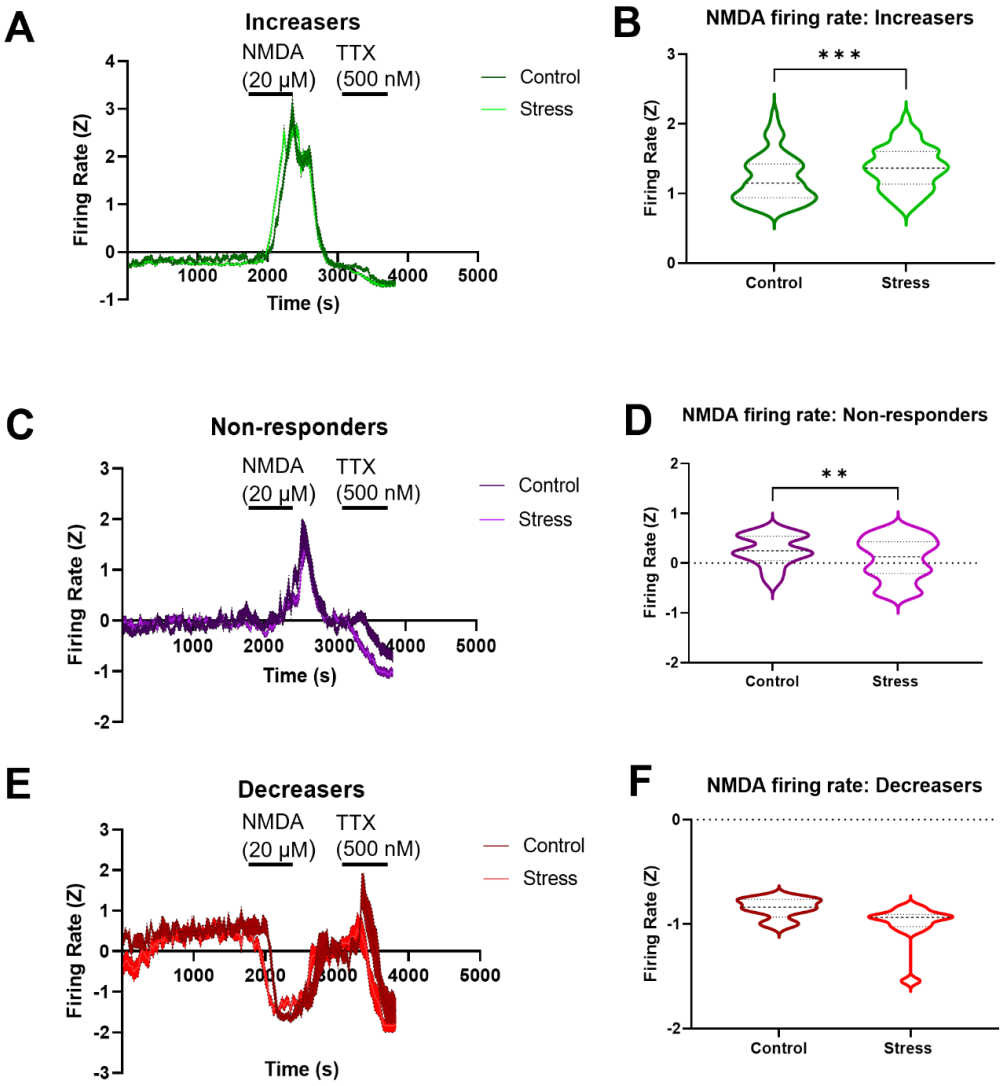

Figure 3.11. Impact of repeated acute restraint stress on the firing rate of putative single units in the anteromedial bed nucleus of the stria terminalis in response to *N*-Methyl-D-Aspartate. (A) Electrophysiological traces of all putative single units which increase their firing in response to NMDA application in slices from mice after acute restraint stress (dark green trace) and stress naïve control animals (light green trace). Firing rate is presented as the mean firing rate against time, with a shaded error bar of the SEM. The black bars indicate the duration of application of NMDA (20 μM) and TTX (500 nM). (B) Quantification of firing rate from all putative single unit increasers from naïve and stress slices. Restraint stress significantly increased the firing rate of increasers in response to NDMA application ($p = 0.0005$). (C) Graphical representation of the firing rate of putative single units in slices from stress naïve (dark purple trace) and stressed mice (light purple trace), which do not respond to NMDA, across the time course of the experiment. (D) Quantification of firing rate from all putative single unit non-responders from naïve and stress slices. Firing rate in response to NMDA was significantly reduced in non-responder putative single units within stress slices compared to units from stress naïve control slices ($p = 0.0093$). (E) Graph of the firing rate of all putative single units which decrease their firing in response to NMDA application in slices from mice after acute restraint stress (light red trace) and stress naïve control animals (dark red trace). (F) Quantification of firing rate from all putative single units from naïve and stress slices. There was no difference in firing rate of decreasers in response to NMDA in slices from stress naïve or stressed mice. Control slices: Increasers: N = 70; Decreasers: N = 5; Non-responders: N = 53. Stress slices: Increasers: N = 149; Decreasers: N = 11; Non-responders: N = 90; n (control) = 6 animals, 8 brain slices; n (stressed) = 7 animals, 10 brain slices. Data are presented as violin plots with mean±SEM indicated (B, D, F); $^{**}p < 0.01$, $^{***}p < 0.001$ vs an indicated group; one-way ANOVA with Tukey's post-hoc test.

To determine whether the differences in firing rate observed between units in the presence of NMDA were also evident under basal conditions, the baseline firing rate of each type of responder was retrospectively analysed in slices from control and stressed mice, separately. The type of firing rate response a particular unit displayed in the presence of NMDA was also indicative of the baseline firing rate of that unit in the slices from stress naïve control mice (Figure 3.12A; $F(2, 125) = 12.03$, $P < 0.0001$). Specifically, at baseline in slices from control animals, decreasers displayed higher firing rates compared to increasers and non-responders (Figure 3.12A; increaser: -0.16 ± 0.03, $p < 0.0001$; non-responder: -0.07 ± 0.05, $p = 0.0002$; vs. decreaser: 0.48 ± 0.12). Similarly, in slices from stressed mice, the behaviour of a unit in response to NMDA, in regard to firing rate, informed the baseline firing rate of that unit (Figure 3.12B; $F(2, 247) = 16.78$, $P < 0.0001$). In stressed slices, the basal firing rate of decreasers was also higher than that of increasers or non-responders (Figure 3.12B; increaser: -0.23 ± 0.02, $p < 0.0001$; non-responder: -0.05 ± 0.05, $p = 0.012$; vs. decreaser: 0.48 ± 0.12). Considering units from stressed slices, non-responders displayed greater firing rates at baseline compared to increasers ($p = 0.0002$).

Exposure to restraint stress had no effect on the interspike interval, or duration of time between spikes, of putative single units in the STMA (Figure 3.12C). To confirm whether the differences in firing rate could be attributed to the properties of the units themselves, the proportion of each type of responder was quantified in both stress and control STMA slices (Figure 3.12D). The proportions of increasers, decreasers and non-responders were similar between groups (Figure 3.12D; control increaser: 54.69%; control decreaser: 3.91%; control non-responder: 41.41%; stress increaser: 59.6%; stress decreaser: 4.4%; stress non-responder: 36.0%). No differences in the basal firing rate of increasers, decreasers or non-responders were identified between stress and control conditions (Appendix 1 Table 6.9).

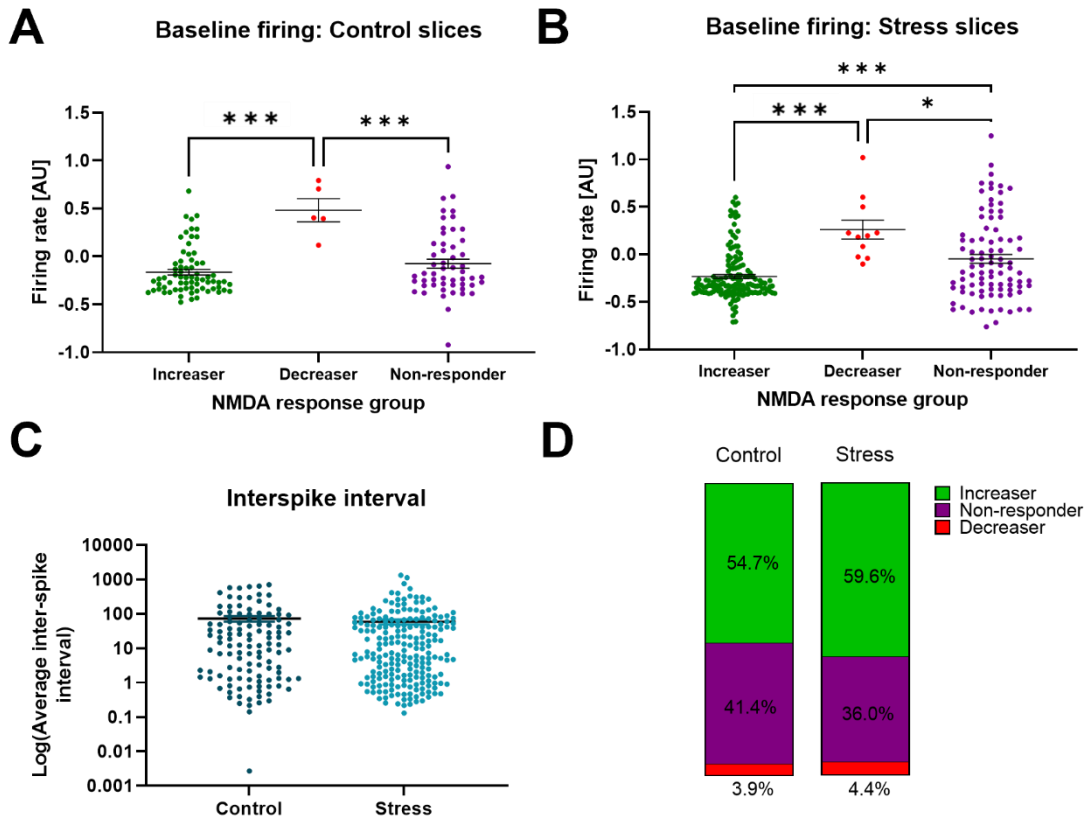

Figure 3.12 Basal firing rate of putative single units in the anteromedial bed nucleus of the stria terminalis following exposure to repeated acute restraint stress. (A) Baseline firing rate of increaser, decreaser and non-responder units, classified by response to NMDA, in the STMA of slices from control mice; at baseline, decreasers fired at a significantly higher rate compared to increasers ($p < 0.0001$) and non-responders ($p = 0.0002$). (B) Baseline firing rate of increaser, decreaser and non-responder units in the STMA of slices from stressed mice; at baseline, decreasers had a significantly higher firing rate compared to increasers ($p < 0.0001$) and non-responders ($p = 0.0002$); non-responders fired at a significantly higher rate compared to increasers at baseline ($p = 0.012$). (C) No difference in interspike interval was observed between conditions. (D) Proportions of each type of NMDA response in the STMA of control and stressed mice were approximately equally distributed. Control slices – Increasers: N = 70; Decreasers: N = 5; Non-responders: N = 53; Total: N = 118 (interspike interval values were not available for all detected units). Stress slices – Increasers: N = 149; Decreasers: N = 11; Non-responders: N = 90; Total: N = 212 (interspike interval values were not available for all detected units). n (control) = 6 animals, 8 brain slices; n (stressed) = 7 animals, 10 brain slices. Data are presented as dot plots with mean±SEM (A-C); $^{**}p < 0.01$, $^{***}p < 0.001$ vs an indicated group; one-way ANOVA with Tukey's post-hoc test.

Finally, the average waveforms of increasers, decreasers and non-responders were investigated to further determine the properties of each type of responder. Firing rate in response to NMDA and subsequent classification of STMA units did not inform the waveform properties of those units in slices from stress naïve control mice (Figure 3.13). Specifically, there were no difference in the halfwidth of the action potential (AP halfwidth) between the three NMDA response groups (Figure 3.13C; increasers: 0.29 ± 0.007; decreasers: 0.34 ± 0.01; non-responders: 0.28 ± 0.007). Similarly, NMDA response did not inform the asymmetry of the action potential waveform (AP asymmetry) in slices from stress naïve control mice, thus no differences were detected between groups (Figure 3.13E; increaser: 2.0 ± 0.08; decreaser: 2.4 ± 0.2; non-responder: 1.9 ± 0.09). See Figure 3.13A for presentation of the average waveform of increasers (green), decreasers (red) and non-responders (purple).

Conversely, response to NMDA did inform the waveform properties, specifically the AP halfwidth, of putative single units in the STMA of mice that were exposed to restraint stress (Figure 3.13D; $F(2, 246) = 4.093$, $P = 0.0178$). The average waveform of decreaser units displayed a greater AP halfwidth compared with increasers and non-responders (Figure 3.13D; increaser: 0.28 ± 0.004, $p = 0.0135$; non-responder: 0.29 ± 0.006, $p = 0.0377$; vs. decreaser: 0.33 ± 0.01). The asymmetry of waveforms was also significantly affected by NMDA response type (Figure 3.13F; $F(2,247) = 13.75$, $P < 0.0001$). Increasers displayed significantly more asymmetric waveforms compared with non-responders (Figure 3.13F; non-responder: 1.93 ± 0.07; vs. increaser: 2.37 ± 0.05, $p < 0.0001$). There was no difference in the waveforms of decreasers compared to increasers or non-responders (Figure 3.13F; decreaser: 2.22 ± 0.18). See Figure 3.13B for the average waveforms of the increaser (green), decreaser (red) and non-responder (purple) NMDA response unit subtypes. Additional t test comparisons were made between units in slices from stressed mice and control mice, for each waveform property, for each responder subtype. Action potential asymmetry was significantly greater in increasers in slices from stressed mice compared to increasers in slices from control mice (Appendix 1 Table 6.11; $p < 0.0001$), however, no other differences in action potential halfwidth or asymmetry were identified between the distinct responder subtypes in stress and control slices (Appendix 1 Table 6.10; Appendix 1 Table 6.11).

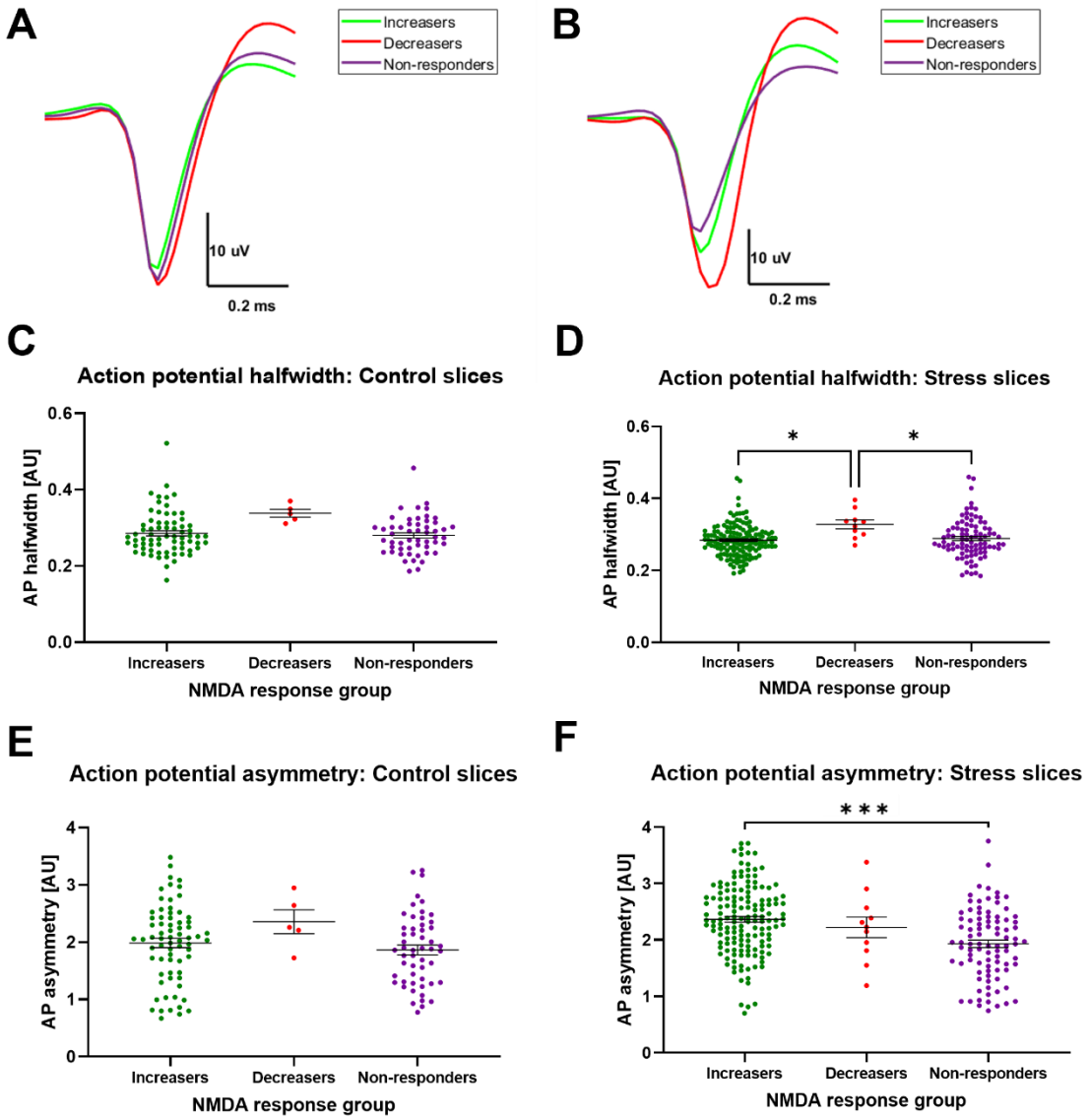

Figure 3.13 Waveform properties of putative single units in the anteromedial bed nucleus of the stria terminalis following exposure to repeated acute restraint stress. (A) Mean waveform traces of putative single unit increasers (green trace), decreasers (red trace), and non-responders (purple trace) to NMDA (20 µM) in slices from control mice. (B) Mean waveform traces of putative single unit increasers (green trace), decreasers (red trace), and non-responders (purple trace) to NMDA in slices from stressed mice. (C) Action potential halfwidth of increasers, decreasers and non-responders to NMDA in slices from control mice. (D) Action potential halfwidth of increasers, decreasers and non-responders to NMDA in slices from stressed mice. Decreasers exhibited a significantly greater action potential halfwidth than increasers ($p = 0.0135$) and non-responders ($p = 0.0377$). (E) Asymmetry of action potentials fired by increasers, decreasers and non-responders in slices from control mice. (F) Asymmetry of action potentials fired by increasers, decreasers and non-responders in slices from stressed mice. Increasers displayed significantly more asymmetric action potentials than those fired by non-responders ($p < 0.0001$). Control slices – N = 70; Decreasers: N = 5; Non-responders: N = 53; Total: N = 118 (interspike interval values were not available for all detected units). Stress slices – Increasers: N = 149; Decreasers: N = 11; Non-responders: N = 90; Total: N = 212. n (control) = 6 animals, 8 brain slices; n (stressed) = 7 animals, 10 brain slices. Data are presented as dot plot with mean±SEM (C-F); *$p < 0.05$, ***$p < 0.001$ vs an indicated group; one-way ANOVA with Tukey's post-hoc test.

3.5 Discussion

In results chapter 3 I experimentally discovered the impact of acute repeated restraint stress on neuronal excitability and PNN expression and morphology within the STMA. An acute, rather than chronic, model of restraint stress was employed in the current study to induce anxiety-like behaviour. Two hours of restraint stress for three consecutive days was previously shown to increase corticosterone levels in both juvenile and adult C57BL/6 mice, consistent with HPA axis activation, however no behavioural changes were observed in the EPM (Sadler & Bailey, 2016).

Here, three consecutive days of two-hour long restraint stress sessions was sufficient to induce anxiety-like behaviour in the EPM as demonstrated by a decrease in open arm entries and time spent in the open arms of the maze (Figure 3.4). For these experiments the increase in anxiety-like behaviour was enough for the stress to be considered sufficient, however the methodology was limited by lack of follow-up physiological measurements including body weight, welfare and plasma corticosterone. Though these have been investigated by other researchers for this paradigm (Sadler & Bailey, 2016), not including them here means that it cannot be certain that the HPA was activated by the restraint protocol. The behavioural results here therefore lack wider context and should be interpreted with some caution.

Anxiety-like behaviour was sustained beyond 24 hours, for at least 7 days, following the last session of restraint. By 14 days post-stress, anxiety-like behaviour in the EPM was similar to stress naïve mice (Figure 3.4). As many acute restraint studies do not evaluate anxiety-like behaviours beyond the 24 hour period, context around the long-term behavioural consequences of acute restraint is limited (Nosek, et al., 2008; Reis, et al., 2011; Busnardo, et al., 2013; Sadler & Bailey, 2016). However, in a study by Wang *et al.* (2015) a single prolonged stress protocol consisting of a two-hour restraint followed by a 20-minute forced swim induced similar behaviours in the EPM as the repeated restraint stress protocol used here (Figure 3.4). Anxiety-like behaviour in the EPM was sustained for at least 7 days post-stress (Figure 3.4). Yet at 14 days, anxiety index scores were comparable to control group levels. Considering the behavioural data obtained following this restraint stress protocol, a potential period of vulnerability was revealed, at the 7 day post-stress time point. Here,

mice spent the least amount of time in the open arms of the maze and made the fewest entries to the open arms (Figure 3.4).

Notably, there were also deficits in locomotor activity in mice 7 days after repeated acute restraint stress when compared with stress naïve mice. Hypolocomotion may confound measures of anxiety-like behaviour and may therefore partially explain the enhanced anxiety-like behaviour observed in mice 7 days post-stress in comparison with stress naïve mice and mice tested 24 hours post-stress. However, increased measures of anxiety-like behaviour were also reported at the 24 hour post-stress time point, and no locomotor deficits were detected in mice at the 24 hour time point (Figure 3.4).

Reduced locomotor activity following stress has previously been reported and considered to be a methodological confound of emotionality, an indication of sedation, malaise, or locomotor incapacity (Royce, 1977; Salmon & Stanford, 1989; Stanford, 2007). However, changes in locomotor activity may also provide insight into emotional status – reduced movement and exploration can be characteristic of a negative emotional state and could thus reciprocally confound measures of emotionality (Schrader, et al., 2018; Stanford, 2007). Hypolocomotion in the EPM following restraint has rarely been reported and has only been tested up to 48-hours post-stress (Padovan & Guimaraes, 2000). Comparing locomotor activity in the EPM between studies is challenging, since most studies preferentially use an open field test to measure overall locomotion following stress (Sestakova, et al., 2013; Seibenhener & Wooten, 2015; Kraeuter, et al., 2018). Due to design differences between the apparatus used to perform each test, locomotion in the EPM and OF are not directly comparable.

The behaviour observed here is consistent with what other researchers have determined to be ‘anxiety-like’ (Pellow, et al., 1985). Considering the human EPM, the results observed here indicate similar behaviours of mice and humans following exposure to stressful stimuli; general avoidance of the open arms (Biedermann, et al., 2017). As humans have self-reported a concomitant increase in their perceived anxiety, it can be inferred that open arm aversion in the maze is indicative of increased anxious perception. It therefore would seem appropriate to consider similar behaviours in mice to be ‘anxiety-like’, in the absence of an ability of mice to self-report their emotions.

A limitation of the present study is the lack of a secondary measure of anxiety-like behaviour, such as the OFT or light dark box which would go some way to addressing the time-sensitive behavioural differences observed in the EPM. As these tests are similar in that the measure approach-avoidance behaviour, including a further test such as the hole board or novelty suppressed feeding would provide a more comprehensive insight into the overall behaviour of mice following repeated acute restraint stress and potentially strengthen the interpretation of anxiety-like behaviour.

The BNST is well documented to be recruited in rodents during restraint stress and to endure plastic changes as a result (Casada & Dafny, 1991; Cecchi, et al., 2002; Lin, et al., 2018; Kovacs, et al., 2018; Fetterly, et al., 2019; Vyas, et al., 2002). Both electrical stimulation of the BNST and restraint stress, separately, produce similar behavioural consequences in rats (Casada & Dafny, 1991). Furthermore, acute restraint stress increases release of norepinephrine in the lateral BNST (Cecchi, et al., 2002). Chronic restraint stress has also been shown to increase dendritic branching in the BNST of Wistar rats (Vyas, et al., 2003).

Though the effects of stress on the BNST are generally well documented, the contribution of the different parts of the BNST to the stress response is less well understood. The organisation of the BNST is incredibly complex and individual subnuclei exert different and often opposing effects on circuitry (Kim, et al., 2013; Jennings, et al., 2013; Giardino, et al., 2018; Yamauchi, et al., 2018; Xiao, et al., 2021). Therefore, labelling for c-Fos, an immediate early gene used as a marker of recent cellular activation (Herrera & Robertson, 1996; Durchdewald, et al., 2009; Chung, 2015), was employed to determine BNST activity following repeated acute restraint stress.

Increased c-Fos expression was detected in the BNST following restraint stress, an indication of BNST engagement in response to this particular stressor (Figure 3.5). Expression of c-Fos was not used here to determine the nuances of subregional responses to restraint in the BNST due to the sensitive timeframe of c-Fos expression following exposure to stimuli. Generally, c-Fos expression is greatest 60 minutes after cellular activation, and blunting of the response after repeated exposure to a stressor has previously been documented (Girotti, et al., 2006; Moench, et al., 2019). Therefore, the c-Fos expression results presented here are intended only to provide a general picture of activity in the BNST during

restraint, as a basis for proceeding experiments. Previously, a single 2 hour long session of restraint stress was shown to significantly increase c-Fos expression in rat brain regions associated with stress: BNST nuclei, with the most pronounced effects in the ventral and dorsomedial BNST, the medial, central and basolateral amygdala, and the dorsal raphe (Kovacs, et al., 2018). Consistent with the observed increase in c-Fos following restraint, the ventral BNST and dorsomedial BNST also show significantly greater c-Fos expression following other acute stressors: electric footshock stress and multimodal stress, including restraint (Lin, et al., 2018).

WFA labelling for PNNs in the anterior BNST, experimentally characterised in the previous chapter (Figures 2.3; 2.4; 2.5; 2.6), was combined here with c-Fos labelling to define the cellular populations contributing to stress responsiveness. I hypothesised that a single population of c-Fos and PNN expressing cells would emerge in the BNST, given the well documented activation of the BNST in response to restraint, together with the importance of long-lasting structural plasticity in the BNST following stress, epitomised by PNN characteristics (Casada & Dafny, 1991; Lin, et al., 2018; Kovacs, et al., 2018; Wang & Fawcett, 2012). However, the populations of PNN expressing neurons and c-Fos expressing cells were mutually exclusive overall (Figure 3.6). Therefore, no direct effect of neuronal activity, as a result of stress, on PNNs could be elucidated.

BNST plasticity is likely to be affected by stressor exposure given that the BNST is a known modulator of both stress response and anxiety-like behaviour. As PNNs are regulators of experience-driven plasticity, changes to their structure or morphology would further evidence a role for the BNST in the stress response. In the absence of a population of cells co-expressing PNNs and c-Fos - following restraint - to study, PNNs were investigated more generally in the STMA following stress.

Gene expression analysis of PNN components was performed to determine effects of restraint stress on PNN composition in the anterior BNST. Changes to the ECM following stress have been reported in other brain regions including the PFC, hippocampus and basolateral amygdala (Pesarico, et al., 2019; Santiago, et al., 2018; Ueno, et al., 2018; Yu, et al., 2020). However, such changes are very much region and stress type specific; for example, scarcity/adversity studies have reported both lower intensity of WFA labelled PNNs in the basolateral amygdala

at P23, and a higher number of PNNs specifically in the right basolateral amygdala of P28 male mice, respectively (Santiago, et al., 2018; Guadango, et al., 2020). Conversely, maternal separation studies have reported both greater intensity of PNNs, and no change to PNNs, in adult female basolateral amygdala at P18 or P28, respectively (Gildawie, et al., 2020; Richardson, et al., 2021). The only study investigating PNN expression following chronic restraint stress in adult rats reported increased numbers of PNNs in the PFC, and reduced numbers of PNNs in the hippocampus, compared with controls (Pesarico, et al., 2019). Furthermore, greater intensity of WFA labelled PNNs in the reticular thalamus and habenula, and no change to PNN number or intensity in the basolateral amygdala, was reported (Pesarico, et al., 2019).

More subtle changes in PNN composition and morphology were observed here following restraint (Figures 3.7 and 3.9), with no change in absolute number of PNNs in the STMA at any time point following stress (Figure 3.8). It is not clear from the experiments performed here the full extent of how these chemical and morphological changes manifest functionally, however the alterations to PNNs observed here following stress merit further investigation. Indeed, the seemingly incredible precision of PNN alterations, observed both in the literature and in the current study, may be exactly how they exert such specific influence functionally, and may require significant time and resources to experimentally resolve.

Stimuli which promote activation of the HPA axis are anticipated to influence PNNs, as almost all of the constituents of PNNs including brevican, neurocan, link protein, HAS and hyaluronan bear glucocorticoid response elements or are documented to be affected by corticosteroids (Rauch, et al., 1997; Rauch, et al., 1995; Rhodes & Yamada, 1995; Zhang, et al., 2000). Here, qRT-PCR revealed an increase in neurocan expression 7 days post-stress and an increase in neurocan and tenascin-R expression 14 days post-stress (Figure 3.7B, C). No change in the expression of brevican was observed at either time point post-stress (Figure 3.7A). As tissue was manually dissected from the STMA for gene expression analysis of PNN components, it is possible that changes specifically occurring in the STMA were diluted by unavoidable inclusion of BNST tissue from adjacent subnuclei.

The observed increase in expression of PNN components, particularly neurocan, also coincides with the time point where the most significant anxiety-like

behaviour was observed in mice tested in the EPM (Figure 3.4). The increase in neurocan expression 7 days post-stress may be indicative of initiation of PNN formation in the BNST as a result of the restraint stress experience. PNNs may therefore encode information pertaining to the stress stimuli. The increase in neurocan and tenascin-R 14 days post-stress suggests further recruitment of PNN components, and tracks with the more complex PNN structure observed at 14 days post-stress (Figure 3.9). Structural vulnerability in the PNNs of the anterior BNST at day 7 post-stress reflects the observed behavioural changes in the EPM. However, from the experiments performed here, it is not possible to disentangle whether the behaviour is a result of PNN vulnerability or whether the timing is coincidental; the 7 day post-stress time point may be a time where changes are simultaneously occurring, independently of one another.

A study to track various morphological parameters of PNNs following stress was undertaken, to reconcile the lack of change in PNN number in the anterior BNST following stress with the reduction in expression of PNN components. There was a critical change to PNN morphology within the STMA 7 days post-stress, while PNN expression remained unchanged. At the 7 days post-stress time point, PNNs exhibited greater hole area and perimeter and reduced intensity of the ECM surrounding the holes, i.e. the matrix of the PNN, compared with PNNs in stress naïve control mice (Figure 3.9). They also displayed greater leakiness, as measured by a reduced minimum intensity of the ECM surrounding the holes of the PNN. No changes in the flatness of PNNs, as measured by the standard deviation of the fluorescence intensity of the PNN across z-planes, were identified (Figure 3.10). Altogether, the results observed here indicate that, following stress, PNNs in the STMA still occupy the same amount of three-dimensional space, however their organisation becomes much less structurally complex and therefore more structurally vulnerable. Reduction in structural integrity of PNNs 7 days post-stress could represent a period of remodelling for PNNs in the anterior BNST. As the measured morphological changes all returned to levels similar to control 14 days after stress, indicating non-permanent alteration to PNNs, further credibility is given to a PNN remodelling period in the STMA post-stress. Recovery of morphological changes 14 days post-stress follows a similar timeline to identified changes in anxiety-like behaviour. A period of vulnerability and increased anxiety-like behaviour was identified 7 days post-stress, but by 14 days

post-stress anxiety index scores were comparable to stress naïve mice (Figure 3.4). However, stressed mice still showed some level of anxiety-like behaviour in the EPM 14 days post-stress, considering open arm entries and time spent in the open arms of the maze (Figure 3.4). The delay in recovery of behaviour to control levels could indicate that fluctuations in the structure and composition of the net precede behavioural changes and therefore contribute to the observed behaviour. Alternatively, the morphological changes occurring in PNNs could encode longer-lasting responses to anxiety-provoking stimuli and could therefore offer some future level of protection against such stimuli.

Next, I performed an electrophysiological study of STMA slices from stress naïve mice and mice 7 days post-stress to elucidate the neuronal underpinnings of the behavioural changes observed post-stress. NMDA was applied to slices to investigate neuronal excitability, since very little spontaneous activity was observed in the STMA (Figure 3.3). It was anticipated that the firing rate of all units would increase in response to NMDA, which was predominantly the case (Figure 3.12D). However, a small population of units that fired at a faster baseline rate, compared to most other units, reduced their firing rate in response to NMDA (Figure 3.11).

One possible explanation for a reduction in firing rate could be NMDA induced excitotoxicity, with excessive Ca^{2+} entering these cells, leading to neuronal death (Choi , et al., 1988; Zhou, et al., 2013). However, firing rate was recovered in decreaser units following wash-off of NMDA (Figure 3.11), suggesting that the reduction in firing rate cannot be explained by excitotoxicity. Another possible feature underlying reduced firing could be that decreaser neurons were hyperpolarised by NMDA and thus unable to fire. NMDA has been reported to hyperpolarise pyramidal-like projection neurons in the guinea pig lateral amygdala (Danober, et al., 2000). While pyramidal-like neurons have not been reported in rodent BNST so far, they have been identified in human BNST, indicating that their existence in rodents could be plausible (Zivanovic-Macuzic, et al., 2007). Hyperpolarisation generally lasts in the order of magnitude of milliseconds to seconds, but not minutes as observed here. Furthermore, in the study of the guinea pig lateral amygdala, hyperpolarisation preceded prolonged depolarisation of pyramidal-like neurons, whereas the units recorded here were generally silent for the entire length of NMDA application (Danober, et al., 2000).

Alternatively, decreaser units in the STMA may be neurons which receive GABAergic projections from neurons elsewhere in the BNST, or even the slice, if connections to other brain regions remained intact. If NMDA were to act on inhibitory projection neurons to increase their firing, as seen in the increaser phenotype, and to a lesser extent the non-responder phenotype, these neurons could project to units with a decreaser phenotype to inhibit their activity. A negative feedback mechanism is more likely than the excitotoxicity or prolonged hyperpolarisation hypotheses discussed, given the proportions of each responder subtype; populations of increasers and non-responders were greater than decreasers, and the STMA is reported to exhibit predominantly GABAergic transmission (Turesson, et al., 2013). The hypothesis could be tested by investigating whether there is a consistent, time-locked delay in response to NMDA by the decreaser population, compared to the increaser and/or non-responder population. Alternatively, a paired experiment to stimulate neurons whilst intracellularly recording from other neurons they may share connections with could resolve the mechanistic underpinnings of NMDA induced firing rate reductions. However, given only ~4% of units were classified as decreasers, it would be a time consuming and potentially laborious process to target sufficient numbers of neurons to determine the mechanism of NMDA induced reduction in firing rate in this population.

The changes in firing rate in response to NMDA following stress will have wider implications for the overall excitatory/inhibitory balance within the BNST. If, as hypothesised, the increaser subtype of neurons in the STMA are GABAergic and fire more frequently following stress, this will lead to greater inhibition. Excitatory neurons within the BNST may be directly inhibited, however, is also possible that these inhibitory neurons project to other inhibitory neurons, in which case there will be a relief of inhibition of these projections, which could result in increased excitation of downstream projections. As the BNST is a complex structure which is highly intra- and inter-connected, it is likely that direct inhibition of excitatory neurons and indirect relief of inhibitory projection neurons is simultaneously occurring. As the BNST expresses a greater proportion of GABAergic neurons than glutamatergic neurons, greater inhibition may indirectly lead to greater excitatory transmission within the BNST and therefore from the BNST via efferent projections.

pMEA recordings are extracellular, and therefore provide a general overview of the electrical activity of a population of cells, at fixed points. While spike sorting analysis can deconvolute signals from multiple neurons and resolve them to the level of individual units, with pMEA recordings it is impossible to know truly how many neurons are being recorded from or exactly where those signals arise from. Therefore, conclusions cannot be drawn on a single cell basis in the way they might for other electrophysiological techniques such as patch clamp. pMEA experiments performed here were further limited due to the prior lack of knowledge about the types of cells being recorded from. Lack of clarity in the literature on the naming conventions of different BNST subnuclei makes it difficult to pinpoint exactly which regions express which types of neurons. Further experiments were not performed here to elucidate the pharmacological nature of the observed changes in putative single unit firing post-stress, but could be undertaken in the future, and would provide additional context to the observations made here.

The separation of units based on their firing responses to NMDA was also applied when investigating the electrophysiological effects of acute immobilisation stress in the mouse BNST. Restraint stress significantly increased the firing rate of the increaser unit subtype in response to NMDA application, indicating an increase in NMDA-mediated excitability of this responder subtype (Figure 3.11). Enhanced NMDA-mediated excitability of neurons has previously been reported in the commissural/associational input to CA3 hippocampal area following chronic restraint stress (Kole, et al., 2002). One possible explanation for the observed increase in excitability is that the NMDA molecules have greater access to pre- and post-synaptic terminals of neurons post-stress. As determined by expression studies, neurons which express PNNs in the STMA are numerous (Figure 2.5) and morphological studies revealed that PNNs are structurally more vulnerable 7 days post-stress (Figure 3.9), the time point chosen for electrophysiological studies. PNNs with less complex structures, observed post-stress, likely have reduced barrier function and therefore exogenous, and endogenous, molecules are more likely to reach the neuron. Increased access of exogenous NMDA to receptors at the synapse would increase the likelihood of neuronal action potential firing and could increase the firing rate of neurons if availability of NMDA was the limiting factor to activation, previously. However, non-responder unit

firing changed in the opposite direction following stress, with units firing at a significantly slower rate compared to those in control slices. The observed changes in excitability are therefore more likely to be generated intrinsically, and as such, are possibly less reflective of the morphological changes occurring in PNNs at this time point, though they may still be a contributing factor.

Alterations in NMDA receptor expression or distribution are most likely to facilitate observed changes in NMDA-mediated excitability. NMDA is a specific partial agonist of NMDA receptors, acting at the glutamate specific site of the receptor, and does not have known additional biological mechanisms of action. Therefore, any observed changes in NDMA-mediated excitability are likely a direct result of changes to NMDA receptors. NMDA receptors regulate the development of intrinsic neuronal excitability, and alterations in their expression have been reported in brain regions involved in anxiety circuitry following stress (Hou & Zhang, 2017; Pawlak, et al., 2005; Calabrese, et al., 2012; Pacheco, et al., 2017). Specifically, chronic restraint stress reduces the expression of NR1, N2A and N2B NMDA receptor subunits in the hippocampus of mice (Pawlak, et al., 2005). However, a more recent study focusing separately on the dorsal and ventral hippocampi reported reductions in NR1 and NR2A subunits in the dorsal hippocampus but an increase in the NR2B subunit, whereas only reduced expression of the NR1 subunit was reported in the ventral hippocampus (Pacheco, et al., 2017). Rats were used in the Pacheco et al. (2017) study, however, and the chronic stress paradigm was of lower intensity and duration than the paradigm employed in the Pawlak et al. (2005) study. Therefore, the type and duration of stress likely has a large impact on the electrophysiological changes observed post-stress. Nevertheless, opposing changes in NDMA receptor subunit expression observed in the hippocampus following stress could support a similar underlying mechanism in the BNST.

The opposing findings in different responder populations suggest that changes in NMDA receptor expression following stress are complex. The expression of different NMDA receptor subunits, and therefore NMDA receptor composition, has not yet been characterised in detail in the BNST. However, N2D subunits which co-localise with CRF transcripts in the dorsolateral BNST have been identified (Salimando, et al., 2020). Furthermore, mice lacking the N2D subunit (GluN2D-/-) exhibit reduced synaptic potentiation in the BNST and exacerbated

negative emotional behaviour. The N1R subunit has also been identified in mouse BNST (Gafford, et al., 2014). However, mice lacking the NR1 subunit in CRF expressing neurons display similar levels of anxiety-like behaviour to control mice (Gafford & Ressler, 2015). Consistent with previous studies, it is likely that functional changes observed here occur as a result of alterations in NR2 subunits, as opposed to NR1 subunits, as NR2 subunits are generally accepted as the site for glutamate, and therefore NMDA, binding (Anson, et al., 1998; Anson, et al., 2000; Laube, et al., 1998). To build on the reported results, further electrophysiological experiments, either using pMEA or patch clamp could be performed using selective antagonists of specific NMDA receptor subunits to elucidate the pharmacological underpinnings of the observed changes in NMDA-mediated excitability in both the increaser and non-responder populations.

3.6 Conclusions

Overall, the experimental findings in results chapter 3 uncover a relationship between PNNs in the STMA and the stress response. Stress-induced morphological alterations to PNNs in the STMA precede measurable changes in anxiety-like behaviour in the EPM. Moreover, the timeframe of morphological and chemical modifications occurring within PNNs appear to directly correlate with observed behavioural changes. At the time point following stress where PNNs show the greatest structural vulnerability, changes in NMDA-mediated excitability of putative single units in the STMA are also apparent. Specific degradation of PNNs in the STMA, using ChABC, may allow further disentanglement of PNN contribution to changes in anxiety-like behaviour and cellular excitability.

Chapter 4 – The role of perineuronal nets in the anteromedial bed nucleus of the stria terminalis in regulating neuronal activity and behaviour following stress

4.1 – Introduction

Electrophysiological properties of neurons within the bed nucleus of the stria terminalis

The BNST is composed of multiple cellular populations within its distinct nuclei. BNST neurons can be divided into at least three types based on their electrophysiological properties, primarily determined by whole cell patch clamp studies: Type I, Type II and Type III (Hammack, et al., 2007; Silberman, et al., 2013; Rodriguez-Sierra, et al., 2013; Daniel & Rainnie, 2016; Daniel, et al., 2017). These neuronal subtypes are observed across species, specifically mouse, rat and primate, and are found in the anterolateral, anteromedial and anteroventral subnuclei (Daniel, et al., 2017; Rodriguez-Sierra, et al., 2013; Silberman, et al., 2013). The distinguishing feature between subnuclei is the incidence of Type II cells – more Type II neurons are found in the anteromedial and anteroventral BNST (approximately 70%) compared to the anterolateral BNST (approximately 40%; Rodriguez-Sierra, et al., 2013). Consequently, less Type III neurons are found in the anteromedial and anteroventral BNST (≤ 8%), compared to the anterolateral BNST (approximately 29%). The prevalence of Type I neurons is similar in all three regions at approximately 25% (Rodriguez-Sierra, et al., 2013).

Type I neurons exhibit a regular spiking pattern in response to depolarising current injection (Hammack, et al., 2007; Rodriguez-Sierra, et al., 2013). Both the resting membrane potential and input resistance of Type I neurons are modulated by the hyperpolarisation-activated cyclic nucleotide (HCN) gated current I_h, encoded by four genes HCN1-4 (Hammack, et al., 2007). The expression of HCN genes determine the distinct properties of I_h channel isoforms. In the BNST, expression levels of HCN1 mRNA are high, moderate expression of HCN3 has been observed, and HCN2 and 4 are comparatively lowly expressed (Monteggia, et al., 2000). Furthermore, I_h channel activity is enhanced by neurotransmitters including serotonin, dopamine and CRF which are all released into the BNST following stressor exposure (Cardenas, et al., 1999; Wu & Hablitz, 2005; Qiu, et al., 2005). As GABA transmission predominates in the BNST, the regular firing of

Type I neurons suggests they evoke tonic GABA release (Hammack, et al., 2007).

Type II neurons are identified by their low threshold bursting in response to depolarising current injection (Hammack, et al., 2007; Rodriguez-Sierra, et al., 2013). As with Type I neurons, the input resistance and resting membrane potential of Type II neurons are modulated by I_h channels, however the burst firing activity of Type II neurons is regulated by an I_T calcium current, in synergy with the I_h current (Hammack, et al., 2007). I_T currents can also be affected by neurotransmitters including acetylcholine, substance P and 5-hydroxytryptamine (5-HT), which exert receptor dependent effects; activation of 5-HT_7 receptors enhances I_T currents, whereas activation of 5-HT_2 receptors inhibits I_T currents (Lenglet, et al., 2002; Placantonakis, et al., 2000). The burst firing of Type II neurons, aside from their regular firing, may suggest a co-release of GABA and other neuropeptides in BNST afferents, as BNST neurons often co-express neuropeptides including cholecystokinin, substance P and CRF (Woodhams, et al., 1983).

Type III neurons are defined by a fast inward rectification in response to hyperpolarising current injection (Hammack, et al., 2007; Rodriguez-Sierra, et al., 2013). Unlike Type I and II neurons, Type III neurons do not express pronounced I_h or I_T currents (Daniel, et al., 2017). Type III neurons have a typically more hyperpolarised resting membrane potential and therefore a higher threshold for action potential firing than Type I or II neurons. The inward rectification is indicative of inwardly rectifying potassium current channels $I_{K(IR)}$, of which there are seven subfamilies (Hazra, et al., 2012). The $I_{KIR}2.3$ channel is expressed in pyramidal neurons within the cortex, which regulate excitatory transmission (Day, et al., 2005; Inanobe, et al., 2002; Takigawa & Alzheimer, 2002). Type III neurons may therefore facilitate excitatory transmission within the BNST (Hammack, et al., 2007).

Two further region-specific populations have also been identified in the BNST: late firing cells and spontaneously active cells. Late firing cells are exclusively found within the anterolateral subnucleus and account for around 4% of cells here (Rodriguez-Sierra, et al., 2013). Late firing cells display the lowest input resistance and the most negative resting membrane potential of all characterised BNST cells and are defined by their delayed firing in response to suprathreshold

depolarising current injection (Rodriguez-Sierra, et al., 2013). Spontaneously active cells reside in the anteroventral BNST and account for approximately 8% of the cells in the region. Of all the characterised cell types in the BNST, spontaneously active cells exhibit the shortest action potential duration, and maintain a stable firing rate, which increases with successive depolarising current injections until spike failure at strong currents (Rodriguez-Sierra, et al., 2013). Notably, no anatomical, chemical, or morphological correlates have yet been identified which correspond to the electrophysiological phenotypes of cells within the BNST.

Impact of PNN digestion on neuronal properties across the brain

While administration of ChABC *in vivo* has provided data to support memory-related behavioural consequences of PNN degradation in individual brain regions, *in vitro* application of ChABC has been used to examine the electrophysiological consequences of PNN degradation on neuronal activity. Most studies have focussed on patch clamp recording of fast-spiking PV-positive interneurons, as these neurons make up a large proportion of PNN expressing neurons throughout the brain (Miyata, et al., 2012; Balmer, 2016; Tewari, et al., 2018; Chu, et al., 2018; Hayani, et al., 2018). Treatment of mouse brain slices with 0.2 U/mL ChABC reduced the excitability of medial nucleus of the trapezoid body neurons – neurons required more current to spike than those in untreated control slices and exhibited reduced firing rates (Balmer, 2016). 0.2 U/mL ChABC is sufficient to fully degrade PNNs such that they are undetectable by WFA labelling (Bukalo, et al., 2001; Balmer, 2016). A dose dependent effect of ChABC has been discussed in the context of tissue engineering, with lower concentrations improving collagen content of grown tissues, but not in the enzymatic degradation of PNNs in the brain. Reduced excitability was also observed in cortical inhibitory interneurons following ChABC treatment. In both the medial nucleus of the trapezoid body and cortical inhibitory neuronal populations, no differences were observed in passive neuronal properties such as input resistance or resting membrane potential (Balmer, 2016).

PNN digestion also reduced neuronal excitability with reduced halfwidth and amplitude of action potentials in an independent study of cortical neurons in

mouse barrel cortex slices (Chu, et al., 2018). However, differences in passive neuronal properties were observed in the Chu et al. (2018) study in disagreement with Balmer et al. (2016) – the resting membrane potential of neurons in ChABC treated mouse slices was significantly more depolarised, and input resistance was significantly reduced (Chu, et al., 2018). Intrinsic excitability was also significantly reduced in the deep cerebellar nuclei following treatment of slices with ChABC (O'Dell, et al., 2021). Large excitatory neurons in the deep cerebellar nuclei required a larger current to spike following treatment of slices with ChABC, similar to the medial nucleus of the trapezoid body neurons. Neurons also showed a prolonged interspike interval, a larger after-hyperpolarisation amplitude and a lower voltage to reach action potential threshold, but unaltered membrane potential and input resistance, after treatment with ChABC in comparison to vehicle treated slices (O'Dell, et al., 2021). Reduced neuronal excitability has also been reported in peritumoral fast-spiking neurons (Tewari, et al., 2018). Gliomas secrete enzymes, including matrix metalloproteinases, known to remodel or degrade PNNs (Fillmore, et al., 2001; Huntley, 2012). Endogenous degradation of PNNs surrounding peritumoral neurons reduced the firing rate of fast-spiking neurons and their specific membrane capacitance in *scid* mice implanted with an epileptogenic patient-derived xenoline (Tewari, et al., 2018). This suggests that PNNs may exhibit an insulator function, analogous to a myelin sheath, allowing the neurons they surround to fire at supraphysiological rates.

Increased neuronal excitability is reported in the hippocampus following PNN degradation, contrary to the reduced excitability of neurons observed in other brain areas (Dityatev, et al., 2007; Hayani, et al., 2018; Bukalo, et al., 2001). In hippocampal cultures treated with ChABC, neurons exhibited faster firing in response to current injection and generated more depolarising action potentials, with reduced after-hyperpolarisation compared with control cultures (Dityatev, et al., 2007). Passive properties including input resistance, capacitance and resting membrane potential were unaffected in ChABC treated slice cultures compared to controls. Fast-spiking interneurons in hippocampal slices from mice injected with ChABC *in vivo* generated action potentials with longer duration and larger amplitudes in response to less depolarising currents, and pyramidal cells were excited at less depolarising membrane potentials (Hayani, et al., 2018). Notably, these alterations in neuronal excitability were not observed with acute treatment

of hippocampal slices with ChABC, suggesting a muti-faceted response to PNN degradation *in vivo*, which could not be replicated *in vitro*. Altogether these data support differing roles of PNNs, dependent on location, type of neuron under investigation, and level of PNN degradation, at both the behavioural and cellular level. The contribution of both *in vivo* and *in vitro* studies which complement one another are therefore invaluable in the investigation of PNNs.

No study to date has investigated the contribution of PNNs to neuronal excitability in the BNST. In addition, the functionality of PNNs within the BNST remains unexplored. In the current chapter I will investigate whether changes in PNN expression within the STMA affect firing properties of BNST neurons and mouse behaviour at baseline and following acute repeated restraint stress.

4.2 Aims

In the current chapter I will address the following three main aims:

(1) determine effects of PNN degradation on synaptic transmission in the anteromedial BNST

(2) examine anxiety-like behaviour following *in vivo* degradation of PNNs in the anteromedial BNST

(3) investigate behavioural response to acute stress following PNN degradation in the anteromedial BNST

4.3 – Methods

4.3.1 Animals

Male, wild-type C57BL/6J mice aged 8-13 weeks, were used in experiments.

4.3.2 The effect of acute perineuronal net degradation on the activity of neurons in the anteromedial bed nucleus of the stria terminalis

Slice preparation

Male mice aged 8-13 weeks were killed by cervical dislocation, followed by decapitation, and the brain was quickly removed and placed into ice-cold sucrose solution. Slices were prepared as described in section 3.3.5. STMA sections were hemisected, and each half of the slice was incubated at ~34°C for 1 hour in 8mL bubbled aCSF with 0.01% BSA (control slices) or aCSF with 0.01% BSA with the addition of 0.2U mL^{-1} ChABC (ChABC-treated slices; Figure 4.3A; Bukalo, et al., 2001; Balmer, et al., 2016).

Multielectrode array recording

Multielectrode array recording was performed, data were transformed, and recordings were analysed, consistent with the methodology described in section 3.3.5.

Verification of PNN degradation

To verify PNN degradation, slices were fixed immediately following pMEA recording in 4% PFA, overnight, at 4°C. The following day, slices were washed with PBST and pre-incubated in blocking solution for one hour at room temperature. Slices were subsequently incubated with WFA in blocking solution (1:500) for a further hour, protected from light. Slices were then washed in PBST for 3 x 15 minutes and mounted on Epredia™ Epoxy Diagnostic Slides (Thermo Fisher Scientific, UK) with Fluorsave mounting media. Slices were left to dry for 24 hours prior to microscope imaging (Scientifica, UK), using µManager software (Cairns Research, UK). A single field of view was imaged for each slice, using a 488 nm wavelength laser for fluorophore excitation.

4.3.3. The effect of perineuronal net degradation *in vivo* on anxiety-like behaviour and responsiveness to stress-inducing restraint

Stereotaxic surgery

All surgeries were performed under stereotaxic guidance using a 'just for mouse' stereotaxic frame (Stoelting, USA), using aseptic techniques. Mice were first anaesthetised in a chamber with isofluorane (2.0%) and oxygen (2 L min^{-1}), and then transferred to a gas mask, where isofluorane and oxygen continued, for surgical preparation. Mice were shaved and cleaned with Hibiscrub from the neck to behind the eyes, and buprenorphine (0.15mg/kg, subcutaneous) was administered to provide analgesia, before transfer to the stereotaxic frame. Depth of anaesthesia was monitored by testing the pedal reflex whilst the mouse was using the gas mask and following transfer to the stereotaxic frame.

Whilst mice were in the frame, anaesthesia was maintained with isofluorane (1.5%) and oxygen (2 L min^{-1}) and was continuously monitored. A small skin incision was made down the midline to facilitate bilateral craniotomies made using a 0.5 mm drill bit (Cooksongold, UK) attached to a drill (Kit K.1090; Foredom, USA). Injection coordinates were determined using the Franklin and Paxinos mouse brain reference atlas (Franklin & Paxinos, 2007). Anteromedial BNST injections were made at 0.38 mm anteroposterior, +/- 0.5 mm mediolateral and -3.75 mm dorsoventral to bregma (Figure 4.1). ChABC enzyme (Sigma Aldrich, UK), or sterile PBS (0.5 M; Sigma Aldrich, UK) in the case of control surgeries, was injected using a 35G bevelled needle (World Precision Instruments, USA) inserted into a 10 µL Hamilton syringe connected to a microsyringe pump and controller (both World Precision Instruments, USA) to control the speed of injection. The needle was lowered to -3.75mm dorsoventral, measured from the top of the brain, and mice were bilaterally injected with enzyme or PBS, 300 nL per site, at a rate of 100 nL min^{-1}. The needle remained in place for five minutes, before slow withdrawal. Each animal was given 0.5 mg kg^{-1} of carprofen analgesic via subcutaneous injection before being allowed to recover on a heat pad. Once fully recovered from anaesthesia animals were singly housed and given diet gel and wet mash diet to aid recovery. Mice were given 0.5 mg kg^{-1} of carprofen once a day for the following three days. Post-surgery, mice were checked three times daily by visual observation and scored, using an in-house monitoring system, based on their movement, appearance, and general demeanour; specifically,

observations were made regarding coat condition, eye/nose secretions, hunching posture, gait, wound appearance and food/water intake. Mice were also weighed once daily until they regained their pre-surgery weight – typically mice lost 5-10% of their bodyweight, but generally regained their body weight within 7 days post-surgery. Regardless of scoring or weight, mice were left to recover for a minimum of 7 days before being subjected to any further experimental procedures. 100% of mice undergoing surgery recovered at 7 days post-surgery and no mice were excluded from the study due to post-surgical complications or exceeding humane end points.

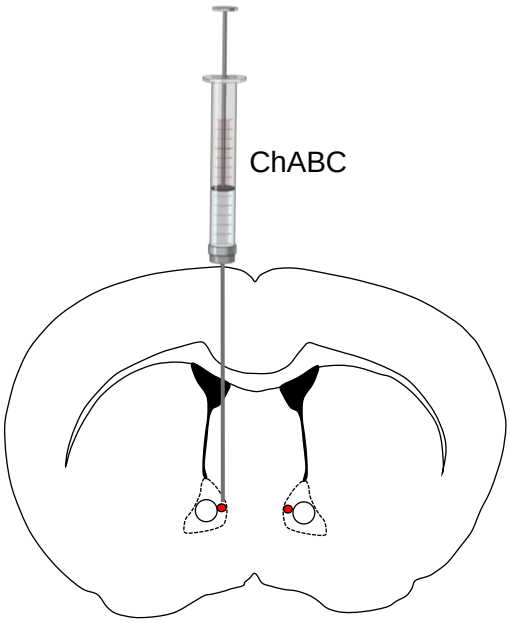

Figure 4.1 Schematic illustration of injection site within the anteromedial bed nucleus of the stria terminalis. Coordinates for all stereotaxic injections were 0.38 mm anteroposterior, +/- 0.5 mm mediolateral and -3.75 mm dorsoventral, as measured from the top of the brain, relative to bregma. The bed nucleus of the stria terminalis is highlighted by the dashed lines, and the injection site is highlighted in red.

Experimental design

Experiment I: effect of PNN degradation in the STMA on anxiety-like behaviour

7, 14, 21 or 30 days following stereotaxic injection with ChABC mice were placed in the EPM for 5 minutes (Figure 4.2). Control mice were injected with PBS and subjected to the EPM 7 days after injection. Mouse behaviour in the EPM was video recorded and scored as described in Chapter 3, section 3.3.2. Mice in Experiment I were allocated to separate groups and were not repeat tested at successive time points. Priority of group number was given to the control group

and 7 day post-stress group as the main comparison of interest. The groups with longer latencies from ChABC injections were included to determine any adverse effects of PNN digestion in the longer term and are therefore of less experimental interest.

Experiment II: effect of PNN degradation in the STMA on anxiety-like behaviour following repeated acute restraint stress

Four experimental groups were used in Experiment II: two experimental groups were exposed to the repeated acute restraint stress protocol, two hours a day for three consecutive days, prior to a PBS (group 1) or ChABC (group 2) injection; another two experimental groups first received either a PBS (group 3) or a ChABC (group 4) injection prior to exposure to the repeated acute restraint stress protocol (Figure 4.2).

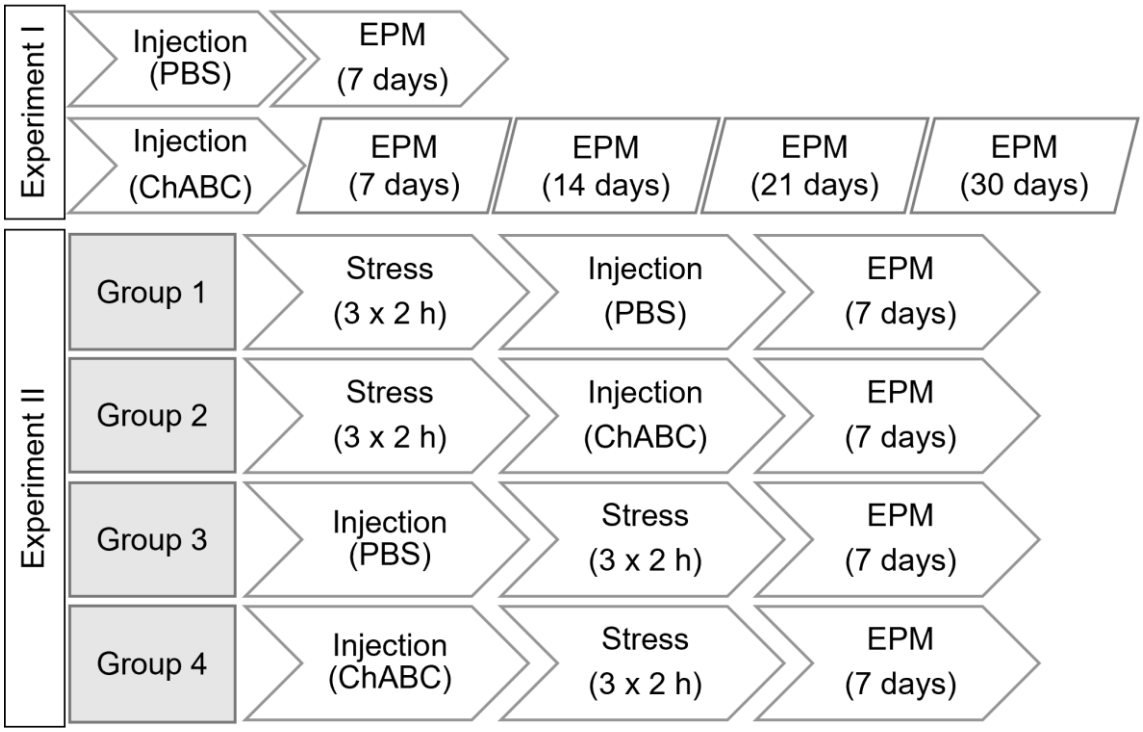

Figure 4.2. Schematic illustration of experimental design to assess the effects of perineuronal net digestion in the anteromedial bed nucleus of the stria terminalis on anxiety-like behaviour. Experiment I: to test whether ChABC mediated degradation of perineuronal nets affected baseline anxiety-like behaviour, PNNs were degraded, and mice were subjected to the elevated plus maze 7, 14, 21 or 30 days following injection. Control mice received a PBS injection and were subjected to the maze 7 days following injection. Number of mice in each group were as follows: control = 5; 7 days post-stress = 6; 14 days post-stress = 3; 21 days post-stress = 3; 30 days post-stress = 4. Experiment II: to test both the anterograde and retrograde effect of ChABC, PNNs were digested before stress in one group and following stress in another, with accompanying control groups who received PBS injections at the corresponding times. Number of mice in each group were as follows: Group 1 = 9; Group 2 = 7; Group 3 = 9; Group 4 = 8.

4.3.4 Statistical analysis

Differences between two groups were determined using an unpaired t-test. Where more than two groups were compared, a one-way ANOVA was performed to determine significant differences between groups. If the ANOVA yielded a statistically significant result, a Tukey *post hoc* test was used to test for multiple comparisons, except where otherwise stated. All data are presented as violin or dot plots with mean ± SEM; *$p < 0.05$, **$p < 0.01$, ***$p < 0.001$.

4.4 – Results

4.4.1 Effect of perineuronal net degradation on the electrophysiological properties of putative single units within the bed nucleus of the stria terminalis *in vitro*

To determine the electrophysiological effects of PNN digestion in the STMA, the incubation protocol designed by Bukalo et al. (2001) was employed in acute slices from the STMA. One hour of slice incubation with 0.2U mL^{-1} ChABC was sufficient to digest PNNs as confirmed by a lack of WFA staining in both the STMA and the cortex (Figure 4.3). Cortical regions were not of experimental interest in the present electrophysiological study – however, images are presented here to demonstrate PNN digestion with more clarity, as cortical regions express PNNs at a high density compared to BNST (Lensjo, et al., 2017a). Slices incubated with BSA show intact PNNs, identified by WFA staining in both the cortex (Figure 4.3B) and BNST (Figure 4.3C). Slices incubated with ChABC show no discernible PNNs in the cortex (Figure 4.3B) or in the BNST (Figure 4.3C) following WFA staining. Every section used for electrophysiology experiments was checked for PNN expression, both control and ChABC treated slices, following recording.

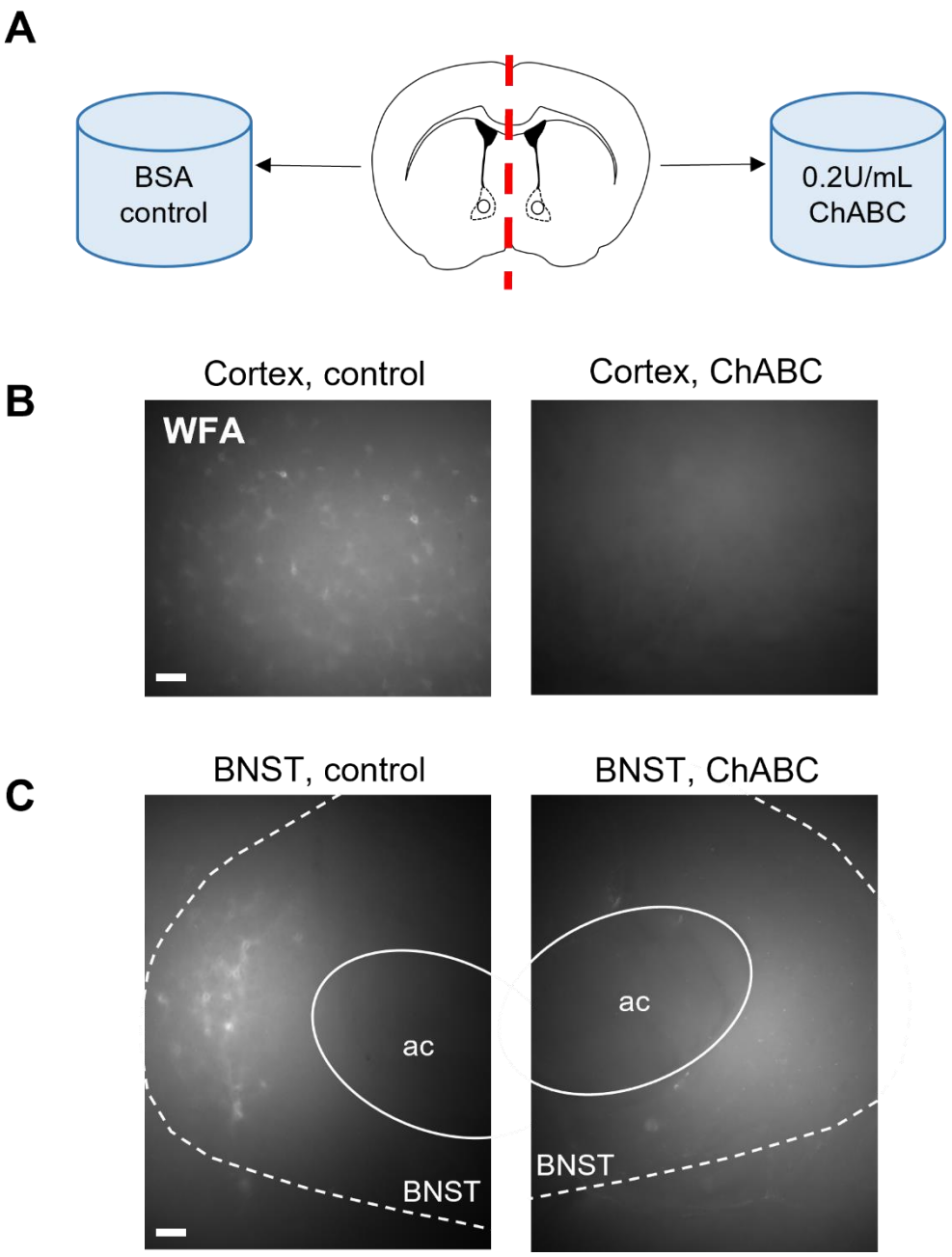

Figure 4.3. Acute treatment of brain slices with chondroitinase ABC. (A) A schematic representation of the treatment of bed nucleus of the stria terminalis containing brain slices prior to electrophysiological recording. Each half of a brain slice was incubated for one hour in aCSF with either BSA (control) or 0.2 U/mL ChABC. Light micrographs of 400 µm brain slices were taken following incubation with ChABC *in vitro*. Perineuronal nets were fully degraded, as no WFA staining was observed in cortex (B) or BNST (C). The anterior commissure is denoted on the images (ac), surrounded by the BNST (BNST). Scale bar = 100 µm.

To account for differences in baseline firing rates between individual slices, firing rates were z-scored to the baseline prior to analysis. Z-scored firing rates are presented as violin plots, to show the relative distribution of the data points, with mean and interquartile range indicated. The width of the violin indicates the relative number of data points with and equivalent firing rate.

ChABC treatment to degrade PNNs in the STMA had no effect on neuronal responsiveness to NMDA, as measured by pMEA recordings (Figure 4.4). There was no difference in the firing rate of increaser units, which display higher firing rates in the presence of NMDA, between control and ChABC treated slices (Figure 4.4B; BSA control: 1.236 ± 0.049; ChABC: 1.183 ± 0.027). Similarly, ChABC treatment did not affect the firing rate of non-responder units, which do not show altered firing rate responses to NMDA, compared with control slices (Figure 4.4D; BSA control: 0.177 ± 0.048; ChABC: 0.090 ± 0.048). Finally, there was no change in the firing rate of decreaser units, which show reduced firing rates in response to NMDA, following PNN degradation with ChABC compared to BSA treated control slices (Figure 4.4F; BSA control: -0.910 ± 0.010; ChABC: -0.967 ± 0.057). The firing rate profiles were strikingly similar between units in control and ChABC treated slices across the length of the recordings for increaser, decreaser and non-responder subtypes (Figure 4.4A, C, E).

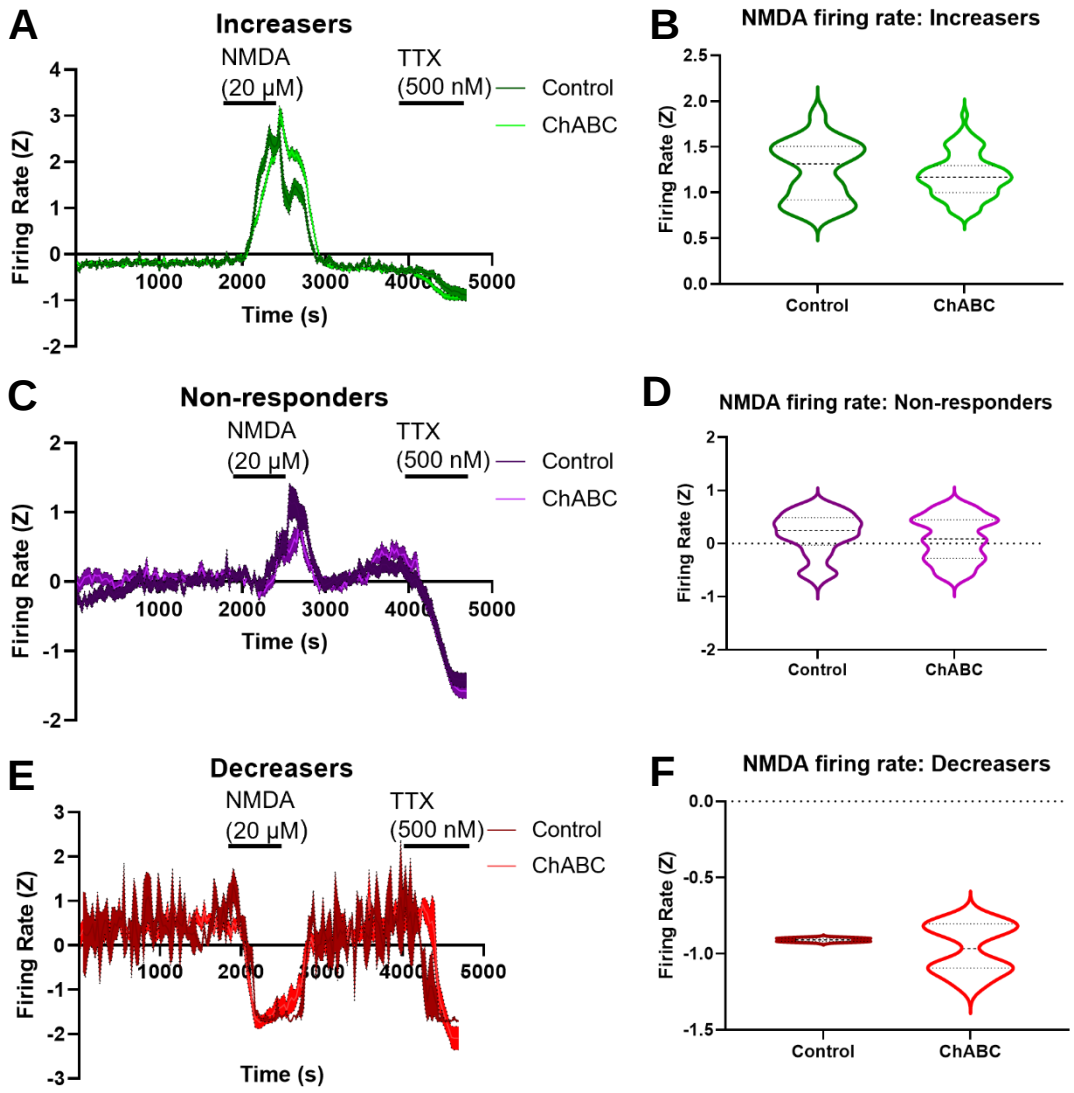

Figure 4.4 The impact of *in vitro* digestion of perineuronal nets on the firing rate of putative single units in the anteromedial bed nucleus of the stria terminalis in response to *N*-Methyl-D-Aspartate. (A) Electrophysiological traces of all putative single units which increase their firing in response to NMDA application in slices from mice after perineuronal net digestion with ChABC (light green trace) and BSA treated control (dark green trace). Firing rates are z-scaled to the baseline firing rate and presented with a shaded error bar of the SEM. The black bars indicate the duration of application of NMDA (20 µM) and TTX (500 nM). (B) Quantification of firing rate of all putative single unit increasers from BSA and ChABC treated slices. There was no difference in firing rate of increasers after NMDA application between BSA and ChABC treated slices. (C) Graph of firing rate of putative single units which do not change their firing rate in response to NMDA application over the experimental time course in slices treated with BSA (dark purple trace) and ChABC (light purple trace). (D) Quantification of firing rate of all putative single unit non-responders to NMDA, from BSA and ChABC treated slices. There was no difference in firing rate of non-responders after NMDA application. (E) Graphical representation of the firing rate of putative single units which decrease their firing rate in response to NMDA, over the course of the multielectrode array recording, in slices treated with ChABC (light red trace) and BSA control (dark red trace). (F) Quantification of firing rate from all putative single unit decreasers from BSA and ChABC treated slices. There was no difference in firing rate in response to NMDA in the non-responder type putative single units. Control N = 7 slices from 7 animals; Increasers: N = 43; Decreasers: N =: 2; Non-responders: N = 67; Total = 112. ChABC N = 7 slices from 7 animals: Increasers: N = 75; Decreasers: N = 8; Non-responders: N = 74; Total = 157. Data are presented as violin plots with mean±SEM (B, D, F); t-test.

Response to NMDA was intrinsically linked to the baseline firing rates of units in both control and ChABC treated slices (Figure 4.5). The decreaser subtype within control slices exhibited a greater firing rate under basal conditions than both the increaser and non-responder unit subtypes (Figure 4.5A; increaser: -0.2 ± 0.04; decreaser: 0.47 ± 0.37; non-responder: -0.07 ± 0.05). However, statistical significance could not be evaluated here due to insufficient numbers of decreaser units detected in control slices (n = 2). Baseline firing rate was different between increaser, decreaser and non-responding putative single unit subpopulations in ChABC treated slices (Figure 4.5B; $F(2,154) = 11.85$, $P < 0.0001$). Decreasers displayed significantly greater firing rates at baseline compared with increasers and non-responders (Figure 4.5B; decreaser: 0.406 ± 0.075; vs. increaser: -0.179 ± 0.032; $p = 0.0003$; and non-responder: -0.050 ± 0.057; $p = 0.0416$). Non-responders also exhibited greater baseline firing rates than increasers ($p = 0.0014$).

ChABC mediated degradation of PNNs in the STMA also significantly affected the overall interspike interval of putative single units in the STMA (Figure 4.5C). Units in slices treated with ChABC exhibited shorter interspike intervals compared with units in control slices (Figure 4.5C; BSA control: 26.80 ± 5.97 s; vs. ChABC: 51.77 ± 11.99 s, $p = 0.044$).

The proportions of each responder subtype were slightly different between ChABC treated slices and controls (Figure 4.5D). More increasers and decreasers were detected in slices treated with ChABC (Figure 4.4D; increaser: 47.8%; decreaser: 5.1%; non-responder: 47.1%) compared to control slices where more non-responders were detected (Figure 4.5D; increaser: 38.4%; decreaser: 1.8%; non-responder: 59.8%). It was not possible to statistically assess whether the proportions of each responder subtype were significantly different between BSA and ChABC treated slices.

Additional statistical comparisons were made between the baseline firing rates of BSA control and ChABC treatment groups for each NMDA responder subtype, but no differences were observed (Appendix 1 Table 6.12).

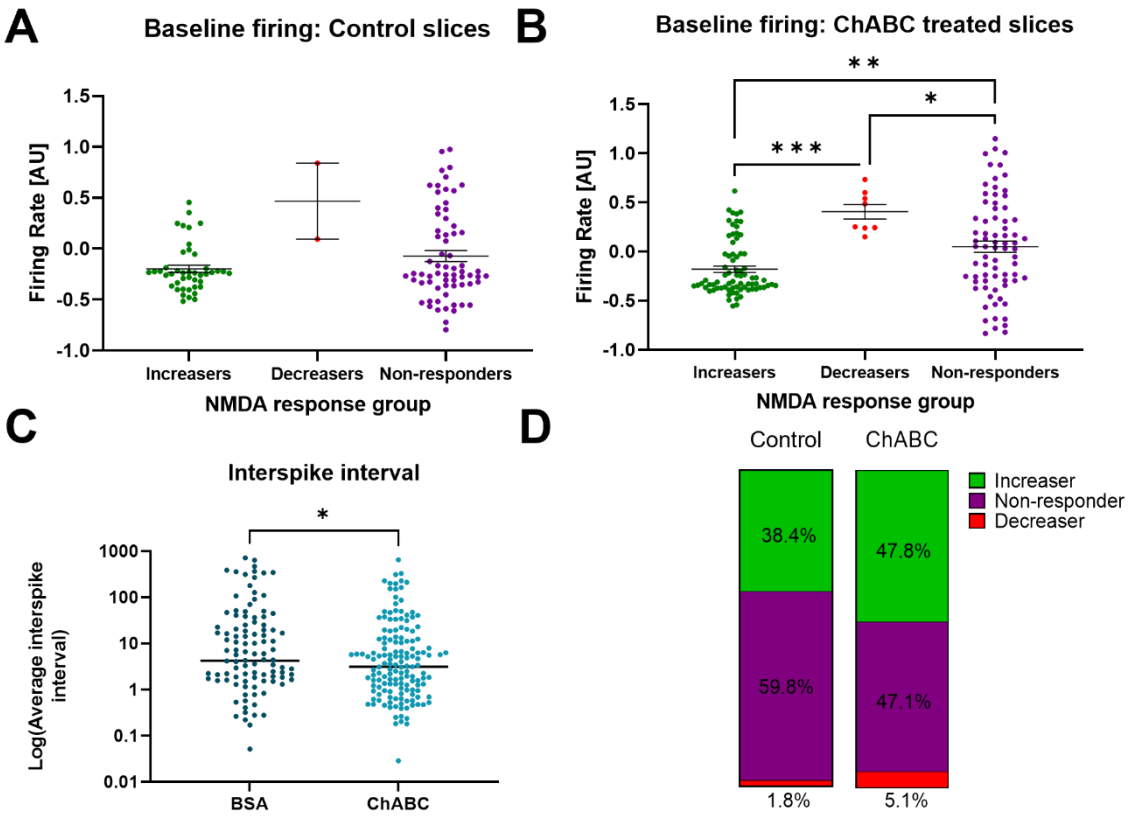

Figure 4.5 Basal firing rate of putative single units in the anteromedial bed nucleus of the stria terminalis following perineuronal net digestion with chondroitinase ABC. Baseline firing rate of increaser, decreaser and non-responder units, classified by response to NMDA, in the STMA of control (A) and ChABC treated (B) slices. PNN removal resulted in increased basal firing rate of decreaser units compared to increasers (p = 0.0003) and non-responders (p = 0.0416) and in non-responders compared to increasers (p = 0.0014). (C) The mean interspike interval of putative single units in the STMA from slices treated with ChABC was significantly shorter in comparison to control slices (p = 0.044). (D) Proportions of each type of NMDA responder in STMA slices treated with BSA (control) and ChABC. Control N = 7 slices from 7 animals; Increasers: N = 43; Decreasers: N =: 2; Non-responders: N = 67; Total = 112. ChABC N = 7 slices from 7 animals: Increasers: N = 75; Decreasers: N = 8; Non-responders: N = 74; Total = 157. Data are presented as dot plots with mean±SEM (A-B); *p < 0.05, **p < 0.01, ***p < 0.001 vs an indicated group, one-way ANOVA with Tukey's post-hoc test; (C) t-test.

NMDA responder subtype did not influence the physical properties of the average waveform of units in control slices (Figure 4.6A). Statistical testing to compare the action potential halfwidth (Figure 4.6C) and the action potential asymmetry (Figure 4.6E) of each NMDA response group was not possible, due to insufficient numbers of decreaser units detected in BSA treated slices (n = 2). In control slices there was no difference in action potential halfwidth metric between subgroups of units (Figure 4.6C; increasers: 0.3 ± 0.01; decreasers: 0.3 ± 0.01; non-responders: 0.3 ± 0.005). However, decreasers showed reduced action potential asymmetry compared with increasers and non-responders in control slices (Figure 4.6E; increasers: 2.2 ± 0.08; decreasers: 1.5 ± 0.3; non-responders: 2.1 ± 0.1). The NMDA responder subtypes had similar action potential halfwidths in ChABC treated slices (Figure 4.6D; increasers: 0.3 ± 0.01; decreasers: 0.3 ± 0.01; non-responders: 0.3 ± 0.005). However, action potential asymmetry was significantly altered between NMDA response groups following PNN degradation (Figure 4.6F; $F(2, 154) = 3.143$, $P = 0.046$). Despite significance reported in the ANOVA, no individual differences between subgroups were identified following Tukey's multiple comparisons *post hoc* testing (Figure 4.6F; increasers: 2.2 ± 0.1; decreasers: 2.6 ± 0.2; non-responders: 2.0 ± 0.1).

Additional t test comparisons were made between units in ChABC-treated and control slices, for each waveform property, for each responder subtype (Appendix 1 Table 6.13; Appendix 1 Table 6.14). No difference in either action potential halfwidth or action potential asymmetry was identified between ChABC and control treated slices for either the increaser or non-responder subtypes. There were insufficient numbers of decreaser units in the control slices for statistical comparisons to be made with the decreasers in the ChABC treated slices (Appendix 1 Table 6.13; Appendix 1 Table 6.14).

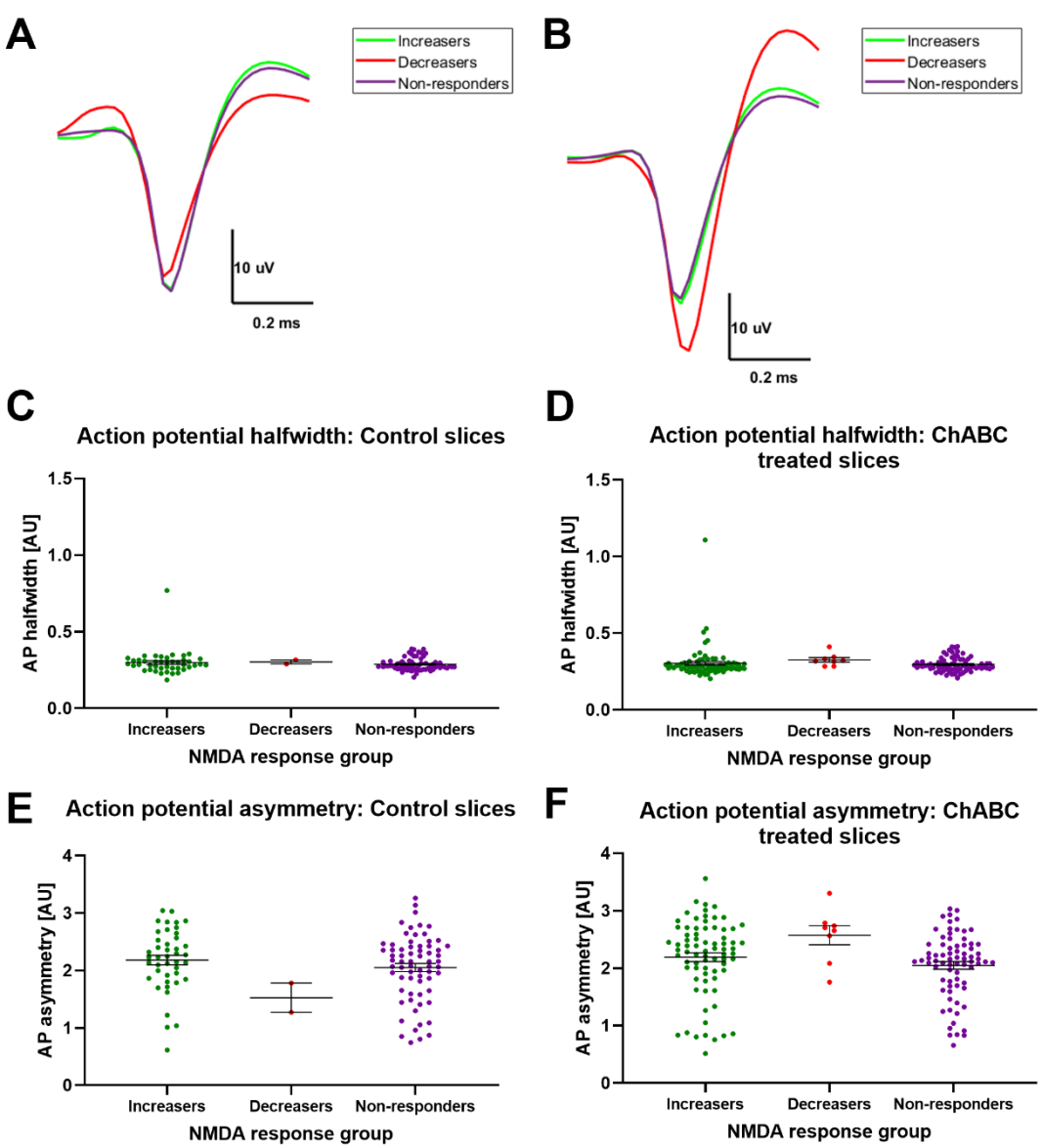

Figure 4.6. Waveform properties of putative single units in the anteromedial bed nucleus of the stria terminalis following perineuronal net degradation. Mean waveform traces of putative single unit increasers (green trace), decreasers (red trace), and non-responders (purple trace) to NMDA in control (A) and ChABC treated (B) slices. Action potential halfwidth of increasers, decreasers and non-responders to NDMA in control (C) and ChABC treated (D) slices. Action potential asymmetry of putative single unit increasers, decreasers and non-responders to NMDA in control (E) and ChABC treated (F) slices. No differences were found between any measured waveform properties of units in slices where perineuronal nets were degraded compared to control slices. Control N = 7 slices from 7 animals; Increasers: N = 43; Decreasers: N =: 2; Non-responders: N = 67; Total = 112. ChABC N = 7 slices from 7 animals: Increasers: N = 75; Decreasers: N = 8; Non-responders: N = 74; Total = 157. Data are presented as dot plots with mean±SEM (C-F); one-way ANOVA.

4.4.2 Effect of perineuronal net degradation within the anteromedial bed nucleus of the stria terminalis on anxiety-like behaviour

In complement with the acute digestion of PNNs in STMA slices, PNNs were also degraded *in vivo* in the STMA to investigate possible behavioural consequences of this manipulation. Administration of ChABC directly to the STMA significantly affected the number of PNNs in the BNST (Figure 4.7; $F(5,28) = 41.83$, $P < 0.0001$). Specifically, PNNs were significantly reduced in the BNST at every experimental time point tested, in comparison with the PBS injected control mice (Figure 4.7B; 3 days post-ChABC: 0.0 ± 0.0, $p < 0.0001$; 7 days post-ChABC: 1.7 ± 0.9, $p < 0.0001$; 14 days post-ChABC: 3.3 ± 0.7, $p < 0.0001$; 30 days post-ChABC: 0.0 ± 0.0; $p < 0.0001$; vs. control: 27.0 ± 4.9). The WFA labelling observed around the STMA at the experimental time points post-ChABC administration is the diffuse extracellular matrix, which is not condensed into perineuronal nets.

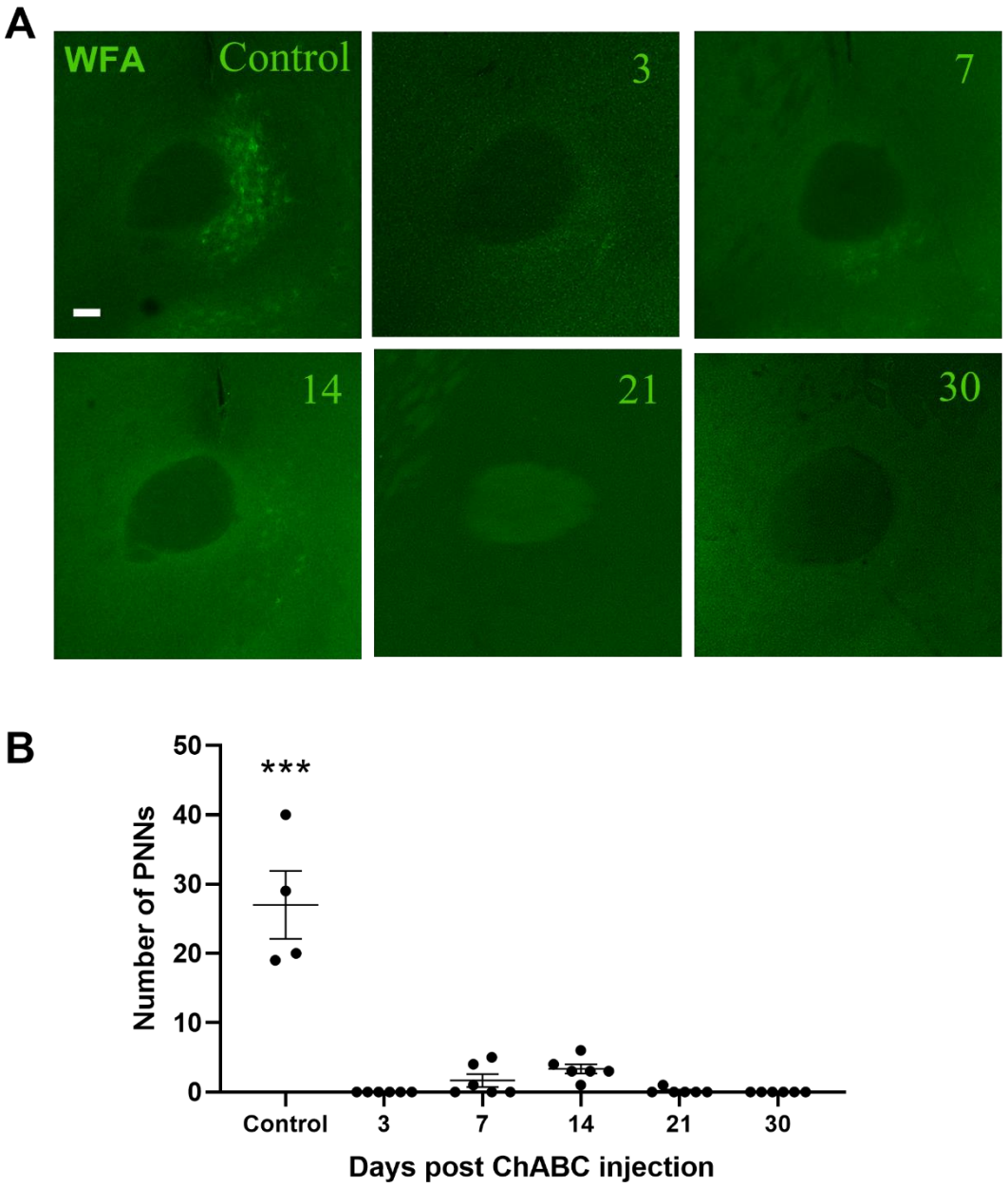

Figure 4.7. Perineuronal net expression in the anteromedial bed nucleus of the stria terminalis following chondroitinase ABC treatment. Mice were sacrificed 3, 7, 14, 21, and 30 days following stereotaxic injection of ChABC at coordinates: 0.38 mm anteroposterior, +/- 0.5 mm mediolateral, - 3.75 mm dorsoventral to bregma. (A) representative images of BNST sections across 3, 7, 14, 21 and 30 days following ChABC administration into the STMA, and at 7 days following PBS injection (control). (B) Quantification of PNN number in the STMA following ChABC injection. Significantly more PNNs were expressed in mice injected with PBS compared with mice administered ChABC ($p < 0.0001$ for comparisons of each experimental group (Day 3, Day 7, Day 14, Day 21 and Day 30) compared to the control group). Control group: N = 4 animals, 3-4 slices per animal; All experimental groups: N = 6 animals, 3-4 slices per animal. Data are presented as a dot plot with mean±SEM (A-C); ***p < 0.001 vs an indicated group; one-way ANOVA with Dunnett's post-hoc test.

To assess the baseline effect of PNN digestion on anxiety-like behaviour, mice were subjected to EPM testing 7, 14, 21 or 30 days following ChABC injection. ChABC administration directly into the STMA did not influence anxiety-like behaviour in the EPM (Figure 4.8). There were no differences in open arm entries made between control and ChABC injected mice, at any measured time point following injection (Figure 4.8A; 7 days post-ChABC: 7.2 ± 1.08 entries; 14 days post-ChABC: 9.3 ± 1.45 entries; 21 days post-ChABC: 7.0 ± 0.58 entries; 30 days post-ChABC: 7.8 ± 1.55 entries; vs. control: 6.40 ± 0.68 entries). In line with the lack of differences observed in open arm entries, there were no differences in the time spent in the open arms of the maze between PBS injected controls and ChABC injected mice, at any time point post-injection (Figure 4.8B; 7 days post-ChABC: 58.3 s ± 7.8 s; 14 days post-ChABC: 83.4 s ± 16.0 s; 21 days post-ChABC: 52.3 s ± 8.4 s; 30-days post-ChABC: 78.7 s ± 18.8 s; vs. control: 62.4 s ± 4.98 s). No difference in EPM anxiety index scores was identified between the PBS injected control mice and ChABC injected mice at any time point post-injection (Figure 4.8C; 7 days post-stress: 0.378 ± 0.047; 14 days post-stress: 0.404 ± 0.069; 21 days post-stress: 0.332 ± 0.052; 30 days post-stress: 0.394 ± 0.039; vs. control: 0.333 ± 0.027). Finally, there was no difference between control and ChABC treated mice in locomotor activity, as determined by the distance travelled in the maze (Figure 4.8D; 7 days post-stress: 1076 cm ± 87 cm; 14 days post-stress: 1266 cm ± 139 cm; 21 days post-stress: 1068 cm ± 224 cm; 30 days post-stress: 978 cm ± 97 cm; vs. control: 1012 cm ± 85 cm).

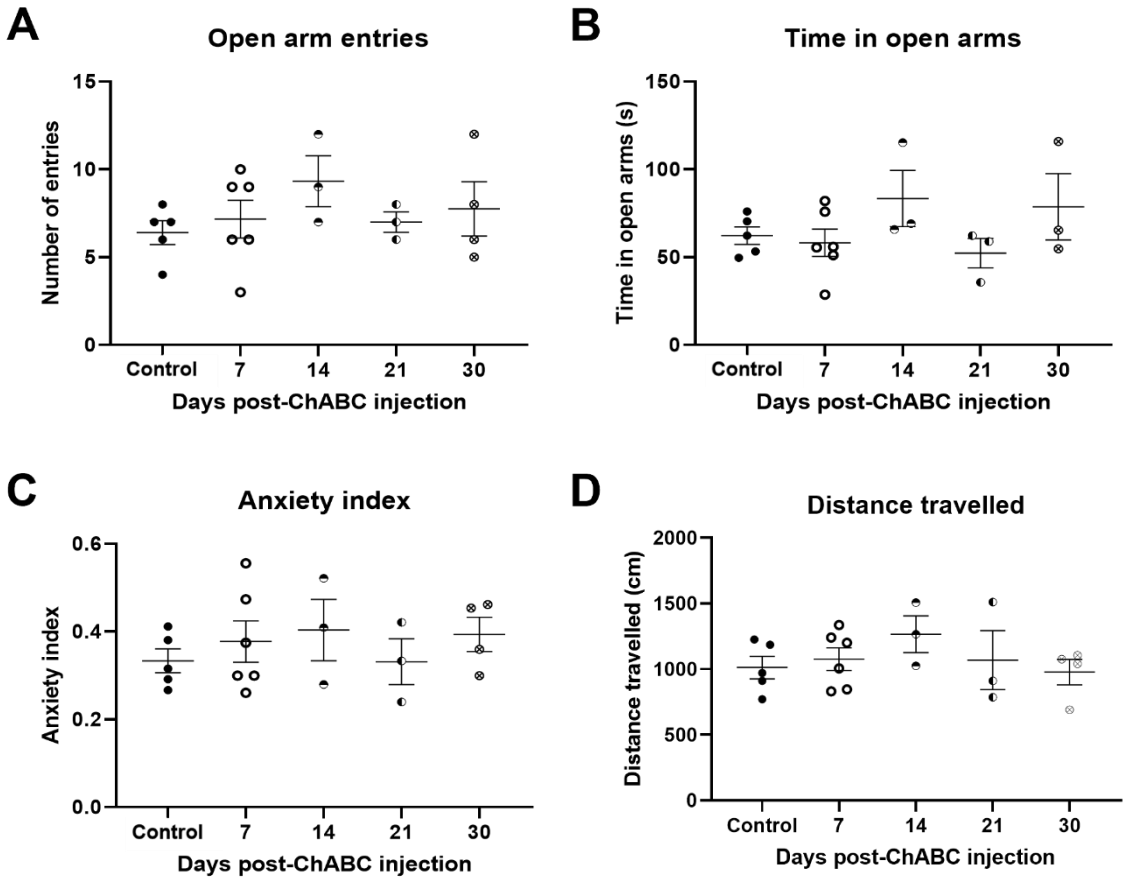

Figure 4.8 Anxiety-like behaviour of mice following perineuronal net degradation in the anteromedial bed nucleus of the stria terminalis. Mice were tested 7, 14, 21 and 30 days post injection. (A) Quantification of open arm entries in the elevated plus maze following bilateral injection of ChABC (50U) into the bed nucleus of the stria terminalis. ChABC injection did not affect open arm entries compared to the sham treated controls. (B) Time spent in the open arms of the elevated plus maze following ChABC injection; mice treated with ChABC spent a similar amount of time in the open arms compared to control mice. (C) Anxiety index in the elevated plus maze following injection of ChABC. No difference in anxiety index was observed between any time points following ChABC injection. (D) Distance travelled in the elevated plus maze following ChABC treatment. Distance travelled did not change in the ChABC injected animals compared to the control animals. Control group: N = 5; 7 days: N = 6; 14 days: N = 3; 21 days: N = 3; 30 days: N = 4. Data are presented as dot plots with mean±SEM; one-way ANOVA.

4.4.3 Effect of perineuronal net degradation within the anteromedial bed nucleus of the stria terminalis on anxiety-like behaviour as a response to repeated acute restraint stress

Next, the effect of perineuronal degradation *in vivo* within the STMA on behavioural response to acute repeated restraint stress was evaluated. Both the anterograde and retrograde activity of ChABC were investigated by administering the enzyme before stress in one experimental cohort (Figure 4.9A), and after stress in another cohort (Figure 4.10A). ChABC administration prior to stressor exposure had no effect on anxiety-like behaviour, as measured in the EPM (Figure 4.9). ChABC injected mice entered the open arms of the maze a similar number of times as control animals (Figure 4.9B; ChABC: 2.88 ± 0.61 entries; vs. control: 3.50 ± 0.63 entries). Similarly, PBS and ChABC injected mice did not significantly differ in the amount of time spent in the open arms of the maze. (Figure 4.9C; ChABC: 17.7 s ± 3.8 s; vs. control: 28.9 s ± 6.6 s). ChABC and PBS injected mice also had similar anxiety index scores (Figure 4.9C; ChABC: 0.315 ± 0.072; vs. control: 0.372 ± 0.067) and locomotor activity, as measured by distance travelled in the maze (Figure 4.9D; ChABC: 1061 cm ± 85 cm; vs. control: 984 cm ± 68 cm).

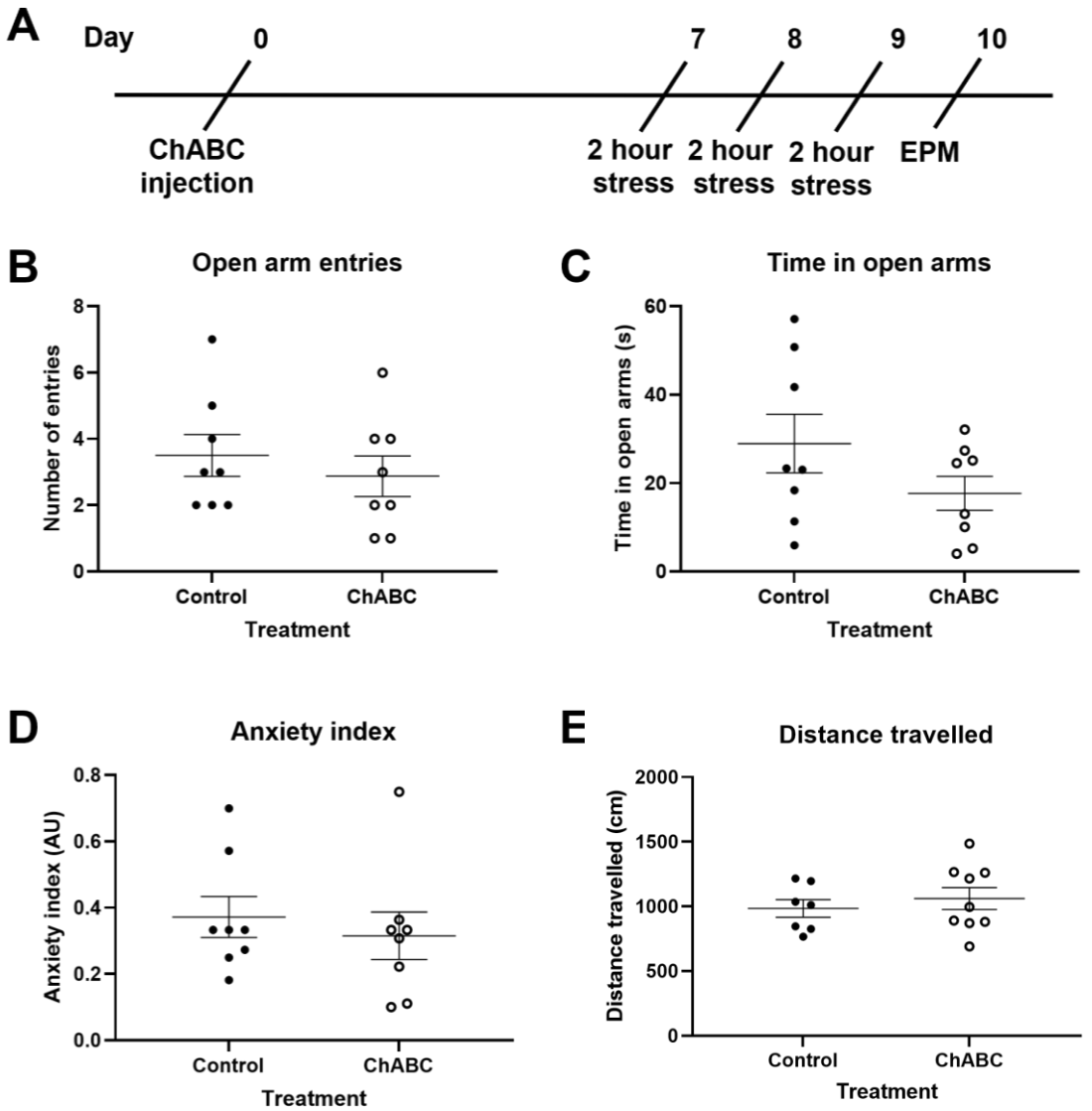

Figure 4.9. Anxiety-like behaviour of mice exposed to repeated acute restraint stress followed by perineuronal net degradation in the anteromedial bed nucleus of the stria terminalis. (A) A schematic timeline of the injection, stress, and behavioural testing. (B) Quantification of entries to the open arms of the elevated plus maze. There was no difference in open arm entries between control and ChABC treated mice. (C) Time spent in the open arms of the elevated plus maze. ChABC treated mice spent a similar amount of time in the open arms compared to control mice. (D) Quantification of anxiety index in the elevated plus maze following treatment injection and acute restraint stress, calculated by the number of open arm entries divided by the number of total arm entries. Anxiety index did not differ between control and ChABC treated mice. (E) Distance travelled in the elevated plus maze. Mice with degraded perineuronal nets travelled a similar distance in the maze compared to control mice. Control group: N = 8; ChABC group: N = 8. Data are presented as dot plots with mean±SEM; t-test.

ChABC administration following stressor exposure had no effect on the anxiety-like behaviour of mice in the EPM (Figure 4.10). Number of entries to the open arms were equivalent between control and enzyme treated groups (Figure 4.10B; control: 3.86 ± 0.96 entries; ChABC: 3.78 ± 0.81 entries). ChABC injected mice spent a similar amount of time in the open arms of the maze, compared with control mice (Figure 4.10C; ChABC: 23.6 s ± 5.8 s; vs. control: 30.7 s ± 6.5 s). There was no difference in the anxiety index scores of PBS and ChABC treated mice in the EPM (Figure 4.10D; ChABC: 0.28 ± 0.05; vs. control: 0.34 ± 0.09). Finally, locomotor activity, as measured by distance travelled in the EPM, was comparable between PBS and ChABC treated groups (Figure 4.10E; ChABC: 782 cm ± 72 cm; vs. control: 772 cm ± 77 cm).

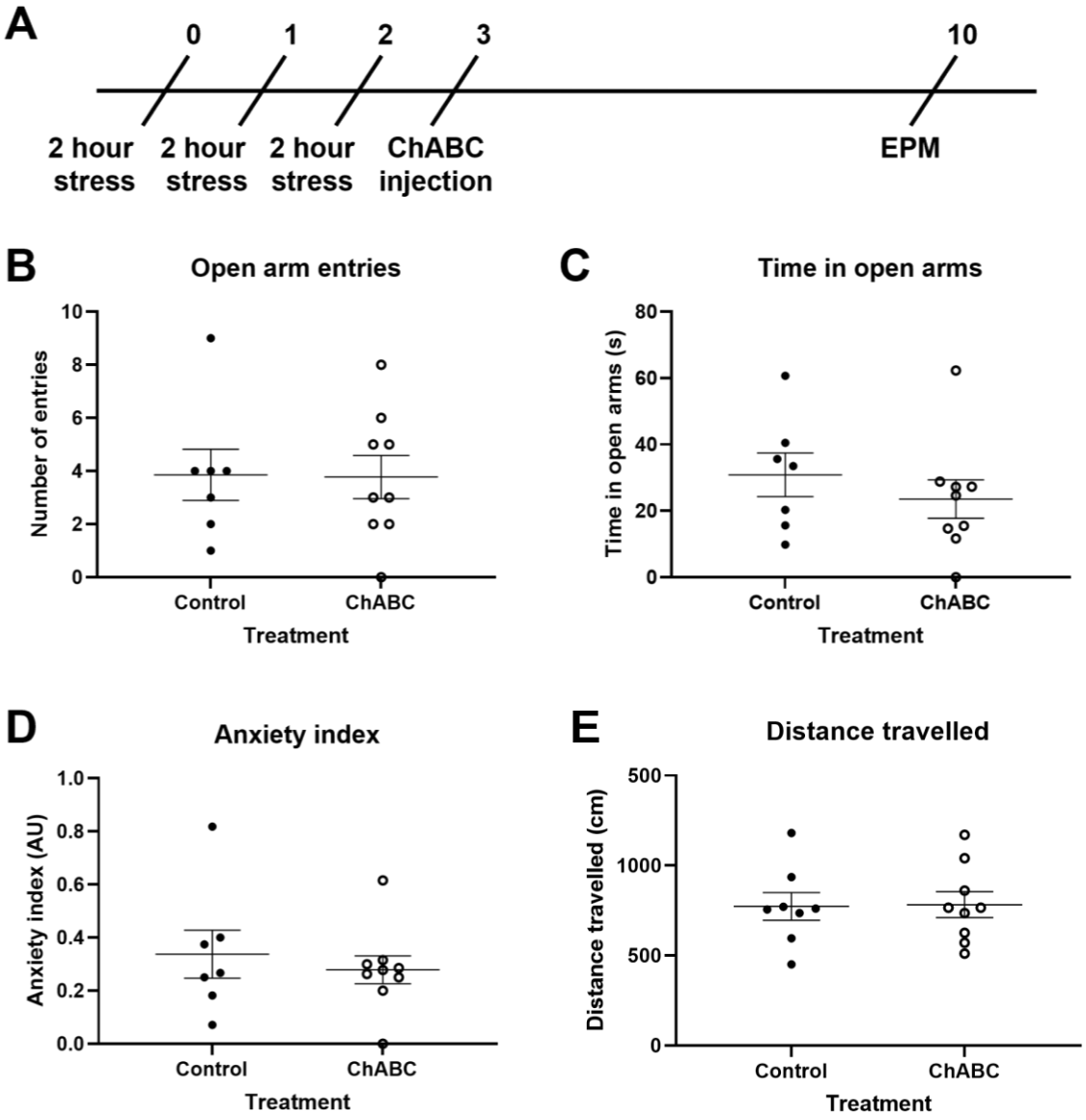

Figure 4.10. Anxiety-like behaviour of mice exposed to perineuronal net degradation in the anteromedial bed nucleus of the stria terminalis followed by repeated acute restraint stress. (A) A schematic timeline of the stress protocol, injection and behavioural testing. (B) Quantification of entries to the open arms of the elevated plus maze. ChABC treated and control mice made similar numbers of entries to the open arms of the maze. (C) Time spent in the open arms of the elevated plus maze. Mice with degraded perineuronal nets spent a similar amount of time in the open arms of the maze compared to control mice. (D) Quantification of anxiety index in the elevated plus maze following treatment injection and acute restraint stress. No difference in anxiety index was observed between ChABC treated and control mice. (E) Distance travelled in the elevated plus maze. Distance travelled was not affected by perineuronal net degradation, as measured by similar total number of arm entries between ChABC treated and control mice. Control group: N = 7; ChABC group: N = 9. Data are presented as dot plots with mean±SEM (A-C); t-test.

4.5 Discussion

In Chapter 4 I investigated the effects of PNN degradation on the electrophysiological properties of cells in the STMA and on anxiety-like behaviour both at baseline and in response to acute repeated restraint stress. PNNs were previously experimentally determined to be densely expressed in the STMA (Figure 2.4; Figure 2.5; Figure 2.6), a region implicated in regulation of the stress response (Dunn, 1987; Feldman, et al., 1990; Gray, et al., 1993; Conrad, et al., 2011; Pego, et al., 2008). Thus, alterations to PNNs in the STMA could be responsible for electrophysiological and behavioural changes previously observed post-stress.

I suggest that neuronal unit subtypes identified in the current study could be potentially mapped to the previously described electrophysiological neuronal phenotypes in the BNST: Type I, Type II and Type III (Hammack, et al., 2007; Rodriguez-Sierra, et al., 2013). Increasers would likely correspond to Type II neurons, as both subtypes make up the biggest percentage of STMA neurons in their respective classifications. Decreasers would map to Type III neurons, as the smallest proportion of each neuronal population, which would leave non-responders as Type I neurons. However, Type III neurons are generally more hyperpolarised at baseline, and require more current to spike, whereas the decreasers observed here were more active at baseline, with a higher basal firing rate than increasers and non-responders, and subsequently quietened upon NMDA application (Figure 4.4). The decreasers identified in the STMA could therefore be a newly discovered population of spontaneously active neurons, similar to those previously described in the anteroventral BNST (Rodriguez-Sierra, et al., 2013). Decreasers made up less than 6% of the neurons captured in the STMA, and therefore could have gone undetected in previous whole cell recording studies.

The proportions of each NMDA responder subtype were different between ChABC treated and control slices, with more increasers and decreasers observed in the ChABC treated slices and more non-responders in the BSA treated slices (Figure 4.5D). The different distribution of unit subtypes could indicate a shift in general responsiveness to NMDA following PNN degradation. However, the period of PNN degradation was short, and alterations such as a change of neuronal phenotype, in this instance responsiveness to NMDA, are likely to

require a greater length of time to occur, if such a change is even possible. PNN presence around a neuron could potentially prevent signal from that neuron being detected by the pMEA. Following PNN degradation, the ability of the pMEA to capture activity from that neuron may be enhanced. Therefore, the proportion of units detected following ChABC treatment may be the true proportion of neurons belonging to each NMDA response group, which were previously obscured by the presence of PNNs.

Few differences were observed in the electrophysiological properties of STMA units in response to NMDA between ChABC and BSA treated slices, suggesting that changes to PNNs in the STMA may not be the biggest driver of changes in neuronal firing following stress. However, as with the slices from control and stressed mice recorded in the previous chapter, decreaser type putative single units were characterised by elevated firing rates at baseline compared with increasers and non-responders (Figure 4.5). Additionally, non-responders exhibited a more rapid baseline firing rate than increasers in slices treated with ChABC; an observation also noted previously, following repeated acute restraint stress exposure (Figure 3.12). Degradation of PNNs in the STMA recapitulated the differences in baseline firing observed post-stress, however, no effect on NMDA responsiveness was identified (Figure 4.5B).

Notably, the biggest change observed in neuronal firing following stress was a decrease in the interspike interval (Figure 4.5C). Such change suggests that removal of PNNs allows neurons in the STMA to fire more rapidly. An increased firing rate could be due to a reduction in the length of time neurons spend in a hyperpolarised state following action potential firing. Alternatively, the reduction in interspike interval may be due to increased availability of the neuron for ion exchange. If the physical barrier which exists around the neuron is structurally weakened, ions may be more freely exchanged between the neuron and the extracellular space. The receptors on the surface of the neuron may also be more available for binding endogenous molecules which promote action potential firing.

The observed results contrast with previous findings from the cerebellum, where large excitatory neurons displayed prolonged interspike intervals following ChABC treatment (O'Dell, et al., 2021). Indeed, the results also contrast with studies of fast-spiking interneurons, which generally fire at a slower rate following PNN degradation (Balmer, 2016; Chu, et al., 2018; Tewari, et al., 2018). Changes

observed in the STMA suggest that the recorded cells are neither excitatory neurons, nor fast-spiking interneurons; this is largely in agreement with the lack of PV expression observed in the region (Figure 2.7). Furthermore, PNNs in the STMA are therefore unlikely to be required for maintenance of a fast-spiking neuronal firing pattern, which agrees with the lack of spontaneous activity observed in MEA baseline recordings of the STMA (Figure 3.3).

Considering the electrophysiological classification of BNST neurons, increasers could correspond to Type II neurons, and non-responders to Type I neurons, based on population size within the STMA. Both subtypes are modulated to some extent by I_h currents, which are known to be affected by neuropeptides released into the BNST following stress (Cardenas, et al., 1999; Wu & Hablitz, 2005; Qiu, et al., 2005). Both increaser and non-responder populations were observed to be affected by stress previously (Figure 3.11), therefore mapping of responder subtypes identified here to the previously defined classes of BNST neuron could be supported. If increasers correspond to Type II neurons and non-responders to Type I neurons, both populations would likely operate via GABAergic transmission, with the potential for increasers to co-release neuropeptides. However, burst activity in BNST neurons was not evaluated in the current study. Hence, it is impossible to track NMDA responder subtypes with the previously defined electrophysiological neuronal phenotypes within the BNST (Hammack, et al., 2007; Rodriguez-Sierra, et al., 2013). It is likely though, that classification of neurons into Type I – III overlaps with the new classification of neurons described here, based on response to NMDA, given similar proportions of BNST neurons classed into each subgroup by two different methods. Whole cell patch clamp experiments to investigate the NMDA responsiveness of each known electrophysiological subtype of BNST neuron would provide further insight into the ways BNST neurons can be classified.

Considering the waveform patterns of the different classes of NMDA responder, little difference between the increaser, decreaser and non-responder waveforms was observed in BSA treated control slices (Figure 4.6A). However, in the ChABC treated slices, the average waveform of the decreaser subpopulation trended towards having greater asymmetry compared to the increaser and non-responder waveforms (Figure 4.6B). With greater numbers of decreaser units it would be possible to determine whether the waveforms significantly differ. However, as the

response group with the smallest population, it may be difficult to obtain enough independent units for analysis.

The pMEA recordings performed here suggest that PNN degradation is not central to the changes in neuronal firing in response to NMDA following exposure to stress. While expression of PNN components was reduced post-stress and morphology of PNNs was more open and less complex, this does not, however, equate to a complete ablation of PNNs, as achieved here. Complete PNN removal may have been too severe to capture changes which occur as a result of structural or chemical alterations to, and not necessarily complete degradation of, PNNs.

One of the limitations of the current study is the lack of electrophysiological experiments performed using slices from mice where PNNs were digested *in vivo,* prior to slice preparation. This may mean that the consequences of PNN degradation in the BNST were not fully captured; PNN degradation *in vivo* is more likely to affect signalling pathways and neuronal communication, both intra- and inter-regionally in a way that cannot be recapitulated *in vitro*. Recording from slices where PNNs have been digested while the brain is still intact and functional would bridge the gap between the experiments performed in the previous and the present chapters.

PNNs in other brain regions were previously shown to mediate region-specific effects. For example, PNNs protect fear memories from erasure in the amygdala, facilitate contextual fear memory formation in the hippocampus and mediate novel object recognition in the perirhinal cortex (Gogolla, et al., 2009; Hylin, et al., 2013; Romberg, et al., 2013). Combining data on the already known role of the BNST in mediating stress response through the HPA axis (Dunn, 1987; Feldman, et al., 1990; Gray, et al., 1993; Herman, et al., 1994; Choi, et al., 2007) and the chemical and morphological changes of PNNs within the BNST discovered in chapter 3 of the current study, I hypothesised that PNNs in the STMA would contribute to the stress response, or to expression of anxiety-like behaviour. To address the hypothesis, anxiety-like behaviour as a result of stress was evaluated following PNN degradation in the STMA *in vivo*. Mice with disrupted PNNs in the STMA displayed unchanged anxiety-like behaviour from Day 7 to Day 30 after ChABC injection (Figure 4.8). Thus, PNNs in the anteromedial BNST are unlikely to determine basal levels of anxiety-like behaviour.

Degradation of PNNs both prior to, and following, exposure to repeated acute restraint stress also had no marked effect on anxiety-like behaviour compared with stress naïve controls (Figure 4.9; Figure 4.10). Thus, disruption of STMA PNNs prior to stress does not affect the way mice process exposure to an emotional stressor. Furthermore, degradation of STMA PNNs following stress does not disrupt stress-related memories formed following stressor exposure. Hence, PNNs in the STMA are unlikely to contribute to stress related learning and memory in the way that PNNs in the amygdala contribute to fear conditioned memories (Gogolla, et al., 2009). This may be because the types of memory formed following the different emotional stressors are underpinned by fundamentally different neural correlates. Whilst stress has been found to facilitate fear conditioning and enhance fear memory consolidation (Conrad, et al., 1999; Rodríguez Manzanares, et al., 2005; Barbayannis, et al., 2017), no studies undertaken to date have looked at potential differences underlying stress-related memories and fear-related memories. Future work into the molecular underpinnings of different types of emotional memory may provide further insight into the role of PNNs in the BNST.

It is possible that PNNs in the BNST have a more predictive role in the stress response; the level of PNN expression may confer responsiveness to stress. Behavioural responses in both the control and ChABC cohorts were incredibly varied, therefore underlying molecular differences between individual subjects may explain some of this variation. To investigate further, as it was determined that PNN expression in the STMA did not change following stress (Figure 3.8), PNN expression in mice which have undergone stress and subsequent behavioural testing could be examined, to determine whether PNN expression correlates with greater or lesser levels of anxiety-like behaviour.

Reflecting on the electrophysiological and behavioural data together, the lack of differences between controls and slices/mice treated with ChABC suggests that the differences observed previously following restraint stress are as a result of broader network effects. The STMA is a highly interconnected region, receiving projections from the subiculum, basomedial amygdala and medial preoptic area and projecting to the hypothalamus. Furthermore, the STMA is reciprocally connected to both the anteroventral and anteromedial regions of the BNST. Therefore, the local changes observed in the STMA, both in PNN morphology

and neuronal activity, will likely impact its afferent and efferent projections too. It will be important in the future to consider the nature of these connections and to experimentally determine how the connectivity of the STMA contributes to the regulation of the underlying network.

One of the main limitations of the behavioural experiments performed in the present study is the small group size for each treatment group or time point. Reduced group numbers subsequently reduce power to detect differences within populations and limit effective power to the size of the smallest group. Reflecting on these preliminary findings, an example power analysis has been conducted to determine sample size required to power analysis in future studies (Appendix 3, Figure 7.4). Considering the 'time in open arms' metric for the behavioural experiments following PNN degradation where a t-test was performed to compare data sets, the power analysis suggests that to achieve 80% power, a sample size of 40-50 animals per group would be necessary (Appendix 3, Figure 7.4). Using this number of samples per group would be significantly more time and financially constraining, so would be important to consider in planning of future experiments.

ChABC mediated degradation of PNNs in the BNST may therefore have greater or more varied effects on anxiety-like behaviour than was measured in the current study. Testing greater numbers of animals per group would be essential in detecting subtle behavioural differences between ChABC-treated and control mice. The addition of further behavioural tests such as the OFT, hole board or acoustic startle would provide additional measures of anxiety-like behaviour for a more comprehensive investigation.

Notably, greater indications of anxiety-like behaviour were observed in both surgical cohorts, compared with mice in earlier studies which had not undergone surgical procedures (Figure 4.9 and Figure 4.10; Figure 3.4). Extending the recovery period of mice post-surgery, prior to behavioural testing, could minimise any surgery-associated anxiety-like behaviour. The duration of action of ChABC in the STMA would support a longer recovery time as PNNs were significantly reduced for at least 30 days following ChABC injection (Figure 4.7).

ChABC has been shown to persist actively in the brain for ten days following nigrostriatal injection in the rat (Lin et al., 2008). After this time, PNNs will presumably begin to regenerate in the region of degradation; in the visual cortex

PNNs are 85% reassembled ~60 days following ChABC mediated degradation (Lensjø, 2013). However, the rate of regeneration may be determined by a number of factors, including brain region, species of animal, age of animal and the environmental experiences of the animal following PNN degradation. As PNNs develop comparatively later in the BNST compared to other brain regions, it may be that their turnover following degradation is also slower. Conversely, PNNs in the BNST may regenerate faster as they have a more granular structure and therefore less extracellular matrix is necessary for PNN synthesis. The mice used in these experiments were young adults; had juvenile mice been used, PNN turnover may have been more rapid as these mice are undergoing critical periods of remodelling in the brain and PNNs are naturally forming around subsets of neurons (Pizzorusso, et al., 2002; Gogolla, et al., 2009; Lensjo, et al., 2017b).

Degradation of PNNs with ChABC is a broad approach. It is a useful and simple to use tool to investigate the effects of PNN absence in brain regions and has led to the discovery of the contribution of PNNs in determining ocular dominance and development of song learning in songbirds among functions (Pizzorusso, et al., 2002; Balmer et al., 2009). However, as ChABC completely degrades PNNs, experimentally it lacks subtlety and greater specificity. Alternative approaches which may be suitable for future experiments could be to target hyaluronan within the PNN with hyaluronidase enzyme or to knock out an individual PNN component, for example tenascin or a non-critical CSPG, to disrupt PNN function but maintain some level of PNN structure.

4.6 Conclusions

Altogether, degradation of PNNs in the STMA did not produce the same effects on neuronal excitability and anxiety-like behaviour as repeated acute restraint stressor exposure, as previously hypothesised. PNNs in the STMA may have a function which is completely independent from the stress response, and alterations to their structure and morphology following stress may simply be a by-product of other molecular interactions. Nevertheless, the questions which have arisen as a result of the studies performed here provide interesting avenues for future research into PNNs in the BNST, and their contribution to brain function.

Chapter 5 – Conclusions and future work

5.1 Conclusions

The experimental work performed and presented in this thesis sought to investigate the expression of PNNs in the anterior BNST and determine their role in regulating synaptic transmission and behaviour at the baseline level and following repeated acute restraint stress. PNNs were determined to be expressed in the BNST from approximately post-natal day 30, which coincides with a previously documented shift in reduced resilience to stress from adolescence to adulthood. PNN expression was densest in the STMA, a subregion with established connections to brain regions known to influence anxiety including the basomedial amygdala and hypothalamus. The STMA also reciprocally connects to both the anteroventral and anterolateral BNST subregions, which in turn influence anxiety circuitry and modulate the stress response.

Here, the impact of emotional stress was examined, in the form of repeated restraint, on the composition and morphology of PNNs in the STMA. Notably, 7 days post-stress PNNs were less structurally complex, as evidenced by greater hole area and perimeter, along with reduced intensity of matrix staining, and showed increased expression of critical component neurocan. Morphological metrics recovered 14 days post-stress, and neurocan and tenascin-R expression were significantly greater than in controls, indicating at least semi-permanent alterations, in addition to more flexible changes, to PNNs as a result of stressor exposure. Anxiety-like behaviour was measured in complement with molecular studies, which highlighted a vulnerable time point 7 days post-stress where mice spent less time in, and made fewer entries to, the open arms of the elevated plus maze, compared to stress naïve controls, indicating increased avoidance behaviour. This increased avoidance behaviour is akin to anxiety in humans; humans behave in a similar way in the elevated plus maze, avoiding the open arms when their perceived anxiety is greater (Biedermann et al., 2017). These observations combined suggest that PNNs in the STMA may exert influence over response to stress and resultant anxiety-like behaviour in mice.

The stress induced changes observed here in the STMA may be consistent with those observed in other brain regions of the stress processing neural network. In the hippocampus, acute restraint increases extracellular glutamate which acts on

NMDA receptors to induce dendritic remodelling (Magarinos et al., 1995; Watanabe et al., 1992). Here, acute restraint stress morphologically altered PNNs in the STMA, creating a more open structure and increased NMDA mediated excitability of neurons. Together, this suggests initiation of a process of NMDA mediated dendritic remodelling within the BNST, as observed in the hippocampus and also the medial prefrontal cortex (Martin & Wellman, 2011). Stress induced remodelling in the hippocampus results in reduced numbers of synapses on remodelled neurons, and in the medial prefrontal cortex leads to dendritic retraction and spine loss; however in the amygdala, stress can induce neuronal hypertrophy and enhanced dendritic branching (Watanabe et al., 1992; Radley et al., 2006 ; Vyas et al., 2002). The reduced complexity of PNNs in the STMA suggest an increase in dendritic branching, or at least the possibility for this to occur, as neurons become less restricted and plasticity is increased.

pMEA recordings were made from the STMA following stress, to determine whether restraint stress also influenced neuronal signalling in the STMA. The STMA was not observed to be spontaneously active, therefore measures of excitability in response to NMDA were investigated. Three types of activity-related response to NMDA were determined: an increase in firing rate, a decrease in firing rate and no change to firing rate. Units whose firing decreased in response to NMDA made up the smallest proportion of units overall, with those increasing their firing and those not responding equally dividing the remaining units. Stress induced an increase in the firing rate of increasers, and a decrease in the firing rate of non-responders, in response to NMDA application, indicating that stress affects neuronal activity in the STMA.

Considering the proportions of the three responders, it is more likely that the increaser and non-responder populations are GABAergic and that the decreaser population is glutamatergic, given GABAergic transmission predominates in the STMA, and indeed the BNST. NMDA application revealed a potential relationship between the increaser and decreaser populations; the increasers may project to the decreasers, and therefore in the presence of NMDA increasers fire more rapidly and silence the decreasers. The downstream implications of this depend on the connections of the decreaser population. If they project to other glutamatergic neurons, then inhibition downstream will lead to a reduction in excitation, but if they project to GABAergic neurons then inhibition downstream

will lead to an increase in excitation; it could be that they project to both glutamatergic and GABAergic neurons. Ultimately, it is likely the balance of excitation/inhibition in the STMA is affected by restraint stress.

Given what is already known about the connectivity of the BNST and the involvement of subregions in the stress response, one potential signalling pathway is that the relief of inhibition on other GABAergic neurons enhances excitation in the STMA, which sends projections to both the dorsal and ventral BNST subregions. Both the dorsal and ventral BNST regions contain CRF expressing cells, many of which project to the hypothalamus, where release of CRF will increase HPA axis activity (Figure 5.1). Notably, stimulation of dorsolateral BNST CRF neurons has been shown to increase aversive behaviours (Salimando et al., 2020), as observed here in the EPM.

To determine whether changes in neuronal activity were due to the morphological alterations to PNNs previously observed, further pMEA recordings were made from STMA slices where PNNs were degraded with ChABC. No changes to neuronal firing in response to NMDA were observed, suggesting that the physical presence of PNNs in the STMA does not alter neuronal activity in the region.

In complement, PNNs were digested *in vivo,* to elucidate their contribution to the stress response. No differences in the basal behaviour of mice in the EPM were identified between ChABC-treated and control groups. To test whether PNN degradation regulated stress responsiveness, PNNs were degraded prior to stress in one cohort and following stress in a second cohort. Neither group of ChABC treated mice showed a difference in anxiety-like behaviour in the EPM when compared with PBS injected control mice, indicating that STMA PNNs may not be important for encoding emotional stress-related memories. However, it should be taken into consideration that it is structural alterations occurring within the PNN, and not full degradation, which accompanies the changes in neuronal signalling and, indeed, the increase in anxiety-like behaviour which manifests as a result of restraint stress. Therefore, the ChABC approach to PNN manipulation may lack the subtlety required to examine the questions of how PNNs contribute to stress responsiveness. If PNNs can, and do, encode information concerning perceived stressful stimuli, then their absence may promote stress resilience. Degradation of PNNs may provide a blank slate for the encoding of new

memories, therefore responses to stress may not be as heightened as seen in mice with intact PNNs.

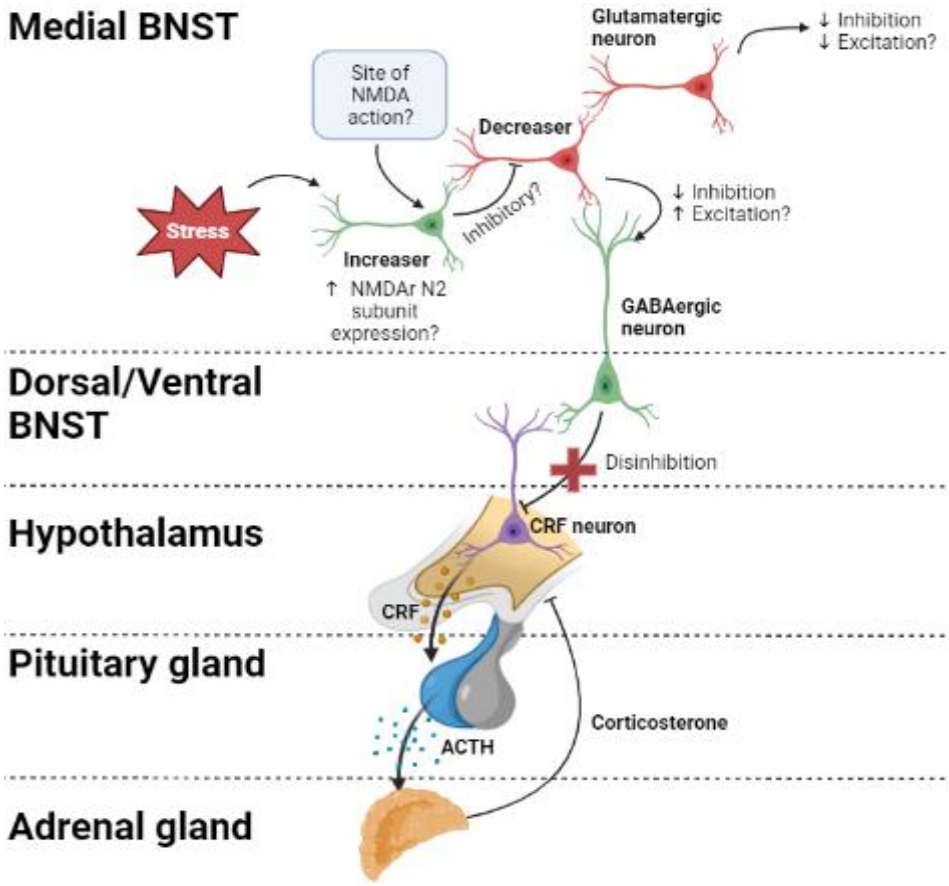

Figure 5.1 Proposed model of the effect of restraint on neuronal activity and downstream connectivity of the anteromedial bed nucleus of the stria terminalis. A proposed site of action for NMDA is the increaser subpopulation of neurons in the anteromedial BNST. When increasers fire rapidly in response to NMDA, they may GABAergically project to the decreaser subpopulation of neurons, which may be glutamatergic given the relative size of these neuronal populations, ultimately inhibiting their activity. If the decreasers project outwards from the STMA, they may project to the ventral or dorsal BNST subregions. Both the ventral and dorsal BNST contain corticotrophin releasing factor (CRF) expressing neurons which project to the hypothalamus, and therefore exert influence over the hypothalamic-pituitary-adrenal axis (HPA), responsible for the processing of stressful stimuli. An increase in HPA axis activity, as a result of increased CRF release could be responsible for the increase in avoidance behaviour observed here in the elevated plus maze following restraint stress. Figure created with BioRender.

Altogether, the studies performed as part of this thesis raise further questions about the role of PNNs in the STMA, and the wider BNST. The observation that PNNs are altered following stress, and that the timeframe of their structural recovery tracks with their molecular composition and changes to anxiety-like behaviour in the EPM does suggest a role in the stress response, however that was not captured in the experiments performed here. The final part of this thesis outlines the potential avenues which could be experimentally explored in the future, to determine the function of PNNs in the STMA.

5.2 Future work

The greatest limitation of this body of work is the focus on the male sex. Anxiety disorders are well documented to disproportionately affect females and the BNST, albeit the posterior part, is known to be sexually dimorphic. As such, any study on anxiety, stress and the BNST incorporating females would need to focus on whether there are underlying differences between males and females – however, such experiments were outside the scope of the present study. The experimental work undertaken in this thesis should therefore be replicated using female animals to explore whether there are any discernible differences between PNNs, stress-induced changes in neuronal activity, or anxiety-like behaviour, between males and females. Where differences are uncovered, this may help explain the sex disparity in the development of anxiety disorders and could provide insight into underlying mechanisms of disease generation which could be therapeutically targeted in the future. If there are no differences between males and females, this would make future research easier, as sex-specific differences will not require the same level of consideration in experimental design or interpretation.

A more specific limitation of the work, and a hinderance to experimental progress throughout, was the inability to determine the type of cell(s) which express PNNs in the BNST. Knowing the genetic or chemical nature of these cells would provide a richer context for discussion of observed experimental results and allow more specific functional experiments to be performed. In the future, it would be advantageous to determine a unique signature for PNN expressing cells in the BNST. This could either be a genetic signature determined by a single cell RNA

sequencing analysis or could be based on cellular expression of proteins determined by single cell proteomics analysis, further immunohistochemistry, or fluorescence *in situ* hybridisation studies. Identification of the qualities specific to PNN expressing cells, but not cells lacking PNNs, in the BNST would allow specific targeting of PNN expressing cells *in vivo*. Use of retrograde and anterograde tracers targeted to PNN expressing cells would provide solid evidence of their afferent and efferent projections, which eventually could lead to resolution of the micro- and macrocircuits that BNST PNN-expressing cells are involved in. Furthermore, BNST PNN-expressing cells could then be specifically activated or inhibited by optogenetic constructs or designer receptors exclusively activated by designer drugs (DREADDs) to eventually inform about novel cell signalling cascades controlling downstream behaviours, either at baseline or in anxiety-inducing or task-based ethological tests.

The ability to specifically label PNN-expressing neurons in the BNST would also further facilitate crucial electrophysiological experiments. Whole cell patch clamp recording of PNN-positive and -negative neurons in the BNST may provide insight into potential differences in their electrophysiological properties and involvement in neuronal function and firing on a single cell basis. Constructing profiles of the firing properties of neurons with and without PNNs would allow mapping of cellular responses to NMDA determined in this work, and may reveal more about the types of neurons in the STMA; whether they are excitatory or inhibitory. Complementary studies applying a variety of drugs to the cells in the STMA could further help determine the corresponding pharmacology of these neurons. Pharmacological experiments, coupled with ChABC-mediated PNN removal, both *in vivo* and *in vitro,* would allow a more detailed picture of the role of PNNs in the BNST at the cellular level to be drawn.

Mouse models with attenuated PNNs, such as the brevican or tenascin-R knockout mice, would be beneficial in investigating the electrophysiological consequences of development in the absence of intact PNNs. Such models will also be of use to determine whether PNNs in the STMA are important for a basal level of stress susceptibility. As these mice express PNNs with disrupted morphology, these models would be an intermediate between mice with degraded PNNs and those with intact PNNs. Both the basal behaviour of these mice and their behaviour following exposure to restraint protocols, would inform

whether PNNs are responsible for encoding stress related memories or response to stress. Altered responsiveness to stress in mice with attenuated PNNs would indicate that PNNs in the STMA influence the susceptibility of individuals to stress.

It will be equally important to determine the underlying signalling mechanisms which link PNNs to stress. Given that the majority of genes which encode PNN components contain glucocorticoid response elements, it is plausible that there are many ways in which PNNs could be altered by stress and how that, in turn, could inform stress responsiveness. At a cellular level, PNNs provide a barrier to neurons, and their negative charge allows them to act as a reservoir for ion exchange, which is likely what allows neurons surrounded by a PNN to fire at supraphysiological rates. Defining the efferent projections of neurons surrounded by PNNs, and examining why these neurons are required to fire with such high frequency, could provide further context about the neuronal processes which STMA PNNs influence.

If future research determines aberrations in PNNs to be important in the development of anxiety- and other stress-related disorders, PNN manipulation could be a future therapeutic strategy for treatment. The therapeutic benefit of ChABC is currently under investigation for diverse conditions including Parkinson's disease, various cancers, and spinal cord injuries. In a phase III trial of patients with herniated discs, those who received ChABC reported greater therapeutic benefit compared to patients who received placebo treatment (Chiba et al., 2018). In a second study, ChABC was well tolerated, with more adverse effects observed at higher doses, however only the lowest dose of enzyme was required for therapeutic benefit (Matsuyama et al., 2018).

While the efficacy and tolerability of ChABC is promising as a future treatment for humans, there are challenges associated with potential use of ChABC to treat psychiatric conditions. Delivery into the brain is presently impractical; the BNST especially is deep in the brain and therefore not easily targetable by direct injection, the delivery method for spinal cord injury. Ensuring specific delivery to a single brain region would also be problematic; there are no boundaries around the BNST which would prevent diffusion of enzyme into other brain regions, and it is not known how ChABC would affect adjacent brain regions.

It would perhaps be more pertinent to invest resources in determining the ways in which current anxiolytics and antidepressants modulate PNNs, as they have been observed to, and whether these alterations are how they exert their therapeutic efficacy (Chen et al., 2016; Alaiyed et al., 2019; Donnegan & Lodge, 2017). It may be possible to modify current compounds in order to enhance their modulation of PNNs, or to design new compounds which will act in more specific ways to achieve greater relief of symptoms.

In summary, this thesis has provided the foundations for future research on PNNs in the BNST. I investigated in detail the spatiotemporal development and expression of PNNs in the BNST, and moved one step towards elucidating their functional role, laying the foundation for an exciting area of future research. If further research is focussed on the physiological contribution of PNNs in the BNST, both in health and disease, they may become a beneficial therapeutic target for psychological disorders, including anxiety disorders, in the future.

Appendix 1

Tukey's multiple comparisons test	Significant?	Summary	Adjusted P Value
STLV vs. STMV	No	ns	0.9733
STLV vs. STMA	No	ns	0.9996
STLV vs. STLP	No	ns	0.8930
STLV vs. STLD	No	ns	0.1181
STMV vs. STMA	No	ns	0.9272
STMV vs. STLP	No	ns	0.9981
STMV vs. STLD	No	ns	0.3234
STMA vs. STLP	No	ns	0.8037
STMA vs. STLD	No	ns	0.0806
STLP vs. STLD	No	ns	0.4834

Table 6.1 Statistics for comparisons of perineuronal net number in the anterior subnuclei of the bed nucleus of the stria terminalis at P30.

Tukey's multiple comparisons test	Significant?	Summary	Adjusted P Value
STLV vs. STMV	No	ns	0.9997
STLV vs. STMA	No	ns	0.0906
STLV vs. STLP	No	ns	0.9909
STLV vs. STLD	No	ns	0.9988
STMV vs. STMA	No	ns	0.1288
STMV vs. STLP	No	ns	0.9673
STMV vs. STLD	No	ns	0.9907
STMA vs. STLP	Yes	*	0.0366
STMA vs. STLD	No	ns	0.0535
STLP vs. STLD	No	ns	0.9997

Table 6.2 Statistics for comparisons of perineuronal net number in the anterior subnuclei of the bed nucleus of the stria terminalis at P60.

Tukey's multiple comparisons test	Significant?	Summary	Adjusted P Value
STLV vs. STMV	No	ns	0.9657
STLV vs. STMA	Yes	***	<0.0001
STLV vs. STLP	No	ns	0.9838
STLV vs. STLD	No	ns	0.9917
STMV vs. STMA	Yes	***	<0.0001
STMV vs. STLP	No	ns	>0.9999
STMV vs. STLD	No	ns	0.9996
STMA vs. STLP	Yes	***	<0.0001
STMA vs. STLD	Yes	***	<0.0001
STLP vs. STLD	No	ns	>0.9999

Table 6.3 Statistics for comparisons of perineuronal net number in the anterior subnuclei of the bed nucleus of the stria terminalis at P210.

Tukey's multiple comparisons test	Significant?	Summary	Adjusted P Value
STLV vs. STMV	Yes	*	0.0426
STLV vs. STMA	Yes	***	<0.0001
STLV vs. STLP	No	ns	0.7316
STLV vs. STLD	No	ns	0.9646
STMV vs. STMA	Yes	***	<0.0001
STMV vs. STLP	No	ns	0.4092
STMV vs. STLD	Yes	**	0.0094
STMA vs. STLP	Yes	***	<0.0001
STMA vs. STLD	Yes	***	<0.0001
STLP vs. STLD	No	ns	0.3496

Table 6.4 Statistics for comparisons of perineuronal net number in the anterior subnuclei of the bed nucleus of the stria terminalis at P365.

Tukey's multiple comparisons test	Significant?	Summary	Adjusted P Value
STLV vs. STMV	No	ns	>0.9999
STLV vs. STMA	No	ns	0.4432
STLV vs. STLP	No	ns	0.9788
STLV vs. STLD	No	ns	0.9179
STMV vs. STMA	No	ns	0.5101
STMV vs. STLP	No	ns	0.9585
STMV vs. STLD	No	ns	0.8752
STMA vs. STLP	No	ns	0.1901
STMA vs. STLD	No	ns	0.1181
STLP vs. STLD	No	ns	0.9988

Table 6.5 Statistics for comparisons of perineuronal net intensity in the anterior subnuclei of the bed nucleus of the stria terminalis at P30.

Tukey's multiple comparisons test	Significant?	Summary	Adjusted P Value
STLV vs. STMV	No	ns	0.9106
STLV vs. STMA	Yes	*	0.0179
STLV vs. STLP	No	ns	0.5793
STLV vs. STLD	No	ns	0.9831
STMV vs. STMA	Yes	**	0.0027
STMV vs. STLP	No	ns	0.9668
STMV vs. STLD	No	ns	0.9975
STMA vs. STLP	Yes	***	0.0006
STMA vs. STLD	Yes	**	0.0055
STLP vs. STLD	No	ns	0.8690

Table 6.6 Statistics for comparisons of perineuronal net intensity in the anterior subnuclei of the bed nucleus of the stria terminalis at P60.

Tukey's multiple comparisons test	Significant?	Summary	Adjusted P Value
STLV vs. STMV	No	ns	0.3283
STLV vs. STMA	Yes	***	<0.0001
STLV vs. STLP	Yes	**	0.0011
STLV vs. STLD	Yes	*	0.0102
STMV vs. STMA	Yes	***	<0.0001
STMV vs. STLP	No	ns	0.0981
STMV vs. STLD	No	ns	0.4515
STMA vs. STLP	Yes	***	<0.0001
STMA vs. STLD	Yes	***	<0.0001
STLP vs. STLD	No	ns	0.8891

Table 6.7 Statistics for comparisons of perineuronal net intensity in the anterior subnuclei of the bed nucleus of the stria terminalis at P210.

Tukey's multiple comparisons test	Significant?	Summary	Adjusted P Value
STLV vs. STMV	No	ns	0.2773
STLV vs. STMA	Yes	***	0.0004
STLV vs. STLP	No	ns	0.4885
STLV vs. STLD	No	ns	0.8429
STMV vs. STMA	Yes	****	<0.0001
STMV vs. STLP	No	ns	0.9942
STMV vs. STLD	No	ns	0.8450
STMA vs. STLP	Yes	****	<0.0001
STMA vs. STLD	Yes	****	<0.0001
STLP vs. STLD	No	ns	0.9712

Table 6.8 Statistics for comparisons of perineuronal net intensity in the anterior subnuclei of the bed nucleus of the stria terminalis at P365.

Unpaired t tests	Significant?	Summary	Adjusted P Value
Increaser: control vs. stress	No	ns	0.0641
Decreaser: control vs. stress	No	ns	0.2137
Non-responder: control vs. stress	No	ns	0.6983

Table 6.9 Statistics for comparisons of baseline firing rate of the three *N*-Methyl-D-Aspartate response types of putative single units in the anteromedial bed nucleus of the stria terminalis, in slices from control and stressed mice.

Unpaired t tests	Significant?	Summary	Adjusted P Value
Increaser: control vs. stress	No	ns	0.8393
Decreaser: control vs. stress	No	ns	0.6031
Non-responder: control vs. stress	No	ns	0.3263

Table 6.10 Statistics for comparisons of action potential halfwidth of the three *N*-Methyl-D-Aspartate response types of putative single units in the anteromedial bed nucleus of the stria terminalis, in slices from control and stressed mice.

Unpaired t tests	Significant?	Summary	Adjusted P Value
Increaser: control vs. stress	Yes	***	< 0.0001
Decreaser: control vs. stress	No	ns	0.6670
Non-responder: control vs. stress	No	ns	0.5299

Table 6.11 Statistics for comparisons of action potential asymmetry of the three *N*-Methyl-D-Aspartate response types of putative single units in the anteromedial bed nucleus of the stria terminalis, in slices from control and stressed mice.

Unpaired t tests	Significant?	Summary	Adjusted P Value
Increaser: control vs. ChABC treated	No	ns	0.7286
Decreaser: control vs. ChABC treated	No	ns	0.7826
Non-responder: control vs. ChABC treated	No	ns	0.1253

Table 6.12 Statistics for comparisons of baseline firing rate of the three *N*-Methyl-D-Aspartate response types of putative single units in the anteromedial bed nucleus of the stria terminalis, in control and chondroitinase ABC treated slices.

Unpaired t tests	Significant?	Summary	Adjusted P Value
Increaser: control vs. ChABC treated	No	ns	0.7890
Decreaser: control vs. ChABC treated	-	Not enough samples	-
Non-responder: control vs. ChABC treated	No	ns	0.2558

Table 6.13 Statistics for comparisons of action potential halfwidth of the three *N*-Methyl-D-Aspartate response types of putative single units in the anteromedial bed nucleus of the stria terminalis, in control and chondroitinase ABC treated slices.

Unpaired t tests	Significant?	Summary	Adjusted P Value
Increaser: control vs. ChABC treated	No	ns	0.9368
Decreaser: control vs. ChABC treated	-	Not enough samples	-
Non-responder: control vs. ChABC treated	No	ns	0.9733

Table 6.14 Statistics for comparisons of action potential asymmetry of the three *N*-Methyl-D-Aspartate response types of putative single units in the anteromedial bed nucleus of the stria terminalis, in control and chondroitinase ABC treated slices.

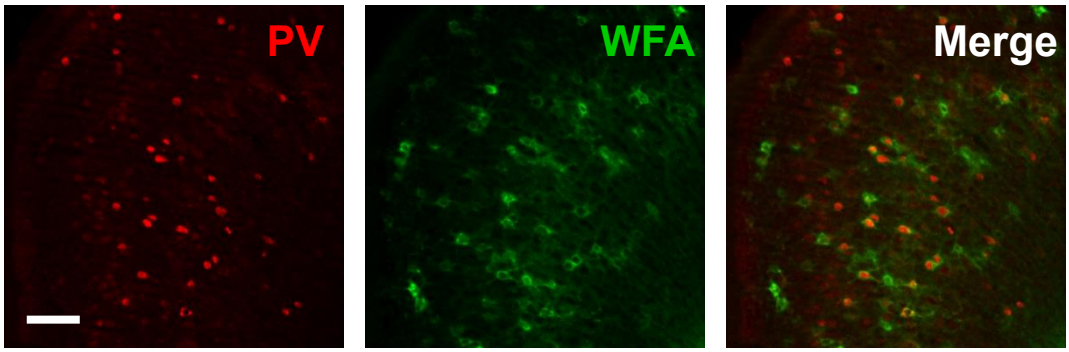

Figure 6.1 Parvalbumin immunolabelling in the adult mouse motor cortex. Positive labelling for parvalbumin (PV; red) and perineuronal nets (WFA; green) in the motor cortex. Scale bar = 100 µm.

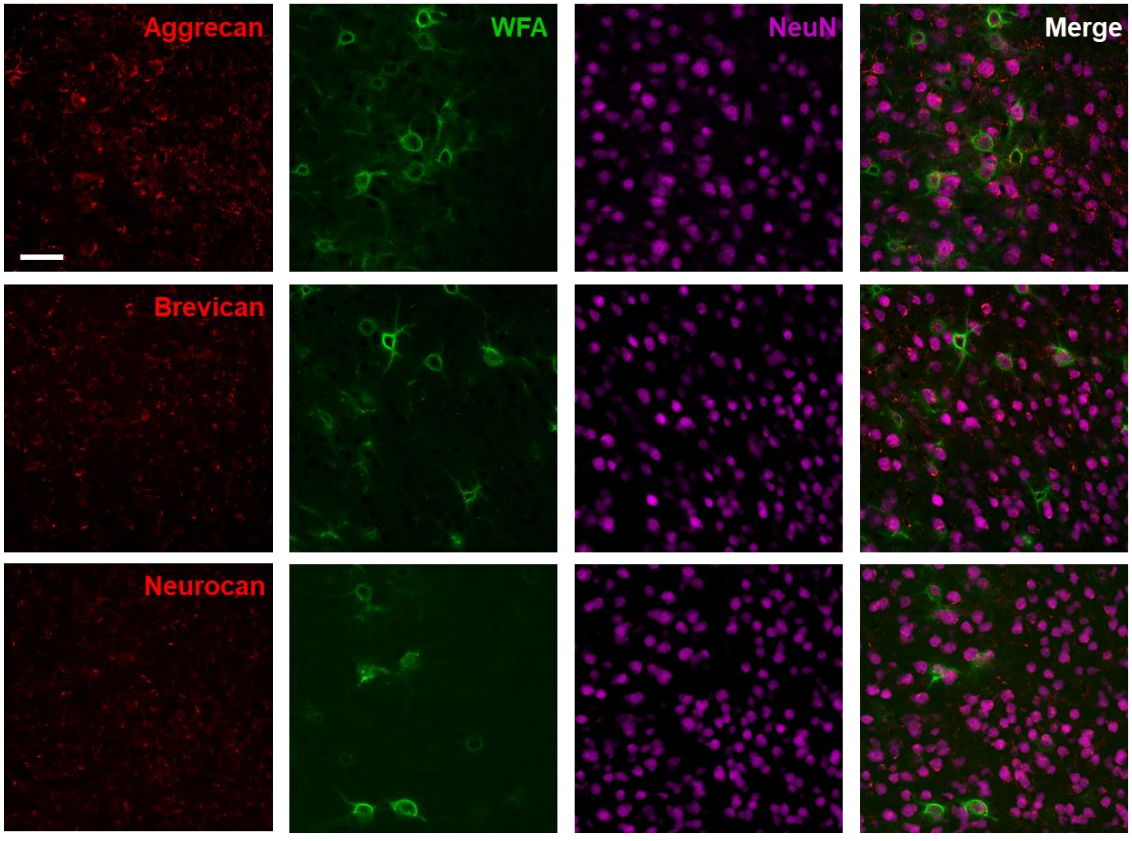

Figure 6.2 Perineuronal net component labelling in the cortex of adult mice. Representative images of immunolabelling for aggrecan (top), brevican (middle) and neurocan (bottom; red) with WFA labelled perineuronal nets (green) and NeuN labelling to show neuronal cell bodies (magenta). Labelling for all CSPGs was stronger in the cortex than the BNST during antibody optimisation, with detection of all three CSPGs, aggrecan, brevican and neurocan in the cortex. CSPG labelling did not directly co-localise with WFA labelling, however, as shown by other research groups (Morawski et al., 2010; Rowlands et al., 2018). Scale bar = 50µm.

Appendix 2

```
% First written - 2018/08/30
% Latest iteration - 11/09/2018
% Author: BES (b.sherlock@exeter.ac.uk)

% Simple script to segment mouse brain images
% Segmentation is based on an overlay of different brain regions that
is
% manually positioned over the fluorescence images
clc
clear all
close all

orig_dir = pwd;

foldr = dir('*2018_08_28 raw images old 1 right*'); % This is the
directory where the images + overlay are currently saved
savedir = '\\isad.isadroot.ex.ac.uk\UOE\User\PhD\Experiments\PNN
quantification\MATLAB\2018_08_28 processed regions'; % This can be any
folder where you want the region images and histogram data to be saved
to

cd(strcat(foldr.folder,'\', foldr.name))

files = dir('*Picture*'); %files contains the names of all the images
that have the word "picture" in their file name

cmap = [linspace(0,0)',linspace(0,1)',linspace(0,0)']; % A green
colour map to make the codes images look similar to those produced by
the microscope

for i = 1:length(files)
pic_with_overlay = imread(files(i).name); % Inside this loop we
sequentially read in each image file into the variable
"pic_with_overlay"
pic = pic_with_overlay(:,:,2);

overlay = imbinarize(pic_with_overlay(:,:,1)); % These two operations
are used
overlay = imdilate(overlay, strel('disk', 2)); % to prepare the image
for region segmentation

overlay_boundaries = bwboundaries(overlay,4); % bwboundaries finds the
boundaries of different regions in the image

%% This section removes certain boundaries that were incorrectly
segmented by the code in each of the 9 images
if i == 1 || i == 2 || i == 3 ||  i == 4 || i == 5 || i == 6 || i == 7
|| i == 9
    overlay_boundaries(1) = [];
    overlay_boundaries(1) = [];
end

if i == 6
    overlay_boundaries(1) = [];
end

if i == 8
    overlay_boundaries(1) = [];
    overlay_boundaries(4) = [];
end
```

```
%%

pix_bins = [0:255]; % Used when contructing a histogram - makes sure
histogram bin width always equals 1


    for j = 1:size(overlay_boundaries,1) % Inside this nested loop, we
sequentially look at each segmented region from each of the 9 images
        figure(j);
        B = overlay_boundaries{j};
        mask = uint8(poly2mask(B(:,2),B(:,1), size(pic,1),
size(pic,2)));

        imagesc(pic.*mask) % Plots an image of the segmented region
        set(gca,'YDir','reverse')
        colormap(cmap)
        caxis([0 100])
        axis equal
        axis off
        title(['Slice ' num2str(i) ' Region ', num2str(j)])

        pause(0.1)

        saveas(figure(j),[savedir '\slice_' num2str(i) '__region_'
num2str(j) '.tiff']) % Saves an image of the segmented region as a
tiff
        region_counts(i,j) = sum(sum(pic.*mask)); % Grand total of all
pixel counts in the segmented region
        region_pixels(i,j) = nnz(mask); % Number of pixels in the
segmented region
        region_counts_per_pixel(i,j) = sum(sum(pic.*mask)) /
nnz(mask); % Mean pixel counts (total pixel counts / total number of
pixels)

         data = pic.*mask; % Data contains all the pixel values from
the segmented region
         data(data == 0) = []; % This removes all the zero pixels from
the data - you might not want to do this, definitely worth thinking
carefull about...
         figure(j+10); histogram(data, pix_bins) % Histogram of pixels
in segmented region with a normal distribution fit
         title(['Slice ' num2str(i) ' Region ', num2str(j)])
         xlabel('Pixel value')
         ylabel('Number of pixels')
         hold on
         [hist_counts] = histcounts(data,pix_bins); % Gets the
histogrammed data
         filename = [savedir '\slice_' num2str(i) '__region_'
num2str(j) ' histogram data.xlsx'];

         xlswrite(filename, {'Pixel Value', 'Number of
pixels'},1,'C3'); %These three lines
         xlswrite(filename, pix_bins(1:end-1)', 1,
'C4');               % just write the histogram data
         xlswrite(filename, hist_counts', 1,
'D4')                     % to an individual .xlsx file

         % Fit a distribution to the histogram, and plot the fitted
function
         % over the top of the histogram figure
         xfitdata = pix_bins(1:end-1);
         % Use MATLAB Gaussian distribution for fitting i.e.  f(x)
=  a1*exp(-((x-b1)/c1)^2)
```

```
        [xData, yData] = prepareCurveData( xfitdata, hist_counts );

        % Set up fittype and options.
        ft = fittype( 'gauss1' );
        opts = fitoptions( 'Method', 'NonlinearLeastSquares' );
        opts.Display = 'Off';
        opts.Lower = [0 0 0];
        opts.StartPoint = [500 25 5];

        [fitresult, gof] = fit( xData, yData, ft, opts ); % This bit
does the fitting
        h = plot(fitresult);
        set(h,'linewidth',2)
        hold off
        saveas(figure(j+10),[savedir '\slice_' num2str(i) '__region_'
num2str(j) ' histogram' '.png'])

        fitvals = coeffvalues(fitresult); % The data from the
histogram fit

        histogram_fit_centres(i,j) = fitvals(2);
        histogram_fit_widths(i,j) = fitvals(3);
    end
    close all
end

%% This section is used to write all the relevant values to a single
Excel spreadsheet

cd(orig_dir)
filename = 'processed regions.xlsx';

for i = 1:9
col_headers{i} = ['Region ' num2str(i)];
row_headers{i} = ['Slice' num2str(i)];
end

xlswrite(filename, {'Total pixel counts / Number of pixels'}, 1,
'B2');
xlswrite(filename, col_headers, 1, 'C3');
xlswrite(filename, row_headers', 1, 'B4');
xlswrite(filename, region_counts_per_pixel, 1, 'C4');

xlswrite(filename, {'Total pixel counts '}, 1, 'B15');
xlswrite(filename, col_headers, 1, 'C16');
xlswrite(filename, row_headers', 1, 'B17');
xlswrite(filename, region_counts, 1, 'C17');

xlswrite(filename, {'Number of pixels '}, 1, 'B28');
xlswrite(filename, col_headers, 1, 'C29');
xlswrite(filename, row_headers', 1, 'B30');
xlswrite(filename, region_pixels, 1, 'C30');

xlswrite(filename, {'Histogram fit centres '}, 1, 'B41');
xlswrite(filename, col_headers, 1, 'C42');
xlswrite(filename, row_headers', 1, 'B43');
xlswrite(filename, histogram_fit_centres, 1, 'C43');

xlswrite(filename, {'Histogram fit widths '}, 1, 'B54');
xlswrite(filename, col_headers, 1, 'C55');
xlswrite(filename, row_headers', 1, 'B56');
xlswrite(filename, histogram_fit_widths, 1, 'C56');
cd(orig_dir)
```

Appendix 3

Beta – actin
Forward primer: TCCTTAGCTTGGTGAGGGTG
Reverse primer (reverse complement): GATGTGGATCAGCAAGCAGG

TATAAAACCCGGCGGCGCAACGCGCAGCCACTGTCGAGTCGCGTCCACCCGCGAGCACAGCTTCTTTGCA
GCTCCTTCGTTGCCGGTCCACACCCGCCACCAGGTAAGCAGGGACGCCGGGCCCAGCGGGCCTTCGCTCT
CTCGTGGCTAGTACCTCACTGCAGGGTCCTGAGGATCACTCAGAACGGACACCATGGGCGGGTGGAGGGT
GGTGCCGGGCCGCGGAGCGGACACTGGCACAGCCAACTTTACGCCTAGCGTGTAGACTCTTTGCAGCCAC
ATTCCCGCGGTGTAGACACTCGTGGGCCCGCTCCCGCTCGGTGCGTGGGGCTTGGGGACACACTAGGGTC
GCGGTGTGGGCATTTGATGAGCCGGTGCGGCTTGCGGGTGTTAAAAGCCGTATTAGGTCCATCTTGAGAG
TACACAGTATTGGGAACCAGACGCTACGATCACGCCTCAATGGCCTCTGGGTCTTTGTCCAAACCGGTTT
GCCTATTCGGCTTGCCGGGCGGGCGGGCGGGCGGGCGGGCGCGGCAGGGCCGGCTCGGCCGGGTGGGGGC
TGGGATGCCACTGCGCGTGCGCTCTCTATCACTGGGCATCGAGGCGCGTGTGCGCTAGGGAGGGAGCTCT
TCCTCTCCCCCTCTTCCTAGTTAGCTGCGCGTGCGTATTGAGGCTGGGAGCGCGGCTGCCCGGGGTTGGG
CGAGGGCGGGGCCGTTGTCCGGAAGGGGCGGGGTCACAGTGGCACGGGCGCCTTGTTTGCGCTTCCTGCT
GGGTGTGGTCGCCTCCCGCGCGCGCACAAGCCGCCCGTCGGCGCAGTGTAGGCGGAGCTTGCGCCCGTTT
GGGGAGGGGGCGGAGGTCTGGCTTCCTGCCCTAGGTCCGCCTCCGGGCCAGCGTTTGCCTTTTATGGTAA
TAATGCGGCCGGTCTGCGCTTCCTTTGTCCCCTGAGCTTGGGCGCGCGCCCCCTGGCGGCTCGAGCCCGC
GGCTTGCCGGAAGTGGGCAGGGCGGCAGCGGCTGCTCTTGGCGGCCCCGAGGTGACTATAGCCTTCTTTT
GTGTCTTGATAGTTCGCCATGGATGACGATATCGCTGCGCTGGTCGTCGACAACGGCTCCGGCATGTGCA
AAGCCGGCTTCGCGGGCGACGATGCTCCCCGGGCTGTATTCCCCTCCATCGTGGGCCGCCCTAGGCACCA
GGTAAGTGACCTGTTACTTTGGGAGTGGCAAGCCTGGGGTTTTCTTGGGGATCGATGCCGGTGCTAAGAA
GGCTGTTCCCTTCCACAGGGTGTGATGGTGGGAATGGGTCAGAAGGACTCCTATGTGGGTGACGAGGCCC
AGAGCAAGAGAGGTATCCTGACCCTGAAGTACCCCATTGAACATGGCATTGTTACCAACTGGGACGACAT
GGAGAAGATCTGGCACCACACCTTCTACAATGAGCTGCGTGTGGCCCCTGAGGAGCACCCTGTGCTGCTC
ACCGAGGCCCCCCTGAACCCTAAGGCCAACCGTGAAAAGATGACCCAGGTCAGTATCCCGGGTAACCCTT
CTCTTTGGCCAGCTTCTCAGCCACGCCCTTTCTCAATTGTCTTTCTTCTGCCGTTCTCCCATAGGACTCC
CTTCTATGAGCTGAGTCTCCCTTGGATCTTTGCAGTTTCTGCTCTTTCCCAGACGAGGTCTTTTTTTCTC
TCAATTGCCTTTCTGACTAGGTGTTTAAACCCTACAGTGCTGTGGGTTTAGGTACTAACAATGGCTCGTG
TGACAAAGCTAATGAGGCTGGTGATAAGTGGCCTTGGAGTGTGTATTGAGTAGATGCACAGTAGGTCTAA
GTGGAGCCCCTGTCCTGAGACTCCCAGCACACTGAACTTAGCTGTGTTCTTGCACTCCTTGCATGTCTCA
GATCTATCCATACAGTTTCACCTGCCCTGAGTGTTTCTTGTGGCTTTCTGAACTTGACAACATTATTTAT
TTTTCTCTACAGATCATGTTTGAGACCTTCAACACCCCAGCCATGTACGTAGCCATCCAGGCTGTGCTGT
CCCTGTATGCCTCTGGTCGTACCACAGGCATTGTGATGGACTCCGGAGACGGGGTCACCCACACTGTGCC
CATCTACGAGGGCTATGCTCTCCCTCACGCCATCCTGCGTCTGGACCTGGCTGGCCGGGACCTGACAGAC
TACCTCATGAAGATCCTGACCGAGCGTGGCTACAGCTTCACCACCACAGCTGAGAGGGAAATCGTGCGTG
ACATCAAAGAGAAGCTGTGCTATGTTGCTCTAGACTTCGAGCAGGAGATGGCCACTGCCGCATCCTCTTC
CTCCCTGGAGAAGAGCTATGAGCTGCCTGACGGCCAGGTCATCACTATTGGCAACGAGCGGTTCCGATGC
CCTGAGGCTCTTTTCCAGCCTTCCTTCTTGGGTAAGTTGTAGCCTAGTCCTTTCTCCATCTAAAGGTGAC
AAAACTCCTGAGGCCATAGTACAAGTTAAGTCTGATTTCTGTCACTCTTCTCTTAGGTATGGAATCCTGT
GGCATCCATGAAACTACATTCAATTCCATCATGAAGTGTGACGTTGACATCCGTAAAGACCTCTATGCCA
ACACAGTGCTGTCTGGTGGTACCACCATGTACCCAGGCATTGCTGACAGGATGCAGAAGGAGATTACTGC
TCTGGCTCCTAGCACCATGAAGATCAAGGTAAGCTAAGCATCCTTAGCTTGGTGAGGGTGGGCCCTGTGG
TTGTCAGAGCAACCTTCTAGGTTTAAGGGGAATCCCAGCACCCAGAGAGCTCACCATTCACCATCTTGTC
TTGCTTTCTTCAGATCATTGCTCCTCCTGAGCGCAAGTACTCTGTGTGGATCGGTGGCTCCATCCTGGCC
TCACTGTCCACCTTCCAGCAGATGTGGATCAGCAAGCAGGAGTACGATGAGTCCGGCCCCTCCATCGTGC
ACCGCAAGTGCTTCTAGGCGGACTGTTACTGAGCTGCGTTTTACACCCTTTCTTTGACAAAACCTAACTT
GCGCAGAAAAAAAAAAAATAAGAGACAACATTGGCATGGCTTTGTTTTTTTAAATTTTTTTTAAAGTTTT
TTTTTTTTTTTTTTTTTTTTTTTTTTAAGTTTTTTTGTTTTGTTTTGGCGCTTTTGACTCAGGATTTAAAA
ACTGGAACGGTGAAGGCGACAGCAGTTGGTTGGAGCAAACATCCCCCAAAGTTCTACAAATGTGGCTGAG
GACTTTGTACATTGTTTTGTTTTTTTTTTTTTTTGGTTTTGTCTTTTTTTAATAGTCATTCCAAGTATCC
ATGAAATAAGTGGTTACAGGAAGTCCCTCACCCTCCCAAAAGCCACCCCCACTCCTAAGAGGAGGATGGT
CGCGTCCATGCCCTGAGTCCACCCCGGGGAAGGTGACAGCATTGCTTCTGTGTAAATTATGTACTGCAAA
AATTTTTTTAAATCTTCCGCCTTAATACTTCATTTTTGTTTTTAATTTCTGAATGGCCCAGGTCTGAGGC
CTCCCTTTTTTTTGTCCCCCCAACTTGATGTATGAAGGCTTTGGTCTCCCTGGGAGGGGGTTGAGGTGTT
GAGGCAGCCAGGGCTGGCCTGTACACTGACTTGAGACCAATAAAAGTGCACACCTTACCTTACACAAACA

Brevican
Forward primer sequence: GATGGAGAGCGAGTCTCGTG
Reverse primer (reverse complement sequence): CCACCTACCGAG

GAGCACAGAAGCAGCCCTGGTGAGGAGCTAGTCCTGCTGAGGAGGACCAGCAGGGTCTCCACAATCACCA
CCTTTGGTAACTCTGTTCATGAGCCCACAGTGCATGCCCTGACATGGGCACAAAGGCTGGCTGTTCCTTC
GCTCCCTTCTGAAATGGGATTGACCTGACCATCCACAAAGTGCTGGGTTACAAGCATTGCTGGGGTGGGG
GGCTGCAGAGGGGAATCTGCTGTTAAGAGTGCTTGCTTTGCTGGCTGTGGTGGTGCACACCTTTCATCAC
AGCACTCAGGAAGCTGAGGCAGGCAGATCTCTGTGGGTTCATGGCCAGCCTGGCCTGCATAATGAGTTCC
AGAACAGTCAGGTCTACATAGAGATCTTGTCTCCAAAAAAGACCAAAACAAAACAAAAGCACTTGCTGAT
CTTGCCGAGGACCTGAGTTCAGTTCCCAGCACTCACTAGGATGGCTCACAACCACCTGTAACCCCAGATC
CAGGGGAGCCAATGCCCTTTCCTGGGCCCCATGGGCACCTGCACACATAGAGATAAAAATAAAATAGGGG
GCTGGTGAGATGGCTCAGCAGTTAAGAACACTGACTGCTCTTCCAAAGGTCCTGAGTTCAAATCCCAGCA
ACCACATGGTGGCTCACAAACATCTGTATGGCTACAGTGTACTCATATACATAAAATAAATAAATAAATC
TTAAAAATAAAATAAAAACCACGTACATGCTCTAACATAAGACCGCTCAACAATGTGTTGGCACCATCTT
ACATGTGGAGAAACTGAGAGAAGGTGCATGCCCCAACACCACAGAGGAGTGAGCCTGCAGGGAAGGTGAT
GCACACCTCTGGTACCTCTAGTGATCTCCTCTGAGCCTGCCCCTGGTGGCCGATACTCAGCTGCAGATCC
AGCTCCAGGCCACAGCTGTGCCATCTCTCAGAACCACCCCCTGGCATTTCTAAGCTTTGCTATGCTTCCT
GGCCCCCTTCTGAGACTATCAAAGCCCCCATTCTCTGAGCACAGCTGTGCCAGCACTGGGCCCCTCCCAG
CCAAGAAGCCAGGTGTCTGGGCCTTGAGGGGGCTGGCTGCCAATGCAGGAGAGGGCGCGAGTCTGAACAG
CCCTCCAGCGGCCACTTCAGATGGGCGCACAGTAAGAGCCAACACCGAAGAGGGGTGTTTGGGAGGCGGG
AGCTTTGCGAGCAGCGTGGGTTCTCACCTTGGGCCACAGCTTTGGCCTGTGTGGAAGCTATTGCCCTGGG
AAAGCGGGAGGAGATTGCTGGTTCTTCAAGAGAGCCTGGAAAAGTCTCCAGGGCAGGCTGGGAGGCAGCC
AGCTGCACCACGTGGGGACAGGGCAGGCGAGCCGCCACTGCCTGGCTTTCTCCAAGCTCGCCTTCCTCCT
CCCTCTTTTCCTGAGCCCTTGGTGCAGCAGTCCTGGGCAGGCCACTTCTGATTCAACCGGCTGACCCTTG
TGACACCGCCGTTTACCATTTGGCATCTAGAAGACCCTTGTGGCTATGAGAACTGTCATGCCCTGTTGCT
AGGACACGGGTTTGCACACGAAAGCCGCCATTCTGGGCTCTGTTGGCTTCCAGTGCCAAGATCTCTGTCT
AAGATCTAAAGGGGATGCAAGGAGCAGGCCAGGGTCCAGGAGCACCTCAGATGGAGAACAGAAATGAGCA
GAGTCCTTTGGCTATGAGTCAAGATGCCAGACTCCATAATTGGGGAAAAGGTACCTATCAGCAATGGCTA
GAGTTGTGTGGGTGTACCTCGATGCAAATGTCCCCAGCTGGAAAAAAGGGGGGCCTTTATAATGCCCATC
TTTTATAGAAAGGGGCCCCTCTCAAAGACTCAGTCCCCATGGGCTGCTGAGCCCCTAACCAGACCTCATA
AGGCTGTGAATGACAAAGAATAGGATTCCACAGGAGTGGTGGGGACCCTGCTTGGTTGATCAGAAGAGGC
CAAGGCATTCCTGGCAGATGGCTGCCTACTGGCTCCACTGGCCCCAGGATTCTTTTCCCCTTCCCCCGGG
TTGTGCACATTGGTAACTCTGAGCTGGGGGCGGGGGCGGGGGGTATCTCTTTCCTGTCTTCCTTGGTCAC
AGTCAGGTTTTCCCAGGCAAAAATTGTGTTATATCCAAGACAGCAACTGGGCTGAACTGCAGCCCCTTGG
TTTCTTTCCTAGCTCCACCTGGGAGACCTGCAGGGCATGGAGCCCATGTGTTGGTGAGCCATGCAGGTGC
AACCCAGAGCTGGCACCCAGCACCTCAGAGTCCTTCCCAACTGGTGACTCCCCCAGTCTTAGGGCCCCAG
ACAGGGCCTGGTACATAGATGACTTGTGGGTCAAGCTTAAGGAATGAATAAATGAAGGCCTCCTGTGCAG
CTTCTTCAGGGGCCCCTTTCTCCTTTCTGCTGGCACCACTGCCTGGTAGTTTTCTCCCTGCGTGACTCTG
CCCTGGGTTTCAAGGTCCTTCTGTCCTGTCCTTACAGTGGGCGGCATTAGCTGGAGTCCTCTCTTTAAAC
TTGTAAGGCTTTGGAGAGGAGTTTGTTTTTTTCCAGAGGTTCTGAAGGCGTTTTTTTTTTTTTTGTTTT
GTTTTGTTTTTTGGTTTTGTTTTGTTTTGTTTTTTTGGAACTCCATCCAAGGCAGGGGGTGGGGCGTGAT
TAGGAAACTGTTCCCTGAGTTGGGGGTGAAGGTGTCTGCAGACAGTCGGCATTTGGGGATCTAGAAATGG
TAAGGTCACAGCCCCCACACCGGCCTTGAGGACAAGGATCTGGCTGAGTGGCCTACAGCTGGTGCCAAGG
CTTTGCCTGGAGTCGCAAGCAAGAGGAGGAAAGTGGGAAGCCTGGGAAAGCAGGGAGAAGCAGCGGGTGA
AGTGGGGGTGGGGGACAGCTGGCAGTCCTCGAGGCCCACCCCCAGGCTCCTGGCTGCACACTGGGCAGCC
CAGCCGAGGCTAGCAGGCTCTCCTGCACACATTGATCTGCAACCTGTGACGCCTGCTCCATCACTCACTG
TACCACTTGATACCGCGCGCCTAGACTCTCTTGACTTGGGTTGCCTAACCCGTAGTTCTGCGAGTCGACC
TCCACCTGGTCAACCACTGCAAAGTCAGCTCCTCCGCCGGGGAGGGAGAGGAGCACCGGGGGAGCACAGC
CCGATCAAAGCTTCCTCAAGAGGGATGGCTGTGGTCATCTGCCTTTTCTCTGGCCTGAGAAAAGGACTTC
CCCTTTTCACCCAGCAGTGCCCTCTTTCCCGGGGCAAAGCTCCTGTCGTCCCTCCATCCTCTGCGCGACT
AAGTTTGAGCCGGTCTTCCTCCCTTTAACCAATGAGAAGTCCCTCCCGTGTTCTAACTCTCCATCCTGCG
TCGCCACAGCGCCCTCCATCGCTCCCTCCCCGCCCCTTCTGCCCTCCCCGCTGCAAGTCTTGGGCTCCCG
TCCGCGGAACCTTGTCCTACTTCGCTTGTCCTCCCTCTGCCCGCTGTCGCCCGGAACCCGCACAGAGAAG
GCAGCGGGTCCCGTGACCGCGCAGAGCCCCCCACGGGGGCGGCAAGGGCCGGGGACGGCGGGGAAGGCGG
GGCGCGTGGGAAGAAAGGGGGTTTTGTGAGGCTCCCGGCGAGCTGGCGCCCCTGTCTGGGTCCCGCGCGC
CCGGCCCTGCTCGCGCCCGCGCATTGCGCCGCAGTCTCGGCTGCGGCTGCGGGACGTGCGGTGTGCGCGG
AGGGGACCTCGCAAGGTGAGTGCGGAGGCCTGGCCCTATCGGTCGCTTGCTTGCTTGCTGTGTGACCTTG
GGTAAGTTTCTTGACCTCTCTGAGCCAAAGGATCCGGGCGAGGGCGAGAGCGGGCCGCGATACTGGCTGC
TGTGGGCGACCGAGACAGTGACCCACCGTAGCTTCCTGGGGTCCCCAGGCACTCGGGGGTGCGGTCGGCA
GCGGCGCCTCTCTGAAGGTGGGCGCGCAGCGCTCTGTGCCGGCTTCGGCACCCTGAGCCACGCGTCTGCT
CGCTCACTGTCCTCGCCGCGCAGCCTTCAGGAGCCAGGGGACGTCTGGGCTGCGGAGCGACTAAGGATGC

CCGGGCTGGAGACGACAGGGGACTGCTGAGCTCCGGTCCTTGTGGTGGCTTTCCTCCGGGAAGTGTCACA
GTAGCCACTCTTGGCCACTTGGATCAAAAATTCATGTCTCAGGGCAGTCGGATCCTCTGGCCTCAGGCTT
CCTTCCTCATCCCGTGCTGCCCCAACACGGGTAAAAGAGGTAGCCACAGGGCCGGGCGGGCGTGTGAGTA
GCTCCTGCTCCCAGCCTCCCCTCCTCAGAACGCTCCAGCACCTGGCTTACTTGCCAGCGGTAACCCGAGT
GACTGCTCGCCCGGCCCGCTGCACAGCACAGGCCAGAGCGCTGCTTAGCAGGGGAGTCTGTCCTGGGAGG
ATCTAGGAGGACCGCTTAGGCTCAGGCTAGCGACTATGAAGGCAGACCGAGTGGGAGATGGAGCCAGTGA
GAATAGGTATGGTCGGTAGGAAATCTTGCCTGACGTTGTAACTGACCCCCGGCTGCATCATTAGCCATGT
AGTCCTGGGTCCCCGAATACTCCCAAGTCTGACTCTTTACAGAGTGTGTTCATTATCTGTGCAGCTTTCC
TTCCTGAGGGCACAGTGACCTGGCTCCCGGTTTGGCTCAGAGTTAGCTCTAACCCTCTCTGGTCATCCAC
CTCACTTTCCCCGTGAGCCTGTATGCGCAATGAGATCTCAGAAAGAGAAACTGTTTCCAGAGCTGAGGGC
CAGGGCGGGGGGGGGGGGGGGACGACTGGCCTCTCCCTGTACCCTTCTCCAGTACACTCCAAGTTGTAGG
CTTTCACAAAAGATGGGTGGGGGAAGGAGCAACTGGATAGAGGCCAGACTGGCAGGGACAGGGTCTTTGT
CCCAGCTGGCTTCTGAGCCAGGAGATCCGGTGGGAAAGCCCGTGCCAGGCAGAGGGGAATGGCTGAGAGC
AAAGTGGGAGGGAGGGAGGGATGGAGGGGGCAGAGGATGTTGGGCACCAGGGGAGCTTCCTTACAAGTCC
TGGTGGAGAGGAAGCAGAGGGAGAAGCCGCTGTTTCAGCAGGGTTCAGTCTAGGAGGCCCTCCTGGAAGA
GGAAGGGTTAGGAAGGGAAGGTTGGAGCTTTACTGTGGGGGAAAGAAACTCCTGGTTGGCACCTGAGGGC
GGGGAGGGGGGTGTTTGCCAAGGGGGTGAAGTAGGACCATAGTTGCGCTCCCAACCCCACCCCTGCGTCT
GTGGGTTTGAGTCTCCAACCCCTAGAGGCTGCCTGGACCTGCAGGTGCCCAAGTCCCTCACACAGAATGA
TGTCTTTGCATCTCACCTACGCATGTCTTTCATACACAGGAACCCGTCTCTAGGTGACTTATAATTCCTA
AGTATATGCATGCTGTTTAGGGAACAGTGACAAAAACCTCTGTATGTGTTCAGAACAGACTCTTTTTTTT
TTCCTGCATGTTTGACGAGTAGCTGGTTTGGATGCATAGATTTTGAATACACGTGCACAGAGAGCTGATT
ACGCAGTACCACCAGCCACTGTGTTACAAGTATTCGCTGGCATCTGTTATGTGTCTGTTGCTGGCCTATG
CACAGGGCATTTTCTGTCGTAGATTATAAATAGGTAAGTAGGTAATAGACAGTGGCAACTGTGTGTAGAT
GACAGCTAGACAGGTAGACAGACAGACAGATCACTCAAGCATACAGCCCCATCAAAATGCGTAAGGTGCT
AATGATGGTGCTTCCCCCCCCCCCCCCCCCAGTTAAGAAGACACAGACTCAGAGAGGGTAAGGAACTTGGC
TTAGGTCACACAGTGAGTTGACTGGGCACACCTCTTGGTGCTTGGAGATAGGAATCAGAAACAGAGTTAG
GGGTGATTCTAGTATGTGCTACCTGCATGGTGGGACAGAGAACGGAGGAAGTCCGTTCCGCAGTCTAACA
ACTTTCCTCTTTCCTCTTCAAGTTCTTCCATCAGTGTGCAGAATGATTCCACTGCTTCTGTCCCTGCTGG
CCGCTCTGGTCCTGACCCAAGCCCCTGCCGCCCTCGCTGATGACCTGAAAGAAGACAGCTCGGGTGAGTA
AGCATCCAGAGGACCATGTCTCTGCTGCATCTTTCTCAGGACAGAGGGCTGTCTCGGTTTAGCCCCAGCT
ACATGCTTCCAGCCTAGGCACACGGAAGGAGATGTGGAAGTGCTGTGGGCAAGGGCTGGAGCCAACTGCA
AAATAGGGATGAATTGGGAACCCTAGTAAGTAGGGGAGTCTTGGGGGTCAGAGTTGCAAAGGAGCACGAG
GCAGGAGGCTAAGGGTAGAGGATCAAATTCAGGACCCTGGGCAGTGCTCAGCACCCTGAGCTGGGCAGTG
CACCCCAGGCGCCTTGGATCGAGGGGCGGGGCTTGGAGCCAAGCGCACAGGCGCACTACGTCCTGCGTCT
GGCTGCAGCCGGCTTTGACCCCTGTCCACAGAGGATCGAGCCTTCCGCGTGCGCATCGGTGCCACGCAGC
TGCGGGGCGTGCTGGGCGGTGCCCTGGCCATCCCATGCCACGTCCACCACCTGCGGCCGCCGCACAGTCG
CCGGGCCGCGCCGGGTTTTCCCCGGGTCAAGTGGACCTTCCTGTCCGGGGACCGGGAGGTAGAGGTACTG
GTGGCTCGTGGGCTGCGCGTCAAGGTAAACGAAGCCTACCGGTTCCGCGTGGCGCTGCCTGCCTACCCCG
CATCGCTCACGGATGTGTCTCTAGTATTGAGCGAACTGCGGCCCAATGATTCCGGGGTCTATCGCTGCGA
GGTCCAGCACGGTATCGACGACAGCAGTGATGCTGTGGAGGTCAAGGTCAAAGGTGAGAGGAGAGTGAGA
TCCCTAGAGAAAGGGAGGAAAGGACTCAGGCCCCCCTCCCCCCGCAAGGAGTTGATTGTGAGGCGGCTTA
GCAAACCCTGCAGGGGAAAGGCACAGGGTGAATAGGGGGCCAGAGATGTGGGGGGAGACAGTCCCACAAG
CTGTAACAGGAGCACAATCGGACTTTAACTTTTGTGAACAGGAAGTGACAGAAGAGAGGGGGAGGTCAGT
GTGCTGGTGGTCCGGCCAACTCAGGAGTTATTTCTTCTCCGCAGGGGTCGTCTTCCTCTACAGAGAGGGC
TCTGCGCGCTATGCTTTCTCCTTTGCTGGAGCCCAGGAAGCCTGCGCTCGCATAGGAGCCCGAATCGCCA
CCCCGGAGCAGCTCTATGCTGCCTACCTCGGCGGCTATGAGCAGTGTGATGCAGGCTGGCTGTCCGACCA
AACTGTGAGGTGGGCTGGGGATGTAGACCAGGAACTCCTGGTCACATCGGGATGCTTGCTACCTCCTCCC
TCCATCGAAGTTCCTCAGGATTCCCTGCCTCTGGAAAGAAAATTGGTCTGCAGCTCTGCCTGGGCCTTAC
TTTCCTGCATCCTGACATCACACACACACACACACACACACACACACACACACACACACACAGCAGCAGCAGCA
GCAGCAGCAGCAGCAGCAGCAGCAGCAGGGTTGACATGGGACAGCCTTCTGGGGGTGGAAGATGCCAGGCA
TTAGCCTCTTCCTCTCTCTTAGGTACCCCATCCAGAACCCACGAGAGGCCTGCTCTGGAGACATGGATGG
CTATCCTGGCGTGCGGAACTACGGAGTGGTGGGTCCTGATGATCTCTATGATGTCTACTGTTATGCCGAA
GACCTAAATGGTAATTGGGAGTGACAAGCCCTTCTGCAACATGGCCCTTGGTTTCTTCTAGGTCCTCCAC
TAGACTTCACATGTCTAAGAGGACAGGCAAATTAGGCAGGCACTTAACGCACGCCTCCAAACACTGTCCC
AGAGGCAAGCCTCTGAGCAGACCTAGCAAATAGCAGACAGAGGGGTGGGGGCGGGGCCGGGGTGGGGGTG
GTGAGTTTCAGCAGAGTCCTGTAGAGCGAGGAACTGGGGCCAGGCTCTCTAAGTACTAATTTTCATCTTG
GGTTTCATGCAGACTTTGGTACTATCAGGTGGGCAAGGTGACCCCCCCACACACACCAGGAATGAGCTTG
CCTAGGAACGTTTAAACGTCTAGGGTGGAAGTACTGCCAACTGCCTGATGACCCAGCTCCTCTTTTACAC
TCAGGAGAACTGTTCCTAGGCGCCCCTCCCAGCAAGCTGACATGGGAGGAGGCTCGGGACTACTGTCTGG
AACGTGGTGCACAGATCGCTAGCACAGGCCAGCTGTACGCAGCCTGGAATGGTGGCCTGGACAGATGTAG
CCCTGGCTGGCTGGCTGATGGCAGCGTGCGCTATCCCATCATCACACCCAGCCAACGCTGTGGGGGCGGC
CTGCCAGGAGTCAAGACCCTCTTCCTCTTTCCCAACCAGACTGGCTTCCCCAGCAAGCAGAACCGCTTCA
ATGTCTACTGCTTCCGAGGTGAGTGGCCTCTGCAGCAGTCAGTGCCAGGCCTGGAATTCAAGCCCTCACC

ATCTTCTTGGTCATTTGCCCTCAGTAATCTGTATTAGCTTCCTCAATCCTTGTGCCTGTCAGCATATTGG
CCAACAGAGGTAGCTGACATTTTTTTCACTTCCATGAACCAACTGTTCTGTGCTTCAGTGAACAAAATGC
ACGTGGGAGTGGAACGCTCCTTAGAATGTTCCAGATCCTACAGCTTATGGGTGACAGGACTTTCAACACT
GCGTGTTGAGGAGGGGACAGAGGGTGGTACTAGGAAGCCAGATGAGTGCAGACTCTGAGCCAAGCACTTT
GTTCTGAAAGAAGCAGTAAGAGGCATGACTGTGGAGGGACAAGGAGGGGAGATGAAGGACAGATGTAGGT
TTGCTGGTCTGTGGTGACCTGGGCAAGGGTCACTGGAACAGGTCATACAGTCCTGTCTGTCCTGCCTAGA
GATAGCTCTCTGGGCTTCTCTTGGCCCAACTCTACGTTGGAGTCATTGGTTCTCTGCTCTGTGTTCCCTC
CCCAGAGGATGAGGTAATTCACTCTGAGCCACTGAGCATCACACCCAGAAAGTGGTCCCTTCCCTTTCCT
TAGCCATAGCTGAGCTCCAAGCTCCTCAGATAGTGACCACTGAGCACTCTTCCTGGGGATGGAGTCTCTA
CCCTTCTCCACACAAGCCTAGCCTGCACGGTACAGAGCCTGCTCCATCCACCCACTCTGTATTCACACTT
AAAGGAGCAGCTCACTCAGCCTTTCTAGACCCATCTGAAGGAAAGTGAGCCTCCACTTCATCTCACTGCT
TCTCAAGTGCCTTTCTATTGTGCAATGTGTTTATTGCCTATGCCTATTTTCTTCAGGTTTCCCTAGCGTT
CTCTATACCATACTCAGAGAAAGCTTGGCCTAAAACTAGAAGGCACTCCATTAGCACTCGAGGGATGGGT
GAAGCACATTCCAGGGCCTGTAGAGGTCTAGCCTAGAGGCTCAGACGCAGCCCACACCCTGGGAGGATTC
AAATGCACACTTAGCTTCTCACTGGCCTTTTCCTCTTGCCACAGACTCTGCCCATCCCTCTGCTTCCTCT
GAGGCCTCTAGCCCAGCCTCAGATGGACTTGAGGCCATTGTCACAGTGACAGAAAAGCTGGAGGAACTGC
AGCTGCCTCAGGAAGCGATGGAGAGCGAGTCTCGTGGGGCCATCTACTCCATCCCCATCTCAGAAGATGG
GGGAGGAGGAAGCTCCACCCCAGAAGACCCAGCAGAGGCCCCCAGGACTCCGCTAGGTAACTGGAAGCCT
TTGCCTTGGGTTCTCACTACCTGAGAGAAGTTGGGGGTAGGAGGGCAAGCCCAAGTGGTCACTAGGGTCA
TGACTGACATAATTCTGCCTTAGGTATCTCTCCTATCACCCTCCCAAATTTTTTATTCAAGTAAATTCCA
CACCCAATTCTCTTTAACTAGAGAAACTTGTGTTTAGAGGGTGCTCTCTGGGAAGGAAATATATTCCTTA
CCCCAAGATTGGAAAATGTTGGCAGACTGGGAGAGGGAGATGCAACAGCCTTTTCTGACCCAGTAAGAGG
CAGTTTGCAGAGCCCTTCAATGCGTAGGCCAGGTCAGAGTTCTTCCAGACAGGCAATGCACCAGGCGCTG
TACCTCTCCCCCTCCCCTTGGGCCCCACCCCCCTCCCCTCCCCTCCCCTCCCCTTGCTTGGTCTGGGGCG
CTGTCCCTGGTGCTGAACTGTCTTGCTGTGGTCAGAATCGGAAACCCAATCCATTGCACCACCTACCGAG
TCCTCAGAAGAGGAAGGCGTAGCCCTGGAGGAAGAAGAAAGATTCAAAGACTTGGAGGCTCTGGAGGAAG
AGAAGGAGCAGGAGGACCTGTGGGTGTGGCCCAGAGAGCTCAGCAGCCCTCTCCCTACTGGCTCAGAAAC
AGAGCATTCACTCTCCCAGGTGTCCCCACCAGCCCAGGCAGTTCTACAGCTGGGTGCCTCACCTTCTCCT
GGGCCTCCAAGGGTCCGTGGACCGCCTGCAGAGACTTTGCTCCCCCCGAGGGAGGGAAGCCCCACATCTA
CTCCTGGTGGGGCAAGAGAAGTAGGGGGGGAAACTGGGAGCCCTGAGCTCTCTGGGGTTCCTCGAGAGAG
CGAGGAGGCAGGGAGCTCCAGCTTGGAGGATGGCCCTTCCCTACTTCCAGCTACATGGGCCCCTGTGGGT
CCCAGGGAGCTGGAGACCCCCTCAGAAGAGAAGTCTGGAAGAACTGTCCTGGCAGGCACCTCAGTGCAGG
CCCAGCCAGTGCTGCCCACCGACAGTGCCAGCCACGGTGGAGTGGCTGTGGCTCCCTCATCAGGTAATTC
TGCTGAAGGCTCAATGCCCGCTTTTCTCCTTTTCCTCCTCCTCCAGCTCTGGGCCACCTGACACGTTGGC
CTTTAATCCACCCTTTTCCCCTGGACCCTCTGGTCCTTTGCCCTCGTTCCCTTTTCTGTCTCTCCCCGTG
GATCTTCCATCTTGGATCTTCCATTCTGTCACTTCCGTCCCAGTTCTCTGATCCTCTGTCCCCTCCCCCA
CCCACCACTGACCCTTGGGCCCTCTGCTGTAGCTCACATCTCACTGGCCACACAGAATGTCCTCATGCCT
CTTCCTGGTGCCCTCATCAGCCTTGAAGGCAGGCCCATTGTCTGCAGTTCCCTCCCTGGGCCCTTTGTTC
CACCCCTTTAACCAACCCCCACTGATTCCAGGGAAGCCTGAGAGGCCATACCTACCCCTCACCTCTGGGG
ACCAGAATACTCACCCCAAAGAGCCTTAAGCCACTACTTCTGTGAAGTATTTTTTGACTGTTTCATGGAA
AACAAACCTTGGAAATAAATCTGTATTAAACTGCTTTGTACCCAGCCGTTGACAACCTCTCCATCTCCAG
CTGTCCTTTCTGCTCATCGCTGTGTCTGAATCAGGAATCTCTGTTTCCCTGTACCCTCTCCATCCTCTGT
GTCTCCACCTGTCTCTTTGCCACTCTTCATTGGCCAACATCCTTGCTGTCACAGCAGGATGGCAGCTTCT
TACTGCTCCCTCTATCTCTCCTTGGGCCATTTACACCTTCCCTTCATACTGCTGGGACCCCAGACTTGAC
TGTACATATCACCCAAGGGAGTCCTCCGTCACCTGCAGAAGAAACCCACACTGCCCGGGTATGATGTGTA
GCCTACCCAGGTAGTTCCTGCTTGGAGCTGGTTCTCTAGCTTCCCAAGGCTTAAACATATCATCTTCCTC
GGTGCACCCAGCAAGAGACAGTACTATTATCCCTGTGCCCAGTGTTCCCTCCCTGCACTAACCCTGCACT
AATGACCCCCCACTCCCGGAGAAATGGCTTATGTTCTTCAACCCAAAGGACCTGGCTCATTCGGAACAGG
GTGGGGTGGGCAGAAAGAAAGGAACTGGTTTCCACCATCTGAAAGAAATCTTCTGTCCCAGAACCATAAG
GTTCCCATTGGAAGTCTTCTCCGGGAAGGCTGAGGCCCTCCCAGGTTCACCTCTCCTCCATGGCTCAAGT
GGAATATCACCCCTACATCACAAAAAGCTTGCCCATTTCAGCTATTGCCTTTCTGCCCACTGGCCTTGGA
GTGAGTGTAGTAAGGAAGAGGGAACCCCTTAGAGGTCACTGAAGTGTCAGCCCACCTGTAAAGAGAGCCA
GAGGCCCCCTGGCCTACTGTCAGAAGGTGGGAAAGAAATGCTTTCTGGTTCTGTGGGGTAGAAAAAGAGG
AGGGAAAATCCAAAGTGGGTCCCTTATACCGCACTGCCCAGCCAAGGTTCAGGCACTGTAGCCCACAGCC
AGGTTGGAACTTAAAGCCAAAAGGGCAAGGACTGAGCTTAAGAGTCTGTCCCCCCAGGGTTAGAGGGCTG
CCCAGGAAGGAGAGGAAACTGGAGAAGCAGAAAGCATGAGGACTCCCGGGGGCCCAGGACTCTTCACCCT
CAGCACCTGAGACCAACAACCTTCACCCTACTTGAAAAACTGTTAGCAGAGGGATGCTCGACATGATAGA
TGTTAGCGGAGGGATGTTCAAAAGACTGCTTGGTCAGTGTACCAATTATAGCTGGGGCACTCCAGCAAAT
TTAATCAGCCCAGCTTCTCCTTCCTCCTCCCCTGCTGCTACCACTGGCATGTGGGCTGTGTTCTCAGCAG
CCACTGCTGGGGAGTAGTCTGAGGGACCTAGTCTGCTCTGTTGGTTAAAGGAGCCATTGTCTCTGGTCAT
CTGGACCAGAAATGGAGTGGATGCTGACAGCTCCTCCAGTACCTAGGCGGGGCCCAGGAAGAAGGCTGGA
GAAGGCTGCCTGAGGCTGGCAGGAATTCAGGTCTCATAATCCACAGCCCTGGGCTTCTTCCCTTCCTTGG
CCTCTTCCCGCTGGCTGCTCAGGGCTCACACTGGTGGCAGTCTGAGCCAGTCAGGAACTGGGAGGTGAGA

Neurocan
Forward primer: GGGCTCTAGGGCTGAAGAAA
Reverse primer (reverse complement): GCTGTGGCTGCTTCTCCTAG

GGAGGCTGCGCCTGGCGTGCTGAGCGCCTGGGCTCTAGGGCTGAAGAAACACCGGGAGCGGGGCGTCGCG
TCCTTTGTGCCCGGAACCGTGGGGATGTGTTCGCGCTAAGGAGCCAGGTGTGGGGGGGCCGGAAGGAGGG
GGGCAACAGAAAATAGGGCTTGGGGAGGACTGACCAGAATGAAGGGGAAGCCCCCTCCTCGATGAAAATG
GGCAGGGAACGATGGGGGAGGGGAACCAAGTTTGGGGGGCCTGAGTGCATGAGGGGCGGCCTTAAGGGTG
TTGGGAATGGAAGGGAGTCTTGAATGAAAAGACTTTCCCATCTCTGGTAGGGAGGATCCCTGGCTGCATA
TAGTTCTCTGGATCAAGCAGGAGGTGCTGAAAGCTAGGGCTAGGGGAGGGGTACCCCGAGTTTGGAATAA
AGACAAGCTGGGAACTTGAAATGGGGACCTCCAATTTACACATGAATGGAAGGCTGTGGTGGGGAAAGGG
TCCCCCAATTTAAGAGTGTGTGTAGCAGAGTCTCTTCCCTGGAAAAGGAAGTCAGACAGGTCTCTGTCCT
CTTACTGCATCCTGAGCTAAGAAGGAGGCTCAGACACCCATCCTAAGAGTCACCCTGGTTTTCTAACAGA
TAAGGAGTTGGGGTGCAGTCCCTTTCCCCAGTAAGCATGTTTACTGTCCTGGCTAATGCTGGGTGTGGGT
TCTGGTATGCCCCAAAATGGATGTTCAGGACCTGGATGGACCCTGTGAGGGGACAGGACCCCCCAGATGC
CTCACATCTCCATGTAATCTCAGCACTCCACCCCAGTGCTTCACCCCCAGTCTACCTGTATGGTGCATTT
TAAAACTCTCTTTGGATGATCAGGTGGTAGAAGGGAAGGGACCCAGTGCTTGGGTATAGGAGTGACCCCC
GTGCATACACCACAGTGTGGCTTTGTTCATTCTAAGTGTGTTTGGGATAAAGCCAGGCTGAGGCAGTCCA
GGATGGGTGACATGTGGGGACCAGTTAGGAAGGTATGAATTCATACATTGTGCCATCCCAGACTCTGGCA
GTCTCGGTGATCCCTGGCCGTCCCTACAGGGAGACAAGGAAGGTTTTCACCCCAGGAATCGGGGGTCTTT
GTGTGTCAACGAGCTATGAGGAGAGGCATGTCTAGGGTCTCCTGTGACTGATATAACTGCTAACAGTGTC
TTTTGTTACAAAACTATGCTGGGGCCACATTATCAGTGGCCCTGCATCGGTCACCAAGGCCACATGCATC
CCAGGGCTGGTGTGGCAGCCTGTGGGAGGAGCCAGACCTGGTGAACGGATTCGTTAGGGGCTTCAGCAGA
GGGCTCCAGATTGTGGGTGTCTTTGTGTAGAGGTCGCGCAGCCTACTCCGCCAACACAGGCATGGTTCCC
TTTGTTAATGTCCCTGAAAGTCTCTGTGTGTGTCTCTCCTGGGGTGTGTCTTGTGAATAGGGAAAGGGGA
TTCAGAGCATGGGAGTGCAAACCTGAGGAGCCACAGTGGGCACGGAGGCCAGGGTGGAGGTCCTCAGCTT
GGCTTCCTTTCTTCTCCAGTGTTCTACACTCATGCACACACATCCAGTGTGAGTCTCGGGCCAGGAACCC
TCAGTGTGTGCAAGAGTGTGTGCATACATGCGTGTGGCTTTCCTCGCCCCCACCCCACCCCCACTCCCGG
GACCAGAAATCCTTCTGGAGCTGATGCACCCACATCACAGGGTGCCGACATAGACATACCCTCGCCTAGA
CACAGCACCACAGATGCACACCGTCACATATCCAGGGACAATAGATGACAACTGCCCAACTCCAACTCAG
TGGAGAGATGAGAGGCAGGGTGGGGGTGGGAACGGAACAGGGGTACAAACACACTGGAGCTTGTGAATGT
GCTTGCCCTCTTCTCTGCAGGCCCCTGCTTGCATATACATGAGGCTAATGCATCATTCATGAGGGGGTGG
GCCCAAACCTCAGCCTAAAAGCTGTCACTCGCCTCTGGTGGCCCAGGAGAGGAAGTATTTTAAGAGAAGA
GTGTGCGGGTGTGAGGATGTGAGGGGGAGAAGGGGTGGTGTTTGGGGAGTGAGGAGCACAAAACTGACAT
AGAGTCTGTCACTGTGTTGGGCTACCTTCGGGTATTTTTAGTGTGTTCCCAAGGCTTTGTGTACAAAGAG
CTGTTTTTAAAGGTGATATAAAATAAGTCTTAGCTCATTCCTCCCTGATGATTTCAGAGGGTTTGTGTTA
AATGAAGCTCATTTTACAGGTGGGGAAACTGAAGCATGGGGCAACAGGGCCACTGGGGCAGAGCTGCATG
GTGGGTAATAGAGTGTGACATGGATTTTTTTATTTTTCCTTTTGAGGGGAGGAAAGAGACAGCGTTTCTC
TGTGTAGCTCTGGCTGTCCTATAGAAATTCTGTAAAACAGGCTGATCTCCAACTCAGAGGTCCACTGTCT
CTGCTTCCCCAGTCCTGGGATTAAAGGGGTGCGCCATCACACCCAGCTGGATTTTTGTTGTTGTTTTTTC
TTTTTCCTCTTTCTTTTCTTTTCTTTCTTTTTCCACTTCTCTCTCTCTCTCTCTTCCTCTCTCTCTCTCT
CTTTGAGGCTAGGTCTCATATAGTACAGGCAGACTTCAAATTTGAAATGAAGTTCAGGGTAGCCTCAAAC
CCTTGATCATCCTACCTCCACCTTCCAAGTGCTAAGATAAGATGACAGACTTTGGCCACAACATCCAGCT
GAACTCAATTATGTGGAGAGGGGAGGGGAGGAAGAAAGAATGAGAGAACACATTTTCTGGCTTTTATCCC
TCTTAAAATGGGGTGATCGTAGGTACTAGGGTACCCCACATTGGCTTGGGGTTCCAAAATGAAGAAACGG
GGATGGCCTGGATTGGCATTAGAGTCTGTGGCATTTACAAATTGGTAGCTTGTGCTCTGCTCTGCAACCC
AAAGCAAAAAGCGAGCCCTCTCTGGGTTCAGAGGCAGGTTGTGCTCAGAGGCCCGGCAATACGCCTCAGA
GTTCAGCACCAAGGACAGATCGTCGACGGGAGTAGCCTTTAGCGTTTGTAGAAACAGGGAGGGCTGAAGG
GAACTGAGCTCTAGAGGCCCCACCCACAAGGCTTGCTCTACTTCCATAGGCTAAAGGGCAGATTTGCAGG
TGGCCTCAGACTCTCTTTCTCCTGACCTCTTTGAACCCCTGTATGAGGCCGGAGTTGAGAGAGGGGCAAA
GTTTTGTTGAATCCTTGTAATAAATATATTTCAGGCATCCGAGGTAGACCTTGCTCATAGTAAGTGCTCA
ATAACTGCCTACTGTATGCCAAGTGGGTCATGGCCCCTATGGAGGGGATAGCTCCAGGGCAGAGGAAGCC
ATATATGTTGGGAGTACTGGGCTTGGGGGAGGGCCTGGGGACCCACTGCTTCCCTTGGGAGCTCCCAATC
TGATTGTGGAAGCTGACTTGAAAAGCAGGACTTCAGACTTGGCAGTGCAAAGTTTAGTGACAATATTAGC
CACAACTAAAATGTTCTCCTTCAAGCCAAGTTACTCAAAGCATTGTGTGTAAGTTCAGTCATCCATCCCT
TCTAGTCAGCTGTTGTCCTCATCTGACCCATAAGGACAGAGAGTCAGAGAAGCTATGCTACTTGCTTAAA
ACCACACAGCAAGGAAGAGGCAGAGGCATAGCATAGGACTTGCTGTGCTCATCAGGTTGGGCTGAAACTG
CCTCCACTGCTCCAGGGCTGAGATGTGGGACCATAAGAGTGAGTCACCAAACCCGCATAGAGGGCTGTGC
AGGACTGCAGTCTGGTCCTTGAAGATACTCAGTGGGTTCTGGGGTCTGAGGCTAGAACTGGGAGCTCCAC
AGGAGTGTGACAAGGGCTAGGAACAGAACCTAAGGCTATGAAAGCCTGGGAGGTGCTGGGGCCAGAACCC
AGGGTCCCTTGTGAGCTGAGATGTGGCACCACTAAGCCGCACCCCGGCCTCACTGCTTGATTGTGAAATG
AAATGCTCTCTCTGGGTACATATCCTGCTTGGCTTCTGCTTCCCTTCTGCTGTGGCATGTTCCTTCAGCA
ACATGCTGGCCTTTATGAGTTCTGGCTCTAATTCTTCCTGGGACTGTCTGGTTCCTCCATGTTGAATGTC

TTGGGGATGCCACGATTCACCTTCCCTTCCTCTCCTTTGCTCCTAGCTCCAGTATGGGGGCCGGATCTGT
GTGGGCCTCAGGCCTCCTGCTGCTGTGGCTGCTTCTCCTAGTGGCTGGGGATCAGGGTGAGTGGGAAGTC
ATCTCAGTTGACATCATAGTGGGTCAGCGGGACGGGGCAAGACTTTTCATGCTAGAACCTTTTTCTGCTG
CTTCTCTAGCTGGGTCTACAATATAAAACAAGAATAGCTGAAACCAGTCTTTGAACAATCGAAAGAGAAC
AAGATACCTGAGAGGTTATTTTTAGTTCTAACCAGCAGTGGAGTTTCCCACCTCTCACTGTCTTCTGCTG
AACTGATCTGAAAAAAAAAAAAAAAGGGTGGGCGACAGAGACAATAACACAGGGGTTGATTGCTGATGTC
TGCCATGGGCAGGACAAGGGAAAGAAGATCTTTGTGTCTCTCCTGGAGTCTCCCCAGTGGTGGTCAGGAG
TCAGACTTTATGAATTCCTTACTGAGTTTCTCTGTGGCTGTACGCAAGAATATTTGTTCTTCTGATCTTC
AGTTTCCCCAATGTCCTACAAGAGGACATTTCCATTGCAGATGATTACAGAAGCTCAGTGGCTTTATTGC
CCTCACAGGACATAGTGGCAAATGCCTGTAATCCCAGCCCTTGGGCAGTAGACCAGGAGCATTATAAGTG
CAAGGTCATCCTTGGCTATAAAGTTGGAGGCCCACCTGTGCTACACAAGACCCTGACTTTAAACAGAAGA
AAGAAAGGGGGAAAAAAAACCTCACAAAGTTGGTTTCCGGTGTCTGCAAATACCCCACAATCACTGCTTC
CAGTGTTTGCCTCTTGACTTAACTTTTGAGGCTCAGAGAAGGAAAGTGAGTTGCTCAGGGCCACACGGCA
AGCCCGTGATGACATCATAGTTCACCCATATATGAAGCCTTTGGAATTTACTACCATATGAAGGAGAACC
ATGAATGGTCCCTTTGCACAGTGACATTGTGTGGGCAGTCTGGCCTCTCTGGCCTTGATCTCTCTAAAGA
GGTGTTAATGAAGCTGAGTGTAGTGGCCCAGGCCTTGAATTCCAGCACTGGGGAGGCAGAGGCAGGAGGA
TCTCTGTGAGTCCGAGGCCAGCCTGGTCTATATATGAGTTTTGTTATCTGAGTTCCAGGACATCCAGGAC
TATATAGTAAGACACTGTCTCAAAAGGGGAAACAAAGTATTAAGGAAAGAAAAAGAAGAAGAAGAAGAAA
CTCACTAAAGCAAGAAATGTTAGTGCCCACCCCTACCTCTGACTCAGGTCCTCTCTCTCCACCCCAGACA
CACAGGACACCACCGCCACGGAAAAGGGGCTTCGCATGCTGAAGTCAGGGTCAGGACCCGTCCGTGCTGC
CCTGGCAGAGCTAGTGGCCCTGCCCTGCTTCTTTACCCTGCAACCACGGCTAAGCTCCCTGCGAGACATT
CCTCGGATCAAGTGGACTAAGGTTCAGACTGCATCAGGCCAGCGACAGGATTTGCCAATCTTGGTGGCCA
AAGACAACGTGGTGCGTGTGGCCAAGGGCTGGCAGGGACGGGTGTCATTGCCTGCTTATCCCCGGCACAG
AGCCAATGCTACCCTTCTGCTGGGGCCACTTCGAGCAAGCGACTCTGGGCTGTATCGCTGCCAAGTGGTA
AAGGGTATCGAAGATGAGCAGGACCTGGTAACCCTGGAAGTGACAGGTGAGTTGGGGGCAGGTAATGGAC
GTGGTCAGATATGAAAGGGGAGGGACCTAGAATGAAGGGGGAAGGGTTGAGGCTGAGAGAAAGGGCCCAA
GAATCGGGAAATTCTAAGAAAGAAAGAACGCTGGAAAAAGAGGATCTGAGGATGGAGAGGAAGGTGCCTA
GGATTGGAGAGGAATCAGGGATGAAGGGCGAGAGACCAAAGTAAAGGAAGAGGAACCGAGAGGATGGATG
GGAGGGGCAAGTGTAGAGGAATGAAAGAAACCGCAGACAGTCAAAGACAGTAGGGGAGGGCTAAGAAAAA
GGGGTGAAGCCAAGGTGGAAGGGGAAGGATTAGACAAGGGGAAGAGTTACAATGGGAAAGGAGGGACCAA
GATGTAAGGGGAGGGGCTAAATCAGGACAGGATGGAGTAAACCCGAGGCCACTGGAGTTCAACTTAGAAG
TCGATCTGTGTAGGGCTCCTCTCAGGTTTTCTGATGCTCTGTATCCAGGCTCAGCCCTCTCTCAGGCTTC
TTTTTAGCAGAGAGGCACCAGCAGTGATGCAGAACTCAGCTCATCTGGATGCAACCCCTTTTTAAGACCC
TTTACCCTCACTTAATTTACTTAAGACAAAATTATTAGCTGTCCATCAAAATAGGAATATGTCCATGTAG
TGGTGCACCCACCCTCTACATTCTAGAATCTGAGGCAGGAGAATCACTAAAAATTCAAGGCCAGCCTGGA
CTAGGAGACACAGTGACGCTAGCCCATTAGCTCTGCCAACTCTGACCTCATCATGCATCACACACATATA
CACAGAGACACATACACTCACACACACATGCACAGCACACAGGTGCACAAAATGAGAAATCAGGGCAGGA
GACAGATGGCTCAGAGGGTAAGAGCACTTGCTGCTCTTCAGAGGGCTTGAGTTCAGTCCCCACATGGTAC
CTCACAACCACATAATTCCATTGTAGAGTACCTAGAACCTTCCTCTGGCCTCTTTGTGCACTAGACACCA
GCATACAATCATATATATATATATATATATATAATAAAGGAAGTAAATAGCCAAGTGGTAATGGCACACA
CCTTTAATCCCAGCACTTGGGATGCAGAGGCAGAAGGATCTCTGTGAGTTCAAGGTCAGCCTGGTCTACA
GAGAGTTCCATGACAACCAGGAATAAACAGAAAATCCTGTCAAGAGACCAGGGCAGGGTTGGGGGGGTGT
GGGGAAACGACAAATCTTTTAAGAGCACAAATCTCTTTAAAAGGCTAAAGTGAGCCTATCTTTAAAATGT
CAGTTAACACATTCCTTCAGGAGACACAGAGTGTGCTTCCCAGATTTTCTGCTAAATTCCACTGCAGTTT
CTGTTTTCCCAACAGTAAAAACCAAGCTGGGTGGAGCAGGGGCTATGAACTCGAGAAGCAGCAGCAGATT
TTGCTGTGTGAGTGTGGGGCCAGCCTGGGCTACATATTGAGACCCTGTCTCAAAAACAGCAACACAGCCT
GGCAGTGGTGGCACTTTAATCCCAGAGGCAGGTGGATCTCTGTGCCTCAGAGGCTACAGGTCTACAGAGC
AAGCCAGGGCTACACAGAGTAAGCCTGACTGAAAAGATCAACTAACCAACCAAAACCAGACATGAGATAA
GGGCTGTGAAGGCAGAAGGAATGAGTTCACAGTCATTCTTCACTAAATGTGTACACACATTCACAGCACA
CAGGTACACAAAATGCAGTAAGTCAGGGCTGGAGAGAGTTGGAGTTGGAAGCCAGCCTAGGGTACATGAG
ACACTTTTTTTTTCTTTCTTTGTGTGTGTTTCATTGTTGTTTTTTGTTTTGAGAAATCTTTGTTCTGTGTA
ACCCTGGCTGGCCAGAAACTCACTCTGTAGTCCAGGCTGGCCTCGGACTCAGAAATTCGCTTGCCTCCGC
CTCCCAAATGCTGGGATTAAAGCCATGCGCCACCACTGCCCTGCGAGTGTTAGGATTAAAGAAATACACC
ACCACACCATATGAGACTCTGTCTTTAGGAAATATGCTCCAAGAAGGTCCTTTCCCTAAGATTCCACAAA
ACCCCTCTCCGGCCTCGTGGCTGTTACCCCACAGGCGTCGTGTTCCATTATCGGGCGGCCCGGGACCGCT
ATGCGCTGACCTTCGCTGAGGCCCAGGAGGCTTGTCGCCTAAGCTCTGCTACCATCGCTGCCCCACGGCA
CCTGCAGGCTGCCTTTGAAGATGGCTTTGACAACTGCGACGCGGGCTGGCTCTCAGACCGCACGGTTCGG
TGAGGGGGTGCGCGGGAGGCATGGAACTGGGGGGTCGCTCCTGGAGAAAGAGGCTCCAAGAACACACGGC
AATAGCCACTCCCCTCGTACTGTTAGGTACCCGATCACTCAGTCGCGTCCTGGTTGCTATGGTGACCGCA
GCAGTCTCCCGGGTGTTCGGAGCTACGGGAGACGCGACCCGCAGGAACTCTACGATGTCTACTGCTTTGC
CCGCGAGCTAGGGGGTAAGGCAAGGCGGGTCTGGGACCCTGTCGTCACCTGTCCGTGAGTGTAAGGTACT
GTCCCAGGTCCCGTATTTCCTACGCCCCATGAATCTCTCCGAATTCTTTGTGCCCTCCAAAGCTGCACGT
GGGATCTGACCACCTCTCCTTGAAAGTGTCAGGTGTTTTTCCAGCCCTCAAGTTCTGCTAAGTCTCCTCA

Tenascin-R
Forward primer: CAACAGCCTTGGGGATACTC
Reverse primer (reverse complement): ATGCTGCCATACGGAATCTC

CACAGGTCAATGTGCCTCTGTTATGATGTGCCCTCTTCACTTCCCGTCACAACAATCCTTCTTCTCTCCA
GCTATATGAAAAATTTCCCTAAGATAAGGCCCTTGTGTGATAACACAGAGCTGTACAACTGGTTAATCAA
ATTAATTGGACCGATTCATGAGCTAATATGTGTTAAACCACTTTATGGTGAGCTACATTCTGACAGAGCA
AATGTGGTTATGACTGCAGGAAAACTGGCACAATCTAGCTCAAATTCAATATGACCCTTTCTTAGTCCAC
CGCTTAAACCATGCTTTAAAAACTGGTTAAACAGAGAAGAGCACCATGCTAGACTCACAGTGCCCAATGC
ATTGGTTCTAACCTTCTAGATGAACTCGCCCTGTATTTGGTTGATGGCTCCAAAAGGAAATTGCCTTACA
GTACTGTAACTGCCTGGTGCCACAGGGAAGAACTCCTTGACAGCAGAGTCTCCGTCTAGTTTCACATGTC
TAACGGGCTTCACCAGTGACCACAAAAGGAAATCATCTCATGCACCCACATTCTTATAGGCCTTATGTAG
TATACGCTGAATGAAAGTCTAGAAGGATGTGCAGCAGTTGTGCAGATTGAAGATAACATTGCTCAGGGAA
GAGGAAGTGAGAGAGCCAAGTCATAGAGAAGGAAGGAGACTGCCCTGAAAATTACTTGATGTATATTCTG
TTACAGGCTGTATATGGATACACAAATAAACTAGGTGTGTGTGGGGGGGGGGGTGGTCATGGTGGTTGTA
TGCTTAGTCAAAGCAAGCTGAATAGGATTTTAGAATGGCTACTAACAAAACCACTCTGTATACCTGTGGT
ATCTGTGTAATTAGATTTAAATGAACAAGAAGGAGGGAAGGTATACATTGCTGGTACTAGGAGACACTTC
AGCTGGGCACTGCCCCCAACAGATACTGGAAAAGGTGGCCCAAGAATCCCCTTCAGCCATAGAAACTTTT
TTTTTTTGCCCAAAGTTGTGCCCACCTACTCACTGGTGGCAGCTCACATGCAAAGAACTGATCCAACGGT
CTGGGCTTCTTCCCAAAGTAAGGAGGCACCAGAGGACCCGGTCATTTCTGTGTCCTCTGTCCCAGCTCAA
TCTGAAAACAGAGTGGGAGAATAGAGTCCACTCTATTAAAGAACCACACGGTGAGAAATGCCAAGATTTC
CCATGTGTGTCTTTATAATGACTCCCTTATACATGCTCATCACTTTATAATTTAAGAATATCAAGTGGAG
AAATTTGAAACATGATAAACATGTTAGTTGAGTGAAATATGACCGTCCCTATATTTTGTTAGAGAGGCGA
GTAATGACAGGCACGCTGCAGGTATTTGGAGTTAAGTGAACTGAACAGAAGAGGATTTCACCAACACATT
CAGTAACATTAACATAGTTGGTTCAAAAAAGATTAGTCCAGCTCTCCCAGAGTGAAGTGACCACACACCT
AGAGGACAGGACAATGGGTGGACAAAATAGGAGAGGGATTTTTAATTCCATGGAAAGAGAGATTGCTTAG
TGTTAGAGCTATCTGTTCGATGAGAAAAGGGAAAATTCTGTATAGATCCAGATTTACTCTCAAATCACCT
GCAGTGCTTCCTTTTGGTGAGCAGGTAGATTCTAATTGGAAGAGGAAAATACCCACCATGTATACAATCT
GTAACCTCTGTCCCCACTACCGGCAAACCCACTTCTAATGATATAGCCCCACAGTGCCTGTAGCCCCACT
CTCCAGGCTGACCCTTCTAAGACCAGACTATCTTTACACTTCCTACCCCTGGGGTTCCAGGAAGGCCTCC
TGGGAAGGAGTATTCATCCAAGGACAATTTAAATAAGATGCCTAGGTCTTAGCAGAACACTTGCTGCTTC
CTTCTTTAGATTGCAACCAATTTTTGCAAATGCATTCTCTTTAGGCATCTACAAATGAGATCCCTAAGGC
TTAGTGTCCCTTTTGGAGAAGGCTTAGTCGCATTTGTGAGCGGGAAGTCCTTGAAGGCTTAATTATCAAG
CCACCAACTGCATTGACAGATCCGTAGAAACTGTGTAGGGGGAGCCCCGTCCAAGCTCTGCACAGTGCCC
CTGATTAAAAAGGGTGACAATACCCTTATACGGAAGCTTCCACTTGCAGTAAATAGCCATGCTTTAGGGT
GACGGTGTGTCTAGCCAGACAGGATTCTTCTGCATCCATGTGTTTGTTATTTATTGAGCTTTCTTGTGTT
AGTATTATGCTTGGACAGGATCCAATAAAGTAGGAGGAGGACAAAGATTCTGACCTTGAGGACAGTCCAG
AAGGTCCTTGAGGATCTGCAGTGATAAGTTGAACAGACAAAGAGACTGATAAACTTTCATCATGAAGGAG
TGTTCAACGTGCTGAAGGCATTAAGGGGGTAAAGGGGACTCCCTTTTGTGGAAGGTGTTGGATGGCAGGC
TTCTTGGAGGAAGTGGCAAACATTTGCTGCTATCAGATCAAGTATTTACACCACCACTTTTAAAGTTGCT
GAACTTGTGATATAAAATATATTTCTGGATTTATAATGATTCTGCAGTTTTGCCTCATATATTTGTCATT
TTTTTCCAAAAGCTTGAGAAACATAAGAAAAAGAATTAATAAAATATATAAATGAAACTCTGGAGAGAAA
CCAATCACTTAATAAGCAGTAATTTCCTTTCTTGTAGAGAGCTATGTGGTCTGCCTCTAAATTCACTTAA
AAGGAAAGAATAGGGAAACTGAGGTTCTCCTCTTAAAGCTACATGTTCATTCCTGTTGCAGGTGTCTGCA
TCAACTCATTGCTCAGAGGTCAGATCTCATCTGGAGTTAGAGTCACAGAGCACGTGGTCAAGAGAAACCA
TCAGAGAGGACGACATCACGAGGTACTGTGTGCTGTGGACCTTTTCCTATCCATCATGCCAATGGCCAGT
TTAAGGCTTTCAGTAGGAATTGCGTATTCCCCGGGACCCGAGACCTTTTGTCACTGAAACAACAGCCTTG
GGGATACTCTCCATGAAATGAGTTGGCCAACAGCGTCAGCTCCTCTGGGCTTCACATGGTCCCTGAAATC
ACTCAAGAAACCAGGTACTAAGATTTTGGCTACTCATAAAATTGTTCTGAAATGCATTTCATGATGTAGT
TGGTAATAAAAATGTCTTAGTGAGCTCAGTCCCTCTAAAAGGCTAGACTTGATTCTCAGCCCAGTGTGCC
TGTACCAGGCCTGCATGAATCAATGCTAAATTATTCACCAGCCTGACTCTAAAAATTCCAGAGTTCCAAA
ACCCCTAATAAAGTATTATGAAAAAATATCCATCTCTTTATCTCTATCCATAACTATTTATATGGCTGGA
AGAAAACCTGTCGTTTTATTTCTTTTAATTTAAAAGCTTTCCTAATTCCTTTTTCCTACCACATATATAT
GTCTGAAAAAATTTGGGTTTGAAATAATAACCTCTAAAAAATGGTCCACAGGAAAGGCTCTGAGGATTCT
GAGTTGACAGGCACAATGAATATTTTGCTCCCTCAATAACTTGCATGGGCAATCAAACCTTATTCACCAA
ATGGAGAAGTTTTCAAACAGGTGTGTCTGTTTTGTTTTTCATTTCTTGCCTTTTTTTTATTGTGAAAAGC
AATGATTATATTATATCTTCCAACCTTCTCTCGCTATTTATTTACACAGTTCGAAAGTTTATTGAGGAAA
AACTCATTTTCTTCCTGTGCCCCATTGTGTACTTGCCATGTATTTGATGTCCCTCCCAGCACTCTACAGA
CACAATACCTGTCTCCTCTGAAGCTCCACACTGGAATCCACCCATAATGTCCTCAGCAGCATCCTGCCTC
AGTTGAGGACACTTAACCATAAAGTATCCCTTGGCCATTTTCTTTCTTAGTTCTTTAAAGCCTCAAGAAA
CGTTATCATATTTAAGCAGGGTTCCAGCCATTCATATTTCAGGGTGGGTTGGTGAATCTGATGGTTCAAG
GCTACCAGCTGAGTGAGATAGATATGCCTGCAACCACATAAAGCTGGAACAGGTTGGACCAGCTAGGCAG
TAGTGGGAGCTACCTGTCACAAAAGTGTCCTGTATTTAGATAGACTTACTTACCTGAACTCTACTCTGAG

GGGTGTGACAACAAGGATGAGCGAGGGAATACCTGGCGGAAGGTACTTAAACAAGCAAGATGAGTCTGGC
TCCCACAGCCCTTACTAGCATGGATGCTGTGGTGCTAAAATTGCAAACACAGCTACCAGTTTTGAGAGTC
TGCAAATCAGGCACTCAGAAAGTAAGAGCGATGAGCCTTTCTATTTTAATATCAGGAAAACACAAGAACA
TGAACTTCTCTATATAGAAAAACAACACAGATTGCCAACATCAATTCTAAAATGCCTTGAAAAGGCTAGG
ATGCTAACATCAGCCAGCAAGATGCTTTAAGCCTCTCTTTCTCTCAAAGTATATTCCTCTGCCTCCACAT
AGCACAGTGGCAGGATGTAAGAAAGTGGCATGATATATTATTTAGACATGAAGCAAGACTTCTACATTCT
GTTCCTCTCCCTGAATGAGTTAAAAAAGAAGATGGGTACAGTTTGTGAGTATGGGGATTGATGTTATTGT
CTGTTCAAAATGTCTGATGTAGGCTCCTGCTCACTGCATCACCCACGATGCCATGATTTATTACCACACT
GTCTCCAGGTGCAGTCCAGCTAGTCTCCCCTGTGATGATCATGCAGAATGTGAGAAGGGGTGTCCACTGG
TAGACTATTTCCAATGAACTCTTGAATCATCCAGACAGAGAGGCAGATGATGAGCTGACACCCGGTAGAG
ATTGTCTGGTTGCTTGAGTATCCCCATGTGGAATAGAGTGGGGGGATATGGAAGTTTGAGAAATCTCAAT
GAGAAAGTGATTGTTGGACATTTGCCTTCACAGCAGCCATTGATAGTTTGTTCCCAATACAAGTCTCCGC
ACCATCTATCACTTTTGTCCTAAGGACACCTTCATTCTTTCATTCAATAAACATCCAATGAACCCTTGCC
AGGAGCTAGGCACCATGCAGCCATGAGATGACGATCACAGGACTCTTTGCCTTTAAGGAACCTAGAAATC
TCTTCCAACTTTGCCTGTTCTGTGAGATGCCATCCTTCTTTCTCTGGGTTCCCAGAGCTCTTTGCCCTGA
CTAACTCATGACATATCTGCCTCTCTTCTGCACTGGTCTGTGAAGTCCTGAGACAAGGAAGAGAAATTCA
TCTCTTCATCCTTACCCGGAGAGGTGTGTTCACCTTGCAGGCACTGGAGGGGTCTGGAAGTCTCCCAGGA
TGGAGAGGCAGTGATGAGAGTGAATACCCAATCTTCACACATGTATGTCAAAGCTAGCATGTGAGCTAAT
AGCAGACTAAGGACCATGAAGGATGTTTCCCTGGAGTACCACATTTGCACATTTCTCTTATTTTTAACTC
CTCTAAAATATGAGATTTGAACTCATCCTAAGGAAGAGCCACATCCTCATAGTCAACCCACATGTTTCCT
AATGCTGAAATATTTTAGGCATCGAGAACAGCATGTTCAACATTCTCCCAGCAATCTCTCCTTGGAAAGA
GTCTAGATTATGCTTTCTGGTATCATTTAGGCTTTGTCCAGGCTCCACTAGAATGCTTGGGTTTCAACAG
TCCGAACAGAGGGCATGTGGTACACTTGGCGTGTATCTTAACATAGACCAGCACAGTCTGTATGTGAGGA
CCTGGGAGACTTTTTAGCATTCAGCACATAGCCAGACATATAAAAAGGAAACTGATAAACAGGCATCCAG
GAGCCTGGTGTCAGGTATCTGCTTGTTCTACAGTCTGTCCAAACCCACCAGTCAGGCATTGACCAGTGTA
GTGGATCCTCCAAAGACATGACCTCCCTAGCAGACAGCAGTTTCTCTGGCCAGAAAGCCCTACCATGTAT
CACCCCTAGAGCAAATGCAAAAATCAATGCTTTCCTCTCAGGGCTGACCTTTCCTGGCCACTCAGCCACC
ACAGAGTTATATCATCGGTGTCAGGCTCTGCCCAGGGGCCGGTGCTGGGTGGGGACTGTTAATCAGCTCC
TACCCCAGATTAACATTCAGACAGAGAGCTCAGTAATGAATAGTTTAATATAATGTTGACTGTTTACCCA
CATGAATGGAAAGAACTTACATCTGCCAGAGCCACCTGTGCCCACAGAACTATAGCTCAGACAGCCATGT
CCCCCAAGAGCCCAGCTGTGTAGAGGAGAGAGGGGGTAGGTTGGAGAAAAGAGCAGGGGAGACAGGATAG
TCTGGGTGGCTGTGGCCAGCAGTTGACCAGACAGCTGGGAAGGGGACACACACACATAACCAGTAGGCAG
AAGACAGAAGCAGGGGGCGGGGGGGGGGGGGGTGGGTGGAGGTCAGCTGCCAATGGAAAGCAGGTTGGAG
GCAGACGTCTAAGAAAAGGAGCGTAGTAACTTCTGAGTCGAGAGGATTTCTGTGGCTGGCATCAAATGGA
GGAAGAGAGCAGGACATGTCTGACTCAGGCACACAGATCCTCCTCGCTGAGGAGTGGGCGTCTTGCTCAA
GTTGGCACAGCTATTTGTGGCCATGCTGCCATACGGAATCTCTGGAAAACAGCTAAGGTTCTCACCTCGT
TGCCCAGGCGCTGGCTCTGCTGGGAGCTGGAGCAGCTGTCGCAGGAATAGAGAAAAGCTGACTCTGGACA
TCCGCGGGCGCTGGGAGGGATCATCCAGAGTGTTGGGTTAGAATGTTCTGTGTTTGGGAAGGATCTTGAA
GGGGCTGCCCTGACCGGAAAGAGAGACATTACTATTTTCATCAAGGCTATTAAAGGATGGGTGGATGGCT

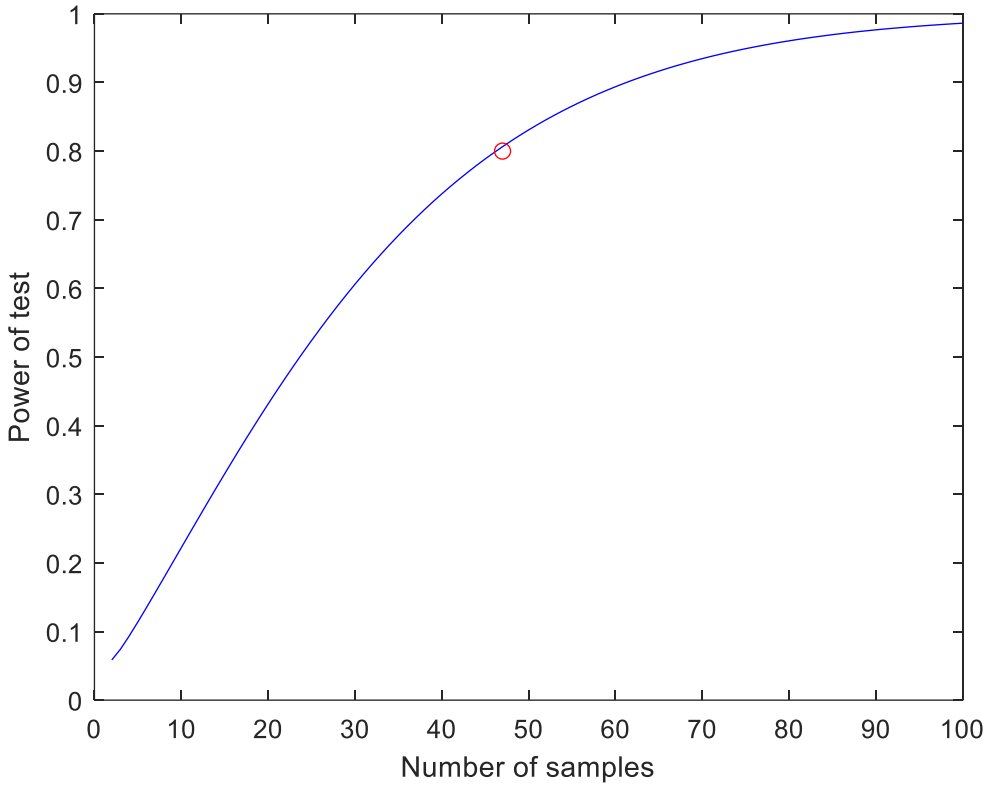

Figure 7.1 Example power analysis. An example power analysis to calculate the number of mice required to achieve 80% power in the elevated plus maze behavioural experiments where two groups were compared using a t-test. Power analysis suggests between 40-50 mice per group would be required to achieve 80% power; specifically, the power analysis shown here is for the 'time in open arms' metric where ChABC was administered prior to stress exposure (Figure 4.9), and suggests 47 mice per group would be required to achieve 80% power.

Bibliography

Adami, Mariane B., Lucas Barretto-de-Souza, Josiane O. Duarte, Jeferson Almeida, and Carlos C. Crestani. 'Both N-Methyl-D-Aspartate and Non-N-Methyl-D-Aspartate Glutamate Receptors in the Bed Nucleus of the Stria Terminalis Modulate the Cardiovascular Responses to Acute Restraint Stress in Rats'. *Journal of Psychopharmacology (Oxford, England)* 31, no. 6 (June 2017): 674–81. https://doi.org/10.1177/0269881117691468.

Adams, I., K. Brauer, C. Arélin, W. Härtig, A. Fine, M. Mäder, T. Arendt, and G. Brückner. 'Perineuronal Nets in the Rhesus Monkey and Human Basal Forebrain Including Basal Ganglia'. *Neuroscience* 108, no. 2 (2001): 285–98. https://doi.org/10.1016/s0306-4522(01)00419-5.

Adhikari, Avishek, Mihir A. Topiwala, and Joshua A. Gordon. 'Synchronized Activity between the Ventral Hippocampus and the Medial Prefrontal Cortex during Anxiety'. *Neuron* 65, no. 2 (28 January 2010): 257–69. https://doi.org/10.1016/j.neuron.2009.12.002.

Alaiyed, Seham, P. Lorenzo Bozzelli, Adam Caccavano, Jian Young Wu, and Katherine Conant. 'Venlafaxine Stimulates PNN Proteolysis and MMP-9-Dependent Enhancement of Gamma Power; Relevance to Antidepressant Efficacy'. *Journal of Neurochemistry* 148, no. 6 (March 2019): 810–21. https://doi.org/10.1111/jnc.14671.

Alheid, G. F., and L. Heimer. 'New Perspectives in Basal Forebrain Organization of Special Relevance for Neuropsychiatric Disorders: The Striatopallidal, Amygdaloid, and Corticopetal Components of Substantia Innominata'. *Neuroscience* 27, no. 1 (1 October 1988): 1–39. https://doi.org/10.1016/0306-4522(88)90217-5.

Allen, Bridget, Esther Ingram, Masaki Takao, Michael J. Smith, Ross Jakes, Kanwar Virdee, Hirotaka Yoshida, et al. 'Abundant Tau Filaments and Nonapoptotic Neurodegeneration in Transgenic Mice Expressing Human P301S Tau Protein'. *Journal of Neuroscience* 22, no. 21 (1 November 2002): 9340–51. https://doi.org/10.1523/JNEUROSCI.22-21-09340.2002.

Allen, Y. S., T. E. Adrian, J. M. Allen, K. Tatemoto, T. J. Crow, S. R. Bloom, and J. M. Polak. 'Neuropeptide Y Distribution in the Rat Brain'. *Science (New York, N.Y.)* 221, no. 4613 (26 August 1983): 877–79. https://doi.org/10.1126/science.6136091.

Alpár, Alán, Ulrich Gärtner, Wolfgang Härtig, and Gert Brückner. 'Distribution of Pyramidal Cells Associated with Perineuronal Nets in the Neocortex of Rat'. *Brain Research* 1120, no. 1 (20 November 2006): 13–22. https://doi.org/10.1016/j.brainres.2006.08.069.

Am, Magariños, and McEwen Bs. 'Stress-Induced Atrophy of Apical Dendrites of Hippocampal CA3c Neurons: Involvement of Glucocorticoid Secretion and

Excitatory Amino Acid Receptors'. *Neuroscience* 69, no. 1 (November 1995). https://doi.org/10.1016/0306-4522(95)00259-l.

American Psychiatric Association. *Diagnostic and Statistical Manual of Mental Disorders: DSM-5*. 5th ed. Washington, DC: American Psychiatric Associations, 2013.

Anlar, Banu, and Ayşen Gunel-Ozcan. 'Tenascin-R: Role in the Central Nervous System'. *The International Journal of Biochemistry & Cell Biology* 44, no. 9 (1 September 2012): 1385–89. https://doi.org/10.1016/j.biocel.2012.05.009.

Anson, L. C., P. E. Chen, D. J. Wyllie, D. Colquhoun, and R. Schoepfer. 'Identification of Amino Acid Residues of the NR2A Subunit That Control Glutamate Potency in Recombinant NR1/NR2A NMDA Receptors'. *The Journal of Neuroscience: The Official Journal of the Society for Neuroscience* 18, no. 2 (15 January 1998): 581–89.

Anson, L. C., R. Schoepfer, D. Colquhoun, and D. J. Wyllie. 'Single-Channel Analysis of an NMDA Receptor Possessing a Mutation in the Region of the Glutamate Binding Site'. *The Journal of Physiology* 527 Pt 2 (1 September 2000): 225–37. https://doi.org/10.1111/j.1469-7793.2000.00225.x.

Arnett, Melinda G., Lisa M. Muglia, Gloria Laryea, and Louis J. Muglia. 'Genetic Approaches to Hypothalamic-Pituitary-Adrenal Axis Regulation'. *Neuropsychopharmacology* 41, no. 1 (January 2016): 245–60. https://doi.org/10.1038/npp.2015.215.

Asher, Richard, and Amico Bignami. 'Localization of Hyaluronate in Primary Glial Cell Cultures Derived from Newborn Rat Brain'. *Experimental Cell Research* 195, no. 2 (1 August 1991): 401–11. https://doi.org/10.1016/0014-4827(91)90390-G.

Attwood, Benjamin K., Julie-Myrtille Bourgognon, Satyam Patel, Mariusz Mucha, Emanuele Schiavon, Anna E. Skrzypiec, Kenneth W. Young, et al. 'Neuropsin Cleaves EphB2 in the Amygdala to Control Anxiety'. *Nature* 473, no. 7347 (19 May 2011): 372–75. https://doi.org/10.1038/nature09938.

Avery, S. N., J. A. Clauss, and J. U. Blackford. 'The Human BNST: Functional Role in Anxiety and Addiction'. *Neuropsychopharmacology* 41, no. 1 (January 2016): 126–41. https://doi.org/10.1038/npp.2015.185.

Avery, Suzanne N., Jacqueline A. Clauss, Danny G. Winder, Neil Woodward, Stephan Heckers, and Jennifer Urbano Blackford. 'BNST Neurocircuitry in Humans'. *NeuroImage* 91 (1 May 2014): 311–23. https://doi.org/10.1016/j.neuroimage.2014.01.017.

Baig, Shabnam, Gordon K. Wilcock, and Seth Love. 'Loss of Perineuronal Net N-Acetylgalactosamine in Alzheimer's Disease'. *Acta Neuropathologica* 110, no. 4 (October 2005): 393–401. https://doi.org/10.1007/s00401-005-1060-2.

Baker, Kathryn D., Arielle R. Gray, and Rick Richardson. 'The Development of Perineuronal Nets around Parvalbumin Gabaergic Neurons in the Medial Prefrontal Cortex and Basolateral Amygdala of Rats'. *Behavioral Neuroscience* 131, no. 4 (August 2017): 289–303. https://doi.org/10.1037/bne0000203.

Ballachey, E. l. *A Study Of The Rats Behavior In A Field*, 1932. http://archive.org/details/in.ernet.dli.2015.214234.

Balmer, Timothy S. 'Perineuronal Nets Enhance the Excitability of Fast-Spiking Neurons'. *ENeuro* 3, no. 4 (August 2016): ENEURO.0112-16.2016. https://doi.org/10.1523/ENEURO.0112-16.2016.

Balmer, Timothy S., Vanessa M. Carels, Jillian L. Frisch, and Teresa A. Nick. 'Modulation of Perineuronal Nets and Parvalbumin with Developmental Song Learning'. *The Journal of Neuroscience: The Official Journal of the Society for Neuroscience* 29, no. 41 (14 October 2009): 12878–85. https://doi.org/10.1523/JNEUROSCI.2974-09.2009.

Bandelow, Borwin, David Baldwin, Marianna Abelli, Carlo Altamura, Bernardo Dell'Osso, Katharina Domschke, Naomi A. Fineberg, et al. 'Biological Markers for Anxiety Disorders, OCD and PTSD – a Consensus Statement. Part I: Neuroimaging and Genetics'. *The World Journal of Biological Psychiatry* 17, no. 5 (3 July 2016): 321–65. https://doi.org/10.1080/15622975.2016.1181783.

Banerjee, Sunayana B., Vanessa A. Gutzeit, Justin Baman, Hadj S. Aoued, Nandini K. Doshi, Robert C. Liu, and Kerry J. Ressler. 'Perineuronal Nets in the Adult Sensory Cortex Are Necessary for Fear Learning'. *Neuron* 95, no. 1 (5 July 2017): 169-179.e3. https://doi.org/10.1016/j.neuron.2017.06.007.

Barbayannis, Georgia, Daly Franco, Solange Wong, Josselyn Galdamez, Russell D. Romeo, and Elizabeth P. Bauer. 'Differential Effects of Stress on Fear Learning and Activation of the Amygdala in Pre-Adolescent and Adult Male Rats'. *Neuroscience* 360 (30 September 2017): 210–19. https://doi.org/10.1016/j.neuroscience.2017.07.058.

Baroncelli, Laura, Manuela Scali, Gabriele Sansevero, Francesco Olimpico, Ilaria Manno, Mario Costa, and Alessandro Sale. 'Experience Affects Critical Period Plasticity in the Visual Cortex through an Epigenetic Regulation of Histone Post-Translational Modifications'. *The Journal of Neuroscience: The Official Journal of the Society for Neuroscience* 36, no. 12 (23 March 2016): 3430–40. https://doi.org/10.1523/JNEUROSCI.1787-15.2016.

Bartoletti, Alessandro, Paolo Medini, Nicoletta Berardi, and Lamberto Maffei. 'Environmental Enrichment Prevents Effects of Dark-Rearing in the Rat Visual Cortex'. *Nature Neuroscience* 7, no. 3 (March 2004): 215–16. https://doi.org/10.1038/nn1201.

Baxter, A. J., K. M. Scott, T. Vos, and H. A. Whiteford. 'Global Prevalence of Anxiety Disorders: A Systematic Review and Meta-Regression'. *Psychological*

Medicine 43, no. 5 (May 2013): 897–910. https://doi.org/10.1017/S003329171200147X.

Baxter, Amanda J., Theo Vos, Kate M. Scott, Rosana E. Norman, Abraham D. Flaxman, Jed Blore, and Harvey A. Whiteford. 'The Regional Distribution of Anxiety Disorders: Implications for the Global Burden of Disease Study, 2010'. *International Journal of Methods in Psychiatric Research* 23, no. 4 (December 2014): 422–38. https://doi.org/10.1002/mpr.1444.

Bekku, Yoko, Wei-Dong Su, Satoshi Hirakawa, Reinhard Fässler, Aiji Ohtsuka, Jeong Suk Kang, Jennifer Sanders, Takuro Murakami, Yoshifumi Ninomiya, and Toshitaka Oohashi. 'Molecular Cloning of Bral2, a Novel Brain-Specific Link Protein, and Immunohistochemical Colocalization with Brevican in Perineuronal Nets'. *Molecular and Cellular Neurosciences* 24, no. 1 (September 2003): 148–59. https://doi.org/10.1016/s1044-7431(03)00133-7.

Belle, Mino D. C., Beatriz Baño-Otalora, and Hugh D. Piggins. 'Perforated Multi-Electrode Array Recording in Hypothalamic Brain Slices'. *Methods in Molecular Biology (Clifton, N.J.)* 2130 (2021): 263–85. https://doi.org/10.1007/978-1-0716-0381-9_20.

Biedermann, Sarah V., Daniel G. Biedermann, Frederike Wenzlaff, Tim Kurjak, Sawis Nouri, Matthias K. Auer, Klaus Wiedemann, et al. 'An Elevated Plus-Maze in Mixed Reality for Studying Human Anxiety-Related Behavior'. *BMC Biology* 15, no. 1 (21 December 2017): 125. https://doi.org/10.1186/s12915-017-0463-6.

Binette, F., J. Cravens, B. Kahoussi, D. R. Haudenschild, and P. F. Goetinck. 'Link Protein Is Ubiquitously Expressed in Non-Cartilaginous Tissues Where It Enhances and Stabilizes the Interaction of Proteoglycans with Hyaluronic Acid.' *Journal of Biological Chemistry* 269, no. 29 (22 July 1994): 19116–22. https://doi.org/10.1016/S0021-9258(17)32282-2.

Bjerke, Ingvild E., Sharon C. Yates, Arthur Laja, Menno P. Witter, Maja A. Puchades, Jan G. Bjaalie, and Trygve B. Leergaard. 'Densities and Numbers of Calbindin and Parvalbumin Positive Neurons across the Rat and Mouse Brain'. *IScience* 24, no. 1 (22 January 2021): 101906. https://doi.org/10.1016/j.isci.2020.101906.

Bjorni, Max, Natalie G. Rovero, Elissa R. Yang, Andrew Holmes, and Lindsay R. Halladay. 'Phasic Signaling in the Bed Nucleus of the Stria Terminalis during Fear Learning Predicts Within- and across-Session Cued Fear Expression'. *Learning & Memory (Cold Spring Harbor, N.Y.)* 27, no. 3 (March 2020): 83–90. https://doi.org/10.1101/lm.050807.119.

Blanchard, Robert J., Errol B. Yudko, R. John Rodgers, and D. Caroline Blanchard. 'Defense System Psychopharmacology: An Ethological Approach to the Pharmacology of Fear and Anxiety'. *Behavioural Brain Research* 58, no. 1–2 (1993): 155–65. https://doi.org/10.1016/0166-4328(93)90100-5.

Bliss, T. V. P., and G. L. Collingridge. ‘A Synaptic Model of Memory: Long-Term Potentiation in the Hippocampus’. *Nature* 361, no. 6407 (January 1993): 31–39. https://doi.org/10.1038/361031a0.

Blosa, M., C. Bursch, S. Weigel, M. Holzer, C. Jäger, C. Janke, R. T. Matthews, T. Arendt, and M. Morawski. ‘Reorganization of Synaptic Connections and Perineuronal Nets in the Deep Cerebellar Nuclei of Purkinje Cell Degeneration Mutant Mice’. *Neural Plasticity* 2016 (2016): 2828536. https://doi.org/10.1155/2016/2828536.

Blosa, M., M. Sonntag, G. Brückner, C. Jäger, G. Seeger, R. T. Matthews, R. Rübsamen, T. Arendt, and M. Morawski. ‘Unique Features of Extracellular Matrix in the Mouse Medial Nucleus of Trapezoid Body--Implications for Physiological Functions’. *Neuroscience* 228 (3 January 2013): 215–34. https://doi.org/10.1016/j.neuroscience.2012.10.003.

Bosiacki, Mateusz, Magdalena Gąssowska-Dobrowolska, Klaudyna Kojder, Marta Fabiańska, Dariusz Jeżewski, Izabela Gutowska, and Anna Lubkowska. ‘Perineuronal Nets and Their Role in Synaptic Homeostasis’. *International Journal of Molecular Sciences* 20, no. 17 (22 August 2019): E4108. https://doi.org/10.3390/ijms20174108.

Bota, Mihail, Olaf Sporns, and Larry W. Swanson. ‘Neuroinformatics Analysis of Molecular Expression Patterns and Neuron Populations in Gray Matter Regions: The Rat BST as a Rich Exemplar’. *Brain Research* 1450 (23 April 2012): 174–93. https://doi.org/10.1016/j.brainres.2012.02.034.

Bourin, Michel, and Martine Hascoët. ‘The Mouse Light/Dark Box Test’. *European Journal of Pharmacology* 463, no. 1–3 (28 February 2003): 55–65. https://doi.org/10.1016/s0014-2999(03)01274-3.

Bouton, M. E. ‘Context, Time, and Memory Retrieval in the Interference Paradigms of Pavlovian Learning’. *Psychological Bulletin* 114, no. 1 (July 1993): 80–99. https://doi.org/10.1037/0033-2909.114.1.80.

Bouton, Mark E., R. Frederick Westbrook, Kevin A. Corcoran, and Stephen Maren. ‘Contextual and Temporal Modulation of Extinction: Behavioral and Biological Mechanisms’. *Biological Psychiatry* 60, no. 4 (15 August 2006): 352–60. https://doi.org/10.1016/j.biopsych.2005.12.015.

Brakebusch, Cord, Constanze I. Seidenbecher, Fredrik Asztely, Uwe Rauch, Henry Matthies, Hannelore Meyer, Manfred Krug, et al. ‘Brevican-Deficient Mice Display Impaired Hippocampal CA1 Long-Term Potentiation but Show No Obvious Deficits in Learning and Memory’. *Molecular and Cellular Biology* 22, no. 21 (November 2002): 7417–27. https://doi.org/10.1128/MCB.22.21.7417-7427.2002.

Brauer, K., L. Werner, and L. Leibnitz. ‘Perineuronal Nets of Glia’. *Journal Fur Hirnforschung* 23, no. 6 (1 January 1982): 701–8.

Brown, Gillian R., and Christopher Nemes. ‘The Exploratory Behaviour of Rats in the Hole-Board Apparatus: Is Head-Dipping a Valid Measure of Neophilia?’ *Behavioural Processes* 78, no. 3 (July 2008): 442–48. https://doi.org/10.1016/j.beproc.2008.02.019.

Brown, M. W., F. A. Wilson, and I. P. Riches. ‘Neuronal Evidence That Inferomedial Temporal Cortex Is More Important than Hippocampus in Certain Processes Underlying Recognition Memory’. *Brain Research* 409, no. 1 (14 April 1987): 158–62. https://doi.org/10.1016/0006-8993(87)90753-0.

Brückner, G., K. Brauer, W. Härtig, J. R. Wolff, M. J. Rickmann, A. Derouiche, B. Delpech, N. Girard, W. H. Oertel, and A. Reichenbach. ‘Perineuronal Nets Provide a Polyanionic, Glia-Associated Form of Microenvironment around Certain Neurons in Many Parts of the Rat Brain’. *Glia* 8, no. 3 (July 1993): 183–200. https://doi.org/10.1002/glia.440080306.

Brückner, G., and J. Grosche. ‘Perineuronal Nets Show Intrinsic Patterns of Extracellular Matrix Differentiation in Organotypic Slice Cultures’. *Experimental Brain Research* 137, no. 1 (March 2001): 83–93. https://doi.org/10.1007/s002210000617.

Brückner, G., J. Grosche, S. Schmidt, W. Härtig, R. U. Margolis, B. Delpech, C. I. Seidenbecher, R. Czaniera, and M. Schachner. ‘Postnatal Development of Perineuronal Nets in Wild-Type Mice and in a Mutant Deficient in Tenascin-R’. *The Journal of Comparative Neurology* 428, no. 4 (25 December 2000): 616–29. https://doi.org/10.1002/1096-9861(20001225)428:4<616::aid-cne3>3.0.co;2-k.

Brückner, G., D. Hausen, W. Härtig, M. Drlicek, T. Arendt, and K. Brauer. ‘Cortical Areas Abundant in Extracellular Matrix Chondroitin Sulphate Proteoglycans Are Less Affected by Cytoskeletal Changes in Alzheimer’s Disease’. *Neuroscience* 92, no. 3 (1999): 791–805. https://doi.org/10.1016/s0306-4522(99)00071-8.

Brückner, Gert, Johannes Kacza, and Jens Grosche. ‘Perineuronal Nets Characterized by Vital Labelling, Confocal and Electron Microscopy in Organotypic Slice Cultures of Rat Parietal Cortex and Hippocampus’. *Journal of Molecular Histology* 35, no. 2 (1 February 2004): 115–22. https://doi.org/10.1023/B:HIJO.0000023374.22298.50.

Bukalo, O., M. Schachner, and A. Dityatev. ‘Modification of Extracellular Matrix by Enzymatic Removal of Chondroitin Sulfate and by Lack of Tenascin-R Differentially Affects Several Forms of Synaptic Plasticity in the Hippocampus’. *Neuroscience* 104, no. 2 (2001): 359–69. https://doi.org/10.1016/s0306-4522(01)00082-3.

Busnardo, Cristiane, Fernando H. F. Alves, Carlos C. Crestani, América A. Scopinho, Leonardo B. M. Resstel, and Fernando M. A. Correa. ‘Paraventricular Nucleus of the Hypothalamus Glutamate Neurotransmission Modulates

Autonomic, Neuroendocrine and Behavioral Responses to Acute Restraint Stress in Rats'. *European Neuropsychopharmacology: The Journal of the European College of Neuropsychopharmacology* 23, no. 11 (November 2013): 1611–22. https://doi.org/10.1016/j.euroneuro.2012.11.002.

Bystritsky, A. 'Treatment-Resistant Anxiety Disorders'. *Molecular Psychiatry* 11, no. 9 (September 2006): 805–14. https://doi.org/10.1038/sj.mp.4001852.

Cabungcal, Jan-Harry, Pascal Steullet, Hirofumi Morishita, Rudolf Kraftsik, Michel Cuenod, Takao K. Hensch, and Kim Q. Do. 'Perineuronal Nets Protect Fast-Spiking Interneurons against Oxidative Stress'. *Proceedings of the National Academy of Sciences* 110, no. 22 (28 May 2013): 9130–35. https://doi.org/10.1073/pnas.1300454110.

Calabrese, Francesca, Gianluigi Guidotti, Raffaella Molteni, Giorgio Racagni, Michele Mancini, and Marco Andrea Riva. 'Stress-Induced Changes of Hippocampal NMDA Receptors: Modulation by Duloxetine Treatment'. *PloS One* 7, no. 5 (2012): e37916. https://doi.org/10.1371/journal.pone.0037916.

Calhoon, Gwendolyn G., and Kay M. Tye. 'Resolving the Neural Circuits of Anxiety'. *Nature Neuroscience* 18, no. 10 (October 2015): 1394–1404. https://doi.org/10.1038/nn.4101.

Camenisch, T. D., A. P. Spicer, T. Brehm-Gibson, J. Biesterfeldt, M. L. Augustine, A. Calabro, S. Kubalak, S. E. Klewer, and J. A. McDonald. 'Disruption of Hyaluronan Synthase-2 Abrogates Normal Cardiac Morphogenesis and Hyaluronan-Mediated Transformation of Epithelium to Mesenchyme'. *The Journal of Clinical Investigation* 106, no. 3 (August 2000): 349–60. https://doi.org/10.1172/JCI10272.

Cardenas, C. G., L. P. Mar, A. V. Vysokanov, P. B. Arnold, L. M. Cardenas, D. J. Surmeier, and R. S. Scroggs. 'Serotonergic Modulation of Hyperpolarization-Activated Current in Acutely Isolated Rat Dorsal Root Ganglion Neurons'. *The Journal of Physiology* 518 (Pt 2) (15 July 1999): 507–23. https://doi.org/10.1111/j.1469-7793.1999.0507p.x.

Cargill, Robert, Steven G. Kohama, Jaime Struve, Weiping Su, Fatima Banine, Ellen Witkowski, Stephen A. Back, and Larry S. Sherman. 'Astrocytes in Aged Non-Human Primate Brain Gray Matter Synthesize Excess Hyaluronan'. *Neurobiology of Aging* 33, no. 4 (April 2012): 830.e13-830.e24. https://doi.org/10.1016/j.neurobiolaging.2011.07.006.

Carstens, Kelly E., Mary L. Phillips, Lucas Pozzo-Miller, Richard J. Weinberg, and Serena M. Dudek. 'Perineuronal Nets Suppress Plasticity of Excitatory Synapses on CA2 Pyramidal Neurons'. *The Journal of Neuroscience: The Official Journal of the Society for Neuroscience* 36, no. 23 (8 June 2016): 6312–20. https://doi.org/10.1523/JNEUROSCI.0245-16.2016.

Carulli, Daniela, Tommaso Pizzorusso, Jessica C. F. Kwok, Elena Putignano, Andrea Poli, Serhiy Forostyak, Melissa R. Andrews, Sathyaseelan S. Deepa,

Tibor T. Glant, and James W. Fawcett. ‘Animals Lacking Link Protein Have Attenuated Perineuronal Nets and Persistent Plasticity’. *Brain: A Journal of Neurology* 133, no. Pt 8 (August 2010): 2331–47. https://doi.org/10.1093/brain/awq145.

Carulli, Daniela, Kate E. Rhodes, David J. Brown, Timothy P. Bonnert, Scott J. Pollack, Kevin Oliver, Piergiorgio Strata, and James W. Fawcett. ‘Composition of Perineuronal Nets in the Adult Rat Cerebellum and the Cellular Origin of Their Components’. *The Journal of Comparative Neurology* 494, no. 4 (1 February 2006): 559–77. https://doi.org/10.1002/cne.20822.

Carulli, Daniela, Kate E. Rhodes, and James W. Fawcett. ‘Upregulation of Aggrecan, Link Protein 1, and Hyaluronan Synthases during Formation of Perineuronal Nets in the Rat Cerebellum’. *The Journal of Comparative Neurology* 501, no. 1 (1 March 2007): 83–94. https://doi.org/10.1002/cne.21231.

Carulli, Daniela, and Joost Verhaagen. ‘An Extracellular Perspective on CNS Maturation: Perineuronal Nets and the Control of Plasticity’. *International Journal of Molecular Sciences* 22, no. 5 (28 February 2021): 2434. https://doi.org/10.3390/ijms22052434.

Casada, J. H., and N. Dafny. ‘Restraint and Stimulation of Bed Nucleus of the Stria Terminalis Produce Similar Stress-like Behaviors’. *Brain Research Bulletin* 27, no. 2 (August 1991): 207–12. https://doi.org/10.1016/0361-9230(91)90069-v.

Cecchi, M., H. Khoshbouei, M. Javors, and D. A. Morilak. ‘Modulatory Effects of Norepinephrine in the Lateral Bed Nucleus of the Stria Terminalis on Behavioral and Neuroendocrine Responses to Acute Stress’. *Neuroscience* 112, no. 1 (2002): 13–21. https://doi.org/10.1016/s0306-4522(02)00062-3.

Celio, M. R., R. Spreafico, S. De Biasi, and L. Vitellaro-Zuccarello. ‘Perineuronal Nets: Past and Present’. *Trends in Neurosciences* 21, no. 12 (December 1998): 510–15. https://doi.org/10.1016/s0166-2236(98)01298-3.

Cheah, Menghon, Melissa R. Andrews, Daniel J. Chew, Elizabeth B. Moloney, Joost Verhaagen, Reinhard Fässler, and James W. Fawcett. ‘Expression of an Activated Integrin Promotes Long-Distance Sensory Axon Regeneration in the Spinal Cord’. *Journal of Neuroscience* 36, no. 27 (6 July 2016): 7283–97. https://doi.org/10.1523/JNEUROSCI.0901-16.2016.

Chen, Na, Die Hu, Lin Lu, and Jie Shi. ‘PS197. Low Level of Perineuronal Nets in the Medial Prefrontal Cortex Predicts Vulnerability to Stress’. *International Journal of Neuropsychopharmacology* 19, no. Suppl 1 (27 May 2016): 72. https://doi.org/10.1093/ijnp/pyw043.197.

Chiba, Kazuhiro, Yukihiro Matsuyama, Takayuki Seo, and Yoshiaki Toyama. ‘Condoliase for the Treatment of Lumbar Disc Herniation: A Randomized Controlled Trial’. *Spine* 43, no. 15 (1 August 2018): E869. https://doi.org/10.1097/BRS.0000000000002528.

Chiba, Shuichi, Tadahiro Numakawa, Midori Ninomiya, Misty C. Richards, Chisato Wakabayashi, and Hiroshi Kunugi. ‘Chronic Restraint Stress Causes Anxiety- and Depression-like Behaviors, Downregulates Glucocorticoid Receptor Expression, and Attenuates Glutamate Release Induced by Brain-Derived Neurotrophic Factor in the Prefrontal Cortex’. *Progress in Neuro-Psychopharmacology & Biological Psychiatry* 39, no. 1 (1 October 2012): 112–19. https://doi.org/10.1016/j.pnpbp.2012.05.018.

Choi, D. W., J. Y. Koh, and S. Peters. ‘Pharmacology of Glutamate Neurotoxicity in Cortical Cell Culture: Attenuation by NMDA Antagonists’. *The Journal of Neuroscience: The Official Journal of the Society for Neuroscience* 8, no. 1 (January 1988): 185–96.

Choi, Dennis C., Amy R. Furay, Nathan K. Evanson, Michelle M. Ostrander, Yvonne M. Ulrich-Lai, and James P. Herman. ‘Bed Nucleus of the Stria Terminalis Subregions Differentially Regulate Hypothalamic–Pituitary–Adrenal Axis Activity: Implications for the Integration of Limbic Inputs’. *The Journal of Neuroscience* 27, no. 8 (21 February 2007): 2025–34. https://doi.org/10.1523/JNEUROSCI.4301-06.2007.

Choi, Dennis C., Mary M. N. Nguyen, Kellie L. K. Tamashiro, Li Yun Ma, Randall R. Sakai, and James P. Herman. ‘Chronic Social Stress in the Visible Burrow System Modulates Stress-Related Gene Expression in the Bed Nucleus of the Stria Terminalis’. *Physiology & Behavior* 89, no. 3 (30 October 2006): 301–10. https://doi.org/10.1016/j.physbeh.2006.05.046.

Chrousos, G. P., and P. W. Gold. ‘The Concepts of Stress and Stress System Disorders. Overview of Physical and Behavioral Homeostasis’. *JAMA* 267, no. 9 (4 March 1992): 1244–52.

Chu, Philip, Reena Abraham, Kumarie Budhu, Usma Khan, Natalia De Marco Garcia, and Joshua C. Brumberg. ‘The Impact of Perineuronal Net Digestion Using Chondroitinase ABC on the Intrinsic Physiology of Cortical Neurons’. *Neuroscience* 388 (15 September 2018): 23–35. https://doi.org/10.1016/j.neuroscience.2018.07.004.

Chung, Leeyup. ‘A Brief Introduction to the Transduction of Neural Activity into Fos Signal’. *Development & Reproduction* 19, no. 2 (June 2015): 61–67. https://doi.org/10.12717/DR.2015.19.2.061.

Chung, Wilson C. J., Geert J. De Vries, and Dick F. Swaab. ‘Sexual Differentiation of the Bed Nucleus of the Stria Terminalis in Humans May Extend into Adulthood’. *The Journal of Neuroscience: The Official Journal of the Society for Neuroscience* 22, no. 3 (1 February 2002): 1027–33.

Ciccarelli, Alessandro, Dilys Weijers, William Kwan, Claire Warner, James Bourne, and Cornelius T. Gross. ‘Sexually Dimorphic Perineuronal Nets in the Rodent and Primate Reproductive Circuit’. *The Journal of Comparative*

Neurology 529, no. 13 (September 2021): 3274–91. https://doi.org/10.1002/cne.25167.

Citri, Ami, and Robert C. Malenka. 'Synaptic Plasticity: Multiple Forms, Functions, and Mechanisms'. *Neuropsychopharmacology* 33, no. 1 (January 2008): 18–41. https://doi.org/10.1038/sj.npp.1301559.

Clauss, Jacqueline. 'Extending the Neurocircuitry of Behavioural Inhibition: A Role for the Bed Nucleus of the Stria Terminalis in Risk for Anxiety Disorders'. *General Psychiatry* 32, no. 6 (2019): e100137. https://doi.org/10.1136/gpsych-2019-100137.

Conrad, C. D., J. E. LeDoux, A. M. Magariños, and B. S. McEwen. 'Repeated Restraint Stress Facilitates Fear Conditioning Independently of Causing Hippocampal CA3 Dendritic Atrophy'. *Behavioral Neuroscience* 113, no. 5 (October 1999): 902–13. https://doi.org/10.1037//0735-7044.113.5.902.

Conrad, Kelly L., Katherine M. Louderback, Caitlin P. Gessner, and Danny G. Winder. 'Stress-Induced Alterations in Anxiety-like Behavior and Adaptations in Plasticity in the Bed Nucleus of the Stria Terminalis'. *Physiology & Behavior* 104, no. 2 (3 August 2011): 248–56. https://doi.org/10.1016/j.physbeh.2011.03.001.

Cook, Susan C., and Cara L. Wellman. 'Chronic Stress Alters Dendritic Morphology in Rat Medial Prefrontal Cortex'. *Journal of Neurobiology* 60, no. 2 (August 2004): 236–48. https://doi.org/10.1002/neu.20025.

Corcoran, Kevin A., and Gregory J. Quirk. 'Activity in Prelimbic Cortex Is Necessary for the Expression of Learned, But Not Innate, Fears'. *Journal of Neuroscience* 27, no. 4 (24 January 2007): 840–44. https://doi.org/10.1523/JNEUROSCI.5327-06.2007.

Corvetti, Luigi, and Ferdinando Rossi. 'Degradation of Chondroitin Sulfate Proteoglycans Induces Sprouting of Intact Purkinje Axons in the Cerebellum of the Adult Rat'. *Journal of Neuroscience* 25, no. 31 (3 August 2005): 7150–58. https://doi.org/10.1523/JNEUROSCI.0683-05.2005.

COVID-19 Mental Disorders Collaborators. 'Global Prevalence and Burden of Depressive and Anxiety Disorders in 204 Countries and Territories in 2020 Due to the COVID-19 Pandemic'. *Lancet (London, England)* 398, no. 10312 (6 November 2021): 1700–1712. https://doi.org/10.1016/S0140-6736(21)02143-7.

Crestani, Carlos C, Fernando HF Alves, Felipe V Gomes, Leonardo BM Resstel, Fernando MA Correa, and James P Herman. 'Mechanisms in the Bed Nucleus of the Stria Terminalis Involved in Control of Autonomic and Neuroendocrine Functions: A Review'. *Current Neuropharmacology* 11, no. 2 (March 2013): 141–59. https://doi.org/10.2174/1570159X11311020002.

Cruz, Joana, Piran C. L. White, Andrew Bell, and Peter A. Coventry. 'Effect of Extreme Weather Events on Mental Health: A Narrative Synthesis and Meta-

Analysis for the UK'. *International Journal of Environmental Research and Public Health* 17, no. 22 (November 2020): 8581. https://doi.org/10.3390/ijerph17228581.

Cullinan, W. E., J. P. Herman, and S. J. Watson. 'Ventral Subicular Interaction with the Hypothalamic Paraventricular Nucleus: Evidence for a Relay in the Bed Nucleus of the Stria Terminalis'. *The Journal of Comparative Neurology* 332, no. 1 (1 June 1993): 1–20. https://doi.org/10.1002/cne.903320102.

Dabrowska, J., D. Martinon, M. Moaddab, and D. G. Rainnie. 'Targeting Corticotropin-Releasing Factor Projections from the Oval Nucleus of the Bed Nucleus of the Stria Terminalis Using Cell-Type Specific Neuronal Tracing Studies in Mouse and Rat Brain'. *Journal of Neuroendocrinology* 28, no. 12 (December 2016). https://doi.org/10.1111/jne.12442.

Dabrowska, Joanna, Rimi Hazra, Jidong Guo, Sarah DeWitt, and Donald Rainnie. 'Central CRF Neurons Are Not Created Equal: Phenotypic Differences in CRF-Containing Neurons of the Rat Paraventricular Hypothalamus and the Bed Nucleus of the Stria Terminalis'. *Frontiers in Neuroscience* 7 (2013). https://www.frontiersin.org/articles/10.3389/fnins.2013.00156.

Daniel, Sarah E., Jidong Guo, and Donald G. Rainnie. 'A Comparative Analysis of the Physiological Properties of Neurons in the Anterolateral Bed Nucleus of the Stria Terminalis in the Mus Musculus, Rattus Norvegicus, and Macaca Mulatta'. *The Journal of Comparative Neurology* 525, no. 9 (15 June 2017): 2235–48. https://doi.org/10.1002/cne.24202.

Daniel, Sarah E., and Donald G. Rainnie. 'Stress Modulation of Opposing Circuits in the Bed Nucleus of the Stria Terminalis'. *Neuropsychopharmacology: Official Publication of the American College of Neuropsychopharmacology* 41, no. 1 (January 2016): 103–25. https://doi.org/10.1038/npp.2015.178.

Danober, L., T. Heinbockel, R. B. Driesang, and H. C. Pape. 'Synaptic Mechanisms of NMDA-Mediated Hyperpolarization in Lateral Amygdaloid Projection Neurons'. *Neuroreport* 11, no. 11 (3 August 2000): 2501–6. https://doi.org/10.1097/00001756-200008030-00031.

Davies, Stephen J. A., David R. Goucher, Catherine Doller, and Jerry Silver. 'Robust Regeneration of Adult Sensory Axons in Degenerating White Matter of the Adult Rat Spinal Cord'. *Journal of Neuroscience* 19, no. 14 (15 July 1999): 5810–22. https://doi.org/10.1523/JNEUROSCI.19-14-05810.1999.

Davis, M. 'The Role of the Amygdala in Fear and Anxiety'. *Annual Review of Neuroscience* 15, no. 1 (1992): 353–75. https://doi.org/10.1146/annurev.ne.15.030192.002033.

Davis, M., L. S. Schlesinger, and C. A. Sorenson. 'Temporal Specificity of Fear Conditioning: Effects of Different Conditioned Stimulus-Unconditioned Stimulus Intervals on the Fear-Potentiated Startle Effect'. *Journal of Experimental Psychology. Animal Behavior Processes* 15, no. 4 (October 1989): 295–310.

Davis, Michael, David L. Walker, Leigh Miles, and Christian Grillon. ‘Phasic vs Sustained Fear in Rats and Humans: Role of the Extended Amygdala in Fear vs Anxiety’. *Neuropsychopharmacology* 35, no. 1 (January 2010): 105–35. https://doi.org/10.1038/npp.2009.109.

Day, Michelle, David B. Carr, Sasha Ulrich, Ema Ilijic, Tatiana Tkatch, and D. James Surmeier. ‘Dendritic Excitability of Mouse Frontal Cortex Pyramidal Neurons Is Shaped by the Interaction among HCN, Kir2, and Kleak Channels’. *The Journal of Neuroscience: The Official Journal of the Society for Neuroscience* 25, no. 38 (21 September 2005): 8776–87. https://doi.org/10.1523/JNEUROSCI.2650-05.2005.

Deepa, Sarama Sathyaseelan, Daniela Carulli, Clare Galtrey, Kate Rhodes, Junko Fukuda, Tadahisa Mikami, Kazuyuki Sugahara, and James W. Fawcett. ‘Composition of Perineuronal Net Extracellular Matrix in Rat Brain: A Different Disaccharide Composition for the Net-Associated Proteoglycans’. *The Journal of Biological Chemistry* 281, no. 26 (30 June 2006): 17789–800. https://doi.org/10.1074/jbc.M600544200.

Delobel, Patrice, Isabelle Lavenir, Graham Fraser, Esther Ingram, Max Holzer, Bernardino Ghetti, Maria Grazia Spillantini, R. Anthony Crowther, and Michel Goedert. ‘Analysis of Tau Phosphorylation and Truncation in a Mouse Model of Human Tauopathy’. *The American Journal of Pathology* 172, no. 1 (January 2008): 123–31. https://doi.org/10.2353/ajpath.2008.070627.

Devienne, Gabrielle, Sandrine Picaud, Ivan Cohen, Juliette Piquet, Ludovic Tricoire, Damien Testa, Ariel A. Di Nardo, Jean Rossier, Bruno Cauli, and Bertrand Lambolez. ‘Regulation of Perineuronal Nets in the Adult Cortex by the Activity of the Cortical Network’. *The Journal of Neuroscience: The Official Journal of the Society for Neuroscience*, 27 May 2021, JN-RM-0434-21. https://doi.org/10.1523/JNEUROSCI.0434-21.2021.

Dick, Gunnar, Chin Lik Tan, Joao Nuno Alves, Erich M. E. Ehlert, Gregory M. Miller, Linda C. Hsieh-Wilson, Kazuyuki Sugahara, et al. ‘Semaphorin 3A Binds to the Perineuronal Nets via Chondroitin Sulfate Type E Motifs in Rodent Brains’. *The Journal of Biological Chemistry* 288, no. 38 (20 September 2013): 27384–95. https://doi.org/10.1074/jbc.M111.310029.

Dilger, Stefan, Thomas Straube, Hans-Joachim Mentzel, Clemens Fitzek, Jürgen R. Reichenbach, Holger Hecht, Silke Krieschel, Ingmar Gutberlet, and Wolfgang H. R. Miltner. ‘Brain Activation to Phobia-Related Pictures in Spider Phobic Humans: An Event-Related Functional Magnetic Resonance Imaging Study’. *Neuroscience Letters* 348, no. 1 (4 September 2003): 29–32. https://doi.org/10.1016/s0304-3940(03)00647-5.

Dityatev, Alexander, Gert Brückner, Galina Dityateva, Jens Grosche, Ralf Kleene, and Melitta Schachner. ‘Activity-Dependent Formation and Functions of Chondroitin Sulfate-Rich Extracellular Matrix of Perineuronal Nets’.

Developmental Neurobiology 67, no. 5 (April 2007): 570–88. https://doi.org/10.1002/dneu.20361.

Dityatev, Alexander, and Melitta Schachner. 'Extracellular Matrix Molecules and Synaptic Plasticity'. *Nature Reviews. Neuroscience* 4, no. 6 (June 2003): 456–68. https://doi.org/10.1038/nrn1115.

Djerbal, L., H. Lortat-Jacob, and JCF Kwok. 'Chondroitin Sulfates and Their Binding Molecules in the Central Nervous System'. *Glycoconjugate Journal* 34, no. 3 (1 June 2017): 363–76. https://doi.org/10.1007/s10719-017-9761-z.

Donegan, Jennifer J., and Daniel J. Lodge. 'Hippocampal Perineuronal Nets Are Required for the Sustained Antidepressant Effect of Ketamine'. *The International Journal of Neuropsychopharmacology* 20, no. 4 (1 April 2017): 354–58. https://doi.org/10.1093/ijnp/pyw095.

Dong, H. W., G. D. Petrovich, A. G. Watts, and L. W. Swanson. 'Basic Organization of Projections from the Oval and Fusiform Nuclei of the Bed Nuclei of the Stria Terminalis in Adult Rat Brain'. *The Journal of Comparative Neurology* 436, no. 4 (6 August 2001): 430–55. https://doi.org/10.1002/cne.1079.

Dong, Hong-Wei, and Larry W. Swanson. 'Organization of Axonal Projections from the Anterolateral Area of the Bed Nuclei of the Stria Terminalis'. *The Journal of Comparative Neurology* 468, no. 2 (6 January 2004): 277–98. https://doi.org/10.1002/cne.10949.

———. 'Projections from Bed Nuclei of the Stria Terminalis, Anteromedial Area: Cerebral Hemisphere Integration of Neuroendocrine, Autonomic, and Behavioral Aspects of Energy Balance'. *The Journal of Comparative Neurology* 494, no. 1 (1 January 2006): 142–78. https://doi.org/10.1002/cne.20788.

Dumont, É. C., B. K. Rycroft, J. Maiz, and J. T. Williams. 'MORPHINE PRODUCES CIRCUIT-SPECIFIC NEUROPLASTICITY IN THE BED NUCLEUS OF THE STRIA TERMINALIS'. *Neuroscience* 153, no. 1 (22 April 2008): 232–39. https://doi.org/10.1016/j.neuroscience.2008.01.039.

Dumont, Éric C. 'What Is the Bed Nucleus of the Stria Terminalis?' *Progress in Neuro-Psychopharmacology & Biological Psychiatry* 33, no. 8 (13 November 2009): 1289–90. https://doi.org/10.1016/j.pnpbp.2009.07.006.

Dunn, J. D. 'Plasma Corticosterone Responses to Electrical Stimulation of the Bed Nucleus of the Stria Terminalis'. *Brain Research* 407, no. 2 (31 March 1987): 327–31. https://doi.org/10.1016/0006-8993(87)91111-5.

———. 'Plasma Corticosterone Responses to Electrical Stimulation of the Bed Nucleus of the Stria Terminalis'. *Brain Research* 407, no. 2 (31 March 1987): 327–31. https://doi.org/10.1016/0006-8993(87)91111-5.

Durchdewald, Moritz, Peter Angel, and Jochen Hess. 'The Transcription Factor Fos: A Janus-Type Regulator in Health and Disease'. *Histology and*

Histopathology 24, no. 11 (November 2009): 1451–61. https://doi.org/10.14670/HH-24.1451.

Duvarci, Sevil, Elizabeth P. Bauer, and Denis Paré. 'The Bed Nucleus of the Stria Terminalis Mediates Inter-Individual Variations in Anxiety and Fear'. *Journal of Neuroscience* 29, no. 33 (19 August 2009): 10357–61. https://doi.org/10.1523/JNEUROSCI.2119-09.2009.

Fanselow, M. S. 'Contextual Fear, Gestalt Memories, and the Hippocampus'. *Behavioural Brain Research* 110, no. 1–2 (1 June 2000): 73–81. https://doi.org/10.1016/s0166-4328(99)00186-2.

Feldman, S., N. Conforti, and D. Saphier. 'The Preoptic Area and Bed Nucleus of the Stria Terminalis Are Involved in the Effects of the Amygdala on Adrenocortical Secretion'. *Neuroscience* 37, no. 3 (1990): 775–79. https://doi.org/10.1016/0306-4522(90)90107-f.

Feldman, Shaul, Nissim Conforti, and Joseph Weidenfeld. 'Limbic Pathways and Hypothalamic Neurotransmitters Mediating Adrenocortical Responses to Neural Stimuli'. *Neuroscience & Biobehavioral Reviews* 19, no. 2 (1 June 1995): 235–40. https://doi.org/10.1016/0149-7634(94)00062-6.

Felix-Ortiz, Ada C., Anna Beyeler, Changwoo Seo, Christopher A. Leppla, Craig P. Wildes, and Kay M. Tye. 'BLA to VHPC Inputs Modulate Anxiety-Related Behaviors'. *Neuron* 79, no. 4 (21 August 2013): 658–64. https://doi.org/10.1016/j.neuron.2013.06.016.

Fetterly, Tracy L., Aakash Basu, Brett P. Nabit, Elias Awad, Kellie M. Williford, Samuel W. Centanni, Robert T. Matthews, Yuval Silberman, and Danny G. Winder. 'A2A-Adrenergic Receptor Activation Decreases Parabrachial Nucleus Excitatory Drive onto BNST CRF Neurons and Reduces Their Activity In Vivo'. *The Journal of Neuroscience: The Official Journal of the Society for Neuroscience* 39, no. 3 (16 January 2019): 472–84. https://doi.org/10.1523/JNEUROSCI.1035-18.2018.

Fillmore, H. L., T. E. VanMeter, and W. C. Broaddus. 'Membrane-Type Matrix Metalloproteinases (MT-MMPs): Expression and Function during Glioma Invasion'. *Journal of Neuro-Oncology* 53, no. 2 (June 2001): 187–202. https://doi.org/10.1023/a:1012213604731.

Finlay-Jones, R., and G. W. Brown. 'Types of Stressful Life Event and the Onset of Anxiety and Depressive Disorders'. *Psychological Medicine* 11, no. 4 (November 1981): 803–15. https://doi.org/10.1017/s0033291700041301.

Flurkey, K, J. Currer, and D. Harrison. 'Mouse Models in Aging Research.' *Faculty Research 2000 - 2009*, 1 January 2007, 637–72.

Forray, María Inés, and Katia Gysling. 'Role of Noradrenergic Projections to the Bed Nucleus of the Stria Terminalis in the Regulation of the Hypothalamic-

Pituitary-Adrenal Axis'. *Brain Research. Brain Research Reviews* 47, no. 1–3 (December 2004): 145–60. https://doi.org/10.1016/j.brainresrev.2004.07.011.

Foscarin, Simona, Danilo Ponchione, Ermira Pajaj, Ketty Leto, Maciej Gawlak, Grzegorz M. Wilczynski, Ferdinando Rossi, and Daniela Carulli. 'Experience-Dependent Plasticity and Modulation of Growth Regulatory Molecules at Central Synapses'. *PloS One* 6, no. 1 (31 January 2011): e16666. https://doi.org/10.1371/journal.pone.0016666.

Fowke, Tania M., Rashika N. Karunasinghe, Ji-Zhong Bai, Shawn Jordan, Alistair J. Gunn, and Justin M. Dean. 'Hyaluronan Synthesis by Developing Cortical Neurons in Vitro'. *Scientific Reports* 7, no. 1 (13 March 2017): 44135. https://doi.org/10.1038/srep44135.

Franklin, K. B. J, and G Paxinos. *The Mouse Brain in Stereotaxic Coordinates*. 3rd ed. New York: Elsevier, 2007.

Fraser, J. R., T. C. Laurent, and U. B. Laurent. 'Hyaluronan: Its Nature, Distribution, Functions and Turnover'. *Journal of Internal Medicine* 242, no. 1 (July 1997): 27–33. https://doi.org/10.1046/j.1365-2796.1997.00170.x.

Frischknecht, Renato, and Eckart D. Gundelfinger. 'The Brain's Extracellular Matrix and Its Role in Synaptic Plasticity'. *Advances in Experimental Medicine and Biology* 970 (2012): 153–71. https://doi.org/10.1007/978-3-7091-0932-8_7.

Frischknecht, Renato, Martin Heine, David Perrais, Constanze I. Seidenbecher, Daniel Choquet, and Eckart D. Gundelfinger. 'Brain Extracellular Matrix Affects AMPA Receptor Lateral Mobility and Short-Term Synaptic Plasticity'. *Nature Neuroscience* 12, no. 7 (July 2009): 897–904. https://doi.org/10.1038/nn.2338.

Gafford, Georgette, Aaron M. Jasnow, and Kerry J. Ressler. 'Grin1 Receptor Deletion within CRF Neurons Enhances Fear Memory'. *PloS One* 9, no. 10 (2014): e111009. https://doi.org/10.1371/journal.pone.0111009.

Gafford, Georgette M., and Kerry J. Ressler. 'GABA and NMDA Receptors in CRF Neurons Have Opposing Effects in Fear Acquisition and Anxiety in Central Amygdala vs. Bed Nucleus of the Stria Terminalis'. *Hormones and Behavior* 76 (November 2015): 136–42. https://doi.org/10.1016/j.yhbeh.2015.04.001.

Galtrey, Clare M., and James W. Fawcett. 'The Role of Chondroitin Sulfate Proteoglycans in Regeneration and Plasticity in the Central Nervous System'. *Brain Research Reviews* 54, no. 1 (April 2007): 1–18. https://doi.org/10.1016/j.brainresrev.2006.09.006.

Galtrey, Clare M., Jessica C. F. Kwok, Daniela Carulli, Kate E. Rhodes, and James W. Fawcett. 'Distribution and Synthesis of Extracellular Matrix Proteoglycans, Hyaluronan, Link Proteins and Tenascin-R in the Rat Spinal Cord'. *The European Journal of Neuroscience* 27, no. 6 (March 2008): 1373–90. https://doi.org/10.1111/j.1460-9568.2008.06108.x.

Gameiro, Gustavo Hauber, Paula Hauber Gameiro, Annicele da Silva Andrade, Lígia Ferrinho Pereira, Mariana Trevisani Arthuri, Fernanda Klein Marcondes, and Maria Cecília Ferraz de Arruda Veiga. 'Nociception- and Anxiety-like Behavior in Rats Submitted to Different Periods of Restraint Stress'. *Physiology & Behavior* 87, no. 4 (15 April 2006): 643–49. https://doi.org/10.1016/j.physbeh.2005.12.007.

Garakani, Amir, James W. Murrough, Rafael C. Freire, Robyn P. Thom, Kaitlyn Larkin, Frank D. Buono, and Dan V. Iosifescu. 'Pharmacotherapy of Anxiety Disorders: Current and Emerging Treatment Options'. *Frontiers in Psychiatry* 11 (2020). https://www.frontiersin.org/articles/10.3389/fpsyt.2020.595584.

Garcia, Andrea Milena Becerra, Fernando Parra Cardenas, and Silvio Morato. 'Effect of Different Illumination Levels on Rat Behavior in the Elevated Plus-Maze'. *Physiology & Behavior* 85, no. 3 (30 June 2005): 265–70. https://doi.org/10.1016/j.physbeh.2005.04.007.

Georges, François, and Gary Aston-Jones. 'Activation of Ventral Tegmental Area Cells by the Bed Nucleus of the Stria Terminalis: A Novel Excitatory Amino Acid Input to Midbrain Dopamine Neurons'. *Journal of Neuroscience* 22, no. 12 (15 June 2002): 5173–87. https://doi.org/10.1523/JNEUROSCI.22-12-05173.2002.

Giamanco, K. A., and R. T. Matthews. 'Deconstructing the Perineuronal Net: Cellular Contributions and Molecular Composition of the Neuronal Extracellular Matrix'. *Neuroscience* 218 (30 August 2012): 367–84. https://doi.org/10.1016/j.neuroscience.2012.05.055.

Giamanco, K. A., M. Morawski, and R. T. Matthews. 'Perineuronal Net Formation and Structure in Aggrecan Knockout Mice'. *Neuroscience* 170, no. 4 (10 November 2010): 1314–27. https://doi.org/10.1016/j.neuroscience.2010.08.032.

Giardino, William J., Ada Eban-Rothschild, Daniel J. Christoffel, Shi-Bin Li, Robert C. Malenka, and Luis de Lecea. 'Parallel Circuits from the Bed Nuclei of Stria Terminalis to the Lateral Hypothalamus Drive Opposing Emotional States'. *Nature Neuroscience* 21, no. 8 (August 2018): 1084–95. https://doi.org/10.1038/s41593-018-0198-x.

Giger, R. J., R. J. Pasterkamp, S. Heijnen, A. J. Holtmaat, and J. Verhaagen. 'Anatomical Distribution of the Chemorepellent Semaphorin III/Collapsin-1 in the Adult Rat and Human Brain: Predominant Expression in Structures of the Olfactory-Hippocampal Pathway and the Motor System'. *Journal of Neuroscience Research* 52, no. 1 (1 April 1998): 27–42. https://doi.org/10.1002/(SICI)1097-4547(19980401)52:1<27::AID-JNR4>3.0.CO;2-M.

Gildawie, Kelsea R., Jennifer A. Honeycutt, and Heather C. Brenhouse. 'Region-Specific Effects of Maternal Separation on Perineuronal Net and

Parvalbumin-Expressing Interneuron Formation in Male and Female Rats'. *Neuroscience* 428 (21 January 2020): 23–37. https://doi.org/10.1016/j.neuroscience.2019.12.010.

Girotti, M., T. W. W. Pace, R. I. Gaylord, B. A. Rubin, J. P. Herman, and R. L. Spencer. 'Habituation to Repeated Restraint Stress Is Associated with Lack of Stress-Induced c-Fos Expression in Primary Sensory Processing Areas of the Rat Brain'. *Neuroscience* 138, no. 4 (2006): 1067–81. https://doi.org/10.1016/j.neuroscience.2005.12.002.

Glangetas, Christelle, and François Georges. 'Pharmacology of the Bed Nucleus of the Stria Terminalis'. *Current Pharmacology Reports* 2, no. 6 (1 December 2016): 262–70. https://doi.org/10.1007/s40495-016-0077-7.

Glangetas, Christelle, Delphine Girard, Laurent Groc, Giovanni Marsicano, Francis Chaouloff, and François Georges. 'Stress Switches Cannabinoid Type-1 (CB1) Receptor-Dependent Plasticity from LTD to LTP in the Bed Nucleus of the Stria Terminalis'. *Journal of Neuroscience* 33, no. 50 (11 December 2013): 19657–63. https://doi.org/10.1523/JNEUROSCI.3175-13.2013.

Glangetas, Christelle, Léma Massi, Giulia R. Fois, Marion Jalabert, Delphine Girard, Marco Diana, Keisuke Yonehara, et al. 'NMDA-Receptor-Dependent Plasticity in the Bed Nucleus of the Stria Terminalis Triggers Long-Term Anxiolysis'. *Nature Communications* 8, no. 1 (20 February 2017): 14456. https://doi.org/10.1038/ncomms14456.

'Global, Regional, and National Burden of 12 Mental Disorders in 204 Countries and Territories, 1990–2019: A Systematic Analysis for the Global Burden of Disease Study 2019'. *The Lancet Psychiatry* 9, no. 2 (1 February 2022): 137–50. https://doi.org/10.1016/S2215-0366(21)00395-3.

Gogolla, Nadine, Pico Caroni, Andreas Lüthi, and Cyril Herry. 'Perineuronal Nets Protect Fear Memories from Erasure'. *Science (New York, N.Y.)* 325, no. 5945 (4 September 2009): 1258–61. https://doi.org/10.1126/science.1174146.

Golgi, C. 'Intorno All'origine Del Quarto Nervo Cerebrale e Una Questione Istofisiologica Che a Questo Argomento Si Collega' 2 (1893): 378–89.

Gomez, D. M., and S. W. Newman. 'Differential Projections of the Anterior and Posterior Regions of the Medial Amygdaloid Nucleus in the Syrian Hamster'. *The Journal of Comparative Neurology* 317, no. 2 (8 March 1992): 195–218. https://doi.org/10.1002/cne.903170208.

Gordon, Joshua A., and Rene Hen. 'Genetic Approaches to the Study of Anxiety'. *Annual Review of Neuroscience* 27 (2004): 193–222. https://doi.org/10.1146/annurev.neuro.27.070203.144212.

Gos, Tomasz, Jay Schulkin, Anna Gos, Joerg Bock, Gerd Poeggel, and Katharina Braun. 'Paternal Deprivation Affects the Functional Maturation of Corticotropin-Releasing Hormone (CRH)- and Calbindin-D28k-Expressing

Neurons in the Bed Nucleus of the Stria Terminalis (BNST) of the Biparental Octodon Degus'. *Brain Structure & Function* 219, no. 6 (2014): 1983–90. https://doi.org/10.1007/s00429-013-0617-4.

Gray, T. S., R. A. Piechowski, J. M. Yracheta, P. A. Rittenhouse, C. L. Bethea, and L. D. Van de Kar. 'Ibotenic Acid Lesions in the Bed Nucleus of the Stria Terminalis Attenuate Conditioned Stress-Induced Increases in Prolactin, ACTH and Corticosterone'. *Neuroendocrinology* 57, no. 3 (March 1993): 517–24. https://doi.org/10.1159/000126400.

Greenberg, Gian D., Abigail Laman-Maharg, Katharine L. Campi, Heather Voigt, Veronica N. Orr, Leslie Schaal, and Brian C. Trainor. 'Sex Differences in Stress-Induced Social Withdrawal: Role of Brain Derived Neurotrophic Factor in the Bed Nucleus of the Stria Terminalis'. *Frontiers in Behavioral Neuroscience* 7 (9 January 2014): 223. https://doi.org/10.3389/fnbeh.2013.00223.

Griffiths, Sarah, Helen Scott, Colin Glover, Alison Bienemann, Mohamed T. Ghorbel, James Uney, Malcolm W. Brown, E. Clea Warburton, and Zafar I. Bashir. 'Expression of Long-Term Depression Underlies Visual Recognition Memory'. *Neuron* 58, no. 2 (24 April 2008): 186–94. https://doi.org/10.1016/j.neuron.2008.02.022.

Gross, Cornelius, Xiaoxi Zhuang, Kimberly Stark, Sylvie Ramboz, Ronald Oosting, Lynn Kirby, Luca Santarelli, Sheryl Beck, and René Hen. 'Serotonin1A Receptor Acts during Development to Establish Normal Anxiety-like Behaviour in the Adult'. *Nature* 416, no. 6879 (28 March 2002): 396–400. https://doi.org/10.1038/416396a.

Guadagno, Angela, Silvanna Verlezza, Hong Long, Tak Pan Wong, and Claire-Dominique Walker. 'It Is All in the Right Amygdala: Increased Synaptic Plasticity and Perineuronal Nets in Male, But Not Female, Juvenile Rat Pups after Exposure to Early-Life Stress'. *The Journal of Neuroscience: The Official Journal of the Society for Neuroscience* 40, no. 43 (21 October 2020): 8276–91. https://doi.org/10.1523/JNEUROSCI.1029-20.2020.

Guirado, Ramon, Marta Perez-Rando, David Sanchez-Matarredona, Eero Castrén, and Juan Nacher. 'Chronic Fluoxetine Treatment Alters the Structure, Connectivity and Plasticity of Cortical Interneurons'. *The International Journal of Neuropsychopharmacology* 17, no. 10 (October 2014): 1635–46. https://doi.org/10.1017/S1461145714000406.

Gungor, Nur Zeynep, and Denis Paré. 'Functional Heterogeneity in the Bed Nucleus of the Stria TerminalisFunctional Heterogeneity in the Bed Nucleus of the Stria Terminalis'. *Journal of Neuroscience* 36, no. 31 (3 August 2016): 8038–49. https://doi.org/10.1523/JNEUROSCI.0856-16.2016.

Hama, Hiroshi, Chikako Hara, Kazuhiko Yamaguchi, and Atsushi Miyawaki. 'PKC Signaling Mediates Global Enhancement of Excitatory Synaptogenesis in

Neurons Triggered by Local Contact with Astrocytes'. *Neuron* 41, no. 3 (5 February 2004): 405–15. https://doi.org/10.1016/s0896-6273(04)00007-8.

Hammack, Sayamwong E., Irakli Mania, and Donald G. Rainnie. 'Differential Expression of Intrinsic Membrane Currents in Defined Cell Types of the Anterolateral Bed Nucleus of the Stria Terminalis'. *Journal of Neurophysiology* 98, no. 2 (August 2007): 638–56. https://doi.org/10.1152/jn.00382.2007.

Hammack, Sayamwong E., Kristen J. Richey, Linda R. Watkins, and Steven F. Maier. 'Chemical Lesion of the Bed Nucleus of the Stria Terminalis Blocks the Behavioral Consequences of Uncontrollable Stress'. *Behavioral Neuroscience* 118, no. 2 (April 2004): 443–48. https://doi.org/10.1037/0735-7044.118.2.443.

Happel, Max F. K., and Renato Frischknecht. *Neuronal Plasticity in the Juvenile and Adult Brain Regulated by the Extracellular Matrix*. *Composition and Function of the Extracellular Matrix in the Human Body*. IntechOpen, 2016. https://doi.org/10.5772/62452.

Harbuz, Michael S., Anjo J. Chover-Gonzalez, and David S. Jessop. 'Hypothalamo-Pituitary-Adrenal Axis and Chronic Immune Activation'. *Annals of the New York Academy of Sciences* 992 (May 2003): 99–106. https://doi.org/10.1111/j.1749-6632.2003.tb03141.x.

Härtig, W., K. Brauer, V. Bigl, and G. Brückner. 'Chondroitin Sulfate Proteoglycan-Immunoreactivity of Lectin-Labeled Perineuronal Nets around Parvalbumin-Containing Neurons'. *Brain Research* 635, no. 1–2 (28 January 1994): 307–11. https://doi.org/10.1016/0006-8993(94)91452-4.

Härtig, W., K. Brauer, and G. Brückner. 'Wisteria Floribunda Agglutinin-Labelled Nets Surround Parvalbumin-Containing Neurons'. *Neuroreport* 3, no. 10 (October 1992): 869–72. https://doi.org/10.1097/00001756-199210000-00012.

Härtig, W., G. Brückner, K. Brauer, C. Schmidt, and V. Bigl. 'Allocation of Perineuronal Nets and Parvalbumin-, Calbindin-D28k- and Glutamic Acid Decarboxylase-Immunoreactivity in the Amygdala of the Rhesus Monkey'. *Brain Research* 698, no. 1–2 (6 November 1995): 265–69. https://doi.org/10.1016/0006-8993(95)01016-o.

Härtig, W., A. Derouiche, K. Welt, K. Brauer, J. Grosche, M. Mäder, A. Reichenbach, and G. Brückner. 'Cortical Neurons Immunoreactive for the Potassium Channel Kv3.1b Subunit Are Predominantly Surrounded by Perineuronal Nets Presumed as a Buffering System for Cations'. *Brain Research* 842, no. 1 (18 September 1999): 15–29. https://doi.org/10.1016/s0006-8993(99)01784-9.

Hausen, D., G. Brückner, M. Drlicek, W. Härtig, K. Brauer, and V. Bigl. 'Pyramidal Cells Ensheathed by Perineuronal Nets in Human Motor and Somatosensory Cortex'. *Neuroreport* 7, no. 11 (29 July 1996): 1725–29. https://doi.org/10.1097/00001756-199607290-00006.

Hayani, Hussam, Inseon Song, and Alexander Dityatev. ‘Increased Excitability and Reduced Excitatory Synaptic Input Into Fast-Spiking CA2 Interneurons After Enzymatic Attenuation of Extracellular Matrix’. *Frontiers in Cellular Neuroscience* 12 (2018): 149. https://doi.org/10.3389/fncel.2018.00149.

Hazra, Rimi, Ji-Dong Guo, Steven J. Ryan, Aaron M. Jasnow, Joanna Dabrowska, and Donald G. Rainnie. ‘A Transcriptomic Analysis of Type I-III Neurons in the Bed Nucleus of the Stria Terminalis’. *Molecular and Cellular Neurosciences* 46, no. 4 (April 2011): 699–709. https://doi.org/10.1016/j.mcn.2011.01.011.

Hebb, D. O. *The Organisation of Behaviour*. New York: Wiley, 1949.

Heine, Martin, Laurent Groc, Renato Frischknecht, Jean-Claude Béïque, Brahim Lounis, Gavin Rumbaugh, Richard L. Huganir, Laurent Cognet, and Daniel Choquet. ‘Surface Mobility of Postsynaptic AMPARs Tunes Synaptic Transmission’. *Science (New York, N.Y.)* 320, no. 5873 (11 April 2008): 201–5. https://doi.org/10.1126/science.1152089.

Herman, J. P., and W. E. Cullinan. ‘Neurocircuitry of Stress: Central Control of the Hypothalamo-Pituitary-Adrenocortical Axis’. *Trends in Neurosciences* 20, no. 2 (February 1997): 78–84. https://doi.org/10.1016/s0166-2236(96)10069-2.

Herman, J. P., W. E. Cullinan, and S. J. Watson. ‘Involvement of the Bed Nucleus of the Stria Terminalis in Tonic Regulation of Paraventricular Hypothalamic CRH and AVP MRNA Expression’. *Journal of Neuroendocrinology* 6, no. 4 (August 1994): 433–42. https://doi.org/10.1111/j.1365-2826.1994.tb00604.x.

Herman, James P., Helmer Figueiredo, Nancy K. Mueller, Yvonne Ulrich-Lai, Michelle M. Ostrander, Dennis C. Choi, and William E. Cullinan. ‘Central Mechanisms of Stress Integration: Hierarchical Circuitry Controlling Hypothalamo-Pituitary-Adrenocortical Responsiveness’. *Frontiers in Neuroendocrinology* 24, no. 3 (July 2003): 151–80. https://doi.org/10.1016/j.yfrne.2003.07.001.

Herman, James P., Michelle M. Ostrander, Nancy K. Mueller, and Helmer Figueiredo. ‘Limbic System Mechanisms of Stress Regulation: Hypothalamo-Pituitary-Adrenocortical Axis’. *Progress in Neuro-Psychopharmacology & Biological Psychiatry* 29, no. 8 (December 2005): 1201–13. https://doi.org/10.1016/j.pnpbp.2005.08.006.

Herrera, D. G., and H. A. Robertson. ‘Activation of C-Fos in the Brain’. *Progress in Neurobiology* 50, no. 2–3 (October 1996): 83–107. https://doi.org/10.1016/s0301-0082(96)00021-4.

Hines, M., F. C. Davis, A. Coquelin, R. W. Goy, and R. A. Gorski. ‘Sexually Dimorphic Regions in the Medial Preoptic Area and the Bed Nucleus of the Stria Terminalis of the Guinea Pig Brain: A Description and an Investigation of Their Relationship to Gonadal Steroids in Adulthood’. *The Journal of Neuroscience:*

The Official Journal of the Society for Neuroscience 5, no. 1 (January 1985): 40–47.

Hirakawa, S., T. Oohashi, W. D. Su, H. Yoshioka, T. Murakami, J. Arata, and Y. Ninomiya. 'The Brain Link Protein-1 (BRAL1): CDNA Cloning, Genomic Structure, and Characterization as a Novel Link Protein Expressed in Adult Brain'. *Biochemical and Biophysical Research Communications* 276, no. 3 (5 October 2000): 982–89. https://doi.org/10.1006/bbrc.2000.3583.

Hoehn, K., C. G. Craig, and T. D. White. 'A Comparison of N-Methyl-D-Aspartate-Evoked Release of Adenosine and [3H]Norepinephrine from Rat Cortical Slices'. *The Journal of Pharmacology and Experimental Therapeutics* 255, no. 1 (October 1990): 174–81.

Horii-Hayashi, Noriko, Takayo Sasagawa, Takashi Hashimoto, Takeshi Kaneko, Kosei Takeuchi, and Mayumi Nishi. 'A Newly Identified Mouse Hypothalamic Area Having Bidirectional Neural Connections with the Lateral Septum: The Perifornical Area of the Anterior Hypothalamus Rich in Chondroitin Sulfate Proteoglycans'. *The European Journal of Neuroscience* 42, no. 6 (September 2015): 2322–34. https://doi.org/10.1111/ejn.13024.

Horii-Hayashi, Noriko, Takayo Sasagawa, Wataru Matsunaga, and Mayumi Nishi. 'Development and Structural Variety of the Chondroitin Sulfate Proteoglycans-Contained Extracellular Matrix in the Mouse Brain'. *Neural Plasticity* 2015 (2015): 256389. https://doi.org/10.1155/2015/256389.

Hou, Guoqiang, and Zhong-Wei Zhang. 'NMDA Receptors Regulate the Development of Neuronal Intrinsic Excitability through Cell-Autonomous Mechanisms'. *Frontiers in Cellular Neuroscience* 11 (2017): 353. https://doi.org/10.3389/fncel.2017.00353.

Huntley, George W. 'Synaptic Circuit Remodelling by Matrix Metalloproteinases in Health and Disease'. *Nature Reviews Neuroscience* 13, no. 11 (November 2012): 743–57. https://doi.org/10.1038/nrn3320.

Hylin, Michael J., Sara A. Orsi, Anthony N. Moore, and Pramod K. Dash. 'Disruption of the Perineuronal Net in the Hippocampus or Medial Prefrontal Cortex Impairs Fear Conditioning'. *Learning & Memory* 20, no. 5 (May 2013): 267–73. https://doi.org/10.1101/lm.030197.112.

Inanobe, Atsushi, Akikazu Fujita, Minoru Ito, Hitonobu Tomoike, Kiyoshi Inageda, and Yoshihisa Kurachi. 'Inward Rectifier K+ Channel Kir2.3 Is Localized at the Postsynaptic Membrane of Excitatory Synapses'. *American Journal of Physiology. Cell Physiology* 282, no. 6 (June 2002): C1396-1403. https://doi.org/10.1152/ajpcell.00615.2001.

Irvine, Sian F., and Jessica C. F. Kwok. 'Perineuronal Nets in Spinal Motoneurones: Chondroitin Sulphate Proteoglycan around Alpha Motoneurones'. *International Journal of Molecular Sciences* 19, no. 4 (12 April 2018): E1172. https://doi.org/10.3390/ijms19041172.

‘ISH Data :: Allen Brain Atlas: Mouse Brain’, 30 August 2022. https://mouse.brain-map.org/.

Jacobson, L., and R. Sapolsky. ‘The Role of the Hippocampus in Feedback Regulation of the Hypothalamic-Pituitary-Adrenocortical Axis’. *Endocrine Reviews* 12, no. 2 (May 1991): 118–34. https://doi.org/10.1210/edrv-12-2-118.

James, Spencer L., Degu Abate, Kalkidan Hassen Abate, Solomon M. Abay, Cristiana Abbafati, Nooshin Abbasi, Hedayat Abbastabar, et al. ‘Global, Regional, and National Incidence, Prevalence, and Years Lived with Disability for 354 Diseases and Injuries for 195 Countries and Territories, 1990–2017: A Systematic Analysis for the Global Burden of Disease Study 2017’. *The Lancet* 392, no. 10159 (10 November 2018): 1789–1858. https://doi.org/10.1016/S0140-6736(18)32279-7.

Jansen, Stephan, Christine Gottschling, Andreas Faissner, and Denise Manahan-Vaughan. ‘Intrinsic Cellular and Molecular Properties of in Vivo Hippocampal Synaptic Plasticity Are Altered in the Absence of Key Synaptic Matrix Molecules’. *Hippocampus* 27, no. 8 (August 2017): 920–33. https://doi.org/10.1002/hipo.22742.

Jennings, Joshua H., Dennis R. Sparta, Alice M. Stamatakis, Randall L. Ung, Kristen E. Pleil, Thomas L. Kash, and Garret D. Stuber. ‘Distinct Extended Amygdala Circuits for Divergent Motivational States’. *Nature* 496, no. 7444 (11 April 2013): 224–28. https://doi.org/10.1038/nature12041.

Jongh, Reinoud de, Lucianne Groenink, Jan van der Gugten, and Berend Olivier. ‘Light-Enhanced and Fear-Potentiated Startle: Temporal Characteristics and Effects of Alpha-Helical Corticotropin-Releasing Hormone’. *Biological Psychiatry* 54, no. 10 (15 November 2003): 1041–48. https://doi.org/10.1016/s0006-3223(03)00468-2.

Ju, G., and L. W. Swanson. ‘Studies on the cellular architecture of the bed nuclei of the stria terminalis in the rat: I. cytoarchitecture’. *Journal of Comparative Neurology* 280, no. 4 (1989): 587–602. https://doi.org/10.1002/cne.902800409.

Kagias, Konstantinos, Camilla Nehammer, and Roger Pocock. ‘Neuronal Responses to Physiological Stress’. *Frontiers in Genetics* 3 (2012). https://www.frontiersin.org/articles/10.3389/fgene.2012.00222.

Kandel, Eric R., and James H. Schwartz. ‘Molecular Biology of Learning: Modulation of Transmitter Release’. *Science* 218, no. 4571 (29 October 1982): 433–43. https://doi.org/10.1126/science.6289442.

Kapp, Bruce S., Paul J. Whalen, William F. Supple, and Jeffrey P. Pascoe. ‘Amygdaloid Contributions to Conditioned Arousal and Sensory Information Processing’. In *The Amygdala: Neurobiological Aspects of Emotion, Memory, and Mental Dysfunction*, 229–54. New York, NY, US: Wiley-Liss, 1992.

Kash, Thomas L., William P. Nobis, Robert T. Matthews, and Danny G. Winder. ‘Dopamine Enhances Fast Excitatory Synaptic Transmission in the Extended Amygdala by a CRF-R1-Dependent Process’. *The Journal of Neuroscience: The Official Journal of the Society for Neuroscience* 28, no. 51 (17 December 2008): 13856–65. https://doi.org/10.1523/JNEUROSCI.4715-08.2008.

Kasten, C. R., K. L. Carzoli, N. M. Sharfman, T. Henderson, E. B. Holmgren, M. R. Lerner, M. C. Miller, and T. A. Wills. ‘Adolescent Alcohol Exposure Produces Sex Differences in Negative Affect-like Behavior and Group I MGluR BNST Plasticity’. *Neuropsychopharmacology: Official Publication of the American College of Neuropsychopharmacology* 45, no. 8 (July 2020): 1306–15. https://doi.org/10.1038/s41386-020-0670-7.

Kaushik, Rahul, Nikita Lipachev, Gabriela Matuszko, Anastasia Kochneva, Anastasia Dvoeglazova, Axel Becker, Mikhail Paveliev, and Alexander Dityatev. ‘Fine Structure Analysis of Perineuronal Nets in the Ketamine Model of Schizophrenia’. *The European Journal of Neuroscience* 53, no. 12 (June 2021): 3988–4004. https://doi.org/10.1111/ejn.14853.

Kessler, R. C., N. A. Sampson, P. Berglund, M. J. Gruber, A. Al-Hamzawi, L. Andrade, B. Bunting, et al. ‘Anxious and Non-Anxious Major Depressive Disorder in the World Health Organization World Mental Health Surveys’. *Epidemiology and Psychiatric Sciences* 24, no. 3 (June 2015): 210–26. https://doi.org/10.1017/S2045796015000189.

Kim, Jeansok J., and Min Whan Jung. ‘Neural Circuits and Mechanisms Involved in Pavlovian Fear Conditioning: A Critical Review’. *Neuroscience and Biobehavioral Reviews* 30, no. 2 (2006): 188–202. https://doi.org/10.1016/j.neubiorev.2005.06.005.

Kim, Sung-Jin, Sang-Ha Park, Song-hyen Choi, Bo-Hyun Moon, Kuem-Ju Lee, Seung Woo Kang, Min-Soo Lee, Sang-Hyun Choi, Boe-Gwun Chun, and Kyung-Ho Shin. ‘Effects of Repeated Tianeptine Treatment on CRF MRNA Expression in Non-Stressed and Chronic Mild Stress-Exposed Rats’. *Neuropharmacology* 50, no. 7 (1 June 2006): 824–33. https://doi.org/10.1016/j.neuropharm.2005.12.003.

Kim, Sung-Yon, Avishek Adhikari, Soo Yeun Lee, James H. Marshel, Christina K. Kim, Caitlin S. Mallory, Maisie Lo, et al. ‘Diverging Neural Pathways Assemble a Behavioural State from Separable Features in Anxiety’. *Nature* 496, no. 7444 (11 April 2013): 219–23. https://doi.org/10.1038/nature12018.

Knight, Lindsay K., and Brendan E. Depue. ‘New Frontiers in Anxiety Research: The Translational Potential of the Bed Nucleus of the Stria Terminalis’. *Frontiers in Psychiatry* 10 (2019). https://www.frontiersin.org/articles/10.3389/fpsyt.2019.00510.

Kochlamazashvili, Gaga, Christian Henneberger, Olena Bukalo, Elena Dvoretskova, Oleg Senkov, Patricia M.-J. Lievens, Ruth Westenbroek, et al.

‘The Extracellular Matrix Molecule Hyaluronic Acid Regulates Hippocampal Synaptic Plasticity by Modulating Postsynaptic L-Type Ca(2+) Channels’. *Neuron* 67, no. 1 (15 July 2010): 116–28. https://doi.org/10.1016/j.neuron.2010.05.030.

Kolb, Bryan, and Robbin Gibb. ‘Plasticity in the Prefrontal Cortex of Adult Rats’. *Frontiers in Cellular Neuroscience* 9 (2015): 15. https://doi.org/10.3389/fncel.2015.00015.

Kole, Maarten H. P., Laura Swan, and Eberhard Fuchs. ‘The Antidepressant Tianeptine Persistently Modulates Glutamate Receptor Currents of the Hippocampal CA3 Commissural Associational Synapse in Chronically Stressed Rats’. *The European Journal of Neuroscience* 16, no. 5 (September 2002): 807–16. https://doi.org/10.1046/j.1460-9568.2002.02136.x.

Korte, S. Mechiel, and Sietse F. De Boer. ‘A Robust Animal Model of State Anxiety: Fear-Potentiated Behaviour in the Elevated plus-Maze’. *European Journal of Pharmacology* 463, no. 1–3 (28 February 2003): 163–75. https://doi.org/10.1016/s0014-2999(03)01279-2.

Kosaka, T., and C. W. Heizmann. ‘Selective Staining of a Population of Parvalbumin-Containing GABAergic Neurons in the Rat Cerebral Cortex by Lectins with Specific Affinity for Terminal N-Acetylgalactosamine’. *Brain Research* 483, no. 1 (27 March 1989): 158–63. https://doi.org/10.1016/0006-8993(89)90048-6.

Kovács, László Ákos, Josef Andreas Schiessl, Anna Elisabeth Nafz, Valér Csernus, and Balázs Gaszner. ‘Both Basal and Acute Restraint Stress-Induced c-Fos Expression Is Influenced by Age in the Extended Amygdala and Brainstem Stress Centers in Male Rats’. *Frontiers in Aging Neuroscience* 10 (2018): 248. https://doi.org/10.3389/fnagi.2018.00248.

Kraeuter, Ann-Katrin, Paul C. Guest, and Zoltán Sarnyai. ‘The Open Field Test for Measuring Locomotor Activity and Anxiety-Like Behavior’. *Methods in Molecular Biology (Clifton, N.J.)* 1916 (2019): 99–103. https://doi.org/10.1007/978-1-4939-8994-2_9.

Krüger, Oliver, Thomas Shiozawa, Benjamin Kreifelts, Klaus Scheffler, and Thomas Ethofer. ‘Three Distinct Fiber Pathways of the Bed Nucleus of the Stria Terminalis to the Amygdala and Prefrontal Cortex’. *Cortex; a Journal Devoted to the Study of the Nervous System and Behavior* 66 (May 2015): 60–68. https://doi.org/10.1016/j.cortex.2015.02.007.

Kulesskaya, Natalia, and Vootele Voikar. ‘Assessment of Mouse Anxiety-like Behavior in the Light-Dark Box and Open-Field Arena: Role of Equipment and Procedure’. *Physiology & Behavior* 133 (22 June 2014): 30–38. https://doi.org/10.1016/j.physbeh.2014.05.006.

Kültz, Dietmar. ‘Defining Biological Stress and Stress Responses Based on Principles of Physics’. *Journal of Experimental Zoology Part A: Ecological and*

Integrative Physiology 333, no. 6 (2020): 350–58. https://doi.org/10.1002/jez.2340.

Kupfer, David J. 'Anxiety and DSM-5'. *Dialogues in Clinical Neuroscience* 17, no. 3 (September 2015): 245–46.

Kwok, Jessica C. F., Daniela Carulli, and James W. Fawcett. 'In Vitro Modeling of Perineuronal Nets: Hyaluronan Synthase and Link Protein Are Necessary for Their Formation and Integrity'. *Journal of Neurochemistry* 114, no. 5 (1 September 2010): 1447–59. https://doi.org/10.1111/j.1471-4159.2010.06878.x.

Lafarga, M., M. T. Berciano, and M. Blanco. 'The Perineuronal Net in the Fastigial Nucleus of the Rat Cerebellum. A Golgi and Quantitative Study'. *Anatomy and Embryology* 170, no. 1 (1984): 79–85. https://doi.org/10.1007/BF00319461.

Larson, Christine L., Hillary S. Schaefer, Greg J. Siegle, Cory A. B. Jackson, Michael J. Anderle, and Richard J. Davidson. 'Fear Is Fast in Phobic Individuals: Amygdala Activation in Response to Fear-Relevant Stimuli'. *Biological Psychiatry* 60, no. 4 (15 August 2006): 410–17. https://doi.org/10.1016/j.biopsych.2006.03.079.

Laube, B., J. Kuhse, and H. Betz. 'Evidence for a Tetrameric Structure of Recombinant NMDA Receptors'. *The Journal of Neuroscience: The Official Journal of the Society for Neuroscience* 18, no. 8 (15 April 1998): 2954–61.

La-Vu, Mimi, Brooke C. Tobias, Peter J. Schuette, and Avishek Adhikari. 'To Approach or Avoid: An Introductory Overview of the Study of Anxiety Using Rodent Assays'. *Frontiers in Behavioral Neuroscience* 14 (2020). https://www.frontiersin.org/articles/10.3389/fnbeh.2020.00145.

Lê, A. D., Douglas Funk, Kathleen Coen, Sahar Tamadon, and Yavin Shaham. 'Role of κ-Opioid Receptors in the Bed Nucleus of Stria Terminalis in Reinstatement of Alcohol Seeking'. *Neuropsychopharmacology: Official Publication of the American College of Neuropsychopharmacology* 43, no. 4 (March 2018): 838–50. https://doi.org/10.1038/npp.2017.120.

Lebow, M. A., and A. Chen. 'Overshadowed by the Amygdala: The Bed Nucleus of the Stria Terminalis Emerges as Key to Psychiatric Disorders'. *Molecular Psychiatry* 21, no. 4 (April 2016): 450–63. https://doi.org/10.1038/mp.2016.1.

LeDoux, Joseph E. 'Emotion Circuits in the Brain'. *Annual Review of Neuroscience* 23, no. 1 (2000): 155–84. https://doi.org/10.1146/annurev.neuro.23.1.155.

Lee, H. K., M. Barbarosie, K. Kameyama, M. F. Bear, and R. L. Huganir. 'Regulation of Distinct AMPA Receptor Phosphorylation Sites during Bidirectional Synaptic Plasticity'. *Nature* 405, no. 6789 (22 June 2000): 955–59. https://doi.org/10.1038/35016089.

Lein, Ed S., Michael J. Hawrylycz, Nancy Ao, Mikael Ayres, Amy Bensinger, Amy Bernard, Andrew F. Boe, et al. 'Genome-Wide Atlas of Gene Expression in the Adult Mouse Brain'. *Nature* 445, no. 7124 (11 January 2007): 168–76. https://doi.org/10.1038/nature05453.

Lenglet, Sebastien, Estelle Louiset, Catherine Delarue, Hubert Vaudry, and Vincent Contesse. 'Activation of 5-HT(7) Receptor in Rat Glomerulosa Cells Is Associated with an Increase in Adenylyl Cyclase Activity and Calcium Influx through T-Type Calcium Channels'. *Endocrinology* 143, no. 5 (May 2002): 1748–60. https://doi.org/10.1210/endo.143.5.8817.

Lensjø, Kristian K. 'Perineuronal Nets in Cortical Processing and Plasticity'. University of Oslo, 2013. https://www.duo.uio.no/bitstream/handle/10852/37196/LensjoeKristian_mastero ppgave.pdf?sequence=1.

Lensjø, Kristian Kinden, Ane Charlotte Christensen, Simen Tennøe, Marianne Fyhn, and Torkel Hafting. 'Differential Expression and Cell-Type Specificity of Perineuronal Nets in Hippocampus, Medial Entorhinal Cortex, and Visual Cortex Examined in the Rat and Mouse'. *ENeuro* 4, no. 3 (June 2017): ENEURO.0379-16.2017. https://doi.org/10.1523/ENEURO.0379-16.2017.

Lensjø, Kristian Kinden, Mikkel Elle Lepperød, Gunnar Dick, Torkel Hafting, and Marianne Fyhn. 'Removal of Perineuronal Nets Unlocks Juvenile Plasticity Through Network Mechanisms of Decreased Inhibition and Increased Gamma Activity'. *The Journal of Neuroscience: The Official Journal of the Society for Neuroscience* 37, no. 5 (1 February 2017): 1269–83. https://doi.org/10.1523/JNEUROSCI.2504-16.2016.

Leserman, J., J. M. Petitto, R. N. Golden, B. N. Gaynes, H. Gu, D. O. Perkins, S. G. Silva, J. D. Folds, and D. L. Evans. 'Impact of Stressful Life Events, Depression, Social Support, Coping, and Cortisol on Progression to AIDS'. *The American Journal of Psychiatry* 157, no. 8 (August 2000): 1221–28. https://doi.org/10.1176/appi.ajp.157.8.1221.

Lesur, A., P. Gaspar, C. Alvarez, and B. Berger. 'Chemoanatomic Compartments in the Human Bed Nucleus of the Stria Terminalis'. *Neuroscience* 32, no. 1 (1 January 1989): 181–94. https://doi.org/10.1016/0306-4522(89)90117-6.

Li, Chia, Jonathan A. Sugam, Emily G. Lowery-Gionta, Zoe A. McElligott, Nora M. McCall, Alberto J. Lopez, Jessica M. McKlveen, Kristen E. Pleil, and Thomas L. Kash. 'Mu Opioid Receptor Modulation of Dopamine Neurons in the Periaqueductal Gray/Dorsal Raphe: A Role in Regulation of Pain'. *Neuropsychopharmacology* 41, no. 8 (July 2016): 2122–32. https://doi.org/10.1038/npp.2016.12.

Li, Gang, Yang Cao, Feifei Shen, Yangsong Wang, Liangjie Bai, Weidong Guo, Yunlong Bi, Gang Lv, and Zhongkai Fan. 'Mdivi-1 Inhibits Astrocyte Activation

and Astroglial Scar Formation and Enhances Axonal Regeneration after Spinal Cord Injury in Rats'. *Frontiers in Cellular Neuroscience* 10 (2016). https://www.frontiersin.org/articles/10.3389/fncel.2016.00241.

Li, Sa, and Gilbert J. Kirouac. 'Projections from the Paraventricular Nucleus of the Thalamus to the Forebrain, with Special Emphasis on the Extended Amygdala'. *The Journal of Comparative Neurology* 506, no. 2 (10 January 2008): 263–87. https://doi.org/10.1002/cne.21502.

Lin, Rachel, Jessica C. F. Kwok, Damaso Crespo, and James W. Fawcett. 'Chondroitinase ABC Has a Long-Lasting Effect on Chondroitin Sulphate Glycosaminoglycan Content in the Injured Rat Brain'. *Journal of Neurochemistry* 104, no. 2 (January 2008): 400–408. https://doi.org/10.1111/j.1471-4159.2007.05066.x.

Lin, Xiaoxiao, Christy A. Itoga, Sharif Taha, Ming H. Li, Ryan Chen, Kirolos Sami, Fulvia Berton, Walter Francesconi, and Xiangmin Xu. 'C-Fos Mapping of Brain Regions Activated by Multi-Modal and Electric Foot Shock Stress'. *Neurobiology of Stress* 8 (February 2018): 92–102. https://doi.org/10.1016/j.ynstr.2018.02.001.

Livak, K. J., and T. D. Schmittgen. 'Analysis of Relative Gene Expression Data Using Real-Time Quantitative PCR and the 2(-Delta Delta C(T)) Method'. *Methods (San Diego, Calif.)* 25, no. 4 (December 2001): 402–8. https://doi.org/10.1006/meth.2001.1262.

Lorenzini, Carlo Ambrogi, Corrado Bucherelli, and Aldo Giachetti. 'Passive and Active Avoidance Behavior in the Light-Dark Box Test'. *Physiology & Behavior* 32, no. 4 (1 April 1984): 687–89. https://doi.org/10.1016/0031-9384(84)90327-5.

Lubbers, Bart R., August B. Smit, Sabine Spijker, and Michel C. van den Oever. 'Neural ECM in Addiction, Schizophrenia, and Mood Disorder'. *Progress in Brain Research* 214 (2014): 263–84. https://doi.org/10.1016/B978-0-444-63486-3.00012-8.

M, Morawski, Brückner G, Jäger C, Seeger G, and Arendt T. 'Neurons Associated with Aggrecan-Based Perineuronal Nets Are Protected against Tau Pathology in Subcortical Regions in Alzheimer's Disease'. *Neuroscience* 169, no. 3 (9 January 2010). https://doi.org/10.1016/j.neuroscience.2010.05.022.

Mabuchi, M., S. Murakami, T. Taguchi, A. Ohtsuka, and T. Murakami. 'Purkinje Cells in the Adult Cat Cerebellar Cortex Possess a Perineuronal Net of Proteoglycans'. *Archives of Histology and Cytology* 64, no. 2 (May 2001): 203–9. https://doi.org/10.1679/aohc.64.203.

Mack, Judith A., Ron J. Feldman, Naoki Itano, Koji Kimata, Mark Lauer, Vincent C. Hascall, and Edward V. Maytin. 'Enhanced Inflammation and Accelerated Wound Closure Following Tetraphorbol Ester Application or Full-Thickness Wounding in Mice Lacking Hyaluronan Synthases Has1 and Has3'. *The Journal*

of Investigative Dermatology 132, no. 1 (January 2012): 198–207. https://doi.org/10.1038/jid.2011.248.

Maggio, Nicola, and Menahem Segal. 'Persistent Changes in Ability to Express Long-Term Potentiation/Depression in the Rat Hippocampus after Juvenile/Adult Stress'. *Biological Psychiatry* 69, no. 8 (15 April 2011): 748–53. https://doi.org/10.1016/j.biopsych.2010.11.026.

Malinow, Roberto, and Robert C. Malenka. 'AMPA Receptor Trafficking and Synaptic Plasticity'. *Annual Review of Neuroscience* 25 (2002): 103–26. https://doi.org/10.1146/annurev.neuro.25.112701.142758.

Maller, Roberta G., and Steven Reiss. 'Anxiety Sensitivity in 1984 and Panic Attacks in 1987'. *Journal of Anxiety Disorders* 6, no. 3 (1 July 1992): 241–47. https://doi.org/10.1016/0887-6185(92)90036-7.

Maren, S., G. Aharonov, and M. S. Fanselow. 'Neurotoxic Lesions of the Dorsal Hippocampus and Pavlovian Fear Conditioning in Rats'. *Behavioural Brain Research* 88, no. 2 (November 1997): 261–74. https://doi.org/10.1016/s0166-4328(97)00088-0.

Martin, Kathryn P., and Cara L. Wellman. 'NMDA Receptor Blockade Alters Stress-Induced Dendritic Remodeling in Medial Prefrontal Cortex'. *Cerebral Cortex (New York, NY)* 21, no. 10 (October 2011): 2366–73. https://doi.org/10.1093/cercor/bhr021.

Martin, S. J., P. D. Grimwood, and R. G. Morris. 'Synaptic Plasticity and Memory: An Evaluation of the Hypothesis'. *Annual Review of Neuroscience* 23 (2000): 649–711. https://doi.org/10.1146/annurev.neuro.23.1.649.

Massey, James M., Charles H. Hubscher, Michelle R. Wagoner, Julie A. Decker, Jeremy Amps, Jerry Silver, and Stephen M. Onifer. 'Chondroitinase ABC Digestion of the Perineuronal Net Promotes Functional Collateral Sprouting in the Cuneate Nucleus after Cervical Spinal Cord Injury'. *Journal of Neuroscience* 26, no. 16 (19 April 2006): 4406–14. https://doi.org/10.1523/JNEUROSCI.5467-05.2006.

Matsuyama, Yukihiro, Kazuhiro Chiba, Hisashi Iwata, Takayuki Seo, and Yoshiaki Toyama. 'A Multicenter, Randomized, Double-Blind, Dose-Finding Study of Condoliase in Patients with Lumbar Disc Herniation'. *Journal of Neurosurgery: Spine* 28, no. 5 (1 May 2018): 499–511. https://doi.org/10.3171/2017.7.SPINE161327.

Matthews, Russell T., Gail M. Kelly, Cynthia A. Zerillo, Grace Gray, Michael Tiemeyer, and Susan Hockfield. 'Aggrecan Glycoforms Contribute to the Molecular Heterogeneity of Perineuronal Nets'. *Journal of Neuroscience* 22, no. 17 (1 September 2002): 7536–47. https://doi.org/10.1523/JNEUROSCI.22-17-07536.2002.

McDonald, A. J. ‘Cortical Pathways to the Mammalian Amygdala’. *Progress in Neurobiology* 55, no. 3 (June 1998): 257–332. https://doi.org/10.1016/s0301-0082(98)00003-3.

McDonald, A. J., S. J. Shammah-Lagnado, C. Shi, and M. Davis. ‘Cortical Afferents to the Extended Amygdala’. *Annals of the New York Academy of Sciences* 877 (29 June 1999): 309–38. https://doi.org/10.1111/j.1749-6632.1999.tb09275.x.

McElligott, Zoé Anastasia, and Danny G. Winder. ‘Modulation of Glutamatergic Synaptic Transmission in the Bed Nucleus of the Stria Terminalis’. *Progress in Neuro-Psychopharmacology & Biological Psychiatry* 33, no. 8 (13 November 2009): 1329–35. https://doi.org/10.1016/j.pnpbp.2009.05.022.

McEwen, B. S. ‘Stress, Adaptation, and Disease. Allostasis and Allostatic Load’. *Annals of the New York Academy of Sciences* 840 (1 May 1998): 33–44. https://doi.org/10.1111/j.1749-6632.1998.tb09546.x.

McEwen, B. S., and E. Stellar. ‘Stress and the Individual. Mechanisms Leading to Disease’. *Archives of Internal Medicine* 153, no. 18 (27 September 1993): 2093–2101.

McEwen, Bruce S. ‘Physiology and Neurobiology of Stress and Adaptation: Central Role of the Brain’. *Physiological Reviews* 87, no. 3 (July 2007): 873–904. https://doi.org/10.1152/physrev.00041.2006.

McKeon, R. J., R. C. Schreiber, J. S. Rudge, and J. Silver. ‘Reduction of Neurite Outgrowth in a Model of Glial Scarring Following CNS Injury Is Correlated with the Expression of Inhibitory Molecules on Reactive Astrocytes’. *The Journal of Neuroscience: The Official Journal of the Society for Neuroscience* 11, no. 11 (November 1991): 3398–3411.

McLaughlin, Katie A., and Mark L. Hatzenbuehler. ‘Stressful Life Events, Anxiety Sensitivity, and Internalizing Symptoms in Adolescents’. *Journal of Abnormal Psychology* 118, no. 3 (August 2009): 659–69. https://doi.org/10.1037/a0016499.

Mikami, Tadahisa, and Hiroshi Kitagawa. ‘Biosynthesis and Function of Chondroitin Sulfate’. *Biochimica Et Biophysica Acta* 1830, no. 10 (October 2013): 4719–33. https://doi.org/10.1016/j.bbagen.2013.06.006.

Mirzadeh, Zaman, Kimberly M. Alonge, Elaine Cabrales, Vicente Herranz-Pérez, Jarrad M. Scarlett, Jenny M. Brown, Rim Hassouna, et al. ‘Perineuronal Net Formation during the Critical Period for Neuronal Maturation in the Hypothalamic Arcuate Nucleus’. *Nature Metabolism* 1, no. 2 (February 2019): 212–21. https://doi.org/10.1038/s42255-018-0029-0.

Mishkin, M, and J Aggleton. ‘Multiple Functional Contributions of the Amygdala in the Monkey’. In *The Amygdaloid Complex*, 409–20, 1981.

Mitra, Rupshi, and Robert M. Sapolsky. ‘Acute Corticosterone Treatment Is Sufficient to Induce Anxiety and Amygdaloid Dendritic Hypertrophy’. *Proceedings of the National Academy of Sciences of the United States of America* 105, no. 14 (8 April 2008): 5573–78. https://doi.org/10.1073/pnas.0705615105.

Miyata, Seiji, Yousuke Nishimura, and Toshihiro Nakashima. ‘Perineuronal Nets Protect against Amyloid Beta-Protein Neurotoxicity in Cultured Cortical Neurons’. *Brain Research* 1150 (30 May 2007): 200–206. https://doi.org/10.1016/j.brainres.2007.02.066.

Miyata, Shinji, Yukio Komatsu, Yumiko Yoshimura, Choji Taya, and Hiroshi Kitagawa. ‘Persistent Cortical Plasticity by Upregulation of Chondroitin 6-Sulfation’. *Nature Neuroscience* 15, no. 3 (15 January 2012): 414–22, S1-2. https://doi.org/10.1038/nn.3023.

Mjaatvedt, C. H., H. Yamamura, A. A. Capehart, D. Turner, and R. R. Markwald. ‘The Cspg2 Gene, Disrupted in the Hdf Mutant, Is Required for Right Cardiac Chamber and Endocardial Cushion Formation’. *Developmental Biology* 202, no. 1 (1 October 1998): 56–66. https://doi.org/10.1006/dbio.1998.9001.

Mobbs, Dean, Rongjun Yu, James B. Rowe, Hannah Eich, Oriel FeldmanHall, and Tim Dalgleish. ‘Neural Activity Associated with Monitoring the Oscillating Threat Value of a Tarantula’. *Proceedings of the National Academy of Sciences* 107, no. 47 (23 November 2010): 20582–86. https://doi.org/10.1073/pnas.1009076107.

Moench, Kelly M., Michaela R. Breach, and Cara L. Wellman. ‘Chronic Stress Produces Enduring Sex- and Region-Specific Alterations in Novel Stress-Induced c-Fos Expression’. *Neurobiology of Stress* 10 (February 2019): 100147. https://doi.org/10.1016/j.ynstr.2019.100147.

Moga, M. M., and C. B. Saper. ‘Neuropeptide-Immunoreactive Neurons Projecting to the Paraventricular Hypothalamic Nucleus in the Rat’. *The Journal of Comparative Neurology* 346, no. 1 (1 August 1994): 137–50. https://doi.org/10.1002/cne.903460110.

Monteggia, L. M., A. J. Eisch, M. D. Tang, L. K. Kaczmarek, and E. J. Nestler. ‘Cloning and Localization of the Hyperpolarization-Activated Cyclic Nucleotide-Gated Channel Family in Rat Brain’. *Brain Research. Molecular Brain Research* 81, no. 1–2 (30 September 2000): 129–39. https://doi.org/10.1016/s0169-328x(00)00155-8.

Moon, L. D., R. A. Asher, K. E. Rhodes, and J. W. Fawcett. ‘Regeneration of CNS Axons Back to Their Target Following Treatment of Adult Rat Brain with Chondroitinase ABC’. *Nature Neuroscience* 4, no. 5 (May 2001): 465–66. https://doi.org/10.1038/87415.

Morawski, Markus, Alexander Dityatev, Maike Hartlage-Rübsamen, Maren Blosa, Max Holzer, Katharina Flach, Sanja Pavlica, et al. ‘Tenascin-R Promotes

Assembly of the Extracellular Matrix of Perineuronal Nets via Clustering of Aggrecan'. *Philosophical Transactions of the Royal Society of London. Series B, Biological Sciences* 369, no. 1654 (19 October 2014): 20140046. https://doi.org/10.1098/rstb.2014.0046.

Morawski, Markus, Tilo Reinert, Wolfram Meyer-Klaucke, Friedrich E. Wagner, Wolfgang Tröger, Anja Reinert, Carsten Jäger, Gert Brückner, and Thomas Arendt. 'Ion Exchanger in the Brain: Quantitative Analysis of Perineuronally Fixed Anionic Binding Sites Suggests Diffusion Barriers with Ion Sorting Properties'. *Scientific Reports* 5 (1 December 2015): 16471. https://doi.org/10.1038/srep16471.

Morikawa, Shota, Yuji Ikegaya, Minoru Narita, and Hideki Tamura. 'Activation of Perineuronal Net-Expressing Excitatory Neurons during Associative Memory Encoding and Retrieval'. *Scientific Reports* 7 (5 April 2017): 46024. https://doi.org/10.1038/srep46024.

Murthy, Sahana, Gary A. Kane, Nicole J. Katchur, Paula S. Lara Mejia, Gracious Obiofuma, Timothy J. Buschman, Bruce S. McEwen, and Elizabeth Gould. 'Perineuronal Nets, Inhibitory Interneurons, and Anxiety-Related Ventral Hippocampal Neuronal Oscillations Are Altered by Early Life Adversity'. *Biological Psychiatry* 85, no. 12 (15 June 2019): 1011–20. https://doi.org/10.1016/j.biopsych.2019.02.021.

Myers, K. M., and M. Davis. 'Mechanisms of Fear Extinction'. *Molecular Psychiatry* 12, no. 2 (February 2007): 120–50. https://doi.org/10.1038/sj.mp.4001939.

Nabel, Elisa M., and Hirofumi Morishita. 'Regulating Critical Period Plasticity: Insight from the Visual System to Fear Circuitry for Therapeutic Interventions'. *Frontiers in Psychiatry* 4 (2013): 146. https://doi.org/10.3389/fpsyt.2013.00146.

Nader, K. O., R. S. Pynoos, L. A. Fairbanks, M. al-Ajeel, and A. al-Asfour. 'A Preliminary Study of PTSD and Grief among the Children of Kuwait Following the Gulf Crisis'. *The British Journal of Clinical Psychology* 32, no. 4 (November 1993): 407–16. https://doi.org/10.1111/j.2044-8260.1993.tb01075.x.

Nakagawa, F., B. A. Schulte, J. Y. Wu, and S. S. Spicer. 'GABAergic Neurons of Rodent Brain Correspond Partially with Those Staining for Glycoconjugate with Terminal N-Acetylgalactosamine'. *Journal of Neurocytology* 15, no. 3 (June 1986): 389–96. https://doi.org/10.1007/BF01611440.

Namburi, Praneeth, Anna Beyeler, Suzuko Yorozu, Gwendolyn G. Calhoon, Sarah A. Halbert, Romy Wichmann, Stephanie S. Holden, et al. 'A Circuit Mechanism for Differentiating Positive and Negative Associations'. *Nature* 520, no. 7549 (30 April 2015): 675–78. https://doi.org/10.1038/nature14366.

Netto, S. M., and F. S. Guimarães. 'Role of Hippocampal 5-HT1A Receptors on Elevated plus Maze Exploration after a Single Restraint Experience'.

Behavioural Brain Research 77, no. 1–2 (May 1996): 215–18. https://doi.org/10.1016/0166-4328(95)00211-1.

Nguyen, Amanda Q., Julie A.D. Dela Cruz, Yanjun Sun, Todd C. Holmes, and Xiangmin Xu. 'Genetic Cell Targeting Uncovers Specific Neuronal Types and Distinct Subregions in the Bed Nucleus of the Stria Terminalis'. *Journal of Comparative Neurology* 524, no. 12 (2016): 2379–99. https://doi.org/10.1002/cne.23954.

Nosek, Katarzyna, Kristen Dennis, Brian M. Andrus, Nasim Ahmadiyeh, Amber E. Baum, Leah C. Solberg Woods, and Eva E. Redei. 'Context and Strain-Dependent Behavioral Response to Stress'. *Behavioral and Brain Functions: BBF* 4 (2 June 2008): 23. https://doi.org/10.1186/1744-9081-4-23.

O'Dell, Deidre E., Bernard G. Schreurs, Carrie Smith-Bell, and Desheng Wang. 'Disruption of Rat Deep Cerebellar Perineuronal Net Alters Eyeblink Conditioning and Neuronal Electrophysiology'. *Neurobiology of Learning and Memory* 177 (January 2021): 107358. https://doi.org/10.1016/j.nlm.2020.107358.

Ohira, Koji, Rika Takeuchi, Tsuyoshi Iwanaga, and Tsuyoshi Miyakawa. 'Chronic Fluoxetine Treatment Reduces Parvalbumin Expression and Perineuronal Nets in Gamma-Aminobutyric Acidergic Interneurons of the Frontal Cortex in Adult Mice'. *Molecular Brain* 6 (5 November 2013): 43. https://doi.org/10.1186/1756-6606-6-43.

Oler, Jonathan A., Do P. M. Tromp, Andrew S. Fox, Rothem Kovner, Richard J. Davidson, Andrew L. Alexander, Daniel R. McFarlin, et al. 'Connectivity between the Central Nucleus of the Amygdala and the Bed Nucleus of the Stria Terminalis in the Non-Human Primate: Neuronal Tract Tracing and Developmental Neuroimaging Studies'. *Brain Structure & Function* 222, no. 1 (January 2017): 21–39. https://doi.org/10.1007/s00429-016-1198-9.

Oliveira, Leandro A., Jeferson Almeida, Ricardo Benini, and Carlos C. Crestani. 'CRF1 and CRF2 Receptors in the Bed Nucleus of the Stria Terminalis Modulate the Cardiovascular Responses to Acute Restraint Stress in Rats'. *Pharmacological Research* 95–96 (June 2015): 53–62. https://doi.org/10.1016/j.phrs.2015.03.012.

Orlando, Clara, Jeanne Ster, Urs Gerber, James W. Fawcett, and Olivier Raineteau. 'Perisynaptic Chondroitin Sulfate Proteoglycans Restrict Structural Plasticity in an Integrin-Dependent Manner'. *The Journal of Neuroscience: The Official Journal of the Society for Neuroscience* 32, no. 50 (12 December 2012): 18009–17, 18017a. https://doi.org/10.1523/JNEUROSCI.2406-12.2012.

Pacheco, Anibal, Felipe I. Aguayo, Esteban Aliaga, Mauricio Muñoz, Gonzalo García-Rojo, Felipe A. Olave, Nicolas A. Parra-Fiedler, et al. 'Chronic Stress Triggers Expression of Immediate Early Genes and Differentially Affects the Expression of AMPA and NMDA Subunits in Dorsal and Ventral Hippocampus

of Rats'. *Frontiers in Molecular Neuroscience* 10 (2017): 244. https://doi.org/10.3389/fnmol.2017.00244.

Padovan, C. M., and F. S. Guimarães. 'Restraint-Induced Hypoactivity in an Elevated plus-Maze'. *Brazilian Journal of Medical and Biological Research = Revista Brasileira De Pesquisas Medicas E Biologicas* 33, no. 1 (January 2000): 79–83. https://doi.org/10.1590/s0100-879x2000000100011.

Park, Yun Kyung, and Yukiko Goda. 'Integrins in Synapse Regulation'. *Nature Reviews. Neuroscience* 17, no. 12 (December 2016): 745–56. https://doi.org/10.1038/nrn.2016.138.

Partridge, John G., Patrick A. Forcelli, Ruixi Luo, Jonah M. Cashdan, Jay Schulkin, Rita J. Valentino, and Stefano Vicini. 'Stress Increases GABAergic Neurotransmission in CRF Neurons of the Central Amygdala and Bed Nucleus Stria Terminalis'. *Neuropharmacology* 107 (August 2016): 239–50. https://doi.org/10.1016/j.neuropharm.2016.03.029.

Pavlov, I. *Conditioned Reflexes*. London: Oxford University Press, 1927.

Pawlak, Robert, B. S. Shankaranarayana Rao, Jerry P. Melchor, Sumantra Chattarji, Bruce McEwen, and Sidney Strickland. 'Tissue Plasminogen Activator and Plasminogen Mediate Stress-Induced Decline of Neuronal and Cognitive Functions in the Mouse Hippocampus'. *Proceedings of the National Academy of Sciences of the United States of America* 102, no. 50 (13 December 2005): 18201–6. https://doi.org/10.1073/pnas.0509232102.

Pecoraro, Norman, Francisca Gomez, and Mary F. Dallman. 'Glucocorticoids Dose-Dependently Remodel Energy Stores and Amplify Incentive Relativity Effects'. *Psychoneuroendocrinology* 30, no. 9 (October 2005): 815–25. https://doi.org/10.1016/j.psyneuen.2005.03.010.

Pêgo, J. M., P. Morgado, L. G. Pinto, J. J. Cerqueira, O. F. X. Almeida, and N. Sousa. 'Dissociation of the Morphological Correlates of Stress-Induced Anxiety and Fear'. *The European Journal of Neuroscience* 27, no. 6 (March 2008): 1503–16. https://doi.org/10.1111/j.1460-9568.2008.06112.x.

Pellow, S., P. Chopin, S. E. File, and M. Briley. 'Validation of Open:Closed Arm Entries in an Elevated plus-Maze as a Measure of Anxiety in the Rat'. *Journal of Neuroscience Methods* 14, no. 3 (August 1985): 149–67. https://doi.org/10.1016/0165-0270(85)90031-7.

Pesarico, Ana Paula, Clara Bueno-Fernandez, Ramón Guirado, María Ángeles Gómez-Climent, Yasmina Curto, Hector Carceller, and Juan Nacher. 'Chronic Stress Modulates Interneuronal Plasticity: Effects on PSA-NCAM and Perineuronal Nets in Cortical and Extracortical Regions'. *Frontiers in Cellular Neuroscience* 13 (2019): 197. https://doi.org/10.3389/fncel.2019.00197.

Pizzorusso, Tommaso, Paolo Medini, Nicoletta Berardi, Sabrina Chierzi, James W. Fawcett, and Lamberto Maffei. 'Reactivation of Ocular Dominance Plasticity

in the Adult Visual Cortex'. *Science (New York, N.Y.)* 298, no. 5596 (8 November 2002): 1248–51. https://doi.org/10.1126/science.1072699.

Placantonakis, D. G., C. Schwarz, and J. P. Welsh. 'Serotonin Suppresses Subthreshold and Suprathreshold Oscillatory Activity of Rat Inferior Olivary Neurones in Vitro'. *The Journal of Physiology* 524 Pt 3 (1 May 2000): 833–51. https://doi.org/10.1111/j.1469-7793.2000.00833.x.

Pleil, Kristen E., Alberto Lopez, Nora McCall, Ana M. Jijon, Jose Peña Bravo, and Thomas L. Kash. 'Chronic Stress Alters Neuropeptide Y Signaling in the Bed Nucleus of the Stria Terminalis in DBA/2J but Not C57BL/6J Mice'. *Neuropharmacology* 62, no. 4 (March 2012): 1777–86. https://doi.org/10.1016/j.neuropharm.2011.12.002.

Polleux, F., T. Morrow, and A. Ghosh. 'Semaphorin 3A Is a Chemoattractant for Cortical Apical Dendrites'. *Nature* 404, no. 6778 (6 April 2000): 567–73. https://doi.org/10.1038/35007001.

Porsolt, R. D., M. Le Pichon, and M. Jalfre. 'Depression: A New Animal Model Sensitive to Antidepressant Treatments'. *Nature* 266, no. 5604 (21 April 1977): 730–32. https://doi.org/10.1038/266730a0.

Prosser, C. Ladd, and Walter S. Hunter. 'The Extinction of Startle Responses and Spinal Reflexes in the White Rat'. *American Journal of Physiology-Legacy Content* 117, no. 4 (30 November 1936): 609–18. https://doi.org/10.1152/ajplegacy.1936.117.4.609.

Qiu, De-Lai, Chun-Ping Chu, Tetsuro Shirasaka, Hiromasa Tsukino, Hiroyuki Nakao, Kazuo Kato, Takato Kunitake, Takahiko Katoh, and Hiroshi Kannan. 'Corticotrophin-Releasing Factor Augments the I(H) in Rat Hypothalamic Paraventricular Nucleus Parvocellular Neurons in Vitro'. *Journal of Neurophysiology* 94, no. 1 (July 2005): 226–34. https://doi.org/10.1152/jn.01325.2004.

Radley, J. J., H. M. Sisti, J. Hao, A. B. Rocher, T. McCall, P. R. Hof, B. S. McEwen, and J. H. Morrison. 'Chronic Behavioral Stress Induces Apical Dendritic Reorganization in Pyramidal Neurons of the Medial Prefrontal Cortex'. *Neuroscience* 125, no. 1 (2004): 1–6. https://doi.org/10.1016/j.neuroscience.2004.01.006.

Radley, Jason J., Kristin L. Gosselink, and Paul E. Sawchenko. 'A Discrete GABAergic Relay Mediates Medial Prefrontal Cortical Inhibition of the Neuroendocrine Stress Response'. *The Journal of Neuroscience: The Official Journal of the Society for Neuroscience* 29, no. 22 (3 June 2009): 7330–40. https://doi.org/10.1523/JNEUROSCI.5924-08.2009.

Radley, Jason J., Anne B. Rocher, Melinda Miller, William G. M. Janssen, Conor Liston, Patrick R. Hof, Bruce S. McEwen, and John H. Morrison. 'Repeated Stress Induces Dendritic Spine Loss in the Rat Medial Prefrontal

Cortex'. *Cerebral Cortex (New York, N.Y.: 1991)* 16, no. 3 (March 2006): 313–20. https://doi.org/10.1093/cercor/bhi104.

Radley, Jason J., and Paul E. Sawchenko. 'A Common Substrate for Prefrontal and Hippocampal Inhibition of the Neuroendocrine Stress Response'. *The Journal of Neuroscience: The Official Journal of the Society for Neuroscience* 31, no. 26 (29 June 2011): 9683–95. https://doi.org/10.1523/JNEUROSCI.6040-10.2011.

Rauch, U., B. Grimpe, G. Kulbe, I. Arnold-Ammer, D. R. Beier, and R. Fässler. 'Structure and Chromosomal Localization of the Mouse Neurocan Gene'. *Genomics* 28, no. 3 (10 August 1995): 405–10. https://doi.org/10.1006/geno.1995.1168.

Rauch, U., H. Meyer, C. Brakebusch, C. Seidenbecher, E. D. Gundelfinger, D. R. Beier, and R. Fässler. 'Sequence and Chromosomal Localization of the Mouse Brevican Gene'. *Genomics* 44, no. 1 (15 August 1997): 15–21. https://doi.org/10.1006/geno.1997.4853.

Reimers, Sabrina, Maike Hartlage-Rübsamen, Gert Brückner, and Steffen Rossner. 'Formation of Perineuronal Nets in Organotypic Mouse Brain Slice Cultures Is Independent of Neuronal Glutamatergic Activity'. *The European Journal of Neuroscience* 25, no. 9 (May 2007): 2640–48. https://doi.org/10.1111/j.1460-9568.2007.05514.x.

Reis, Daniel G., América A. Scopinho, Francisco S. Guimarães, Fernando M. A. Corrêa, and Leonardo B. M. Resstel. 'Behavioral and Autonomic Responses to Acute Restraint Stress Are Segregated within the Lateral Septal Area of Rats'. *PloS One* 6, no. 8 (2011): e23171. https://doi.org/10.1371/journal.pone.0023171.

Ressler, Reed L., Travis D. Goode, Carolyn Evemy, and Stephen Maren. 'NMDA Receptors in the CeA and BNST Differentially Regulate Fear Conditioning to Predictable and Unpredictable Threats'. *Neurobiology of Learning and Memory* 174 (October 2020): 107281. https://doi.org/10.1016/j.nlm.2020.107281.

Reynolds, Sheila M., and Daniel S. Zahm. 'Specificity in the Projections of Prefrontal and Insular Cortex to Ventral Striatopallidum and the Extended Amygdala'. *The Journal of Neuroscience: The Official Journal of the Society for Neuroscience* 25, no. 50 (14 December 2005): 11757–67. https://doi.org/10.1523/JNEUROSCI.3432-05.2005.

Rhodes, C., and Y. Yamada. 'Characterization of a Glucocorticoid Responsive Element and Identification of an AT-Rich Element That Regulate the Link Protein Gene'. *Nucleic Acids Research* 23, no. 12 (25 June 1995): 2305–13. https://doi.org/10.1093/nar/23.12.2305.

Richardson, Rick, Jeremy Bowers, Bridget L. Callaghan, and Kathryn D. Baker. 'Does Maternal Separation Accelerate Maturation of Perineuronal Nets and

Parvalbumin-Containing Inhibitory Interneurons in Male and Female Rats?' *Developmental Cognitive Neuroscience* 47 (February 2021): 100905. https://doi.org/10.1016/j.dcn.2020.100905.

Rittenhouse, E., L. C. Dunn, J. Cookingham, C. Calo, M. Spiegelman, G. B. Dooher, and D. Bennett. 'Cartilage Matrix Deficiency (Cmd): A New Autosomal Recessive Lethal Mutation in the Mouse'. *Journal of Embryology and Experimental Morphology* 43 (February 1978): 71–84.

Rodgers, R. J., and A. Dalvi. 'Anxiety, Defence and the Elevated plus-Maze'. *Neuroscience and Biobehavioral Reviews* 21, no. 6 (November 1997): 801–10. https://doi.org/10.1016/s0149-7634(96)00058-9.

Rodgers, R. J., J. Haller, A. Holmes, J. Halasz, T. J. Walton, and P. F. Brain. 'Corticosterone Response to the Plus-Maze: High Correlation with Risk Assessment in Rats and Mice'. *Physiology & Behavior* 68, no. 1–2 (1 December 1999): 47–53. https://doi.org/10.1016/s0031-9384(99)00140-7.

Rodríguez Manzanares, Pablo A., Nora A. Isoardi, Hugo F. Carrer, and Víctor A. Molina. 'Previous Stress Facilitates Fear Memory, Attenuates GABAergic Inhibition, and Increases Synaptic Plasticity in the Rat Basolateral Amygdala'. *The Journal of Neuroscience: The Official Journal of the Society for Neuroscience* 25, no. 38 (21 September 2005): 8725–34. https://doi.org/10.1523/JNEUROSCI.2260-05.2005.

Rodríguez-Sierra, Olga E., Hjalmar K. Turesson, and Denis Pare. 'Contrasting Distribution of Physiological Cell Types in Different Regions of the Bed Nucleus of the Stria Terminalis'. *Journal of Neurophysiology* 110, no. 9 (November 2013): 2037–49. https://doi.org/10.1152/jn.00408.2013.

Rogers, Stephanie L., Elyse Rankin-Gee, Rashmi M. Risbud, Brenda E. Porter, and Eric D. Marsh. 'Normal Development of the Perineuronal Net in Humans; In Patients with and without Epilepsy'. *Neuroscience* 384 (1 August 2018): 350–60. https://doi.org/10.1016/j.neuroscience.2018.05.039.

Roman, Carolyn W., Kimberly R. Lezak, Margaret Kocho-Schellenberg, Mark A. Garret, Karen Braas, Victor May, and Sayamwong E. Hammack. 'Excitotoxic Lesions of the Bed Nucleus of the Stria Terminalis (BNST) Attenuate the Effects of Repeated Stress on Weight Gain: Evidence for the Recruitment of BNST Activity by Repeated, but Not Acute, Stress'. *Behavioural Brain Research* 227, no. 1 (1 February 2012): 300–304. https://doi.org/10.1016/j.bbr.2011.11.010.

Romberg, Carola, Sujeong Yang, Riccardo Melani, Melissa R. Andrews, Alexa E. Horner, Maria G. Spillantini, Timothy J. Bussey, James W. Fawcett, Tommaso Pizzorusso, and Lisa M. Saksida. 'Depletion of Perineuronal Nets Enhances Recognition Memory and Long-Term Depression in the Perirhinal Cortex'. *The Journal of Neuroscience: The Official Journal of the Society for Neuroscience* 33, no. 16 (17 April 2013): 7057–65. https://doi.org/10.1523/JNEUROSCI.6267-11.2013.

Rossier, J., A. Bernard, J.-H. Cabungcal, Q. Perrenoud, A. Savoye, T. Gallopin, M. Hawrylycz, et al. 'Cortical Fast-Spiking Parvalbumin Interneurons Enwrapped in the Perineuronal Net Express the Metallopeptidases Adamts8, Adamts15 and Neprilysin'. *Molecular Psychiatry* 20, no. 2 (February 2015): 154–61. https://doi.org/10.1038/mp.2014.162.

Rowlands, Daire, Kristian K. Lensjø, Tovy Dinh, Sujeong Yang, Melissa R. Andrews, Torkel Hafting, Marianne Fyhn, James W. Fawcett, and Gunnar Dick. 'Aggrecan Directs Extracellular Matrix-Mediated Neuronal Plasticity'. *The Journal of Neuroscience: The Official Journal of the Society for Neuroscience* 38, no. 47 (21 November 2018): 10102–13. https://doi.org/10.1523/JNEUROSCI.1122-18.2018.

Royce, J. R. 'On the Construct Validity of Open Field Measures'. *Psychological Bulletin* 84, no. 6 (20 February 1977): 1098–1106.

Rozario, Tania, and Douglas W. DeSimone. 'The Extracellular Matrix in Development and Morphogenesis: A Dynamic View'. *Developmental Biology* 341, no. 1 (1 May 2010): 126–40. https://doi.org/10.1016/j.ydbio.2009.10.026.

S, Makino, Gold Pw, and Schulkin J. 'Effects of Corticosterone on CRH MRNA and Content in the Bed Nucleus of the Stria Terminalis; Comparison with the Effects in the Central Nucleus of the Amygdala and the Paraventricular Nucleus of the Hypothalamus'. *Brain Research* 657, no. 1–2 (19 September 1994). https://doi.org/10.1016/0006-8993(94)90961-x.

Sadler, Annelisa M., and Sarah J. Bailey. 'Repeated Daily Restraint Stress Induces Adaptive Behavioural Changes in Both Adult and Juvenile Mice'. *Physiology & Behavior* 167 (1 December 2016): 313–23. https://doi.org/10.1016/j.physbeh.2016.09.014.

Salimando, Gregory J., Minsuk Hyun, Kristen M. Boyt, and Danny G. Winder. 'BNST GluN2D-Containing NMDA Receptors Influence Anxiety- and Depressive-like Behaviors and ModulateCell-Specific Excitatory/Inhibitory Synaptic Balance'. *The Journal of Neuroscience: The Official Journal of the Society for Neuroscience* 40, no. 20 (13 May 2020): 3949–68. https://doi.org/10.1523/JNEUROSCI.0270-20.2020.

Salmon, P., and S. C. Stanford. 'Beta-Adrenoceptor Binding Correlates with Behaviour of Rats in the Open Field'. *Psychopharmacology* 98, no. 3 (1989): 412–16. https://doi.org/10.1007/BF00451697.

Santiago, Adrienne N., Kayla Y. Lim, Maya Opendak, Regina M. Sullivan, and Chiye Aoki. 'Early Life Trauma Increases Threat Response of Peri-Weaning Rats, Reduction of Axo-Somatic Synapses Formed by Parvalbumin Cells and Perineuronal Net in the Basolateral Nucleus of Amygdala'. *The Journal of Comparative Neurology* 526, no. 16 (1 November 2018): 2647–64. https://doi.org/10.1002/cne.24522.

Saper, C. B., and A. D. Loewy. ‘Efferent Connections of the Parabrachial Nucleus in the Rat’. *Brain Research* 197, no. 2 (22 September 1980): 291–317. https://doi.org/10.1016/0006-8993(80)91117-8.

Saroja, Sivaprakasam R., Ajinkya Sase, Susanne G. Kircher, Jia Wan, Johannes Berger, Harald Höger, Arnold Pollak, and Gert Lubec. ‘Hippocampal Proteoglycans Brevican and Versican Are Linked to Spatial Memory of Sprague-Dawley Rats in the Morris Water Maze’. *Journal of Neurochemistry* 130, no. 6 (September 2014): 797–804. https://doi.org/10.1111/jnc.12783.

Sartor, Gregory C., and Gary Aston-Jones. ‘Regulation of the Ventral Tegmental Area by the Bed Nucleus of the Stria Terminalis Is Required for Expression of Cocaine Preference’. *The European Journal of Neuroscience* 36, no. 11 (December 2012): 3549–58. https://doi.org/10.1111/j.1460-9568.2012.08277.x.

Sawchenko, P. E., and L. W. Swanson. ‘The Organization of Forebrain Afferents to the Paraventricular and Supraoptic Nuclei of the Rat’. *The Journal of Comparative Neurology* 218, no. 2 (1 August 1983): 121–44. https://doi.org/10.1002/cne.902180202.

Schmidt, Karl T., Viren H. Makhijani, Kristen M. Boyt, Elizabeth S. Cogan, Dipanwita Pati, Melanie M. Pina, Isabel M. Bravo, et al. ‘Stress-Induced Alterations of Norepinephrine Release in the Bed Nucleus of the Stria Terminalis of Mice’. *ACS Chemical Neuroscience* 10, no. 4 (17 April 2019): 1908–14. https://doi.org/10.1021/acschemneuro.8b00265.

Schmidt, N. B., D. R. Lerew, and R. J. Jackson. ‘Prospective Evaluation of Anxiety Sensitivity in the Pathogenesis of Panic: Replication and Extension’. *Journal of Abnormal Psychology* 108, no. 3 (August 1999): 532–37. https://doi.org/10.1037//0021-843x.108.3.532.

———. ‘The Role of Anxiety Sensitivity in the Pathogenesis of Panic: Prospective Evaluation of Spontaneous Panic Attacks during Acute Stress’. *Journal of Abnormal Psychology* 106, no. 3 (August 1997): 355–64. https://doi.org/10.1037//0021-843x.106.3.355.

Schoenfeld, Timothy J., Alexander D. Kloth, Brian Hsueh, Matthew B. Runkle, Gary A. Kane, Samuel S.-H. Wang, and Elizabeth Gould. ‘Gap Junctions in the Ventral Hippocampal-Medial Prefrontal Pathway Are Involved in Anxiety Regulation’. *The Journal of Neuroscience: The Official Journal of the Society for Neuroscience* 34, no. 47 (19 November 2014): 15679–88. https://doi.org/10.1523/JNEUROSCI.3234-13.2014.

Schrader, Andrew J., Rachel M. Taylor, Emily G. Lowery-Gionta, and Nicole L. T. Moore. ‘Repeated Elevated plus Maze Trials as a Measure for Tracking Within-Subjects Behavioral Performance in Rats (Rattus Norvegicus)’. *PloS One* 13, no. 11 (2018): e0207804. https://doi.org/10.1371/journal.pone.0207804.

Schüppel, Karin, Kurt Brauer, Wolfgang Härtig, Jens Grosche, Bernadette Earley, Brian E. Leonard, and Gert Brückner. ‘Perineuronal Nets of Extracellular Matrix around Hippocampal Interneurons Resist Destruction by Activated Microglia in Trimethyltin-Treated Rats’. *Brain Research* 958, no. 2 (27 December 2002): 448–53. https://doi.org/10.1016/s0006-8993(02)03569-2.

Seibenhener, Michael L., and Michael C. Wooten. ‘Use of the Open Field Maze to Measure Locomotor and Anxiety-like Behavior in Mice’. *Journal of Visualized Experiments: JoVE*, no. 96 (6 February 2015): e52434. https://doi.org/10.3791/52434.

———. ‘Use of the Open Field Maze to Measure Locomotor and Anxiety-like Behavior in Mice’. *Journal of Visualized Experiments: JoVE*, no. 96 (6 February 2015): e52434. https://doi.org/10.3791/52434.

Sengpiel, Frank. ‘The Critical Period’. *Current Biology: CB* 17, no. 17 (4 September 2007): R742-743. https://doi.org/10.1016/j.cub.2007.06.017.

Sestakova, Natalia, Angelika Puzserova, Michal Kluknavsky, and Iveta Bernatova. ‘Determination of Motor Activity and Anxiety-Related Behaviour in Rodents: Methodological Aspects and Role of Nitric Oxide’. *Interdisciplinary Toxicology* 6, no. 3 (September 2013): 126–35. https://doi.org/10.2478/intox-2013-0020.

Sherman, Larry S., and Stephen A. Back. ‘A “GAG” Reflex Prevents Repair of the Damaged CNS’. *Trends in Neurosciences* 31, no. 1 (January 2008): 44–52. https://doi.org/10.1016/j.tins.2007.11.001.

Shinozaki, Munehisa, Akio Iwanami, Kanehiro Fujiyoshi, Syoichi Tashiro, Kazuya Kitamura, Shinsuke Shibata, Hiroshi Fujita, Masaya Nakamura, and Hideyuki Okano. ‘Combined Treatment with Chondroitinase ABC and Treadmill Rehabilitation for Chronic Severe Spinal Cord Injury in Adult Rats’. *Neuroscience Research* 113 (December 2016): 37–47. https://doi.org/10.1016/j.neures.2016.07.005.

Siebert, Justin R., Amanda Conta Steencken, and Donna J. Osterhout. ‘Chondroitin Sulfate Proteoglycans in the Nervous System: Inhibitors to Repair’. *BioMed Research International* 2014 (2014): 845323. https://doi.org/10.1155/2014/845323.

Silberman, Yuval, Robert T. Matthews, and Danny G. Winder. ‘A Corticotropin Releasing Factor Pathway for Ethanol Regulation of the Ventral Tegmental Area in the Bed Nucleus of the Stria Terminalis’. *The Journal of Neuroscience: The Official Journal of the Society for Neuroscience* 33, no. 3 (16 January 2013): 950–60. https://doi.org/10.1523/JNEUROSCI.2949-12.2013.

Sim, Hosung, Bin Hu, and Mariano S. Viapiano. ‘Reduced Expression of the Hyaluronan and Proteoglycan Link Proteins in Malignant Gliomas’. *The Journal of Biological Chemistry* 284, no. 39 (25 September 2009): 26547–56. https://doi.org/10.1074/jbc.M109.013185.

Simerly, Richard B. ‘Wired for Reproduction: Organization and Development of Sexually Dimorphic Circuits in the Mammalian Forebrain’. *Annual Review of Neuroscience* 25 (2002): 507–36. https://doi.org/10.1146/annurev.neuro.25.112701.142745.

Slaker, Megan, Lynn Churchill, Ryan P. Todd, Jordan M. Blacktop, Damian G. Zuloaga, Jacob Raber, Rebecca A. Darling, Travis E. Brown, and Barbara A. Sorg. ‘Removal of Perineuronal Nets in the Medial Prefrontal Cortex Impairs the Acquisition and Reconsolidation of a Cocaine-Induced Conditioned Place Preference Memory’. *The Journal of Neuroscience: The Official Journal of the Society for Neuroscience* 35, no. 10 (11 March 2015): 4190–4202. https://doi.org/10.1523/JNEUROSCI.3592-14.2015.

Slaker, Megan L., John H. Harkness, and Barbara A. Sorg. ‘A Standardized and Automated Method of Perineuronal Net Analysis Using Wisteria Floribunda Agglutinin Staining Intensity’. *IBRO Reports* 1 (December 2016): 54–60. https://doi.org/10.1016/j.ibror.2016.10.001.

Slaker, Megan L., Emily T. Jorgensen, Deborah M. Hegarty, Xinyue Liu, Yan Kong, Fuming Zhang, Robert J. Linhardt, Travis E. Brown, Sue A. Aicher, and Barbara A. Sorg. ‘Cocaine Exposure Modulates Perineuronal Nets and Synaptic Excitability of Fast-Spiking Interneurons in the Medial Prefrontal Cortex’. *ENeuro* 5, no. 5 (October 2018): ENEURO.0221-18.2018. https://doi.org/10.1523/ENEURO.0221-18.2018.

Smithers, Hannah E., John R. Terry, Jonathan T. Brown, and Andrew D. Randall. ‘Sex-Associated Differences in Excitability within the Bed Nucleus of the Stria Terminalis Are Reflective of Cell-Type’. *Neurobiology of Stress* 10 (19 December 2018): 100143. https://doi.org/10.1016/j.ynstr.2018.100143.

Smith-Thomas, L. C., J. Fok-Seang, J. Stevens, J. S. Du, E. Muir, A. Faissner, H. M. Geller, J. H. Rogers, and J. W. Fawcett. ‘An Inhibitor of Neurite Outgrowth Produced by Astrocytes’. *Journal of Cell Science* 107 (Pt 6) (June 1994): 1687–95. https://doi.org/10.1242/jcs.107.6.1687.

Somerville, Leah H., Paul J. Whalen, and William M. Kelley. ‘Human Bed Nucleus of the Stria Terminalis Indexes Hypervigilant Threat Monitoring’. *Biological Psychiatry* 68, no. 5 (1 September 2010): 416–24. https://doi.org/10.1016/j.biopsych.2010.04.002.

Sorg, Barbara A., Sabina Berretta, Jordan M. Blacktop, James W. Fawcett, Hiroshi Kitagawa, Jessica C. F. Kwok, and Marta Miquel. ‘Casting a Wide Net: Role of Perineuronal Nets in Neural Plasticity’. *The Journal of Neuroscience: The Official Journal of the Society for Neuroscience* 36, no. 45 (9 November 2016): 11459–68. https://doi.org/10.1523/JNEUROSCI.2351-16.2016.

Souter, Luke, and Jessica C. F. Kwok. ‘Visualization of Perineuronal Nets in Central Nervous System Tissue Sections’. *Methods in Molecular Biology*

(Clifton, N.J.) 2043 (2020): 251–60. https://doi.org/10.1007/978-1-4939-9698-8_20.

Spijker, Heleen M. van 't, and Jessica C. F. Kwok. 'A Sweet Talk: The Molecular Systems of Perineuronal Nets in Controlling Neuronal Communication'. *Frontiers in Integrative Neuroscience* 11 (2017): 33. https://doi.org/10.3389/fnint.2017.00033.

Spreafico, R., S. De Biasi, and L. Vitellaro-Zuccarello. 'The Perineuronal Net: A Weapon for a Challenge'. *Journal of the History of the Neurosciences* 8, no. 2 (August 1999): 179–85. https://doi.org/10.1076/jhin.8.2.179.1834.

Stanford, S. Clare. 'The Open Field Test: Reinventing the Wheel'. *Journal of Psychopharmacology (Oxford, England)* 21, no. 2 (March 2007): 134–35. https://doi.org/10.1177/0269881107073199.

Steensel, Francisca J. A. van, Susan M. Bögels, and Sean Perrin. 'Anxiety Disorders in Children and Adolescents with Autistic Spectrum Disorders: A Meta-Analysis'. *Clinical Child and Family Psychology Review* 14, no. 3 (September 2011): 302–17. https://doi.org/10.1007/s10567-011-0097-0.

Stein, Dan J., Kate M. Scott, Peter de Jonge, and Ronald C. Kessler. 'Epidemiology of Anxiety Disorders: From Surveys to Nosology and Back'. *Dialogues in Clinical Neuroscience* 19, no. 2 (June 2017): 127–36.

Straube, Thomas, Hans-Joachim Mentzel, and Wolfgang H. R. Miltner. 'Waiting for Spiders: Brain Activation during Anticipatory Anxiety in Spider Phobics'. *NeuroImage* 37, no. 4 (1 October 2007): 1427–36. https://doi.org/10.1016/j.neuroimage.2007.06.023.

Sullivan, Chelsea S., Ingo Gotthard, Elliott V. Wyatt, Srihita Bongu, Vishwa Mohan, Richard J. Weinberg, and Patricia F. Maness. 'Perineuronal Net Protein Neurocan Inhibits NCAM/EphA3 Repellent Signaling in GABAergic Interneurons'. *Scientific Reports* 8, no. 1 (18 April 2018): 6143. https://doi.org/10.1038/s41598-018-24272-8.

Sullivan, G. M., J. Apergis, D. E. A. Bush, L. R. Johnson, M. Hou, and J. E. Ledoux. 'Lesions in the Bed Nucleus of the Stria Terminalis Disrupt Corticosterone and Freezing Responses Elicited by a Contextual but Not by a Specific Cue-Conditioned Fear Stimulus'. *Neuroscience* 128, no. 1 (2004): 7–14. https://doi.org/10.1016/j.neuroscience.2004.06.015.

Sun, N., L. Roberts, and M. D. Cassell. 'Rat Central Amygdaloid Nucleus Projections to the Bed Nucleus of the Stria Terminalis'. *Brain Research Bulletin* 27, no. 5 (November 1991): 651–62. https://doi.org/10.1016/0361-9230(91)90041-h.

Surget, A., and C. Belzung. 'Unpredictable Chronic Mild Stress in Mice'. edited by A. V. Kalueff and J. L. LaPorte, 79–112. New York, NY, USA: Nova Science, 2008. https://eprints.gla.ac.uk/79773/.

Suttkus, A., S. Rohn, S. Weigel, P. Glöckner, T. Arendt, and M. Morawski. 'Aggrecan, Link Protein and Tenascin-R Are Essential Components of the Perineuronal Net to Protect Neurons against Iron-Induced Oxidative Stress'. *Cell Death & Disease* 5 (13 March 2014): e1119. https://doi.org/10.1038/cddis.2014.25.

Swanson, Larry. *Brain Maps: Structure of the Rat Brain*. Gulf Professional Publishing, 2004.

Sylvers, Patrick, Scott O. Lilienfeld, and Jamie L. LaPrairie. 'Differences between Trait Fear and Trait Anxiety: Implications for Psychopathology'. *Clinical Psychology Review* 31, no. 1 (February 2011): 122–37. https://doi.org/10.1016/j.cpr.2010.08.004.

Takigawa, Tomoko, and Christian Alzheimer. 'Phasic and Tonic Attenuation of EPSPs by Inward Rectifier K+ Channels in Rat Hippocampal Pyramidal Cells'. *The Journal of Physiology* 539, no. Pt 1 (15 February 2002): 67–75. https://doi.org/10.1113/jphysiol.2001.012883.

Tewari, Bhanu P., Lata Chaunsali, Susan L. Campbell, Dipan C. Patel, Adam E. Goode, and Harald Sontheimer. 'Perineuronal Nets Decrease Membrane Capacitance of Peritumoral Fast Spiking Interneurons in a Model of Epilepsy'. *Nature Communications* 9, no. 1 (9 November 2018): 4724. https://doi.org/10.1038/s41467-018-07113-0.

Thibaut, Florence. 'Anxiety Disorders: A Review of Current Literature'. *Dialogues in Clinical Neuroscience* 19, no. 2 (June 2017): 87–88.

Thompson, Elise Holter, Kristian Kinden Lensjø, Mattis Brænne Wigestrand, Anders Malthe-Sørenssen, Torkel Hafting, and Marianne Fyhn. 'Removal of Perineuronal Nets Disrupts Recall of a Remote Fear Memory'. *Proceedings of the National Academy of Sciences of the United States of America* 115, no. 3 (16 January 2018): 607–12. https://doi.org/10.1073/pnas.1713530115.

Torres, D. B., A. Lopes, A. J. Rodrigues, J. J. Cerqueira, N. Sousa, J. a. R. Gontijo, and P. A. Boer. 'Anxiety-like Behavior and Structural Changes of the Bed Nucleus of the Stria Terminalis (BNST) in Gestational Protein-Restricted Male Offspring'. *Journal of Developmental Origins of Health and Disease* 9, no. 5 (October 2018): 536–43. https://doi.org/10.1017/S2040174418000399.

Tovote, Philip, Jonathan Paul Fadok, and Andreas Lüthi. 'Neuronal Circuits for Fear and Anxiety'. *Nature Reviews. Neuroscience* 16, no. 6 (June 2015): 317–31. https://doi.org/10.1038/nrn3945.

Tsien, Roger Y. 'Very Long-Term Memories May Be Stored in the Pattern of Holes in the Perineuronal Net'. *Proceedings of the National Academy of Sciences of the United States of America* 110, no. 30 (23 July 2013): 12456–61. https://doi.org/10.1073/pnas.1310158110.

Turesson, Hjalmar K., Olga E. Rodríguez-Sierra, and Denis Pare. ‘Intrinsic Connections in the Anterior Part of the Bed Nucleus of the Stria Terminalis’. *Journal of Neurophysiology* 109, no. 10 (May 2013): 2438–50. https://doi.org/10.1152/jn.00004.2013.

Ueno, Hiroshi, Shunsuke Suemitsu, Shinji Murakami, Naoya Kitamura, Kenta Wani, Yosuke Matsumoto, Motoi Okamoto, Shozo Aoki, and Takeshi Ishihara. ‘Juvenile Stress Induces Behavioral Change and Affects Perineuronal Net Formation in Juvenile Mice’. *BMC Neuroscience* 19, no. 1 (16 July 2018): 41. https://doi.org/10.1186/s12868-018-0442-z.

Ueno, Hiroshi, Shunsuke Suemitsu, Shinji Murakami, Naoya Kitamura, Kenta Wani, Yosuke Matsumoto, Motoi Okamoto, and Takeshi Ishihara. ‘Layer-Specific Expression of Extracellular Matrix Molecules in the Mouse Somatosensory and Piriform Cortices’. *IBRO Reports* 6 (June 2019): 1–17. https://doi.org/10.1016/j.ibror.2018.11.006.

Ueno, Hiroshi, Shunsuke Suemitsu, Motoi Okamoto, Yosuke Matsumoto, and Takeshi Ishihara. ‘Parvalbumin Neurons and Perineuronal Nets in the Mouse Prefrontal Cortex’. *Neuroscience* 343 (20 February 2017): 115–27. https://doi.org/10.1016/j.neuroscience.2016.11.035.

———. ‘Sensory Experience-Dependent Formation of Perineuronal Nets and Expression of Cat-315 Immunoreactive Components in the Mouse Somatosensory Cortex’. *Neuroscience* 355 (4 July 2017): 161–74. https://doi.org/10.1016/j.neuroscience.2017.04.041.

Umemori, Juzoh, Frederike Winkel, Eero Castrén, and Nina N. Karpova. ‘Distinct Effects of Perinatal Exposure to Fluoxetine or Methylmercury on Parvalbumin and Perineuronal Nets, the Markers of Critical Periods in Brain Development’. *International Journal of Developmental Neuroscience: The Official Journal of the International Society for Developmental Neuroscience* 44 (August 2015): 55–64. https://doi.org/10.1016/j.ijdevneu.2015.05.006.

Untergasser, Andreas, Ioana Cutcutache, Triinu Koressaar, Jian Ye, Brant C. Faircloth, Maido Remm, and Steven G. Rozen. ‘Primer3--New Capabilities and Interfaces’. *Nucleic Acids Research* 40, no. 15 (August 2012): e115. https://doi.org/10.1093/nar/gks596.

Vo, Tam, Daniela Carulli, Erich M. E. Ehlert, Jessica C. F. Kwok, Gunnar Dick, Vasil Mecollari, Elizabeth B. Moloney, et al. ‘The Chemorepulsive Axon Guidance Protein Semaphorin3A Is a Constituent of Perineuronal Nets in the Adult Rodent Brain’. *Molecular and Cellular Neurosciences* 56 (September 2013): 186–200. https://doi.org/10.1016/j.mcn.2013.04.009.

Vos, Theo, Stephen S. Lim, Cristiana Abbafati, Kaja M. Abbas, Mohammad Abbasi, Mitra Abbasifard, Mohsen Abbasi-Kangevari, et al. ‘Global Burden of 369 Diseases and Injuries in 204 Countries and Territories, 1990–2019: A Systematic Analysis for the Global Burden of Disease Study 2019’. *The Lancet*

396, no. 10258 (17 October 2020): 1204–22. https://doi.org/10.1016/S0140-6736(20)30925-9.

Vyas, Ajai, Savita Bernal, and Sumantra Chattarji. ‘Effects of Chronic Stress on Dendritic Arborization in the Central and Extended Amygdala’. *Brain Research* 965, no. 1–2 (7 March 2003): 290–94. https://doi.org/10.1016/s0006-8993(02)04162-8.

Vyas, Ajai, Rupshi Mitra, B. S. Shankaranarayana Rao, and Sumantra Chattarji. ‘Chronic Stress Induces Contrasting Patterns of Dendritic Remodeling in Hippocampal and Amygdaloid Neurons’. *The Journal of Neuroscience: The Official Journal of the Society for Neuroscience* 22, no. 15 (1 August 2002): 6810–18. https://doi.org/20026655.

Walker, Claire-Dominique, Kevin G. Bath, Marian Joels, Aniko Korosi, Muriel Larauche, Paul J. Lucassen, Margaret J. Morris, et al. ‘Chronic Early Life Stress Induced by Limited Bedding and Nesting (LBN) Material in Rodents: Critical Considerations of Methodology, Outcomes and Translational Potential’. *Stress (Amsterdam, Netherlands)* 20, no. 5 (September 2017): 421–48. https://doi.org/10.1080/10253890.2017.1343296.

Walker, D. L., and M. Davis. ‘Double Dissociation between the Involvement of the Bed Nucleus of the Stria Terminalis and the Central Nucleus of the Amygdala in Startle Increases Produced by Conditioned versus Unconditioned Fear’. *The Journal of Neuroscience: The Official Journal of the Society for Neuroscience* 17, no. 23 (1 December 1997): 9375–83.

Walker, David L., Donna J. Toufexis, and Michael Davis. ‘Role of the Bed Nucleus of the Stria Terminalis versus the Amygdala in Fear, Stress, and Anxiety’. *European Journal of Pharmacology* 463, no. 1–3 (28 February 2003): 199–216. https://doi.org/10.1016/s0014-2999(03)01282-2.

Walter, A., J. K. Mai, L. Lanta, and T. Görcs. ‘Differential Distribution of Immunohistochemical Markers in the Bed Nucleus of the Stria Terminalis in the Human Brain’. *Journal of Chemical Neuroanatomy* 4, no. 4 (August 1991): 281–98. https://doi.org/10.1016/0891-0618(91)90019-9.

Wang, Difei, and James Fawcett. ‘The Perineuronal Net and the Control of CNS Plasticity’. *Cell and Tissue Research* 349, no. 1 (July 2012): 147–60. https://doi.org/10.1007/s00441-012-1375-y.

Wang, Hua-Ning, Yuan-Han Bai, Yun-Chun Chen, Rui-Guo Zhang, Huai-Hai Wang, Ya-Hong Zhang, Jing-Li Gan, Zheng-Wu Peng, and Qing-Rong Tan. ‘Repetitive Transcranial Magnetic Stimulation Ameliorates Anxiety-like Behavior and Impaired Sensorimotor Gating in a Rat Model of Post-Traumatic Stress Disorder’. *PloS One* 10, no. 2 (2015): e0117189. https://doi.org/10.1371/journal.pone.0117189.

Watanabe, H., K. Kimata, S. Line, D. Strong, L. Y. Gao, C. A. Kozak, and Y. Yamada. ‘Mouse Cartilage Matrix Deficiency (Cmd) Caused by a 7 Bp Deletion

in the Aggrecan Gene'. *Nature Genetics* 7, no. 2 (June 1994): 154–57. https://doi.org/10.1038/ng0694-154.

Weber, P., U. Bartsch, M. N. Rasband, R. Czaniera, Y. Lang, H. Bluethmann, R. U. Margolis, et al. 'Mice Deficient for Tenascin-R Display Alterations of the Extracellular Matrix and Decreased Axonal Conduction Velocities in the CNS'. *The Journal of Neuroscience: The Official Journal of the Society for Neuroscience* 19, no. 11 (1 June 1999): 4245–62.

Weller, K. L., and D. A. Smith. 'Afferent Connections to the Bed Nucleus of the Stria Terminalis'. *Brain Research* 232, no. 2 (28 January 1982): 255–70. https://doi.org/10.1016/0006-8993(82)90272-4.

Wen, Teresa H., Sonia Afroz, Sarah M. Reinhard, Arnold R. Palacios, Kendal Tapia, Devin K. Binder, Khaleel A. Razak, and Iryna M. Ethell. 'Genetic Reduction of Matrix Metalloproteinase-9 Promotes Formation of Perineuronal Nets Around Parvalbumin-Expressing Interneurons and Normalizes Auditory Cortex Responses in Developing Fmr1 Knock-Out Mice'. *Cerebral Cortex (New York, N.Y.: 1991)* 28, no. 11 (1 November 2018): 3951–64. https://doi.org/10.1093/cercor/bhx258.

Willner, Paul, Richard Muscat, and Mariusz Papp. 'Chronic Mild Stress-Induced Anhedonia: A Realistic Animal Model of Depression'. *Neuroscience & Biobehavioral Reviews* 16, no. 4 (1 January 1992): 525–34. https://doi.org/10.1016/S0149-7634(05)80194-0.

Winter, F. de, J. C. F. Kwok, J. W. Fawcett, T. T. Vo, D. Carulli, and J. Verhaagen. 'The Chemorepulsive Protein Semaphorin 3A and Perineuronal Net-Mediated Plasticity'. *Neural Plasticity* 2016 (2016): 3679545. https://doi.org/10.1155/2016/3679545.

Wittchen, Hans-Ulrich, Ron C. Kessler, Katja Beesdo, Petra Krause, Michael Höfler, and Jürgen Hoyer. 'Generalized Anxiety and Depression in Primary Care: Prevalence, Recognition, and Management'. *The Journal of Clinical Psychiatry* 63 Suppl 8 (2002): 24–34.

Wonders, Carl P., and Stewart A. Anderson. 'The Origin and Specification of Cortical Interneurons'. *Nature Reviews. Neuroscience* 7, no. 9 (September 2006): 687–96. https://doi.org/10.1038/nrn1954.

Woodhams, P. L., G. W. Roberts, J. M. Polak, and T. J. Crow. 'Distribution of Neuropeptides in the Limbic System of the Rat: The Bed Nucleus of the Stria Terminalis, Septum and Preoptic Area'. *Neuroscience* 8, no. 4 (April 1983): 677–703. https://doi.org/10.1016/0306-4522(83)90003-9.

Xiao, Qian, Xinyi Zhou, Pengfei Wei, Li Xie, Yaning Han, Jie Wang, Aoling Cai, Fuqiang Xu, Jie Tu, and Liping Wang. 'A New GABAergic Somatostatin Projection from the BNST onto Accumbal Parvalbumin Neurons Controls Anxiety'. *Molecular Psychiatry* 26, no. 9 (September 2021): 4719–41. https://doi.org/10.1038/s41380-020-0816-3.

Y, Watanabe, Gould E, and McEwen Bs. ‘Stress Induces Atrophy of Apical Dendrites of Hippocampal CA3 Pyramidal Neurons’. *Brain Research* 588, no. 2 (21 August 1992). https://doi.org/10.1016/0006-8993(92)91597-8.

Yamada, J., and S. Jinno. ‘Spatio-Temporal Differences in Perineuronal Net Expression in the Mouse Hippocampus, with Reference to Parvalbumin’. *Neuroscience* 253 (3 December 2013): 368–79. https://doi.org/10.1016/j.neuroscience.2013.08.061.

Yamada, J., T. Ohgomori, and S. Jinno. ‘Perineuronal Nets Affect Parvalbumin Expression in GABAergic Neurons of the Mouse Hippocampus’. *The European Journal of Neuroscience* 41, no. 3 (February 2015): 368–78. https://doi.org/10.1111/ejn.12792.

Yamada, Jun, and Shozo Jinno. ‘Molecular Heterogeneity of Aggrecan-Based Perineuronal Nets around Five Subclasses of Parvalbumin-Expressing Neurons in the Mouse Hippocampus’. *The Journal of Comparative Neurology* 525, no. 5 (1 April 2017): 1234–49. https://doi.org/10.1002/cne.24132.

Yamauchi, Naoki, Daiki Takahashi, Yae K. Sugimura, Fusao Kato, Taiju Amano, and Masabumi Minami. ‘Activation of the Neural Pathway from the Dorsolateral Bed Nucleus of the Stria Terminalis to the Central Amygdala Induces Anxiety-like Behaviors’. *The European Journal of Neuroscience* 48, no. 9 (November 2018): 3052–61. https://doi.org/10.1111/ejn.14165.

Yang, Sujeong, Matthias Cacquevel, Lisa M. Saksida, Timothy J. Bussey, Bernard L. Schneider, Patrick Aebischer, Riccardo Melani, Tommaso Pizzorusso, James W. Fawcett, and Maria Grazia Spillantini. ‘Perineuronal Net Digestion with Chondroitinase Restores Memory in Mice with Tau Pathology’. *Experimental Neurology* 265 (March 2015): 48–58. https://doi.org/10.1016/j.expneurol.2014.11.013.

Ye, Jian, George Coulouris, Irena Zaretskaya, Ioana Cutcutache, Steve Rozen, and Thomas L. Madden. ‘Primer-BLAST: A Tool to Design Target-Specific Primers for Polymerase Chain Reaction’. *BMC Bioinformatics* 13 (18 June 2012): 134. https://doi.org/10.1186/1471-2105-13-134.

Yu, Zhoulong, Na Chen, Die Hu, Wenxi Chen, Yi Yuan, Shiqiu Meng, Wen Zhang, Lin Lu, Ying Han, and Jie Shi. ‘Decreased Density of Perineuronal Net in Prelimbic Cortex Is Linked to Depressive-Like Behavior in Young-Aged Rats’. *Frontiers in Molecular Neuroscience* 13 (2020): 4. https://doi.org/10.3389/fnmol.2020.00004.

Zhang, W., C. E. Watson, C. Liu, K. J. Williams, and V. P. Werth. ‘Glucocorticoids Induce a Near-Total Suppression of Hyaluronan Synthase MRNA in Dermal Fibroblasts and in Osteoblasts: A Molecular Mechanism Contributing to Organ Atrophy’. *The Biochemical Journal* 349, no. Pt 1 (1 July 2000): 91–97. https://doi.org/10.1042/0264-6021:3490091.

Zhao, Rong-Rong, and James W. Fawcett. ‘Combination Treatment with Chondroitinase ABC in Spinal Cord Injury--Breaking the Barrier’. *Neuroscience Bulletin* 29, no. 4 (August 2013): 477–83. https://doi.org/10.1007/s12264-013-1359-2.

Zhou, X. H., C. Brakebusch, H. Matthies, T. Oohashi, E. Hirsch, M. Moser, M. Krug, et al. ‘Neurocan Is Dispensable for Brain Development’. *Molecular and Cellular Biology* 21, no. 17 (September 2001): 5970–78. https://doi.org/10.1128/MCB.21.17.5970-5978.2001.

Zhou, X., D. Hollern, J. Liao, E. Andrechek, and H. Wang. ‘NMDA Receptor-Mediated Excitotoxicity Depends on the Coactivation of Synaptic and Extrasynaptic Receptors’. *Cell Death & Disease* 4 (28 March 2013): e560. https://doi.org/10.1038/cddis.2013.82.

Zhu, W., H. Umegaki, Y. Suzuki, H. Miura, and A. Iguchi. ‘Involvement of the Bed Nucleus of the Stria Terminalis in Hippocampal Cholinergic System-Mediated Activation of the Hypothalamo--Pituitary--Adrenocortical Axis in Rats’. *Brain Research* 916, no. 1–2 (19 October 2001): 101–6. https://doi.org/10.1016/s0006-8993(01)02871-2.

Zivanovic-Macuzic, Ivana, Maja Vulovic, Dejan Jeremic, D. Stojadinovic, M. Sazdanovic, and J. Tosevski. ‘The Neurons of Human Bed Nucleus of the Stria Terminalis’. *Medicus* 8 (1 September 2007): 87–92.

6 September 2022. https://www.exeter.ac.uk/media/universityofexeter/recruitmentsites/images/uoe-logo.svg.